
Possible Directions for Advanced Accelerator R&D at the ILC test accelerator at Fermilab

**Tuesday November 28th, 2006,
Fermilab, Wilson Hall room 1 North**

Philippe Piot, Sergei Nagaitsev and Vladimir Shitkev

Goal

Fermilab is currently building a test facility with the prime purpose of testing and characterizing sub-systems associated to the international linear collider (ILC) proposal. This ILC test accelerator (ILCTA) will eventually produced bright electron beams with energies ranging from 40 to 750 MeV. The purpose of this mini-workshop is to identify possible advanced accelerator R&D activities that could be pursued at this facility along with needed infrastructure to successfully carry these experiments. Topics that were discussed included:

- generation, manipulation and diagnostics of high brightness electron beams,
 - plasma-wakefield based acceleration technique,
 - electromagnetic structure and laser-based acceleration methods,
 - radiation sources.
-

Agenda:

Introduction

- 8.30: V. Shiltsev , Introduction
- 8.45: S. Nagaitsev , ILC test accelerator: Overview & Schedule
- 9:00: P. Piot, beamline overview and anticipated beam parameters

Generation, manipulation and diagnostics of high brightness electron beams

Chair: Kwang-Je Kim, Argonne National Lab. & University of Chicago

- 9:30-12:15 -- Talks
- 09:30-10:00 -- K.-J. Kim, ANL, Emittance manipulations & beam conditioning
- 10:00-10:15 -- COFFEE BREAK
- 10:15-10:35 -- A. Mikhailichenko, Cornell, Damping ring for test of optical stochastic cooling
- 10:35-10:55 -- T. Koeth (R. Fillier presenter), Rutgers, Emittance exchanger experiment at FNPL
- 10:55-11:15 -- W. Gai, ANL, Possible low intensity "keep-alive" positron sources
- 11:15-11:35 -- J. Ruan, FNAL, Beam diagnostics based on EO sampling
- 11:35-11:55 -- Y. Li (P. Piot presenter), ANL, Beam diagnostics with <10 fs resolution (optical replica)
- 11:55-12:15 -- A. Lumpkin, ANL, Diffraction radiation (TBC)
- 12:15-12:30 -- Discussion

12:30 to 01:30 Lunch break

- 01:30-02:00 -- Discussion

Plasma-wakefield based acceleration technique

- 02:00-02:20 Talks
- 02:00-02:20 -- P. Muggli, USC (via phone), possible plasma wakefield acceleration experiment

Radiation sources

Chair: Jean Delaen, Thomas Jefferson Lab & Old Dominion University

- 02:20-03:55 -- Talks
- 02:20-02:40 -- G. Krafft (J. Delaysen presenter), JLAB/ODU, Radiation Sources
- 02:40-03:00 -- K. Chouffani, Idaho Accelerator Center, Dual applications of laser-electron beam interaction,
- 03:00-03:15 -- COFFEE BREAK
- 03:15-03:35 -- C. Chen, MIT, Ribbon-beam klystron for ILC [talk not available]
- 03:35-03:55 -- Y. Li (P. Piot presenter), ANL, X-ray sources with 20 fs duration
- 03:55-04:10 -- Discussion

Electromagnetic structure and laser-based acceleration methods

Chair: Alexander Mikhailichenko, Cornell University

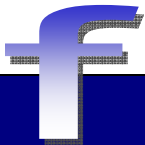
- 04:10-05:30 -- Talks
- 04:10-04:30 -- A. Mikhailichenko, Cornell, Acceleration by swept laser burst
- 04:30-04:50 -- B. Shen, Chinese Academy of Sciences Shanghai, Laser acceleration: overview
- 04:50-05:10 -- J.Power, ANL, Wakefield structure accelerators
- 05:10-05:30 -- J. Zhou, MIT, Photonic band gap HOM Coupler for ILC
- 05:30-05:45 -- Discussion

List of participant (who attended all or part of the workshop)

1. Alexander Mikhailichenko, Cornell
2. Philippe Piot, FNAL/NIU
3. Patric Muggli, USC
4. Alex Lumpkin, ANL
5. Alvin Tollstrup, FNAL
6. Wei Gai, ANL
7. John Power, ANL
8. David Yu, Duli Inc
9. Dick Carrigan, FNAL
10. Khalid Chouffani, Idaho Accelerator Center
11. Slava Yakovlev, Omega-P, Inc./Yale Beam Physics Laboratory
12. Vladimir Shiltsev, FNAL
13. Sergei Nagaitsev, FNAL
14. Mike Church, FNAL
15. Alexander Valishev, FNAL
16. Jea Zhou, MIT
17. Chiping Chen, MIT
18. Alexei Kanareykin, Euclid Concept Inc.
19. Yin-e Sun, ANL
20. Marwan Rihaoui, NIU
21. Kwang-Je Kim, ANL & U. of Chicago
22. Jihao Ruan, FNAL
23. Raymond Filler, FNAL
24. Young-Kee Kim, U. of Chicago
25. Manfred Wendt, FNAL
26. Eliana Gianfelice-Wendt, FNAL
27. Bafei Shen, Institute of fine Mechanics & Optics of Shanghai
28. Randy Thurmman-Keup, FNAL
29. Vic Scarpine, FNAL
30. Leo Bellantoni, FNAL
31. Rodney Gerig, ANL

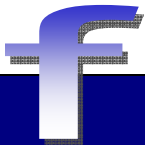
Fermilab's New Take on Advanced Accelerator R&D

Vladimir Shiltsev



4 weeks ago: Nov. 1 2006

“... BATAVIA, ILLINOIS -- The U.S. Department of Energy (DOE) has awarded a new \$1.575 billion, five-year contract for management and operation of Fermi National Accelerator Laboratory (FNAL) to the Fermi Research Alliance, LLC (FRA), owned jointly by the University of Chicago (UChicago) and Universities Research Association, Inc. (URA)...”



...starting Jan 01 2007: FRA



THE UNIVERSITY OF
CHICAGO

Robert Zimmer, President



Fred Bernthal, President



Robert Zimmer, Chair
Fred Bernthal, Vice-Chair
Pier Oddone, President

**Fermi
Research
Alliance**



11/28/2006

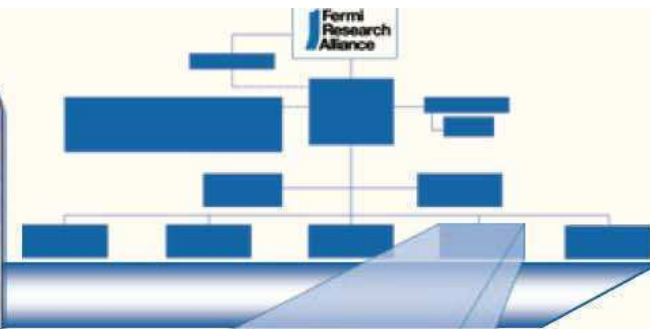
mini-Workshop on AARD@NML


01/01/07: Fermi Research Alliance

- Presidents of IL Universities on FRA Board
 - Northern Illinois University
 - Illinois Institute of Technology
 - Northwestern
 - University of Illinois



Accelerator Programs



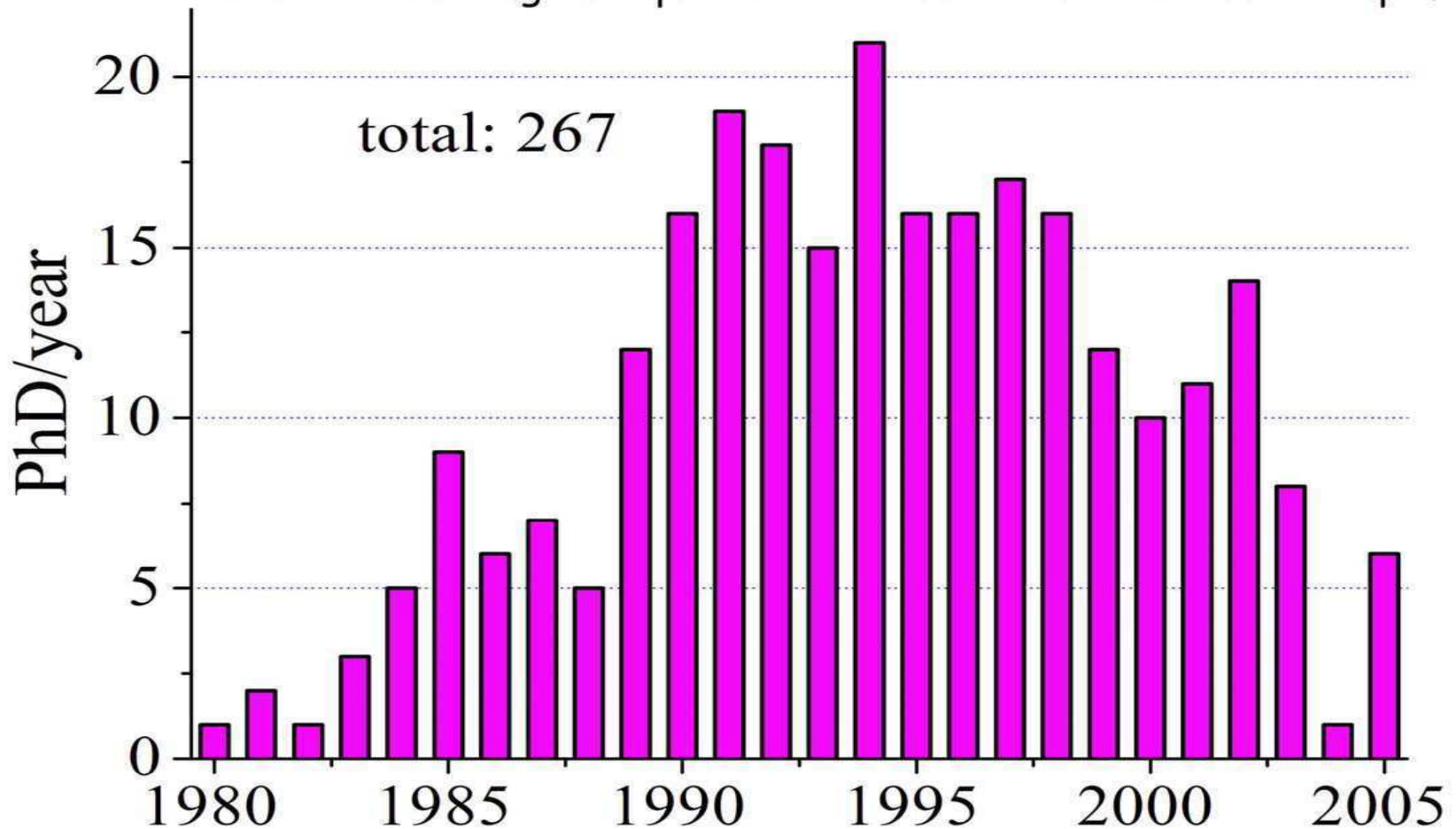
- ❖ New Accelerator Physics Research Center ensures forward-looking R&D for LHC, ILC, and beyond
 - ❖ Enhanced scope of division attracts new skill sets to adapt to changing mission
- 
- ```
graph TD
 AP[CERN Accelerator Physics] --- AP_C[Accelerator Physics Center]
 AP --- T[Technical]
 AP_C --- AP_C_S1[ILC Accelerator Physics]
 AP_C --- AP_C_S2[LHC Accelerator Physics]
 AP_C --- AP_C_S3[Future Accelerator Physics]
 T --- T_S1[ILC Accelerator Physics]
 T --- T_S2[LHC Accelerator Physics]
 T --- T_S3[Future Accelerator Physics]
```

- Accelerator
- Technical
- Accelerator Physics Center

# APC Rationale (2)

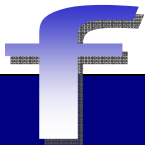
DOE Advanced Technology R&D Yearbook

[www.science.doe.gov/hep/AdvTechR&D2005/TechR&D2005.pdf](http://www.science.doe.gov/hep/AdvTechR&D2005/TechR&D2005.pdf)

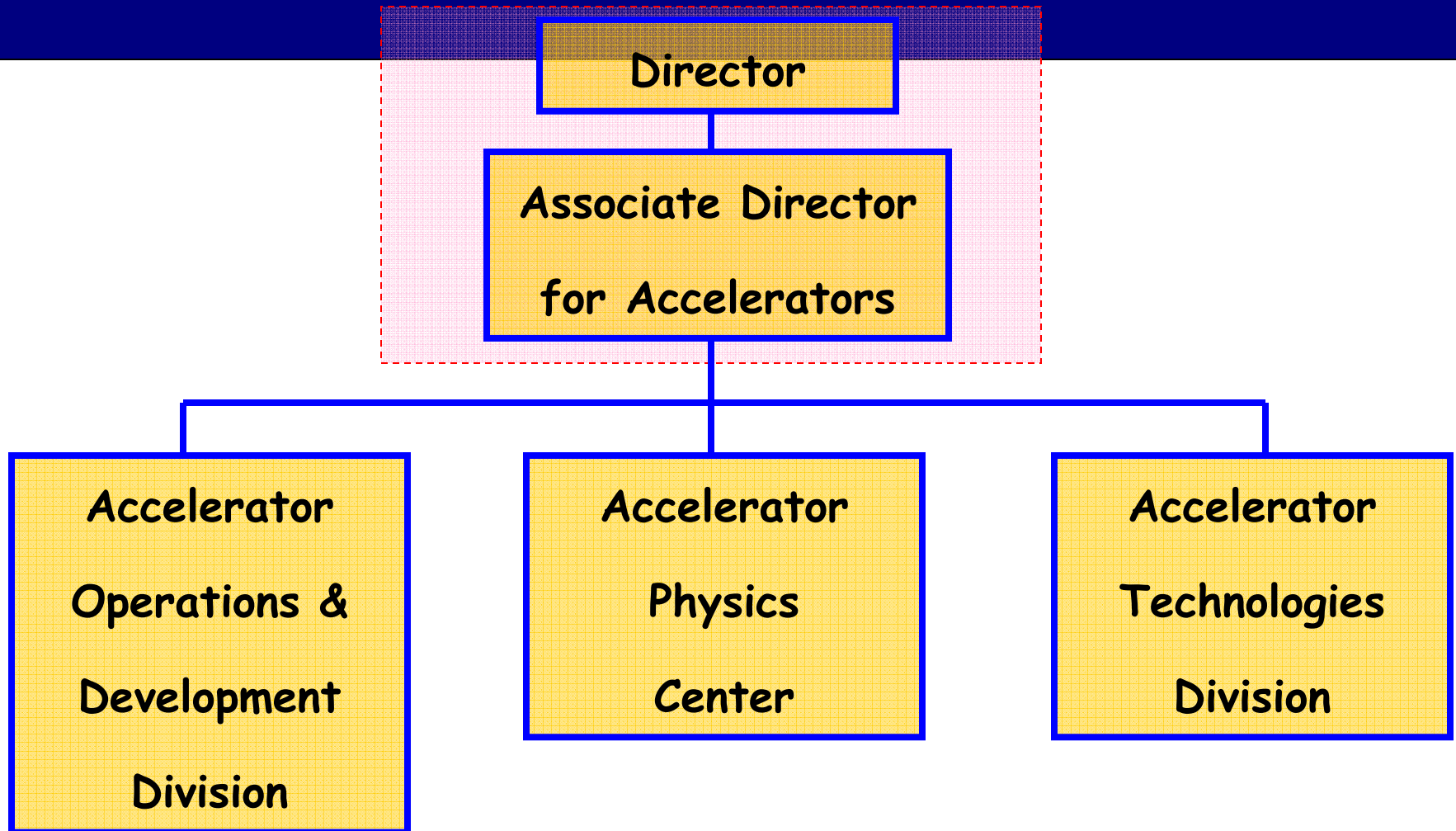


# Accelerator Physics Center Mission

- Coordinate and conduct accelerator R&D aimed at next-generation and beyond accelerator facilities
- Provide Accelerator Physics support for existing operational programs
- Train accelerator physicists and engineers



# APC Organization

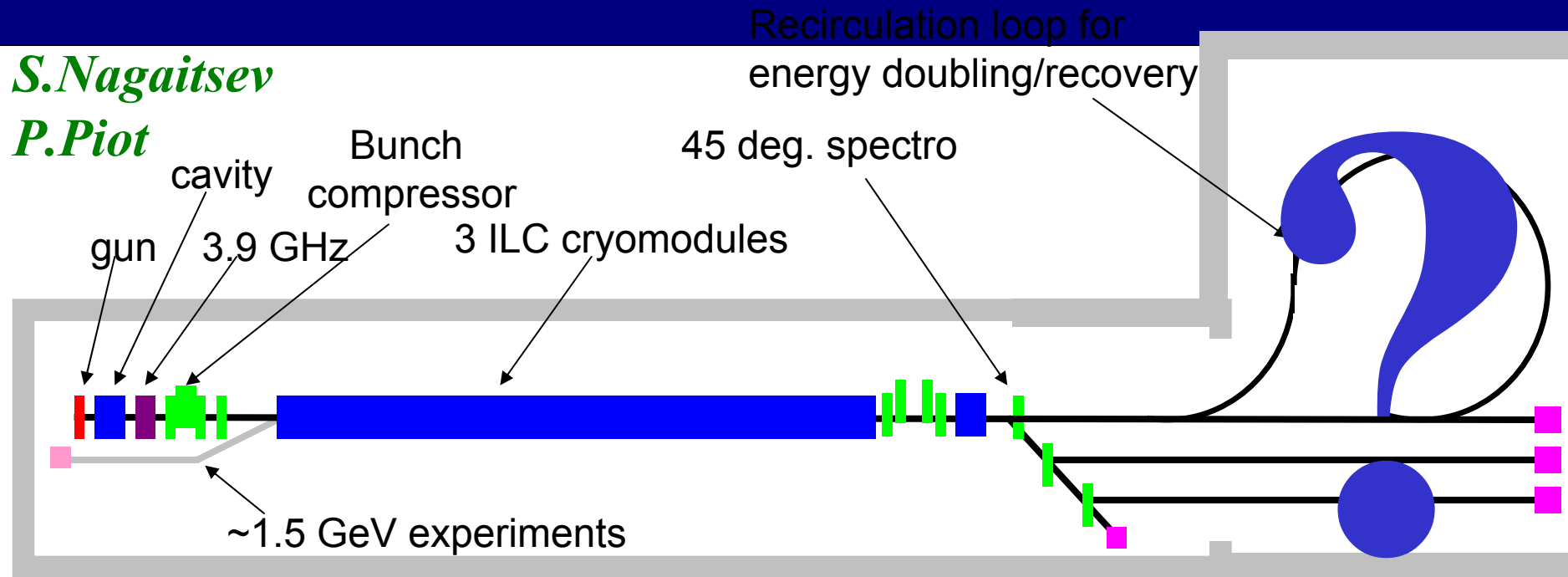




# NML setup as AAR&D user facility

*S. Nagaitsev*

*P. Piot*



- Several user beam line independent of each other will maximize productivity (see model of ATF at Brookhaven),
- In an SCRF linac one could also include a recirculation loop to either operate the linac in either energy recovery or energy doubler,
- The loop in itself could be a very rich “beam dynamics object”, such a loop as actually been proposed for CW operation of X-ray free-electron laser

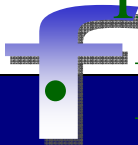


# This Mini-Workshop

The purpose of this mini-workshop is to identify possible advanced accelerator R&D activities that could be pursued at the NML facility along with needed infrastructure to successfully carry these experiments.

Topics that will be discussed include:

- Generation, manipulation, diagnostics of high brightness e-beams
- Plasma-wakefield based acceleration technique,
- EM structure & laser-based acceleration methods



Radiation sources

# Focus points of the mini-Workshop

## Expectations for the mini-Workshop:

- get input from AAR&D community on the NML Users facility experimental program
- focus on possibilities to carry out unique research
- make the first look into what's needed for that
  - lab space
  - infrastructure
  - beam parameters

**All that is very needed for the NML planning!**



# WELCOME TO FNAL!

## Thank you for coming!

Thanks to Philippe for organization of the Workshop

... *and let's do a good job!*

---

# **NML facility overview and schedule**

Sergei Nagaitsev (Fermilab)

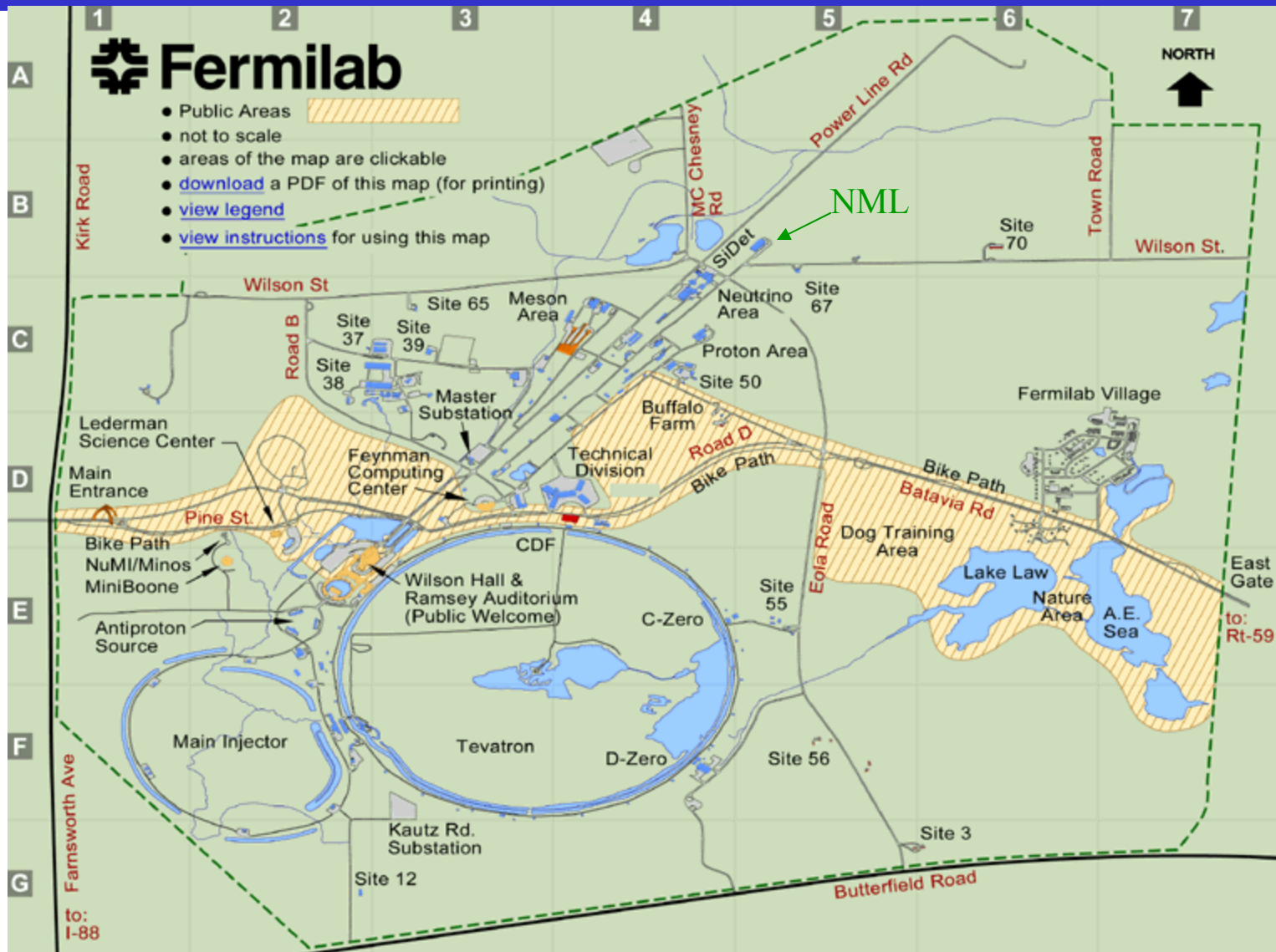
Nov 28, 2006

## What is NML?

---

- NML is an existing building at Fermilab (New Muon Lab)
- NML building is part of Fermilab's ILC Test Areas
  - Other areas are: MDB (horizontal SCRF cavity test stand), IB1 (vertical test stand) etc.
- NML accelerator test facility is being developed as part of SCRF infrastructure at Fermilab.
- The first NML user will be the ILC program.
  - The AARD portion may first piggy-back on the ILC program
  - Will increase with time

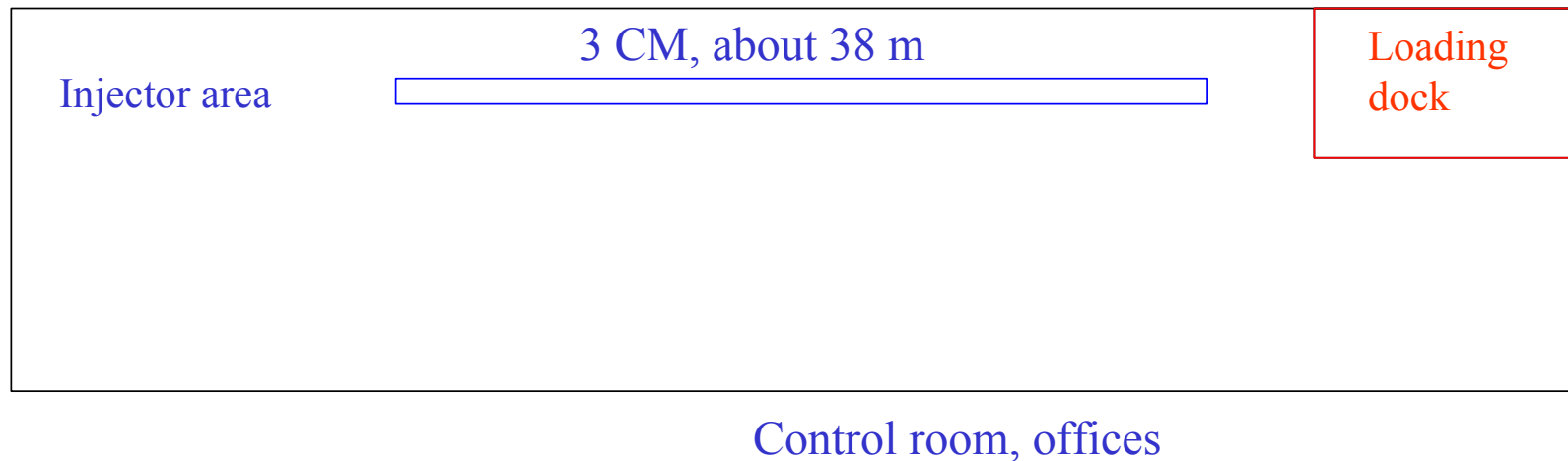
# Location



## New Muon Building

---

- Below-grade area is 73m x 18m.
- Loading dock (NW corner): 12m x 7m





## NewMuon: South Side



## West side





## Facing north wall



## North side, loading dock



## ILC-like beam parameters

---

|                     |                       |
|---------------------|-----------------------|
| ■ # Electrons/bunch | $2 \times 10^{10}$    |
| ■ # bunches/train   | 2820                  |
| ■ Bunch rep. rate   | 3 MHz                 |
| ■ Train rep. rate   | 5 Hz                  |
| ■ Ave. current      | $\sim 50 \mu\text{A}$ |

## ILC Plans for NML

---

0. Use NML as a cryomodule test facility (must be able to replace CM's quickly)
1. Demonstrate stable long-term high-gradient beam operation at ILC-like bunch parameters.
2. While operating at high gradient and ILC-like beam currents, demonstrate a LLRF controls system such that the beam energy and beam phase stability meet the ILC specs.
3. Evaluate effects of cavity gradient spreads, dark current, cryogenic load, radiation levels with beam operation.
4. Measure beam kicks due to couplers, cavity tilt, quad rotations + tilt errors characterize focusing properties of SCRF cavities.
5. Measure vibrations of cavities and quads.
6. Test beam diagnostics.
7. Test ILC crab cavities.
8. Test the ILC installation procedure and tunnel layout.



## AARD plans for NML

---

- Fermilab wants to establish an AARD program at NML
- Requires a flexible beam injector to support various beam parameters (emittance, bunch charge, bunch length)
  - Flexibility requires space
- Requires building extension to provide a users area.
  - Money for extension will not come from the ILC. In fact, the GDE might argue that it will cause delays.
  - Will have to compete for funds against other projects at Fermilab.
  - Must create a convincing story as to why we need to extend the building.

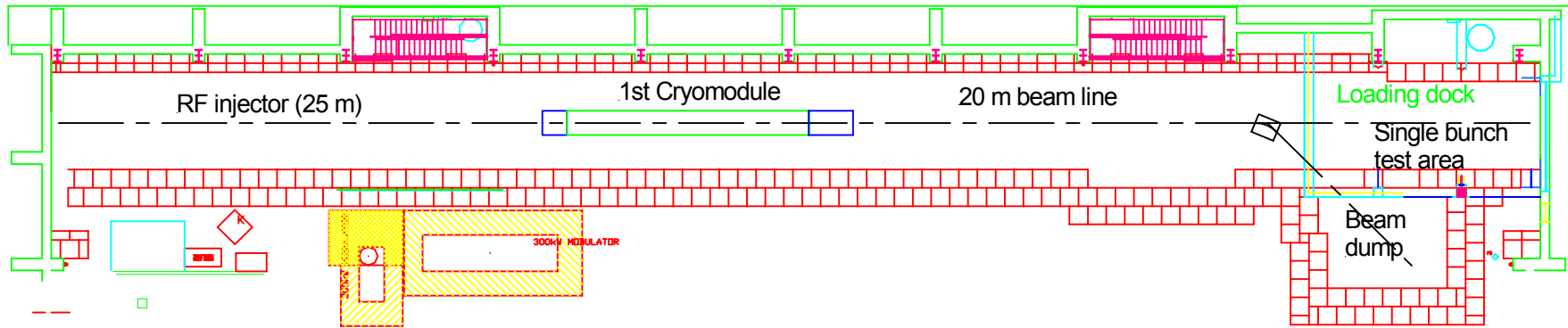
## Cryomodule delivery

---

- 1<sup>st</sup> cryomodule will be delivered to NML in July, 2007
- 2<sup>nd</sup> CM – summer 2008
- 3<sup>rd</sup> CM – Mid FY09

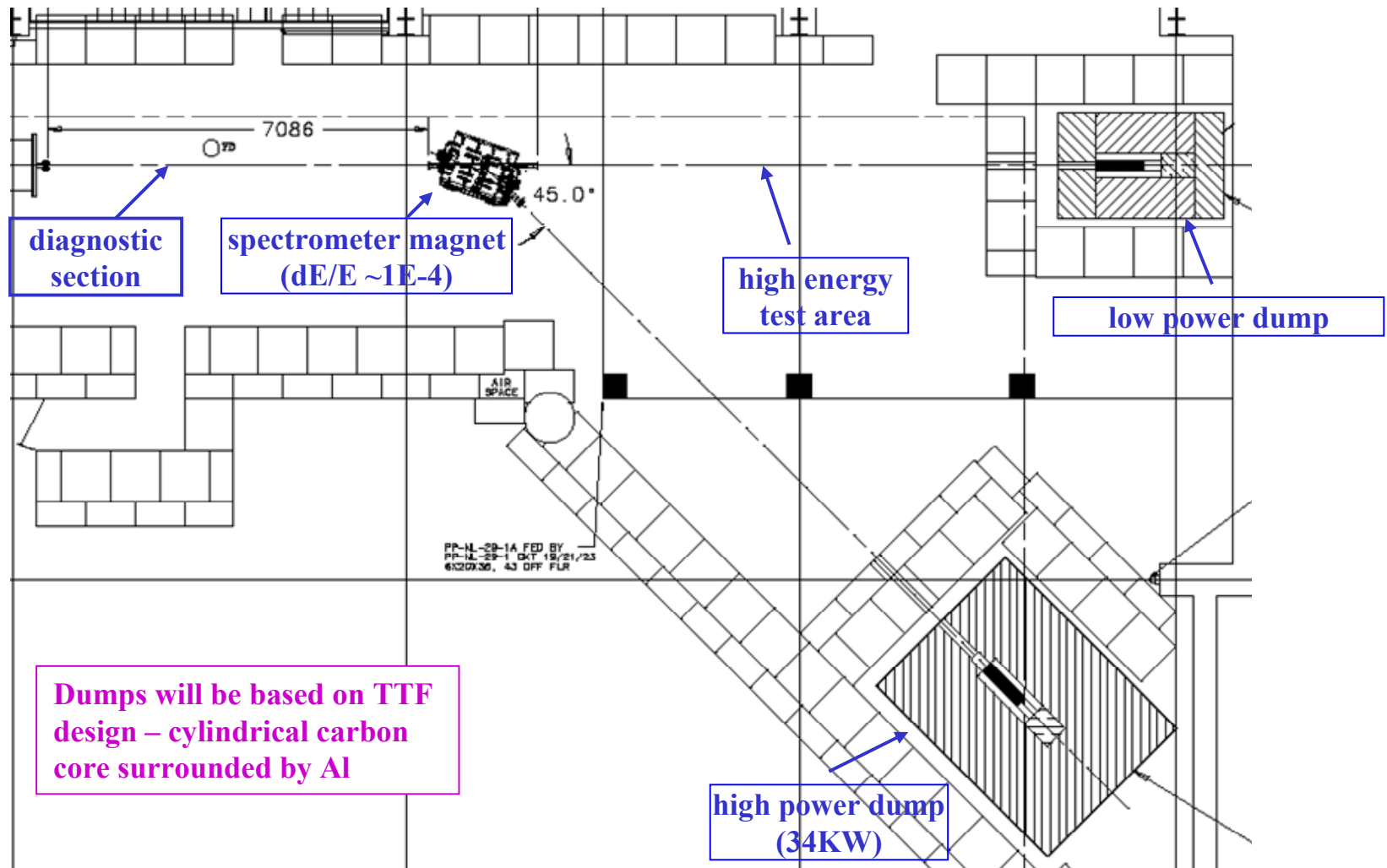


# Stage 1: a single cryomodule with beam

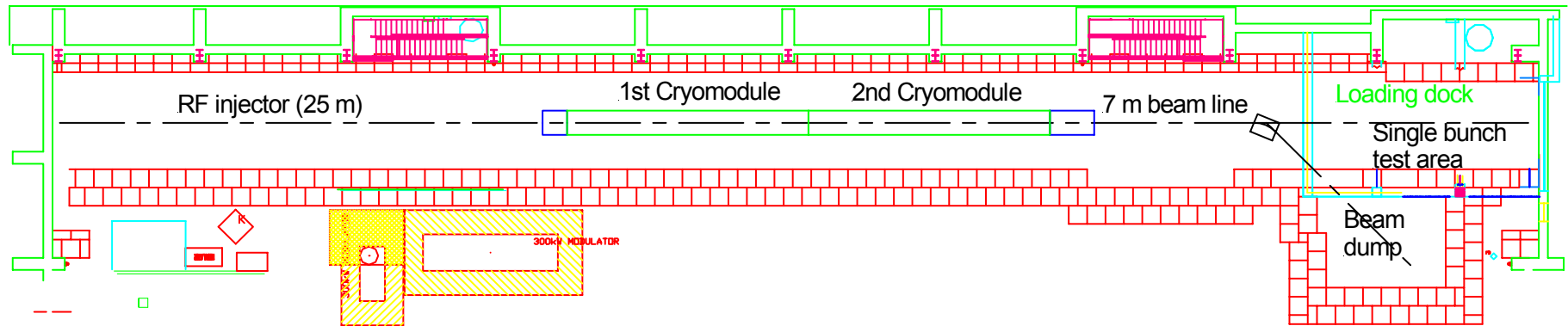


- July, 2007: Cryomodule delivered by TD to NewMuon
- First several months: cryo and rf system integration
- Coupler conditioning
- Injector to supply beam in Apr. 2008

# Experimental beam lines at NML

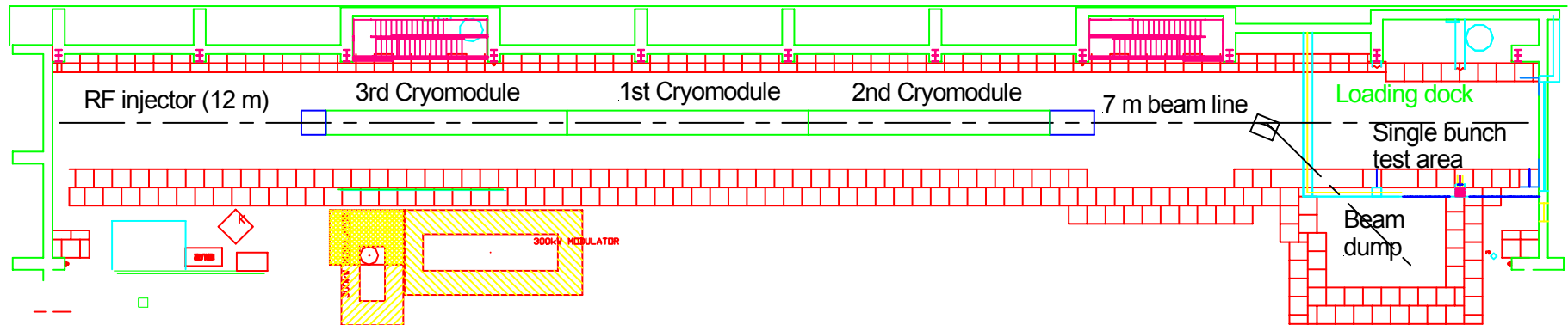


## Stage 2: two cryomodules (summer 2008)



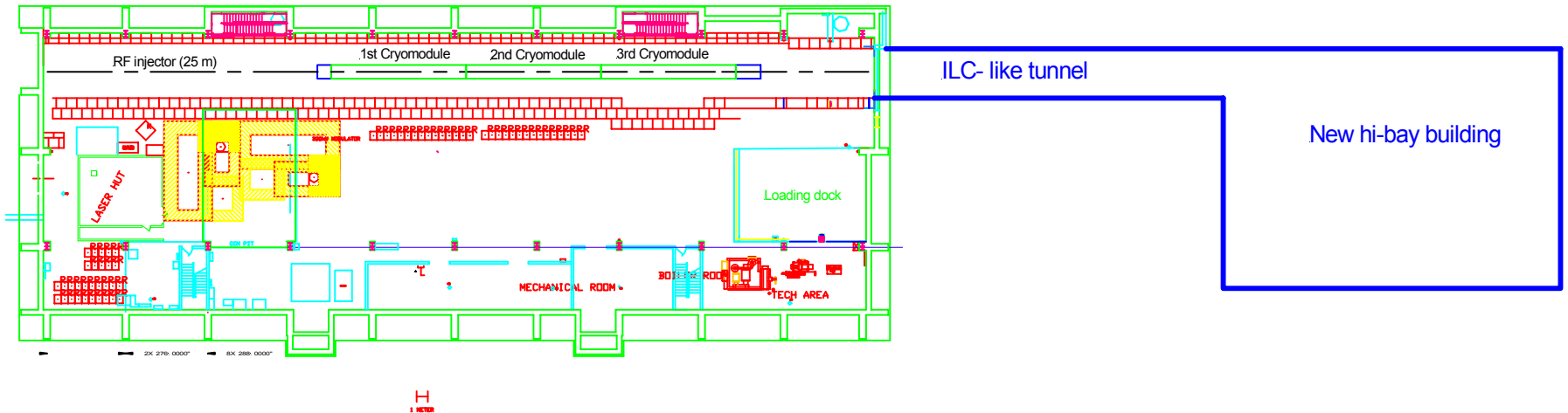
- Mid 2008 - two CM's, 500 MeV, 25 kW beam power

## Stage 3A: three cryomodules (fit everything into NM)



- Mid 2009 - three CM's, 750 MeV, 40 kW beam power
- Minimal injector

## Stage 3B: three cryomodules (Building extension)

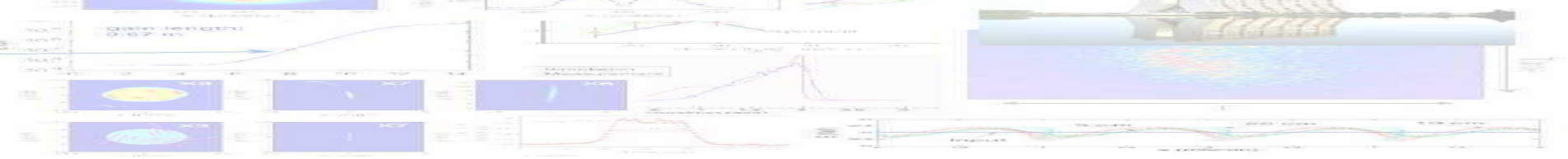


- Mid 2009 - three CM's, 750 MeV, 40 kW beam power
- Flexible injector
- ILC-like tunnel, space for 3 more cryomodules

## This workshop:

---

- We are seeking your advice on
  - what possible advanced accelerator R&D activities could be pursued at this facility;
  - what infrastructure is needed to successfully carry these activities.

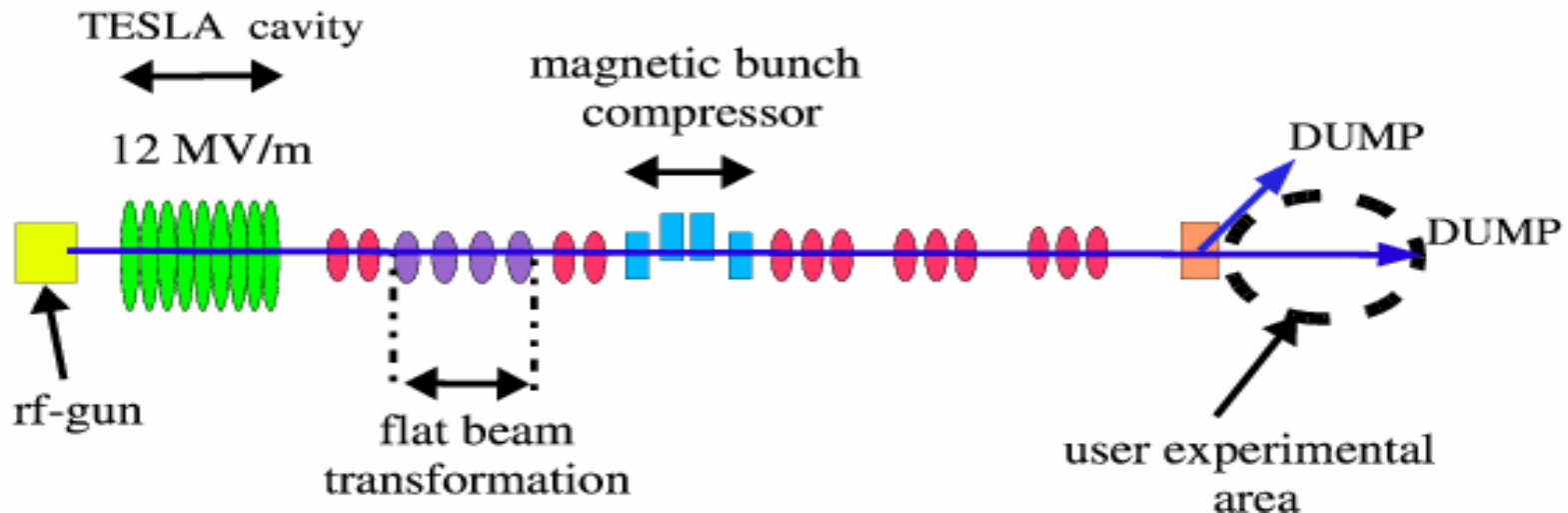


# *Anticipated beam parameters for the ILC test accelerator (NML)*

*Philippe Piot*

## *Introduction: FNAL experience with AARD*

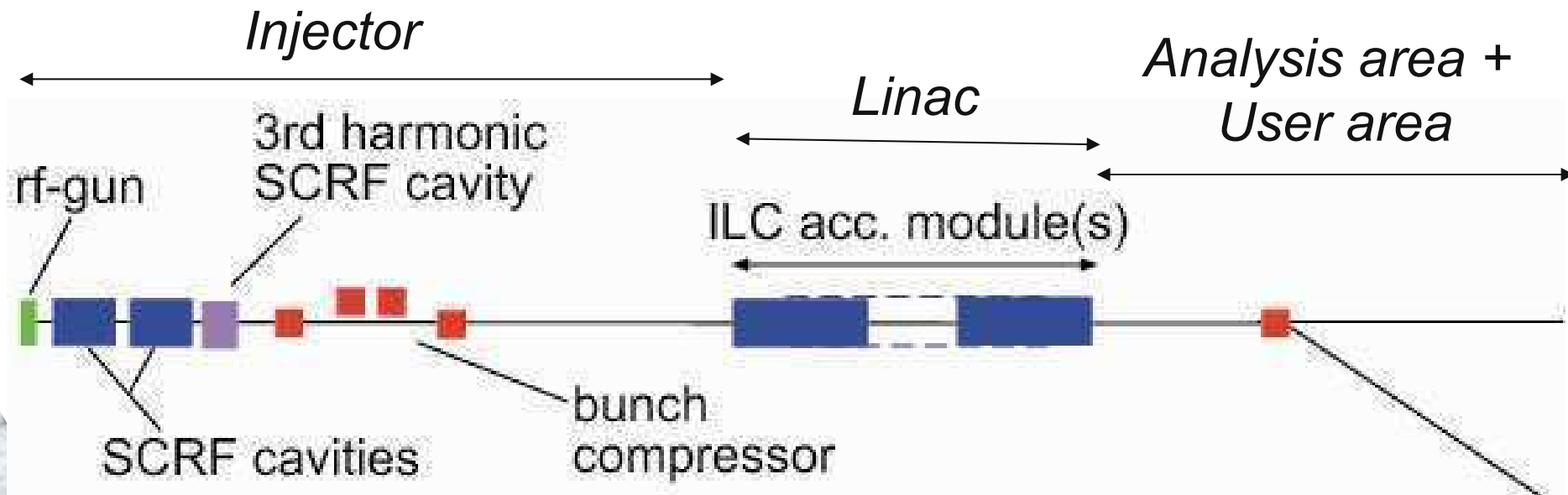
- **beam dynamics:** optimization of high brightness beam emittance,
- **Phase space manipulations:** bunch compression, flat beam, and transverse-to-longitudinal emittance exchange
- **Novel beam acceleration R&D:** PWFA, laser-based.
- **R&D on beam diagnostics**



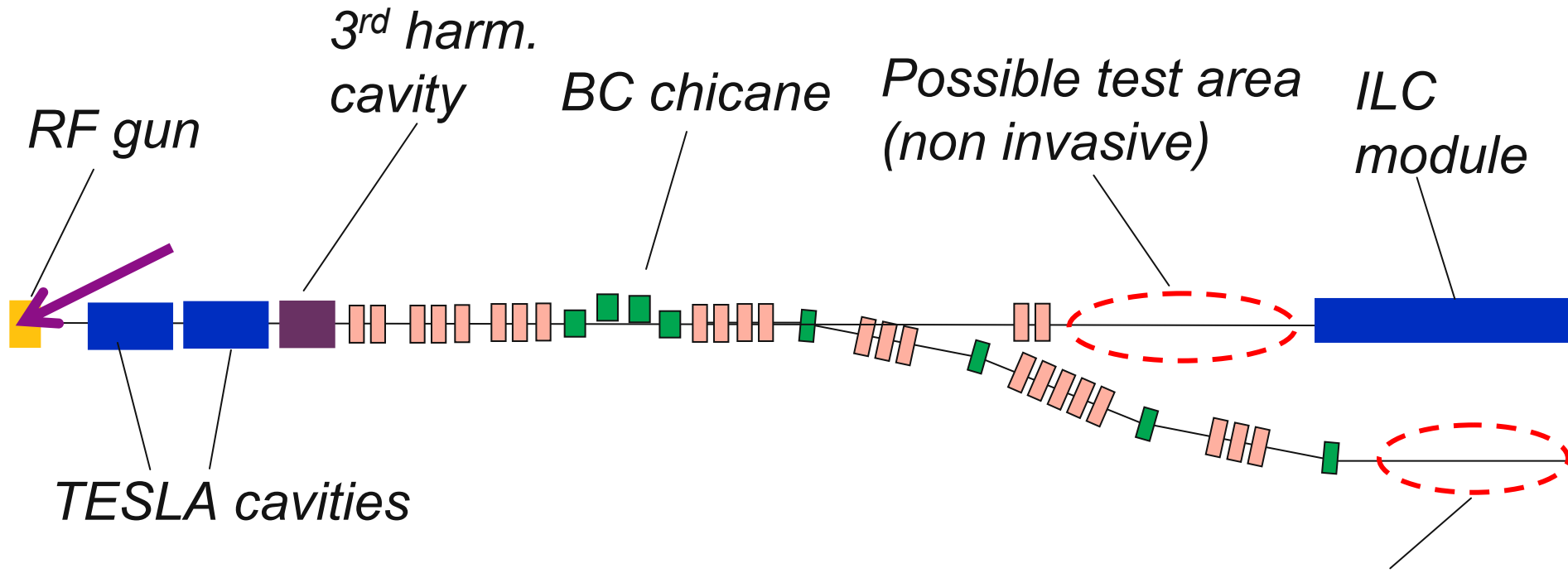


# Introduction

- Need to upgrade/extend A0
- Need a facility with beam to test and develop subsystem associated to ILC proposal
- Use the upgraded version of A0 as an injector for the ILC test accelerator (NML)



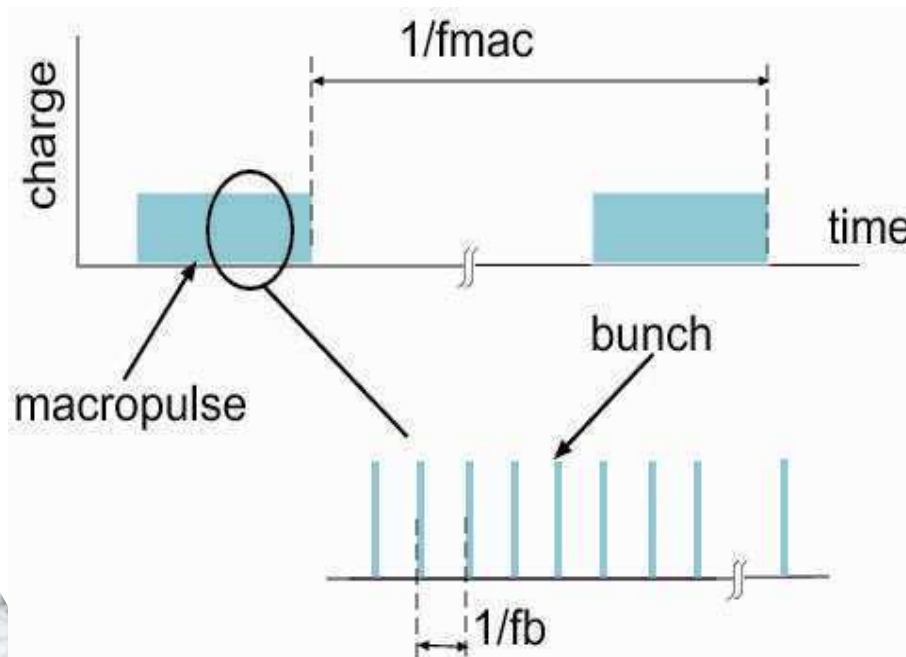
# Injector (Fall 2006 version)



- Rf-gun
- 40-50 MeV injector
- Bunch compressor chicane
- Off-axis beam line (dogleg w tunable R56)

# *Pulse format*

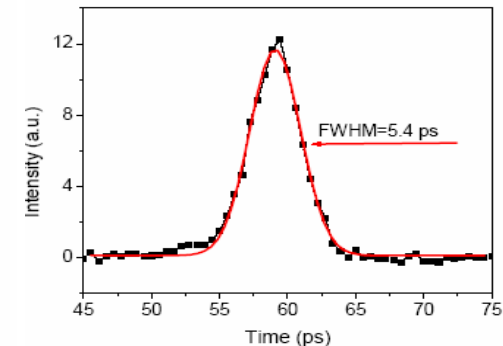
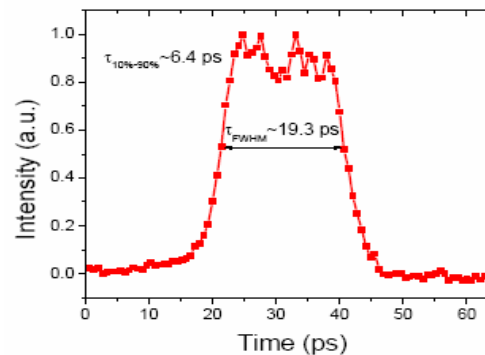
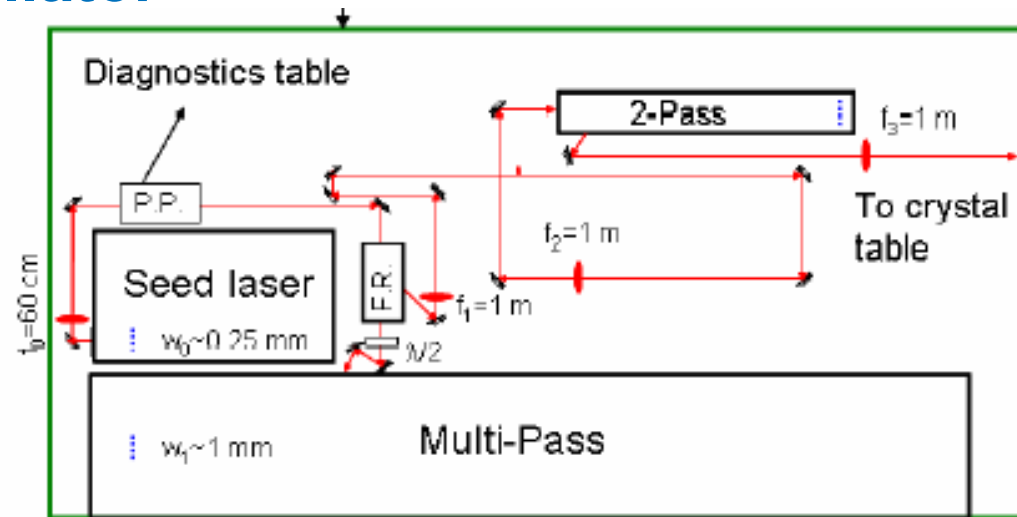
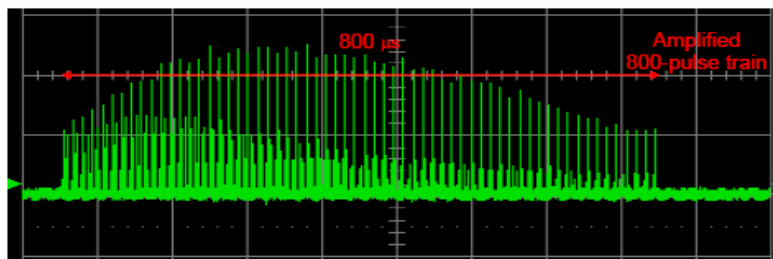
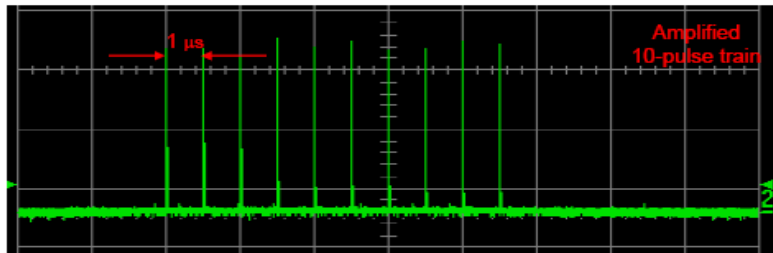
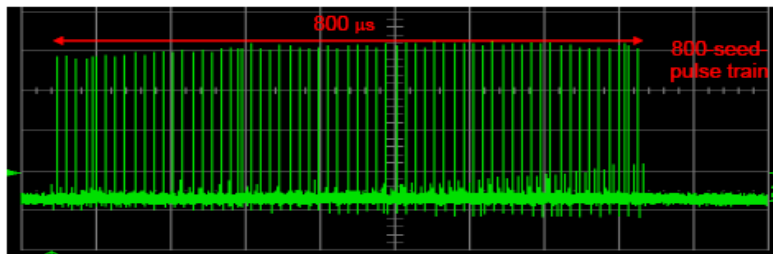
- NML is based on a superconducting linear accelerator
  - long pulse train can be generated
  - control system allow flexibility (e.g. energy ramp along a macropulse, etc...)



- $Q = 3.2$  (0 to 20) nC
- $f_{mac} = 5$  (1 to 5) Hz
- $f_b = 3$  (1 to 3) MHz
- $N_b = 2850$  (1 to 3000)

# Photocathode drive laser

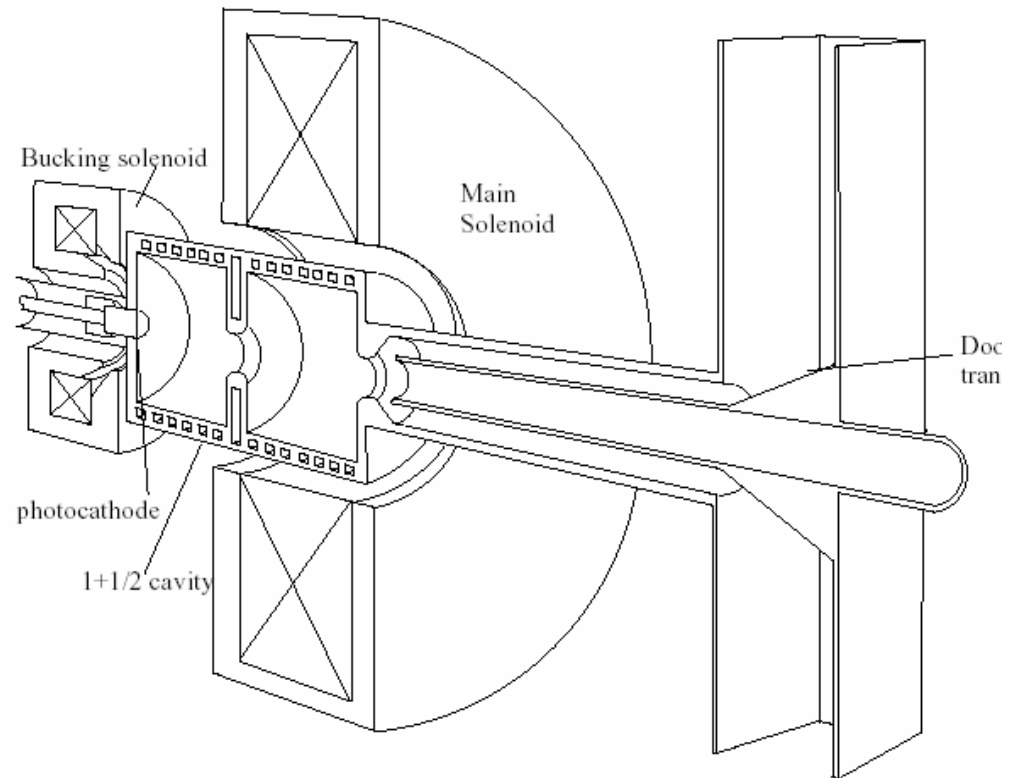
- laser is an upgrade of the laser presently in operation at A0 based on a YLF oscillator



J. Li and R. Tikhoplav (U. of Rochester)

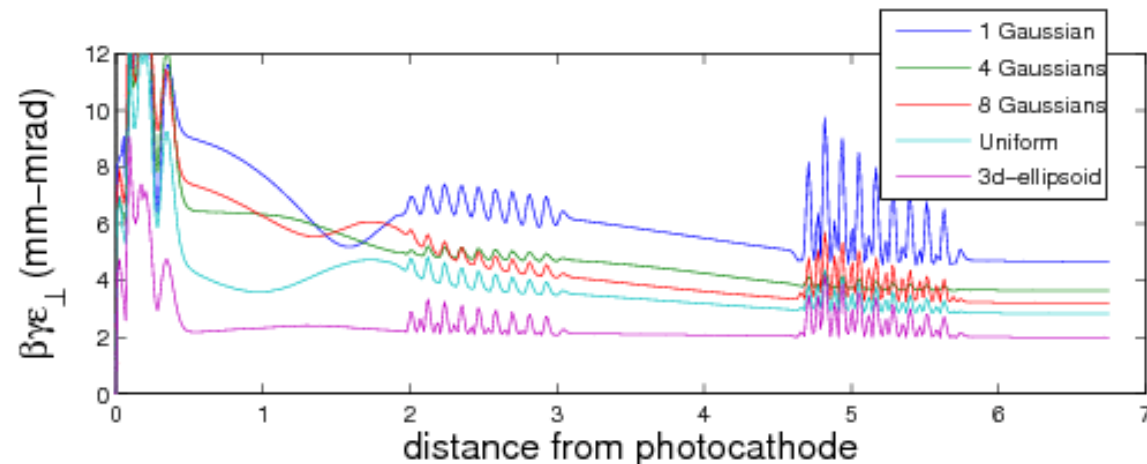
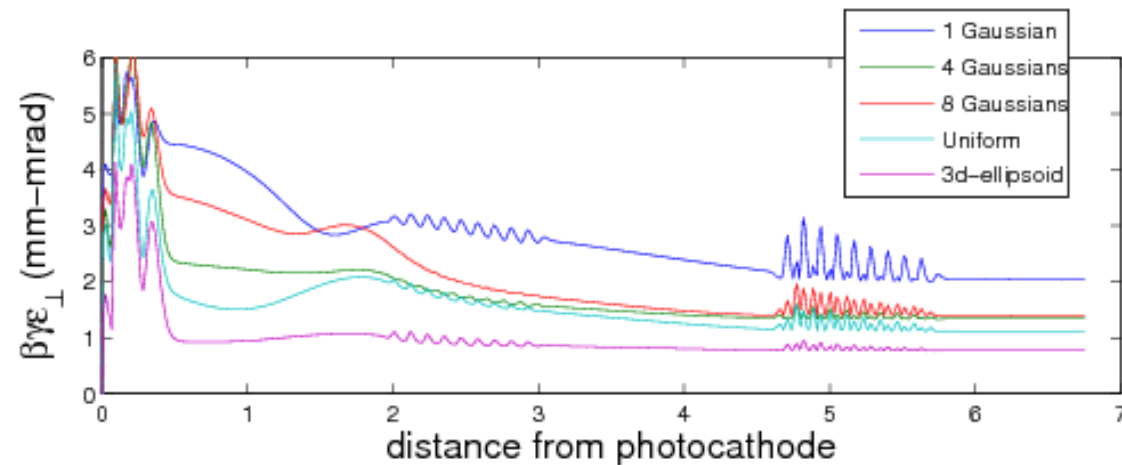
# *RF-gun + Photocathode*

- Copy of the rf-gun currently in use at DESY in **Free electron LASer Source in Hamburg (FLASH)** facility
- Cylindrical-symmetric
- CsTe photocathode can produce up to 20 nC bunches (from A0 experience)



# Injector performances

- Emittance optimized for  $Q=1$  and 3.2 nC
- Compromise in injector design to accommodate various possible laser distribution
- Depending on laser configuration e-longitudinal phase space get distorted



# Bunch compression

- “Long” bunch length results in a nonlinear distortion of the longitudinal phase space

$$\delta_i = \kappa z_i + \mu z_i^2 + O(z_i^3)$$

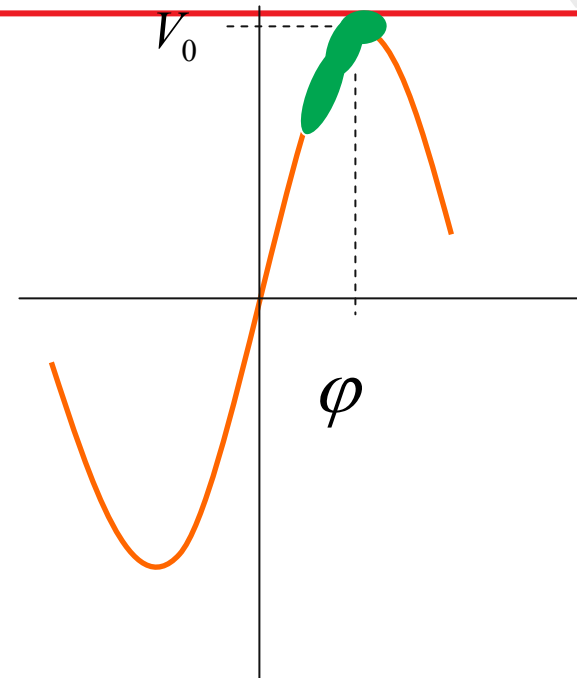
- Downstream of a bunch compressor

$$z_f = z_i + R_{56} \delta_i + T_{566} \delta_i^2$$

- So we want perfect compression i.e.

$$0 = z_i (1 + \kappa R_{56}) + z_i^2 (\mu R_{56} + \kappa^2 T_{566})$$

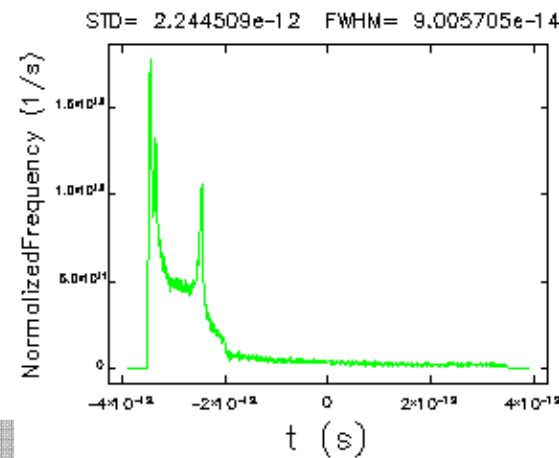
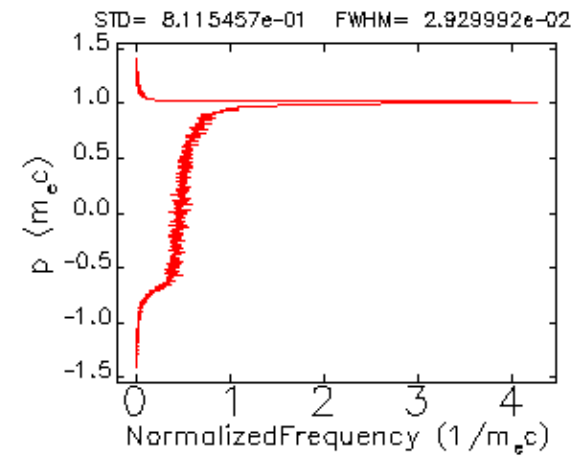
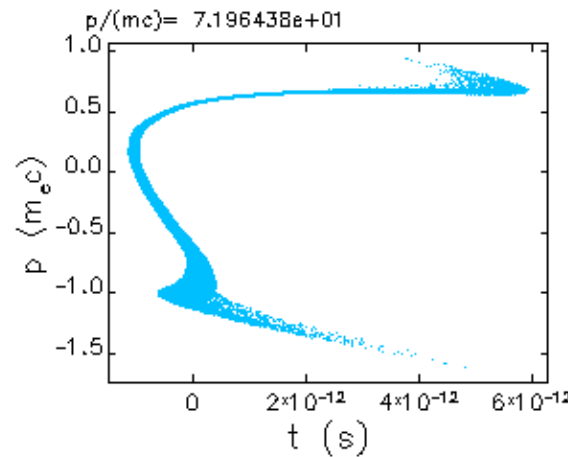
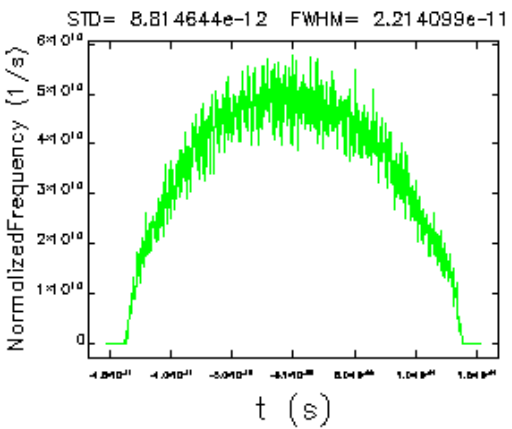
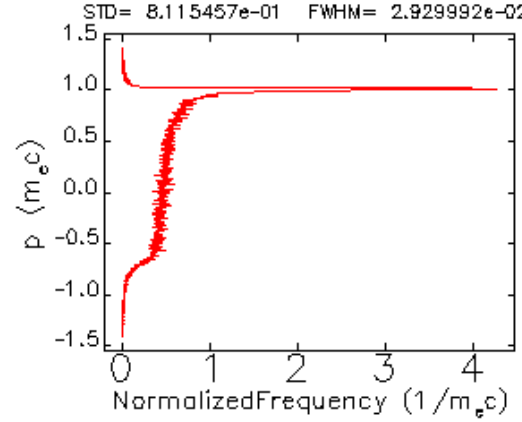
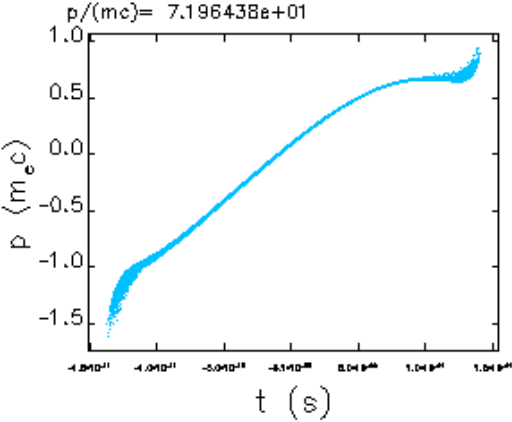
- We plan on using a higher order harmonic accelerating cavity to “linearize” the phase space.



$$\sigma_{z,f} = \sqrt{(1 + \kappa R_{56})^2 \sigma_{z,i}^2 + R_{56}^2 \sigma_{\delta,i}^2 E_0^2 / E^2}, \sigma_{\delta,f} = \sqrt{\kappa^2 \sigma_{z,i}^2 + \sigma_{\delta,i}^2 E_0^2 / E^2}$$

# Bunch compression

## Linearizer OFF

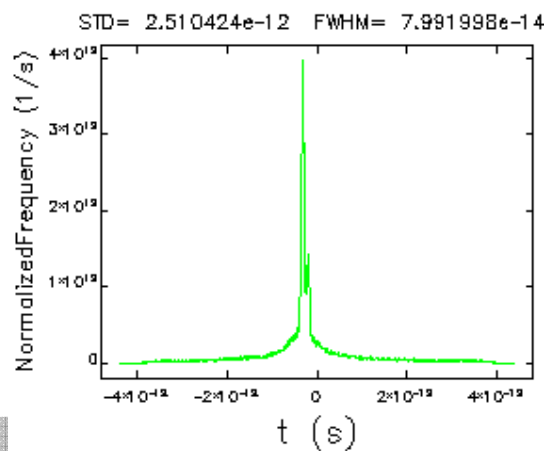
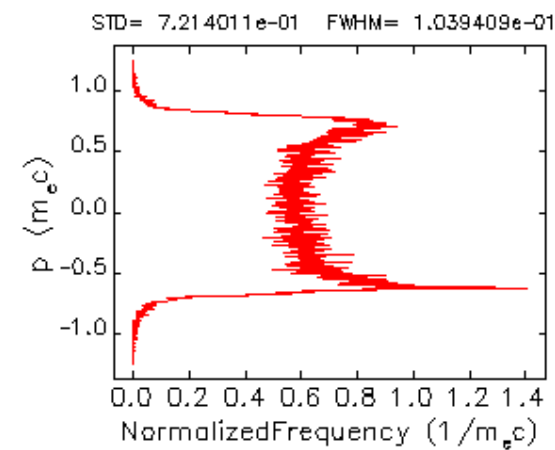
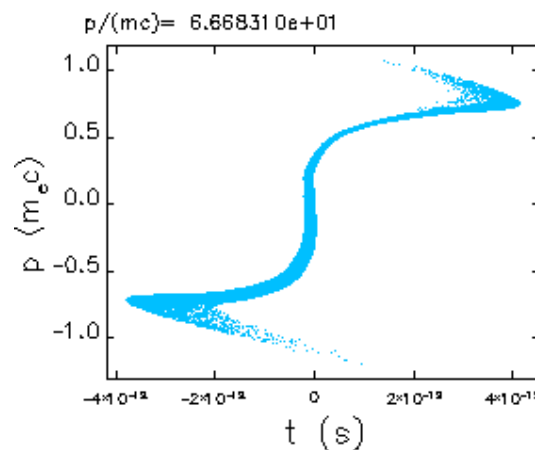
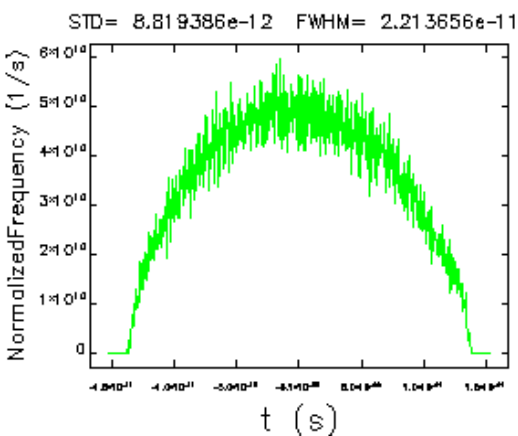
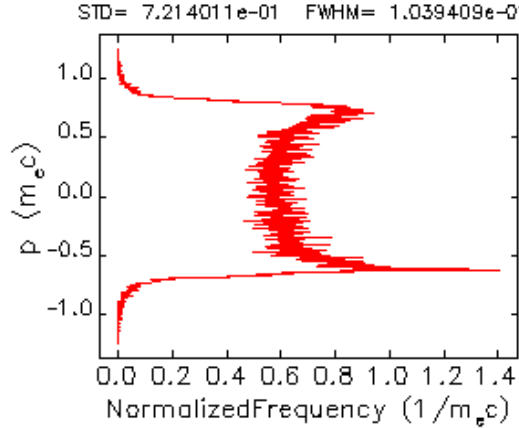
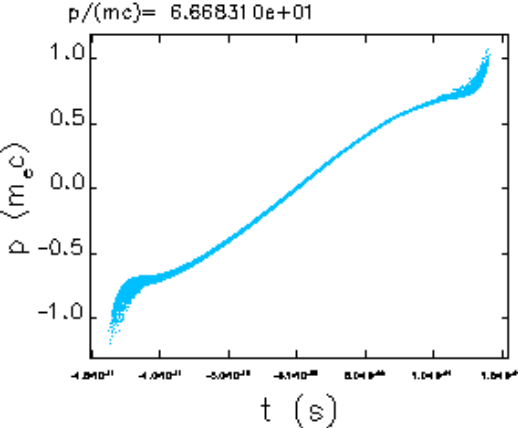


Before compressor

After compressor



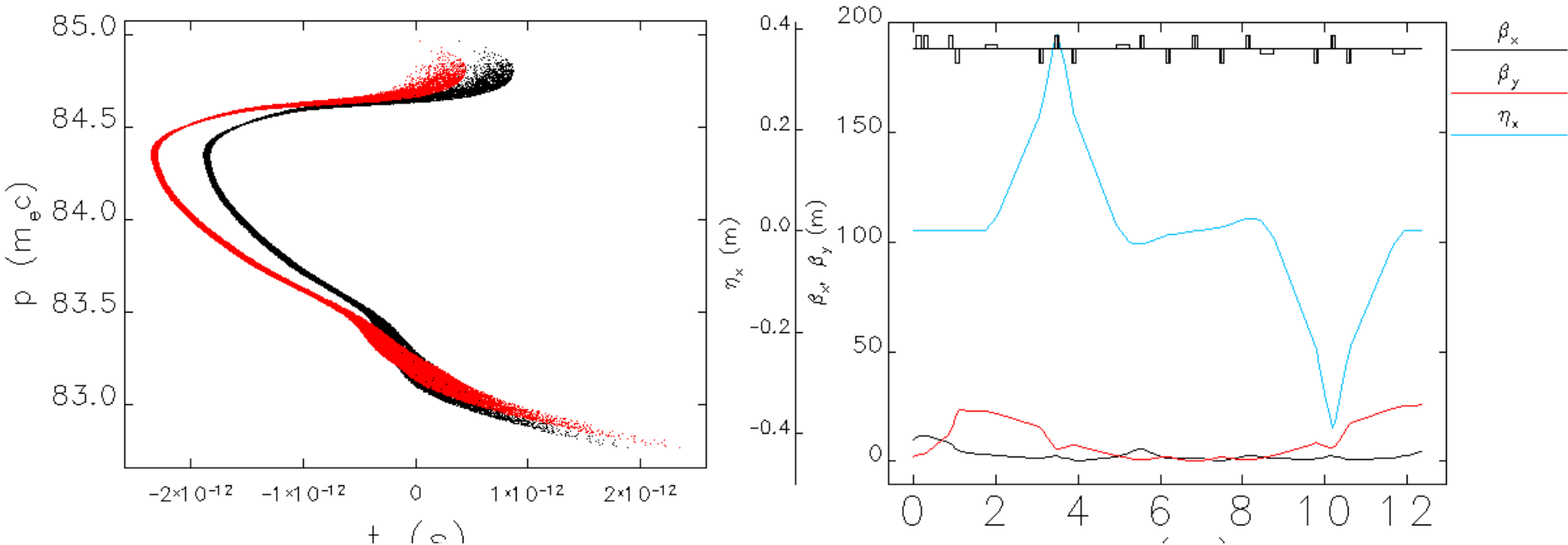
# Bunch compression Linearizer ON



Before compressor

After compressor

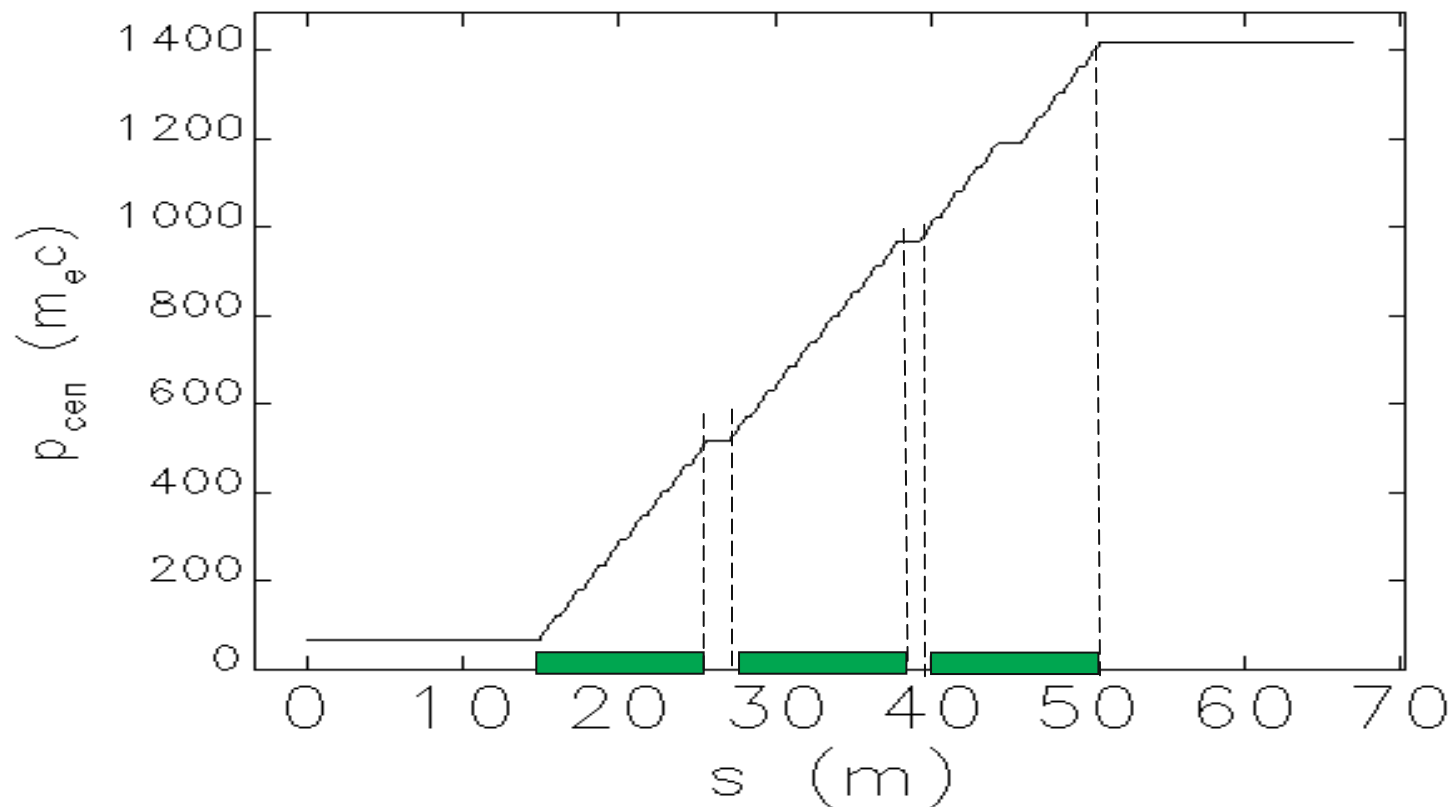
# Off axis 40 MeV beamline (Isochronous mode)



- Emittance increase is tolerable
- longitudinal phase space still distorted but this is tolerable for bunch length diagnostics tests
- Plan to initially install deflecting mode cavity (to streak the beam)

# Acceleration in the linac

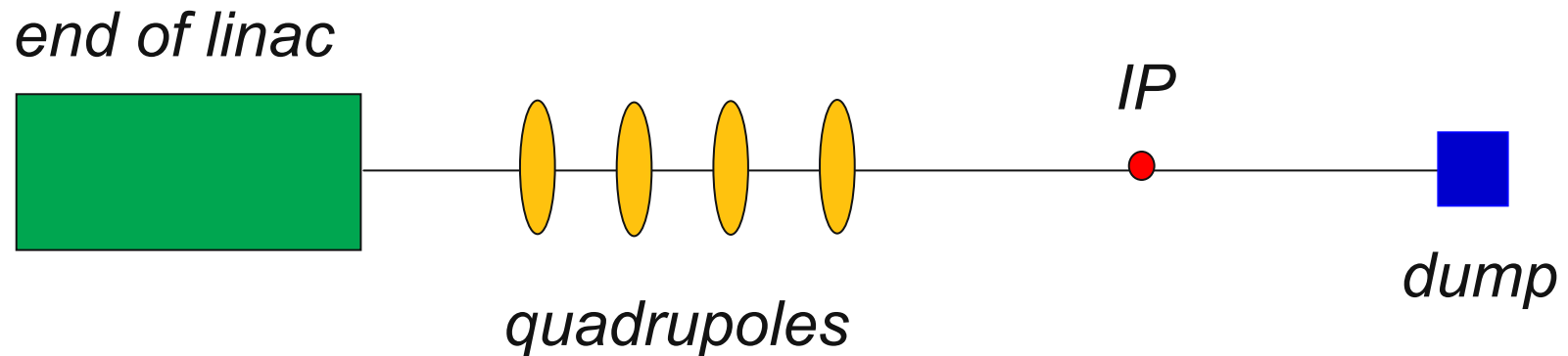
- Beam envelope along the accelerator (example of 3.2 nC)



centroid output--input: ilcta\_all.ele lattice: ilcta.lte

## *Final beam at IP*

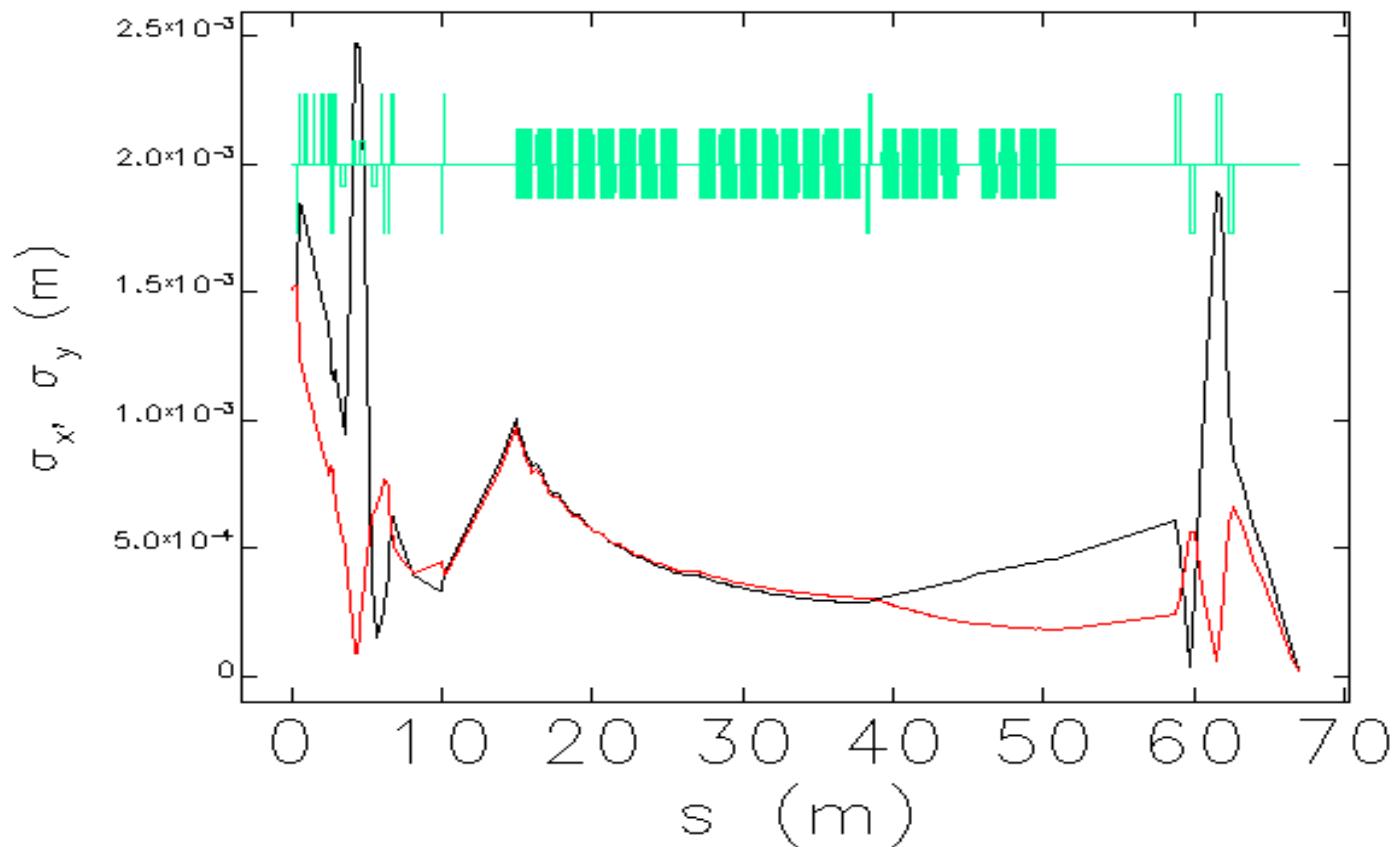
- IP is made up with quadrupoles
- Arbitrarily target  $\beta$ -functions of 0.1 m
- No chromatic corrections (so some emittance growth in some cases)



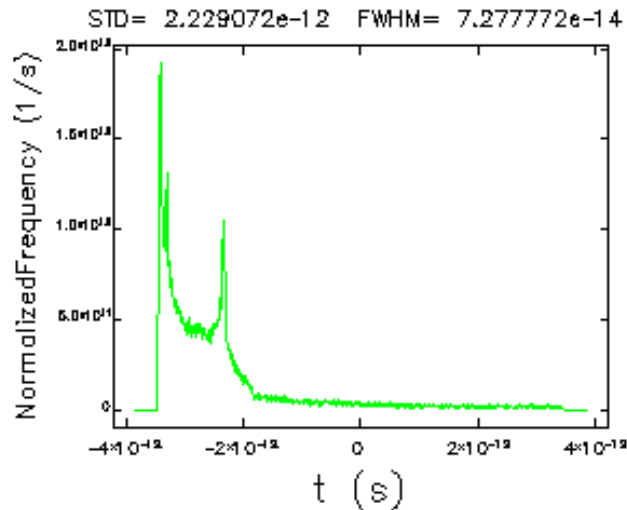
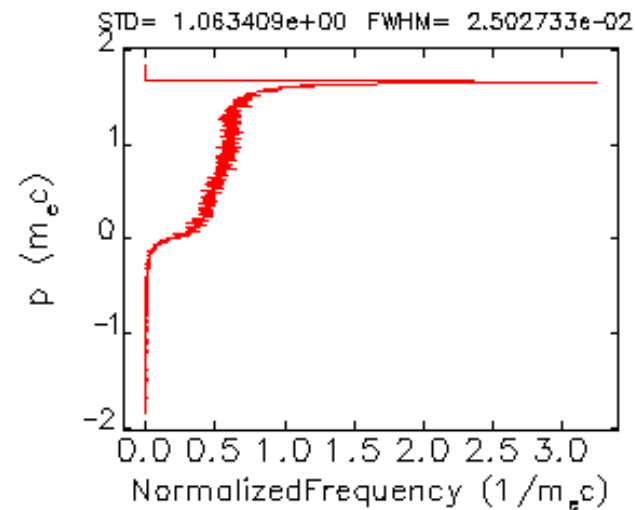
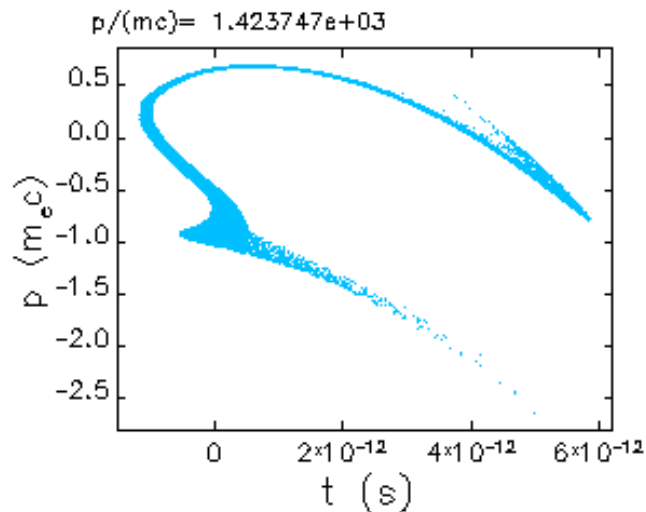
- *Is straight ahead dump what people really want?*

## *Final beam at IP*

- Beam envelope along the accelerator (example of 3.2 nC)

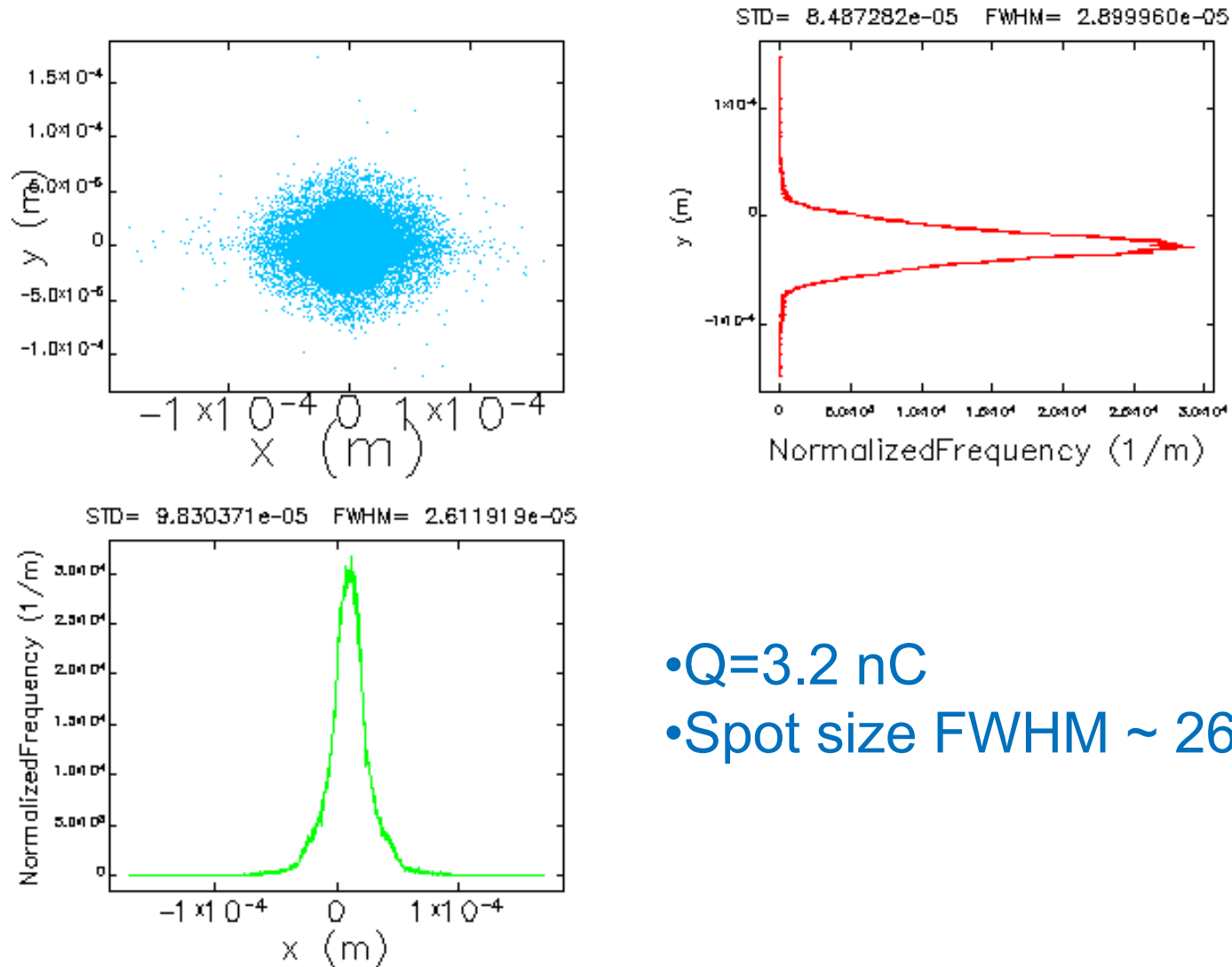


# Longitudinal phase space at IP (no linearization)



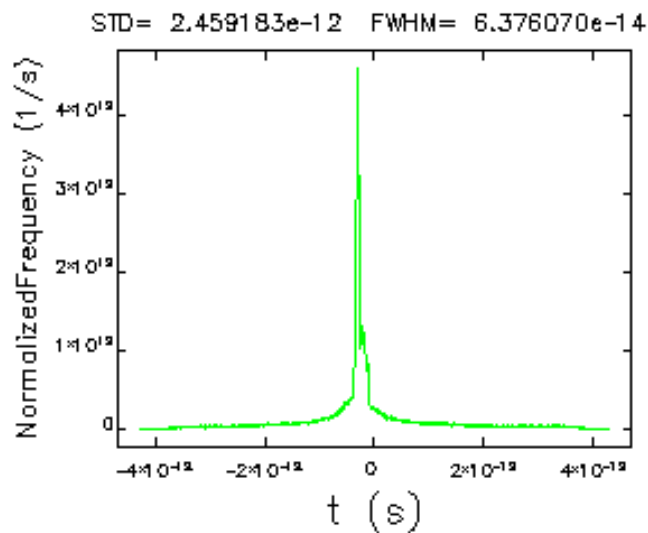
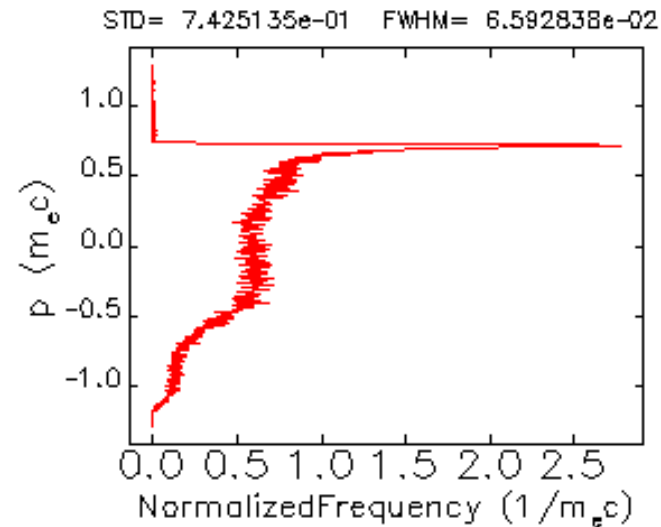
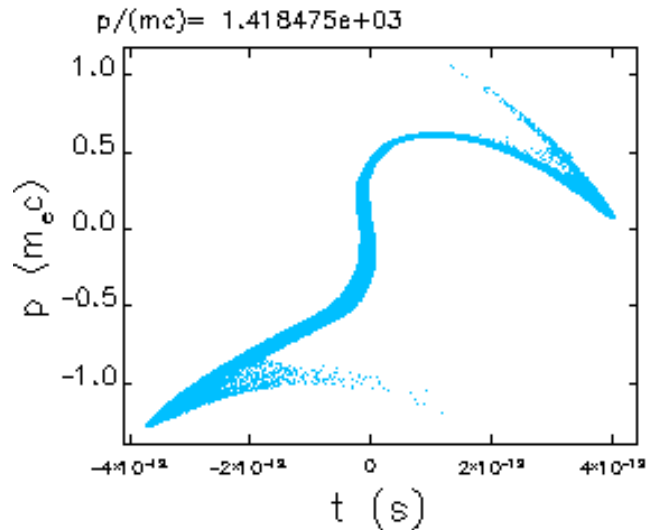
- $Q = 3.2$  nC
  - $I_{peak} = 1800 \times 3.2 = 5.8$  kA
- (Space charge + wakefield not included at high energy)

# *Longitudinal phase space at IP (no linearization)*



- $Q=3.2$  nC
- Spot size FWHM  $\sim 26\text{-}28\ \mu\text{m}$

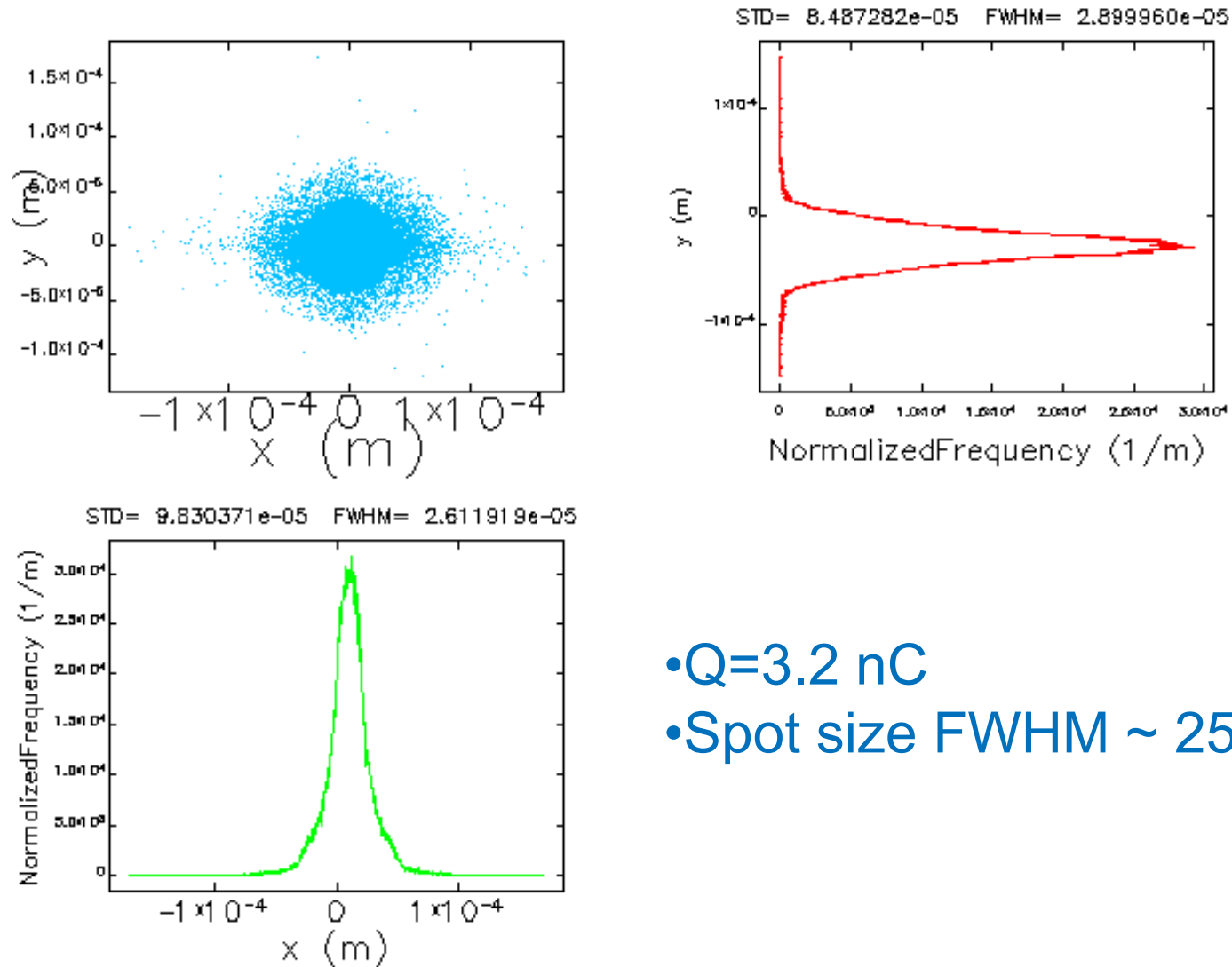
# Longitudinal phase space at IP (linearization)



- $Q=3.2$  nC
- $I_{peak}=4500 \times 3.2=14.4$  kA  
(Space charge + wakefield not included at high energy)



# Longitudinal phase space at IP (linearization)



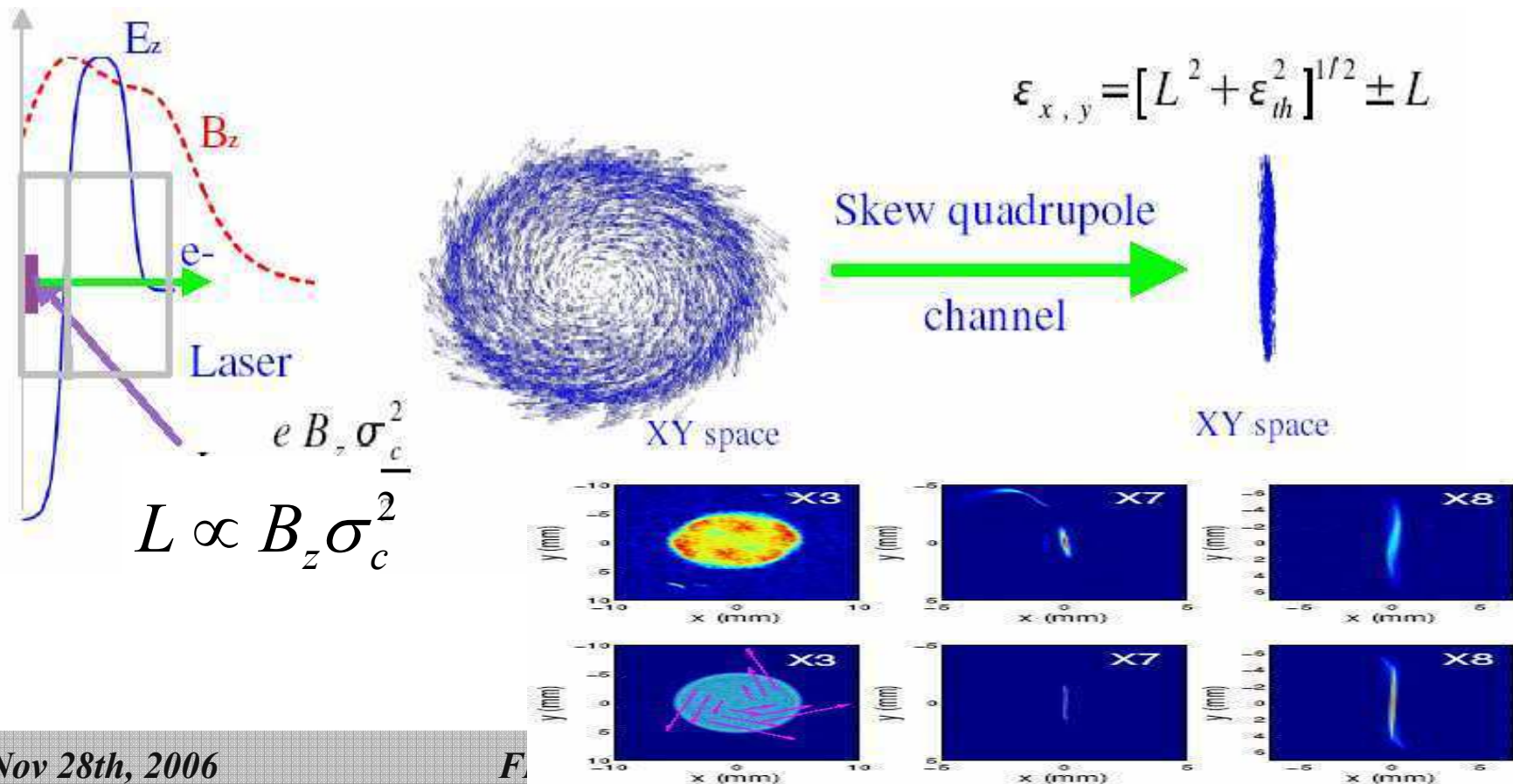
- $Q=3.2$  nC
- Spot size FWHM  $\sim 25\text{-}30 \mu\text{m}$

## *Summary of expected parameter for $Q=3.2 \text{ nC}$*

| Parameter                                   | Phase 1        | Phase 2        | Phase 3        | Units         |
|---------------------------------------------|----------------|----------------|----------------|---------------|
| maximum total energy                        | 280            | 520            | 700            | MeV           |
| rms transverse normalized emittance (round) | 4-5            | 4-5            | 4-5            | $\mu\text{m}$ |
| rms beam sizes (round)                      | 20             | 14             | 12             | $\mu\text{m}$ |
| rms transverse normalized emittance (flat)  | $\sim 0.5, 50$ | $\sim 0.5, 50$ | $\sim 0.5, 50$ | $\mu\text{m}$ |
| rms beam sizes (flat)                       | $\sim 7, 60$   | $\sim 5, 42$   | $\sim 4, 36$   | $\mu\text{m}$ |
| Peak current                                | $< 5$          | $< 5$          | $< 5$          | kA            |
| Peak current (w. linearizer)                | $10 < I < 15$  | $10 < I < 15$  | $10 < I < 15$  | kA            |

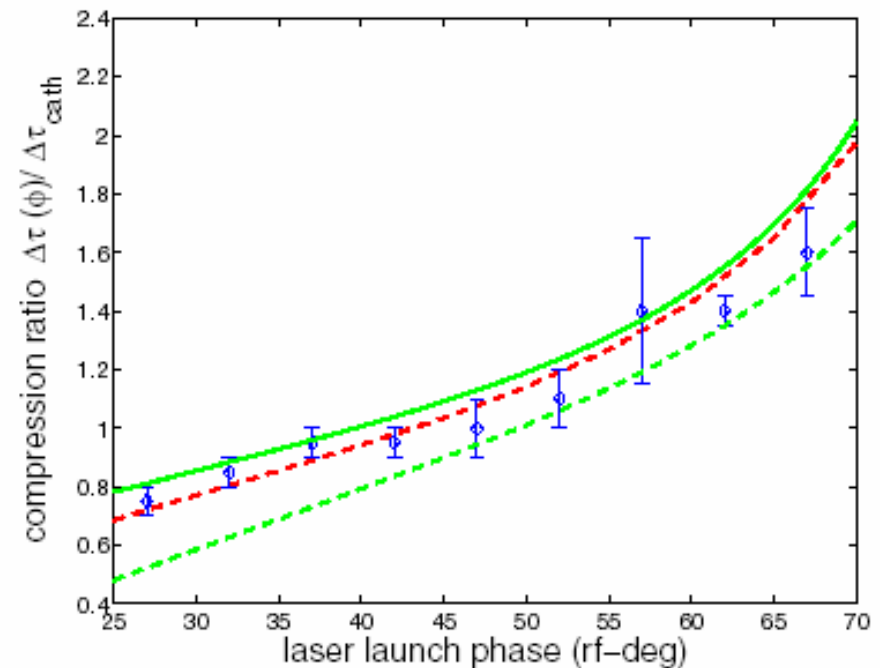
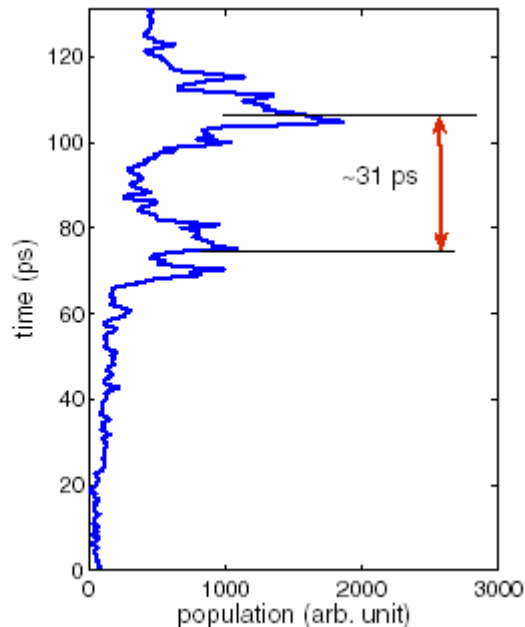
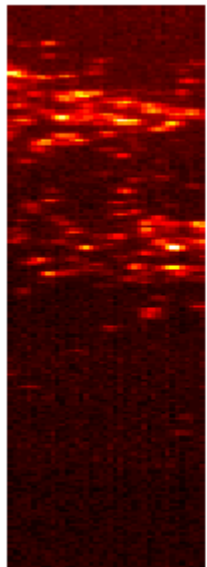
## *Other possibilities: Flat beam generation*

- Manipulations in **two-degree-of-freedom** to generate flat beam is incorporated in the design
- A0 generated flat beam w emittance ratio of  $100=40/0.4$



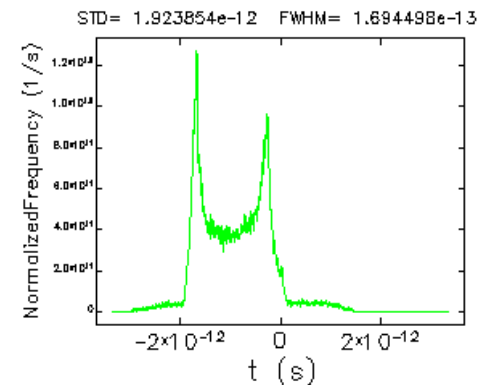
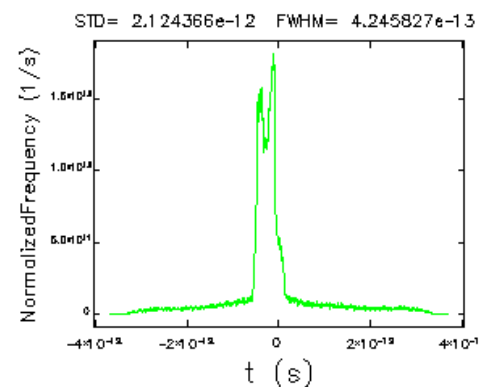
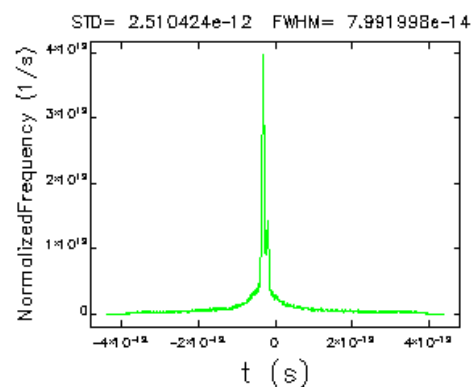
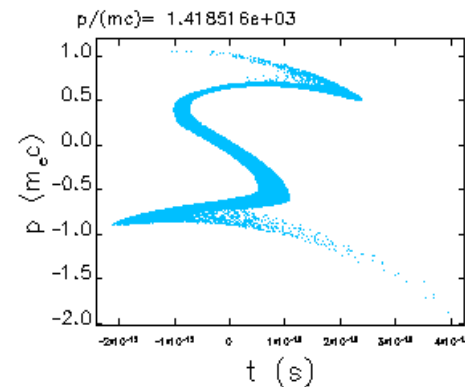
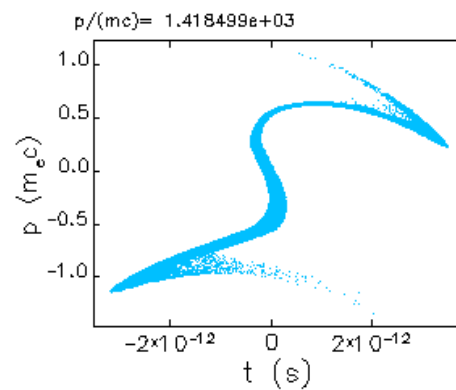
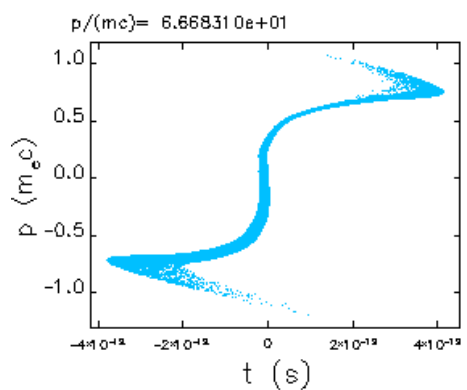
## Other possibilities: “Pump-probe” electron beams

- Can generate a “two macroparticle” bunches done at A0 (initially developed for PWFA experiment)
- Later use to study longitudinal focusing effect in rf-gun and cavity



# Other possibilities: Tailoring the bunch shape

- e- bunch shape can be tailored (within some limit) by fine tuning the compression settings



## *Summary*

- NML can generate promising parameters (peak current transverse spot size) to support exciting advanced accelerator R&D program
- Optimization and beam dynamics studies still on-going,
  - space-charge, wakefield and other collective effects need to be included all the way,
  - Optimization for other charges (e.g. 1, 10 nC) need to be performed.
- Would be nice to have a set of requirement for what potential user would like for beam parameter at the IP



*... for a brighter future*

# *Phase Space Manipulation*

**Kwang-Je Kim**

**AAI, Argonne**

*Possible Directions for AA R&D at  
the ILCTA at Fermilab*

**November 28, 2006**

**Fermilab**



U.S. Department  
of Energy

UChicago ►  
Argonne<sub>LLC</sub>



**Office of  
Science**

U.S. DEPARTMENT OF ENERGY

A U.S. Department of Energy laboratory  
managed by UChicago Argonne, LLC

# Why Phase Space Manipulation?

## ■ To improve x-ray FEL performance

- *Emittance Exchange*: Reduce transverse emittance in each dimensions by 10 at the expense of longitudinal emittance increase by 100
- *Conditioning*: Produce a correlation in energy-betatron amplitude

## ■ To obviate electron damping rings in a linear collider

- Produce damping ring like beams directly from a gun-manipulation system

## ■ Improve the performance of a Terahertz Smith-Purcell FEL



# SASE FEL for 30 keV



## ■ LCLS reference parameters:

$\lambda = 8 \text{ keV}$ ,  $\lambda_u = 3 \text{ cm}$ ,  $K = 3.7$ ,  $I_p = 3.5 \text{ kA}$ ,  $E_e = 15 \text{ GeV}$ ,  
 $\Delta E/E = 10^{-4}$ ,  $\varepsilon_n = 1.2 \text{ mm-mrad}$ ,  $L_{\text{sat}} = 100 \text{ m}$

## ■ Vary $K$ , $\varepsilon_n$ , and $E_e$

| $K$ | $E_e$<br>(GeV) | $\varepsilon_n$<br>(mm-mrad) | $L_{\text{sat}}$<br>(m) |
|-----|----------------|------------------------------|-------------------------|
| 3.7 | 30             | 1.2                          | 300                     |
| 3.7 | 30             | 0.5                          | 130                     |
| 3.7 | 30             | 0.1                          | 40                      |
| 1   | 12             | 0.1                          | 60                      |

**shorter undulator**

← **shorter undulator**  
← **and shorter linac**

## ■ *It pays to strive for an ultralow emittance e-beam*

# *Emittance Exchange for X-ray FEL*

## ■ RF Photocathode Gun

- Transverse emittance  $\varepsilon_n \sim 1 \times 10^{-6} \text{ m}$
- Energy spread very small

$$\sigma_{\Delta E} \sim 1.5 \text{ keV}$$

$$\sigma_{\Delta E/E} = \frac{\sigma_{\Delta E}}{E} = 10^{-7} @ \quad E \sim 15 \text{ GeV}$$

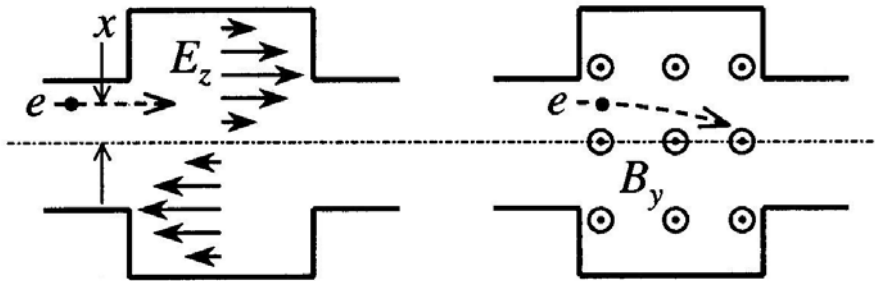
## ■ FEL requires $\sigma_{\Delta E/E} < 10^{-4}$ , $\varepsilon_n \sim 1 \times 10^{-6} \text{ m}$

## ■ Can we do the transformation?

$$(\gamma\varepsilon_x, \gamma\varepsilon_y, \sigma_{\Delta E/E}) = (10^{-6} \text{ m}, 10^{-6} \text{ m}, 10^{-7}) \rightarrow (10^{-7} \text{ m}, 10^{-7} \text{ m}, 10^{-5})$$

# Optical Building Blocks for the Exchange

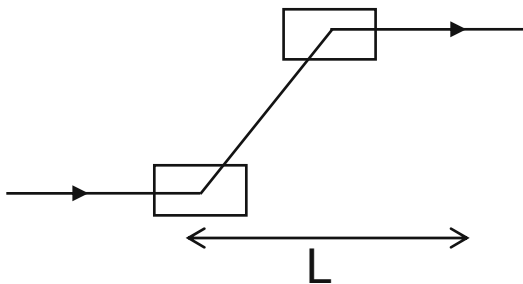
## ■ Dipole mode cavity:



$$\Delta\delta = kx, \Delta x' = kz; k = eV_o/eE$$

$$M_C(k) = \begin{bmatrix} 1 & 0 & 0 & 0 \\ 0 & 1 & k & 0 \\ 0 & 0 & 1 & 0 \\ k & 0 & 0 & 1 \end{bmatrix}$$

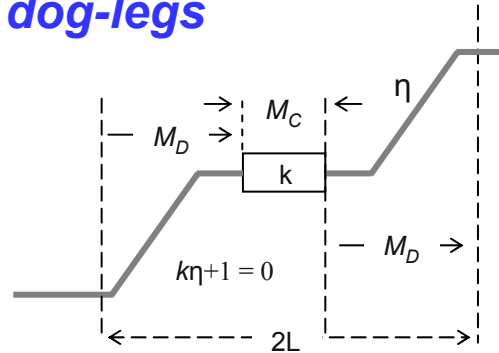
## ■ Dog leg



$$M_D(\eta, \xi, L) = \begin{bmatrix} 1, & L, & 0, & +\eta \\ 0 & 1 & 0 & 0 \\ 0 & \eta & 1 & \xi \\ 0 & 0 & 0 & 1 \end{bmatrix}$$

# An Exact Exchange Optics

## ■ Transverse cavity between two dog-legs



## ■ Choose $k\eta = -1$

## ■ Then transfer matrix becomes:

$$M = \begin{bmatrix} 0 & B \\ C & 0 \end{bmatrix}$$

## ■ The beam matrix:

$$\begin{bmatrix} \Sigma_x & 0 \\ 0 & \Sigma_z \end{bmatrix} \rightarrow \begin{bmatrix} B\Sigma_z\tilde{B} & 0 \\ 0 & C\Sigma_x\tilde{C} \end{bmatrix}$$

## ■ Please someone explain to me why this works but not the Cornnachie-Emma scheme of reverse dogleg!!

# Exchange Alone Does Not Work

- For a symplectic transport from an uncoupled to another uncoupled system, the exchange is wholesome:

$$(\varepsilon_a, \varepsilon_b) \rightarrow (\varepsilon_a, \varepsilon_b) \text{ or } (\varepsilon_b, \varepsilon_a)$$

*but not, for example,  $(0.1\varepsilon_b, 10\varepsilon_a)$*

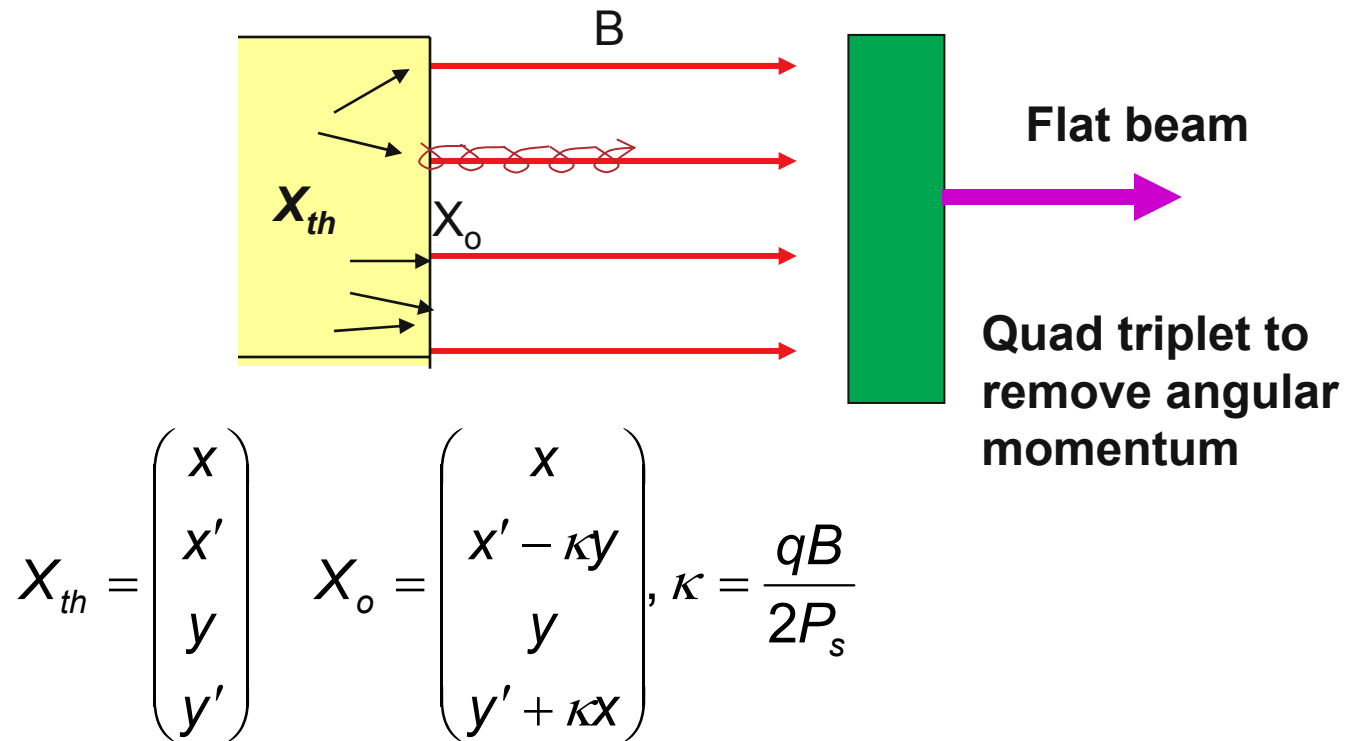
- We need another, non symplectic, step to do

$$(\gamma\varepsilon_x, \gamma\varepsilon_y, \sigma_{\Delta E/E}) = (10^{-6}m, 10^{-6}m, 10^{-7}) \rightarrow (10^{-7}m, 10^{-7}m, 10^{-5})$$

- The flat beam technique is the required step

# Flat Beam Generation

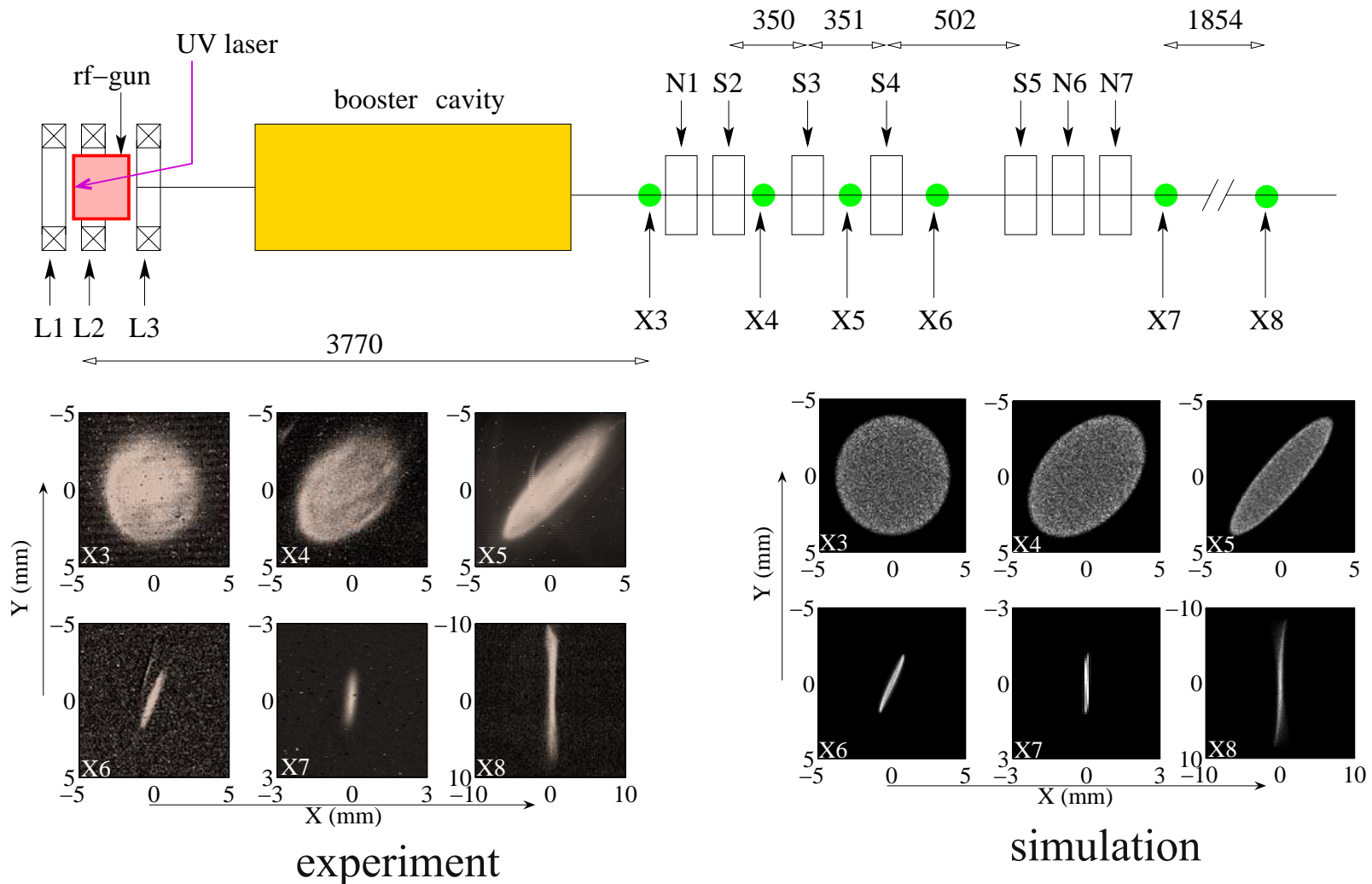
(Y. Derbenev), (R. Brinkmann, Y. Derbenev, K. Flöttmann)



$(\varepsilon_{th}, \varepsilon_{th}) \rightarrow (\rho \varepsilon_{th}, \rho^{-1} \varepsilon_{th})$ : arbitrarily adjustable  $\rho$

# Generating a Flat Beam with Angular Mom. Dominated Beam

(D. Edwards, ...), (Ph. Piot, Y.-e Sun)



# An Emittance Exchange Scheme for Improved X-Ray FEL Performance

(P. Emma, Z. Huang, P. Piot, and KJK, PRSTAB)

- Flat beam technique (units in m-rad)

$$\gamma\epsilon_x \otimes \gamma\epsilon_y : (10^{-6})^2 \rightarrow 10^{-5} \otimes 10^{-7}$$

- Use short electron beam  $\sigma_z = 33 \mu$

$$\gamma\epsilon_z = \sigma_z \sigma_{\Delta\gamma} = 33 \mu \otimes 3 \times 10^{-3} = 10^{-7} m \left( \sigma_{\Delta\gamma} = 1.5 \text{ keV}/mc^2 \right)$$

**Q = 33 pC, I = 100 A**

- Exchange ( $x \leftrightarrow z$ )

$$\gamma\epsilon_x \otimes \gamma\epsilon_y \otimes \gamma\epsilon_z : (10^{-6}, 10^{-6}, 10^{-7}) \rightarrow (10^{-5}, 10^{-7}, 10^{-7}) \rightarrow (10^{-7}, 10^{-7}, 10^{-5})$$

- Final bunch length

$$\gamma\epsilon_z = \gamma\sigma_z\sigma_\delta = \gamma\sigma_z \times 10^{-4} = 10^{-5}, \quad \gamma = 3 \times 10^4$$

$$\sigma_z = 3.3 \times 10^{-6} \Rightarrow \text{Compression by 10}$$

$$I = 100 \rightarrow 1000 \text{ A}$$



# Gun-Transformer Parameters

(P. Emma, Z. Huang, Ph. Piot, KJK, PRSTAB)

## ■ Gun

- Bunch charge= 20pC, rms laser spot size=300 $\mu$ m, rms laser pulse length=80fs, peak rf field=138 MV, B-field on cathode=0.19 T
- Trans. thermal emit.=0.23 $\mu$ m, trans. projected (coupled) emit.=4.96  $\mu$ m
- Long. emit.=0.071  $\mu$ m

## ■ Accelerator

- Tesla cavity, peak acc. field=36MV/m, electron final energy=216 MeV

## ■ After flat-beam transformation

- $\gamma\epsilon_x=9.9 \mu\text{m}$
- $\gamma\epsilon_y=0.0054 \mu\text{m}$
- $\gamma\epsilon_x=0.08 \mu\text{m}$

# *Watch Out for Non-ideal Effects*

## ■ **Space charge**

- Emittance growth & flat beam performance

## ■ **Higher order effects**

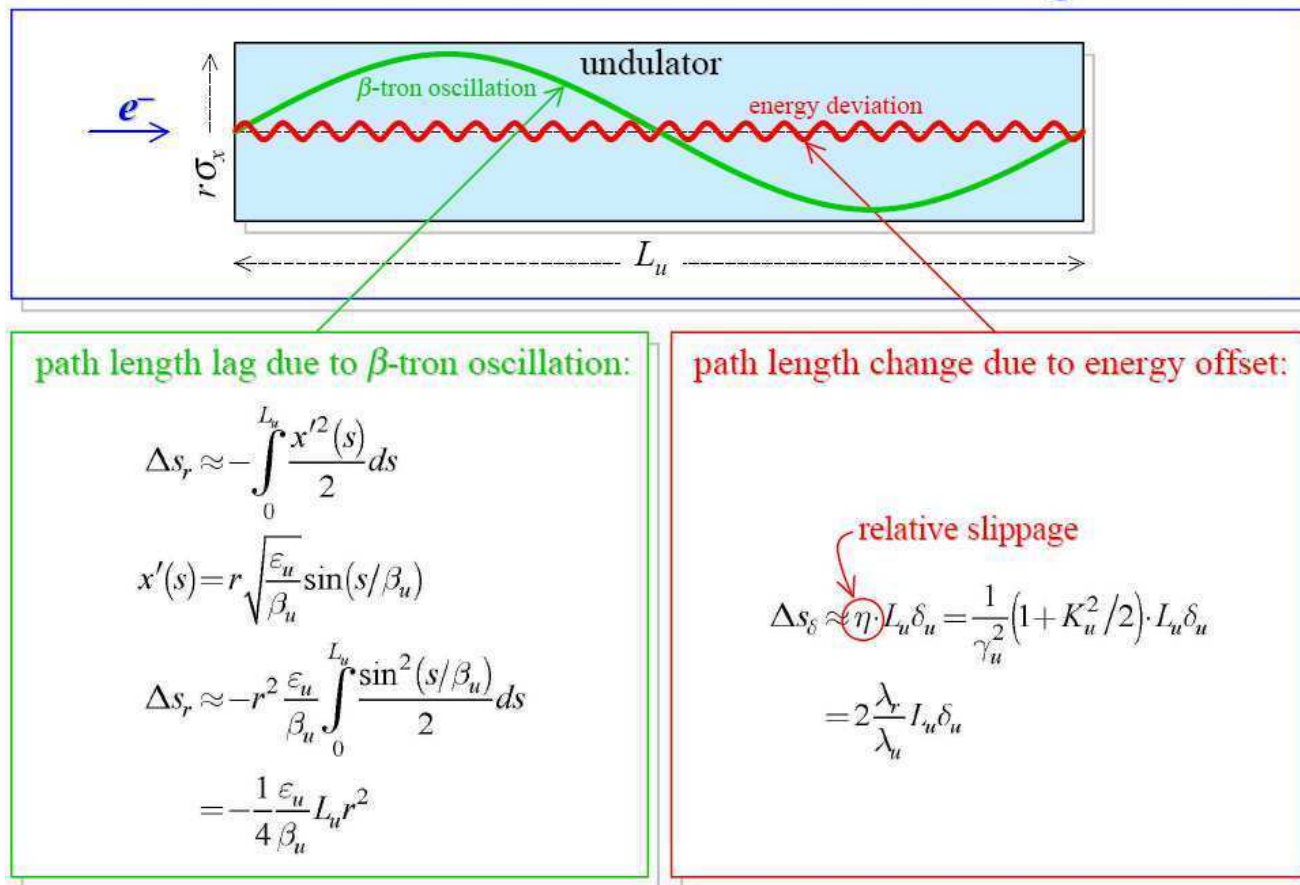
- Second order dispersion ( may be minimized by a suitable chirping according to P. Emma)

## ■ **Alignment**

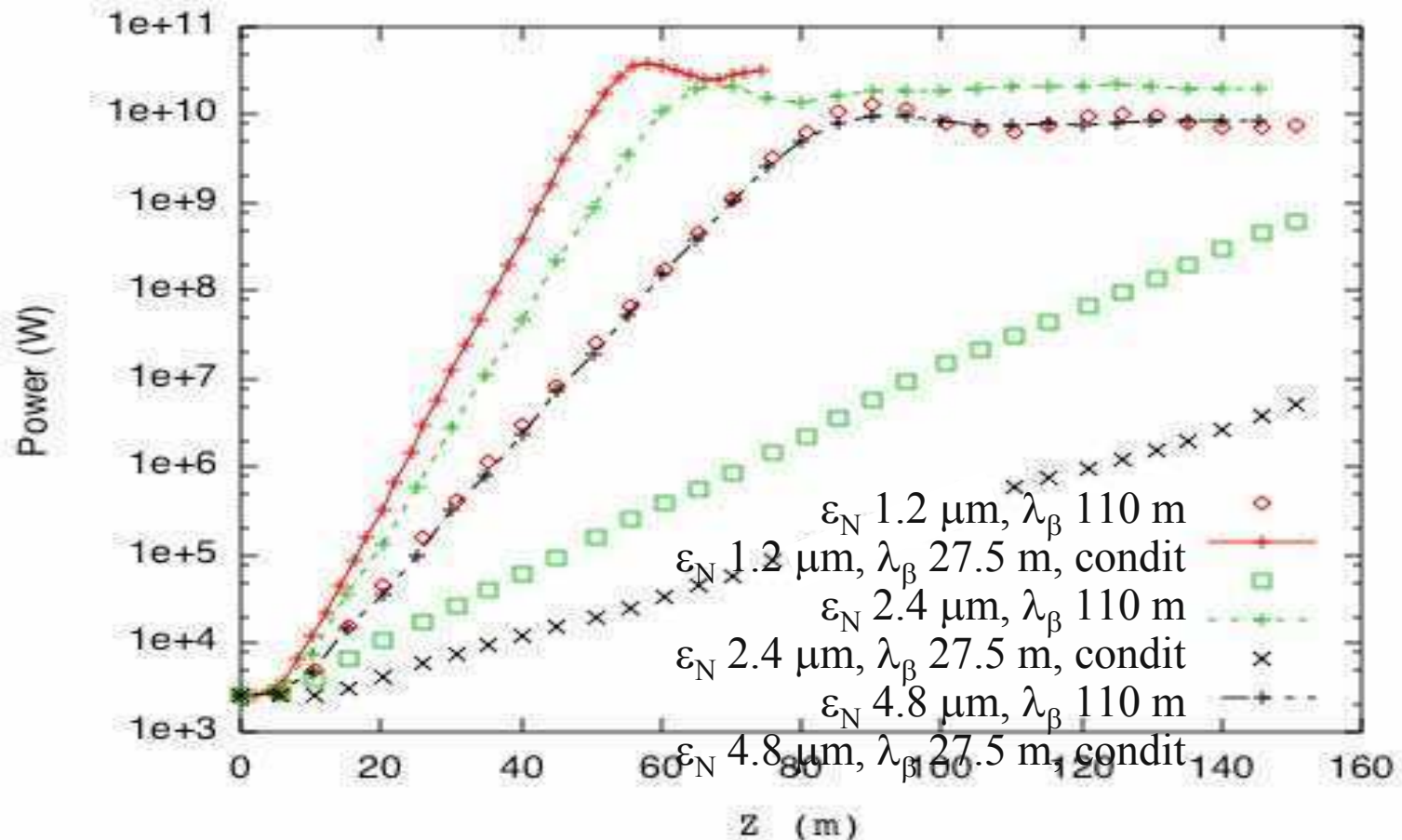
# *Obviating Electron Damping Ring in ILC*

- Require  $(\varepsilon_x, \varepsilon_y, \varepsilon_z) = (8, 0.02, 3000) \mu\text{m}$  at 3 nC
- $\varepsilon_T = (\varepsilon_x \varepsilon_y)^{1/2}$  too small for photocathode
- A possibility:  $(5, 5, 8) \rightarrow (1500, 0.02, 8) \rightarrow (8, 0.02, 1500)$
- Proposal by NIU-ANL Collaboration

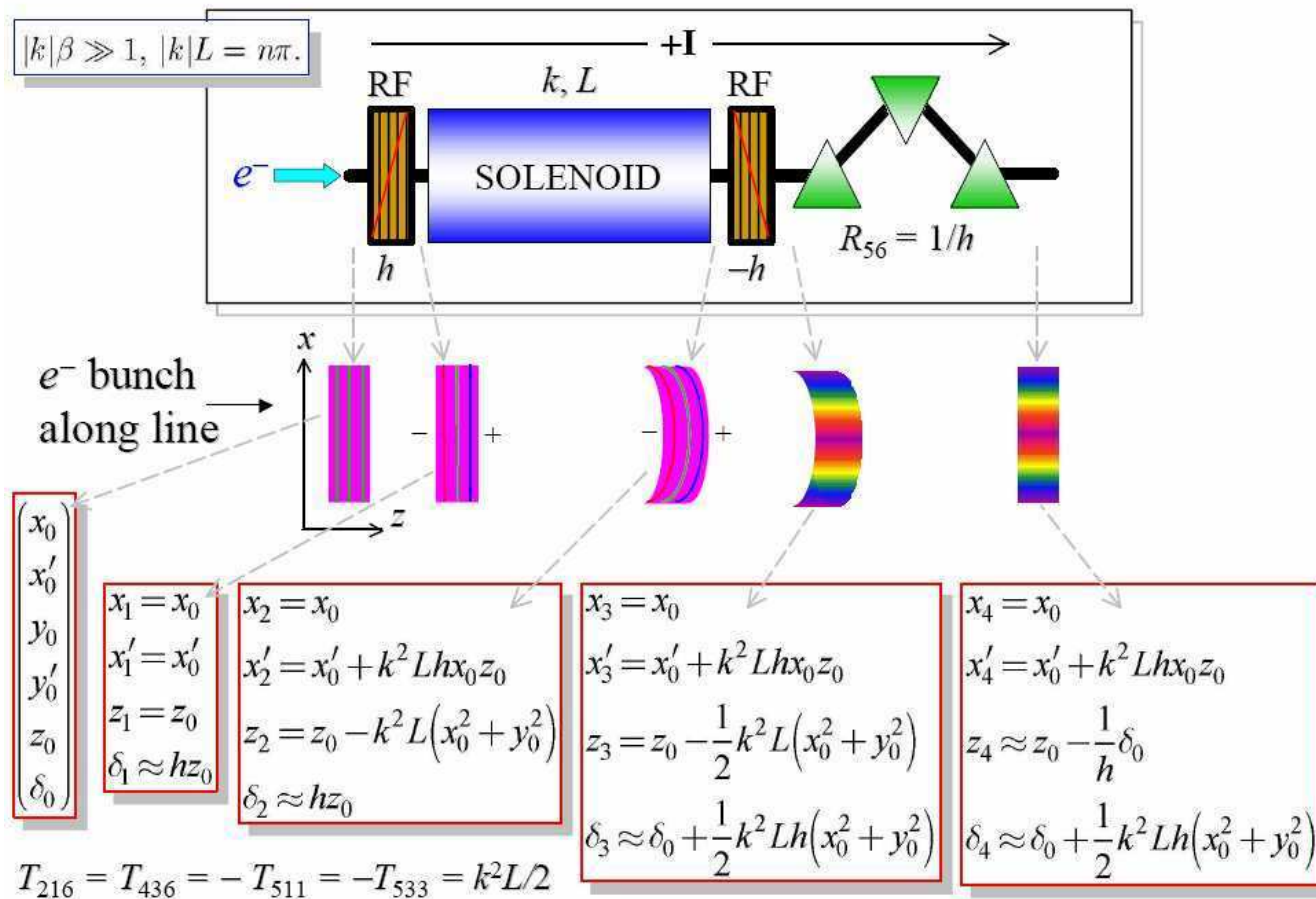
# Beam Conditioning: reducing the path length spread by introducing a correlation between energy and betatron amplitude (A.Sessler, D.H. Whittum, and L.-H. Yu, PRL 1992)



# *LCLS, vary emittance, optimal $\lambda_\beta$*

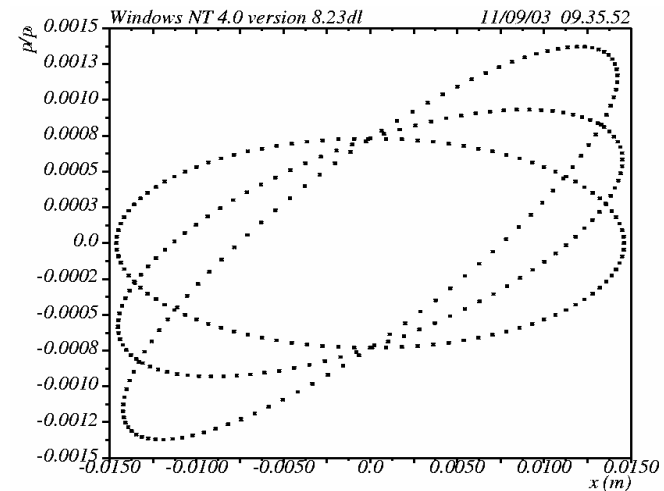


# A Simple Conditioning System using RF Chirp and Solenoid ( N. Vinokurov)



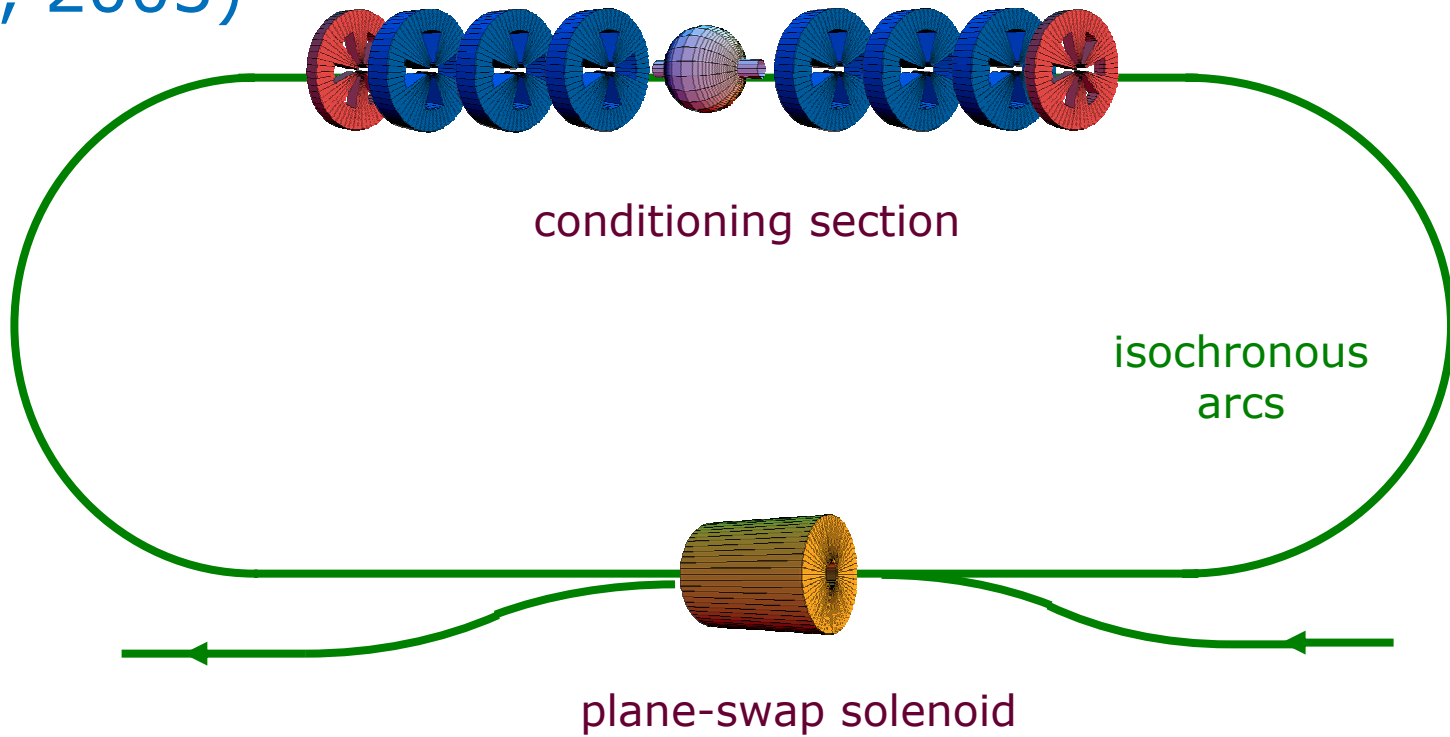
# *Problem: Emittance Dilution due to Chromatic Aberration (G. Stupakov)*

- **Betatron phase advance in solenoid is inversely proportional to electron energy**
- **There will be a large emittance growth unless the beam phase space is matched to the solenoidal focusing**
- **This restricts the conditioning to be weak, requiring long section (several hundred meters?)**



*A recirculating system with sextupole conditioning was proposed by A. Wolski*

# A Recirculating scheme using sextupoles and aTM110 cavity (A. Wolski, Argonne WS, 2003)





# *Concluding Remarks*

- (Emittance exchange + flat beam technique ) is a linear transformation and may find important applications in FELs and ILC
- Experimental demonstration of the concept may proceed in two steps; a “simple” exchange POP to full demonstration of emittance manipulation
- Beam conditioning is a nonlinear process and harder to implement, and is challenging us for further ideas

# **DAMPING RING FOR TEST THE OPTICAL STOCHASTIC COOLING**

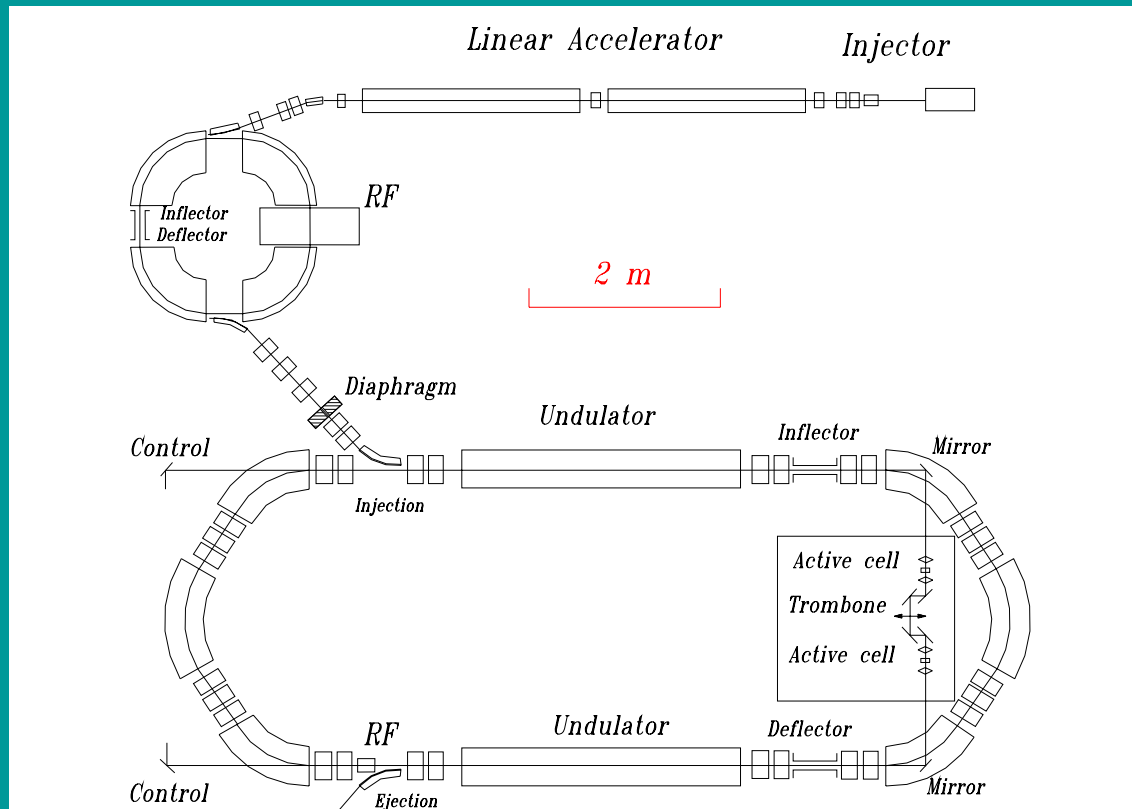
Alexander Mikhailichenko  
LEPP, Ithaca, NY 14853

A compact ring can be used to verify the OSC principles.  
Possible parameters of such ring described here.

Latest interest to this subject initiated by Vladimir Shiltsev

# INTRODUCTION

After proposal to extend Stochastic Cooling method to optical bandwidths, the idea about testing this method on specially designed compact damping ring was described soon after.



A. Mikhailichenko, "*Damping ring for Testing the Optical Stochastic Cooling*", Published in EPAC 94, London, England, 27 Jun - 1 Jul 1994: Proceedings. Edited by V. Suller and Ch. Petit-Jean-Genaz. River Edge, N.J., World Scientific, 1994. vol. 2\*, p. 1214-1216.

Transverse fluctuation of the center of gravity position of  $N$  particles each having transverse coordinate  $x_j$  is

$$\langle x \rangle \cong \frac{\sum_{j=1}^{N_s} x_j}{N_s} \approx \frac{A}{\sqrt{N_s}}$$

where  $A$  is an effective amplitude of transverse oscillation,  $N_s$ —is the number of particles in the bandwidth.

After kick:

$$x_i^{new} \cong x_i^{old} - G \frac{\sum_{j=1}^{N_s} x_j^{old}}{N_s} \rightarrow x_i^{old} - G \frac{x_i^{old}}{N_s} - G \frac{\sum_{j \neq i}^{N_s} x_j^{old}}{N_s} \quad G\text{-amplification}$$

One can see, that the damping associated with the signal from the particle itself is  $\approx G \frac{x_i}{N_s} \cong G \frac{A}{N_s}$  and the rest part  $\approx G \frac{\sum x_j}{N_s} \cong G \frac{A}{\sqrt{N_s}}$  represents the heating for this particle selected.

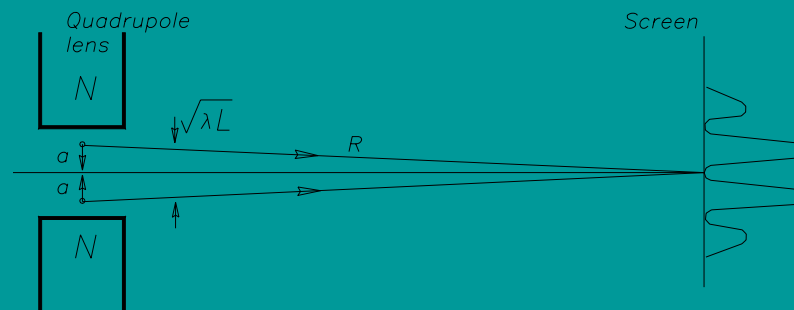
$$\frac{d \langle x^2 \rangle}{dn} + \frac{2G - G^2}{N_s} \langle x^2 \rangle = 0$$

where  $n$  marks the turns. Maximal cooling rate corresponds to  $G = 1$ , this means, that the kicker must eliminate the amplitude, corresponding to the picked averaged displacement in the pick-up. One can see that the cooling rate is simply associated with the number of the particles in the bandwidth.

$$\vec{E}(t) = -\frac{e}{cR} \frac{\vec{n} \times ((\vec{n} - \dot{\vec{\beta}}) \times \vec{n})}{(1 - \vec{n} \cdot \dot{\vec{\beta}})} \bigg|_{t'=t-R(t')/c}$$

$$\vec{E}_i(t) \big| \cong -\frac{e}{mc^2 \gamma R} \cdot \frac{4\gamma^2 g}{(1 + K^2 + \gamma^2 \mathcal{G}^2)^2} \cdot x_i \bigg|_{t'=t-R(t')/c}$$

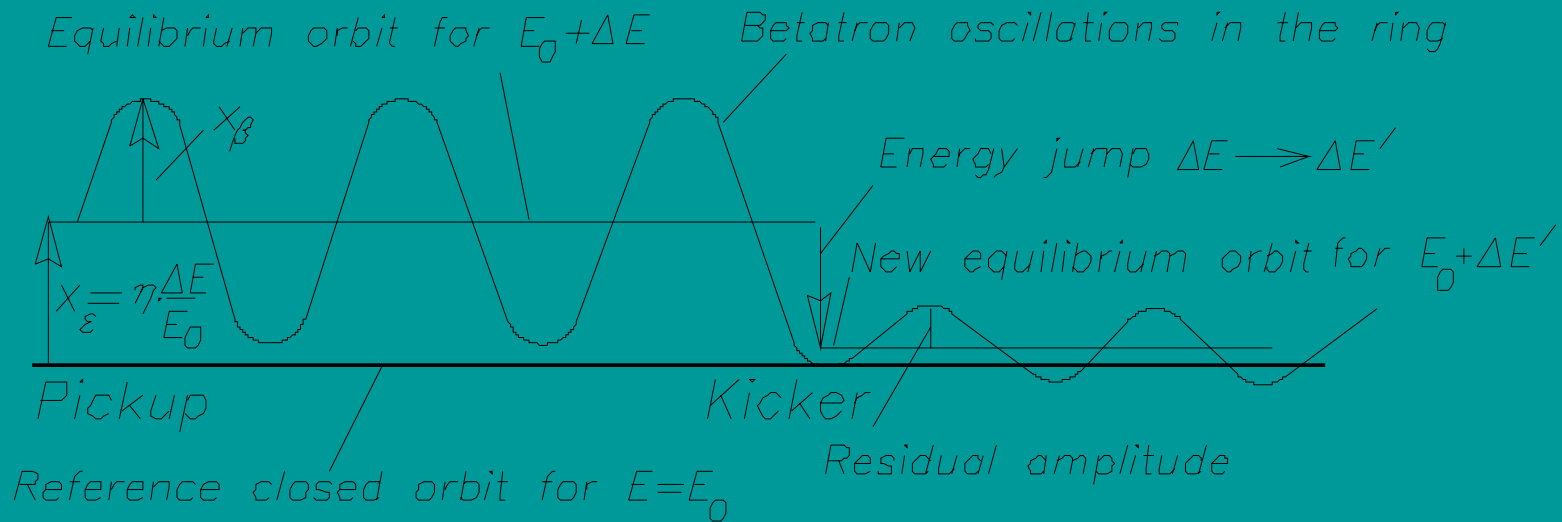
Diagram illustrating the FEL setup and the resulting radiation field. The top part shows the electron beam (blue line) moving through a series of undulator magnets (N and S poles). The beam is deflected vertically (Betatron oscillation) and horizontally (Quadrupole wiggler). The beam is observed by an Observer on the right. The beam's position is labeled  $x$ , and the observer's position is labeled  $k$ . The beam's acceleration is shown as a series of peaks and valleys. The beam's position is labeled  $x_i(t')$ . The beam's position is labeled  $x_i(t')$ . The beam's position is labeled  $x_i(t')$ .



Total number of the photons, radiated by the beam with  $N$  particles, becomes

$$\Delta N_{\gamma} \cong \alpha N \varepsilon / \varepsilon_0$$

# TRANSVERSE KICK OVER ENERGY CHANGE



. Transverse kick through the change of energy

$$\frac{\Delta E}{E} \cong \frac{eE_\perp KLM}{E\gamma} = \frac{A}{\eta\sqrt{N_s}}$$

Electric field strength required

$$E_\perp \cong \frac{AE\gamma}{eKLM\eta\sqrt{N_s}}$$

## AMPLIFICATION

$$\kappa = \sqrt{\frac{W_{kick}}{W_{pick}}} \cong \frac{\gamma l_B}{r_0} \frac{\Delta E}{E} \frac{1}{N} \frac{\Delta f}{f}$$

$$W_{kick} \cong \frac{1}{4\pi} E_{\perp}^2 V \qquad V \cong \pi A_0^2 l_B \cong \pi 2LM\lambda l_B$$

$$\frac{d\varepsilon}{dn} = -\frac{\varepsilon}{N_S} \qquad \varepsilon_{fin} \cong \varepsilon_0 \frac{1}{\alpha N_S}$$

$$N_S \sim \frac{N}{\Delta f} \frac{c}{l_B} \cong MN \frac{\lambda}{l_B} \cong MNL \frac{l_B}{\gamma^2}$$

# BEAM PASS

The necessity to keep the bunch length unperturbed from pickup to the kicker within the level of the wavelength of the optical system is obvious. With the same accuracy the congruence of the light amplified and particle's beam must be arranged in the kicker as well.

$$x(s) = x_0 \cdot C(s, s_0) + x'_0 \cdot S(s, s_0) + D(s, s_0) \cdot (\Delta E / E)$$

$$D(s, s_0) = -S(s, s_0) \cdot \int_{s_0}^s \frac{C(\tau)}{\rho(\tau)} d\tau - C(s, s_0) \cdot \int_{s_0}^s \frac{S(\tau)}{\rho(\tau)} d\tau$$

$$x(s) = x_{0\beta} \cdot C(s, s_0) + x'_{0\beta} \cdot S(s, s_0) + [\eta_0 \cdot C(s, s_0) + \eta'_0 \cdot S(s, s_0) + D(s, s_0)] \frac{\Delta E}{E}$$

$$x^{pick} = x_{\beta}^{pick} + \eta^{pick} \frac{\Delta E}{E}$$

$$x^{kicker} = x_{\beta}^{kick} + [\eta^{kick} + D^{kick}] \frac{\Delta E}{E}$$

$$\Delta l = -\int_{s_0}^s \frac{x}{\rho} d\tau = -x_0 \int_{s_0}^s \frac{C}{\rho} d\tau - x'_0 \int_{s_0}^s \frac{S}{\rho} d\tau - \frac{\Delta E}{E} \int_{s_0}^s \frac{D}{\rho} d\tau = -x_0 M_{51}(s, s_0) - x'_0 M_{52}(s, s_0) - \frac{\Delta E}{E} M_{56}(s, s_0)$$

$$\Delta l \cong -x'_0 2\eta_0 = -[x'_{0\beta} + \eta'_0 \cdot (\Delta E / E)] \cdot 2\eta_0$$

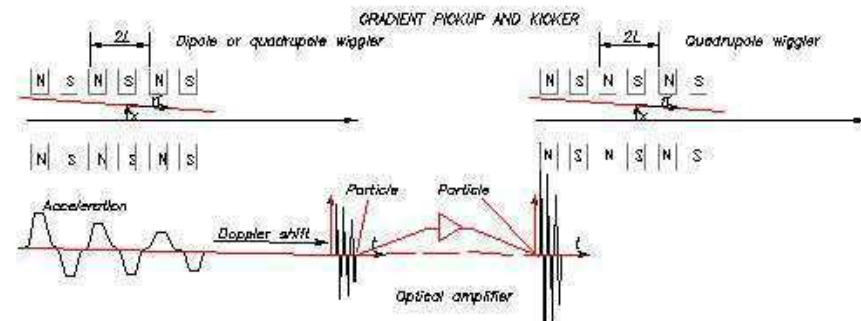
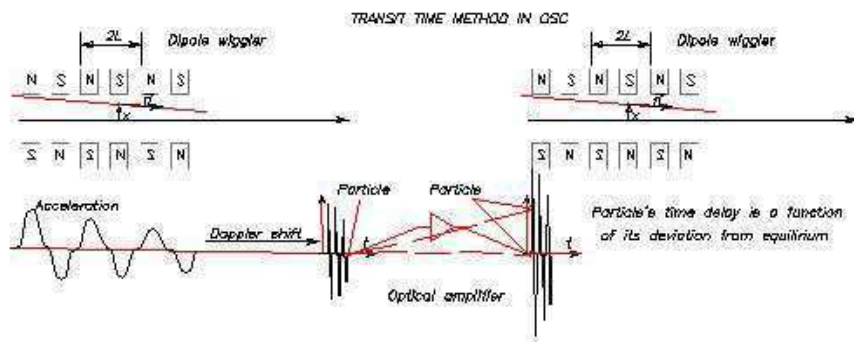
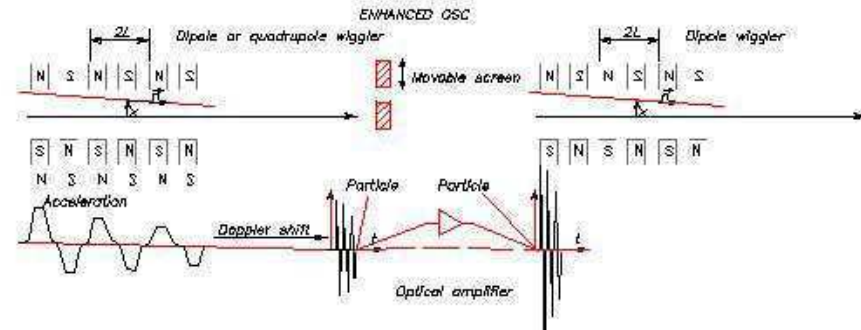
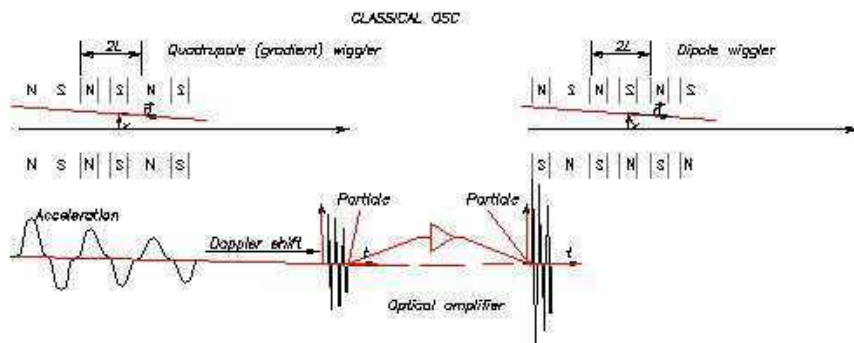
Simultaneous cooling requires

$$\eta^{kick} + D^{kick} = -\eta^{pick}$$

Threshold emittance  $\gamma \varepsilon_{th} \cong \lambda \cdot \gamma \frac{\Delta E}{E} \cong \frac{\lambda}{l_B} \cdot \gamma l_B \frac{\Delta E}{E} \quad \gamma \varepsilon_{th} \cong 10^{-4} cm \cdot rad$

If simultaneous cooling in x and s coordinates required





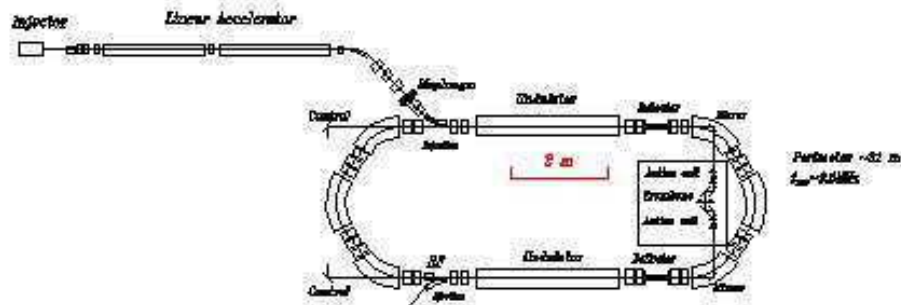
Types of OSC. In transit time method arriving to the second wiggler depends on parameters of particle at the pickup undulator [7]. Enhanced OSC [14] deals with screening of optical image for some parts of radiation from the beam.

[7] M. Zolotarev, A. Zholents, Phys. Rev. E, **50**, 3087(1994).

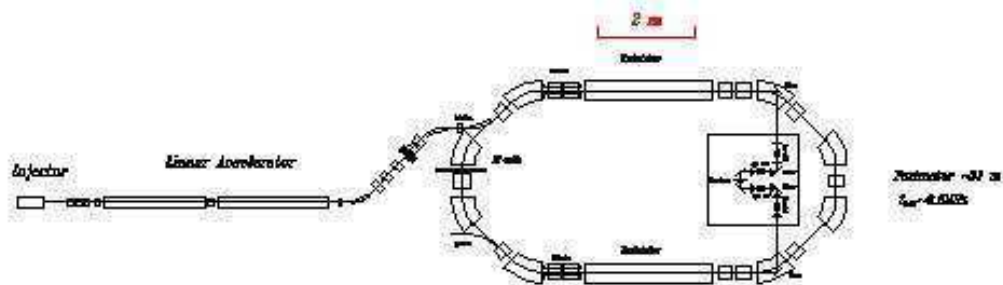
[14] E.G.Bessonov, M.V.Gorbunkov, A.A.Mikhailichenko, "Enhanced Optical Cooling of Ion Beams for LHC", EPAC 2006 Proceedings, TUPLS001, Edinburgh, UK, 2006.

Different shapes

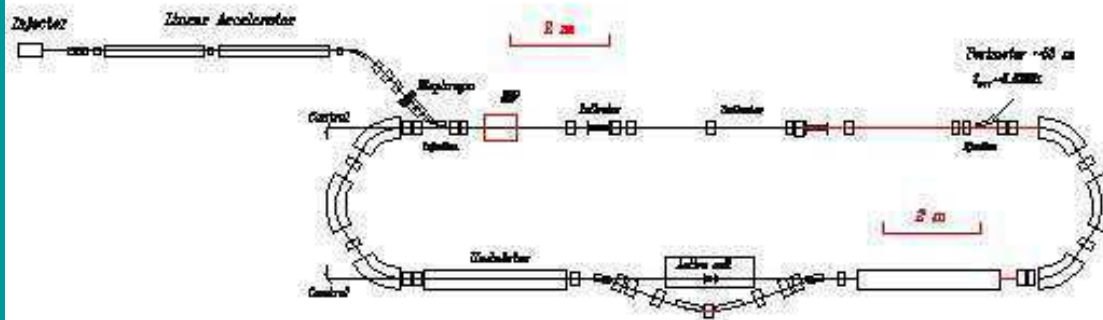
Three-magnet achromat



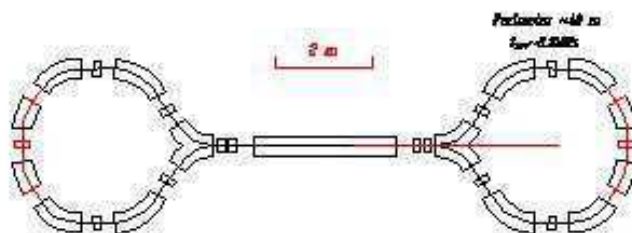
Four magnet achromat



Bypass achromat

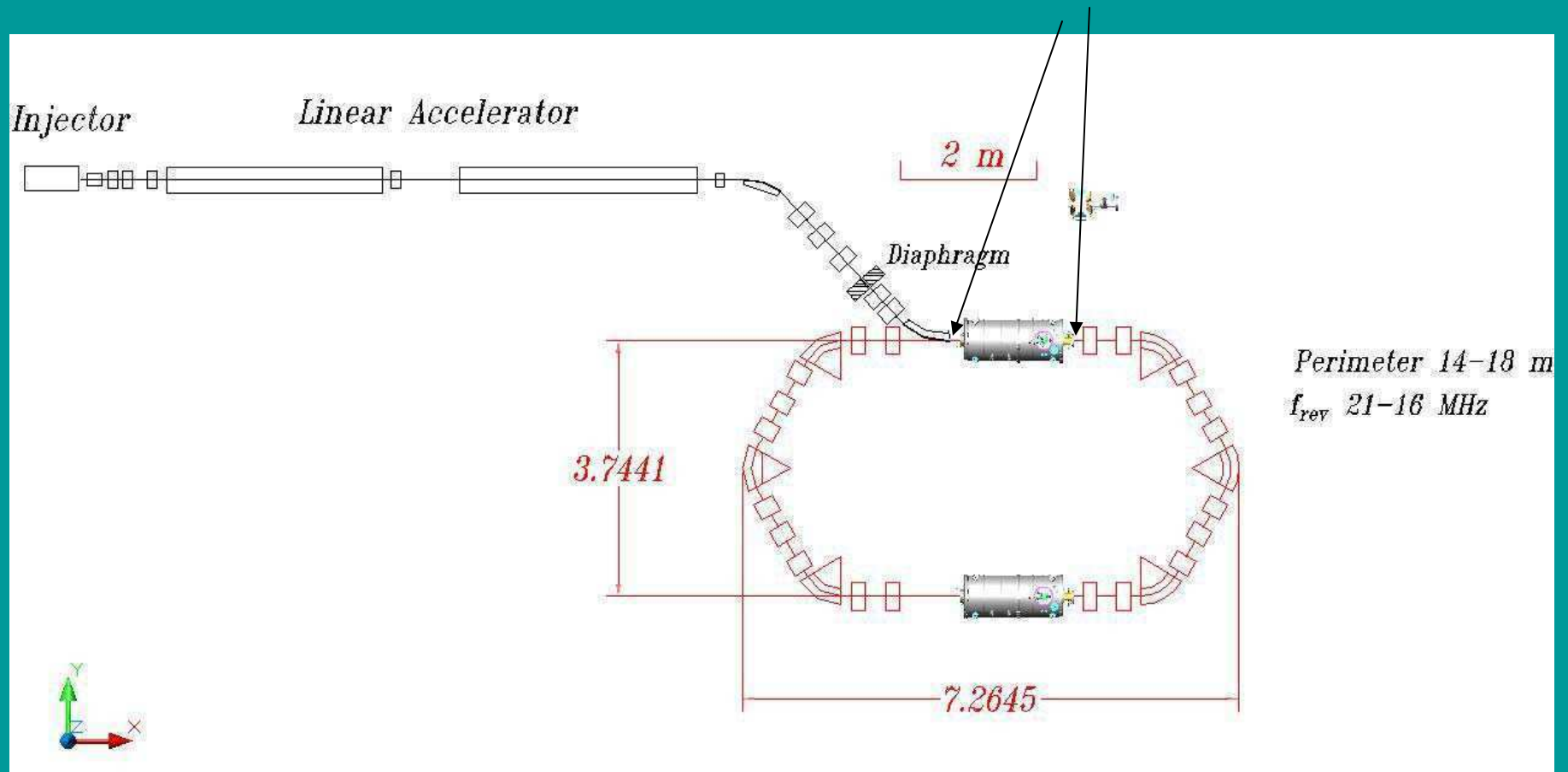


Kayak paddle. Achromatic bends

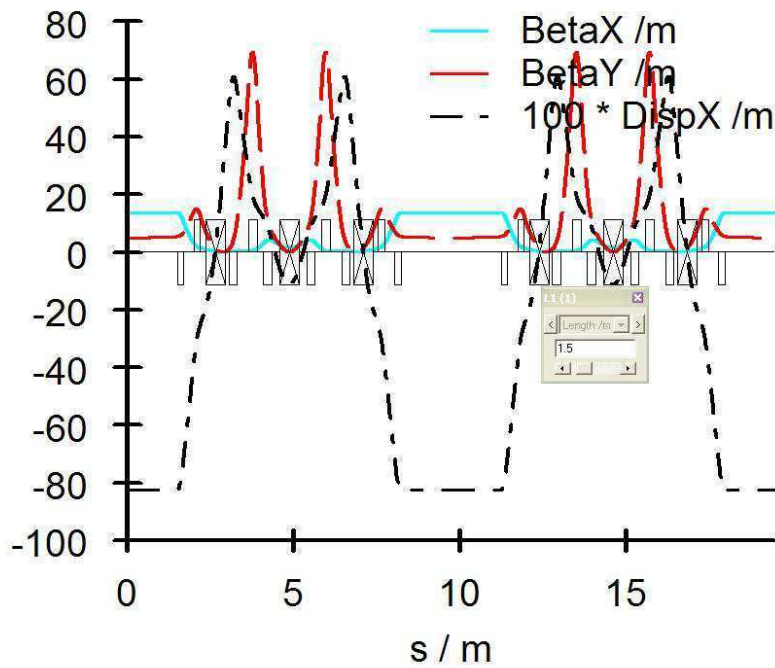


Three-magnet achromat is probably the best choice

Straight sections can be extended up to 4 meters



Machinefunction / m

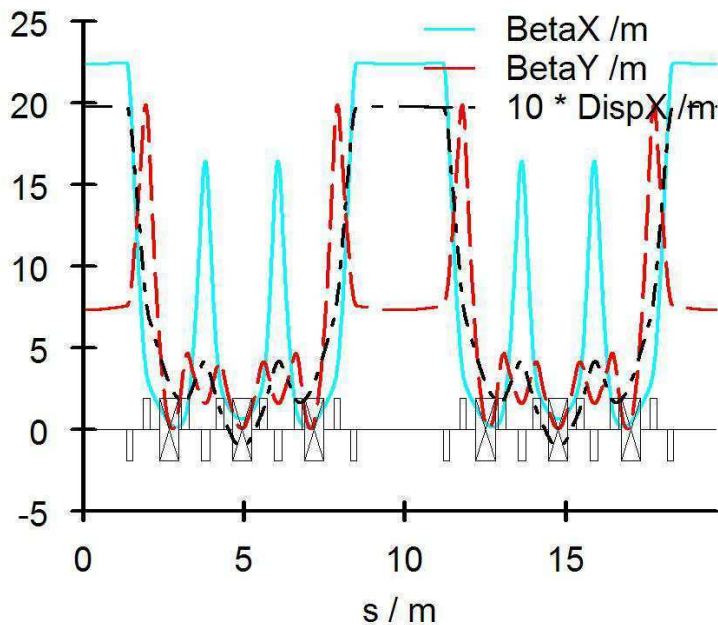


Points: 2037  
 Period: 1  
 Total length: 19.4960m  
 Energy: 0.2500GeV  
 I1: -0.0387  
 I2: 10.9646  
 I3: 19.1354  
 I4: 2.6103  
 I5: 4.9545  
 I6x: 18.0090  
 I6y: 19.8866  
 I7x: -77.2347  
 I7y: -761.4688  
 alpha: -0.0020  
 Uo: 0.6033keV  
 Emit0: 1.00E-08  
 Coubl: 0.0200  
 EmitX: 9.80E-09  
 EmitY: 1.96E-10  
 Sig: 0.0003  
 Jx: 0.7619  
 Je: 2.2381  
 Tx: 70.7391ms  
 Ty: 53.8987ms  
 Te: 24.0827ms  
 Kx: -6.1461  
 Ky: -60.5958

Optics allows broad change of dispersion

Alpha can be made negative or positive

Machinefunction / m



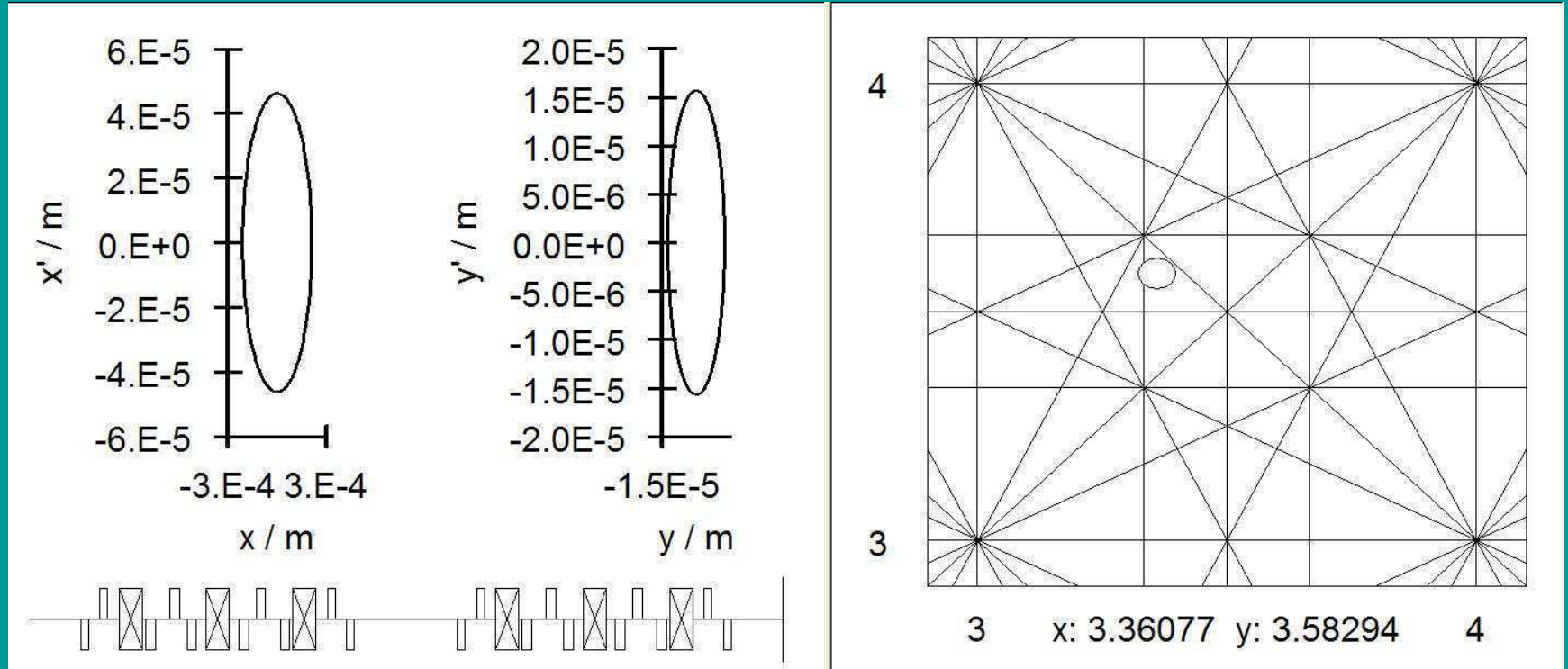
Points: 2021  
 Period: 1  
 Total length: 19.7000m  
 Energy: 0.2500GeV  
 I1: 1.0786  
 I2: 10.9646  
 I3: 19.1354  
 I4: 5.7180  
 I5: 3.4266  
 I6x: 14.5062  
 I6y: 20.9744  
 I7x: -209.8641  
 I7y: -210.4747  
 alpha: 0.0547  
 Uo: 0.6033keV  
 Emit0: 1.00E-08  
 Coubl: 0.0200  
 EmitX: 9.80E-09  
 EmitY: 1.96E-10  
 Sig: 0.0003  
 Jx: 0.4785  
 Je: 2.5215  
 Tx: 113.8177ms  
 Ty: 54.4627ms  
 Te: 21.5994ms  
 Kx: -16.7005  
 Ky: -16.7490

Longitudinal mass and beam temperature

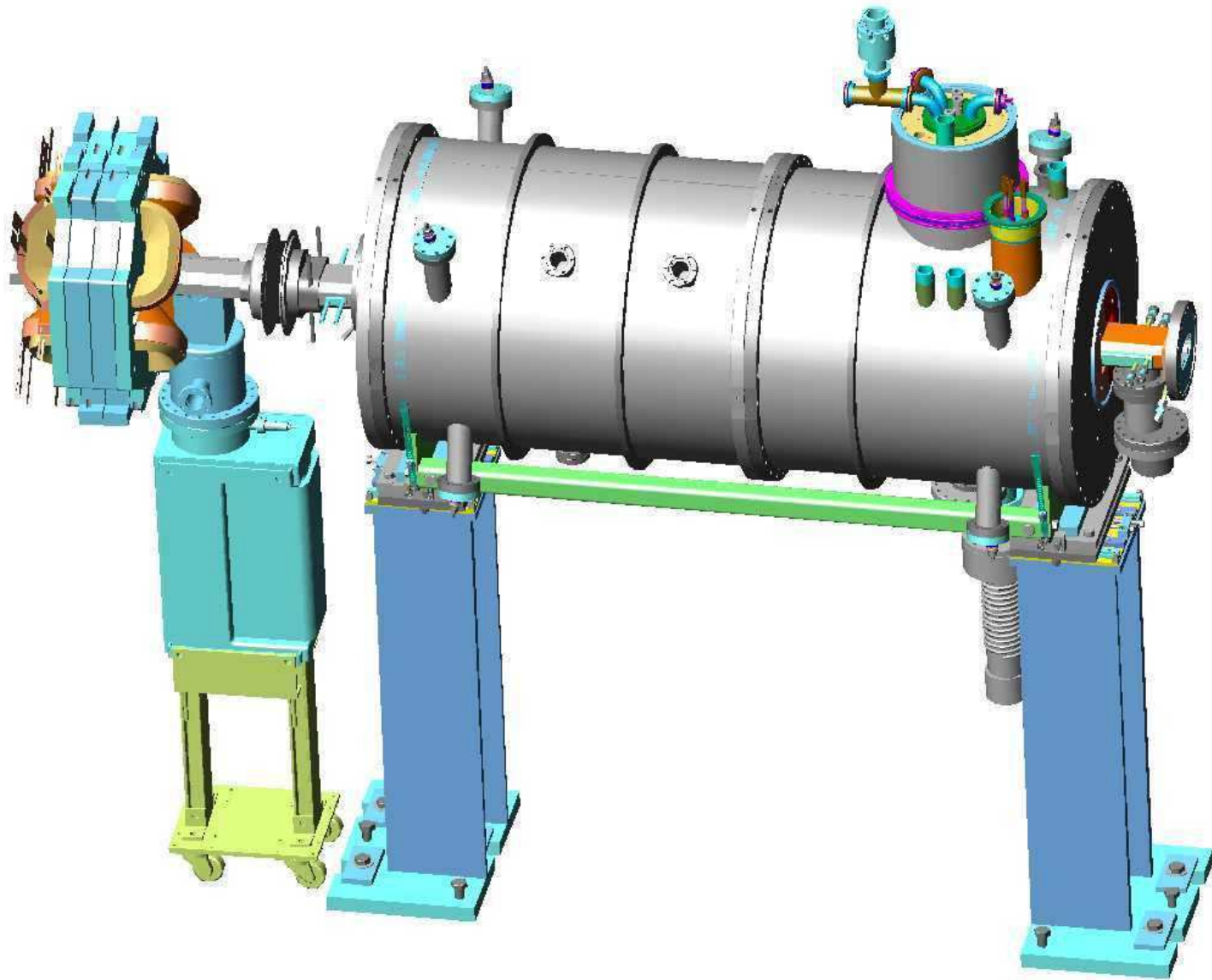
$$\frac{1}{m_{\parallel}} = \frac{1}{m\gamma} \left( \frac{1}{\gamma^2} - \alpha \right)$$

$$\frac{3}{2} N k_B T \cong N \cdot m c^2 \gamma \left[ \frac{\gamma \epsilon_x}{\beta_x} + \frac{\gamma \epsilon_y}{\beta_y} + \gamma \left( \frac{1}{\gamma^2} - \left\langle \frac{D^2}{\beta_x} \right\rangle \right) \left( \frac{\Delta p_{\parallel}}{p_0} \right)^2 \right]$$

## Tune diagram

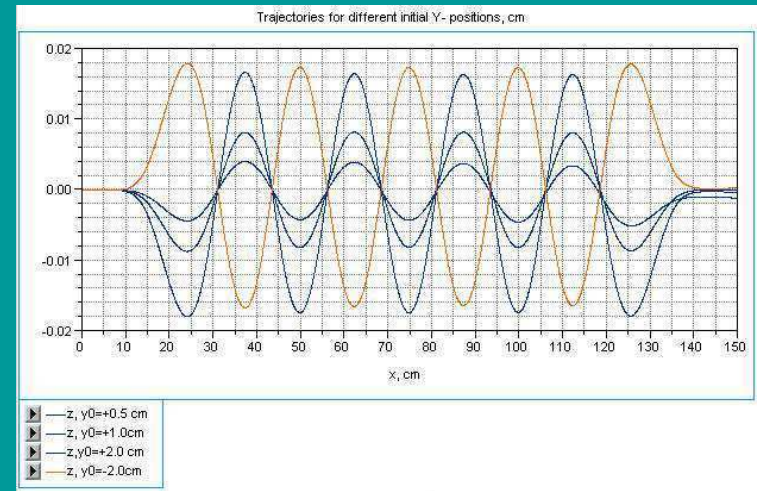
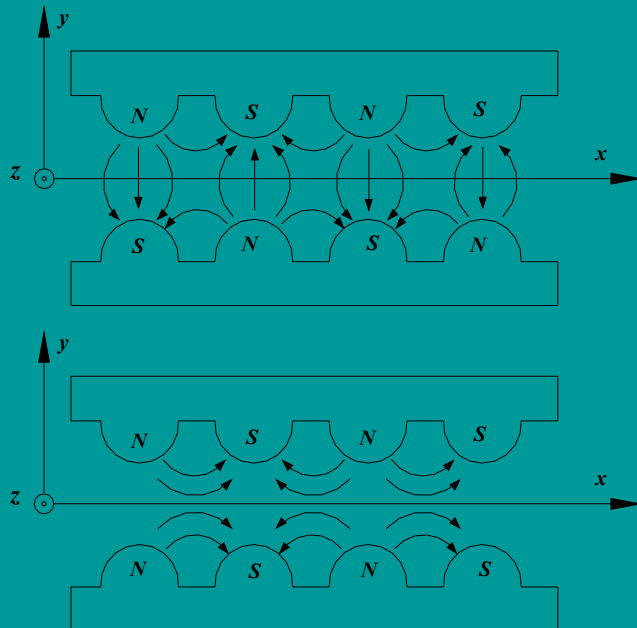






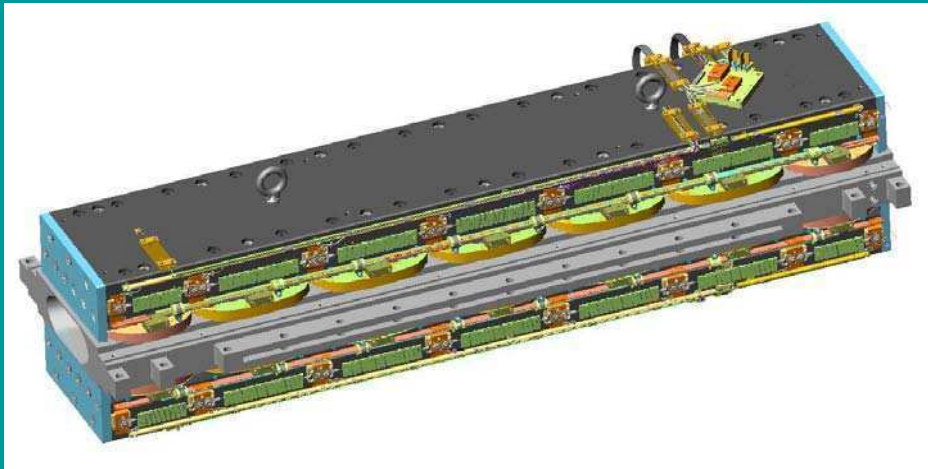
Cornell Wiggler

Any wiggler can be commutated to so called gradient wiggler/undulator



Trajectories in gradient undulator

for different values of vertical coordinate



Basically for test in electron ring wiggler can operate without LHe cooling

#### CORNELL

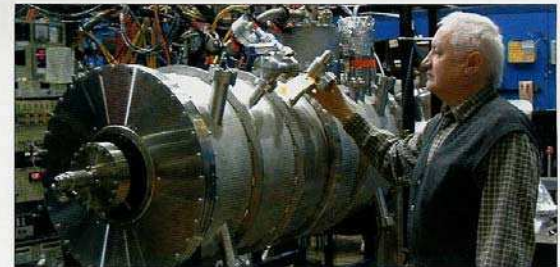
### Wigglers give CESR a new charmed life

In early March, after more than 23 years of continuous operation, the CESR staff and the CLEO collaboration at Cornell completed their programme of b quark physics. Now the conversion of CESR to operate in the lower-energy region of the c quark, or charm, threshold has begun, with the installation of the first new "wiggler" magnets, which are a key component of the conversion (*CERN Courier* January/February 2002 p13). The US National Science Foundation has approved the proposal for this new programme and awarded a five-year grant to support it. At the same time, the NSF approved the continuation of the CHESS facility, which supports the utilization of synchrotron radiation X-rays produced in CESR.

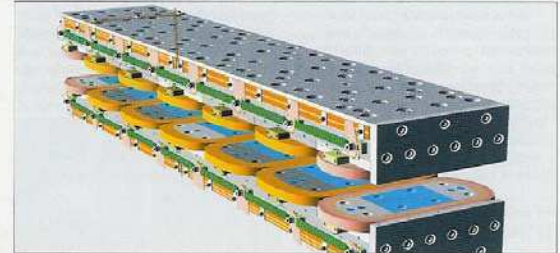
Conversion of CESR's  $e^+e^-$  storage ring to operate with sufficient luminosity in the charm-threshold region requires the installation of 18 m of wiggler magnets operating at magnetic fields of 2.1 T. Wiggler magnets have alternating north and south poles which induce rapid radial oscillations of the beams, increasing dramatically the emission of synchrotron radiation in the form of X-rays. Emission of synchrotron radiation "damps" the beams – that is, it decreases the sizes of the beams and increases the luminosity that the collider can provide.

When CESR was operating in the region of the  $\psi$  particle, near 5 GeV per beam, the emission of synchrotron radiation in the collider's bending magnets was sufficient to achieve small beams and high luminosity. At the lower energies of the c quark threshold region, between 1.5 and 2 GeV per beam, a factor of 20 in the radiation damping rate is lost. The wigglers will make up for this loss and achieve the high luminosities required.

The wigglers for "CESR-c" are superferic magnets, with iron poles excited by superconducting coils. A prototype wiggler, constructed in early 2002, was placed in CESR last August. Beam tests showed that the effects from the wiggler are consistent with estimates based on computer tracking and dynamic aperture analysis. With the extra damping of this one wiggler, as well as two weaker wigglers from the CHESS synchrotron



Designer Alexander Mikhailichenko with the sixth CESR-c wiggler in its cryostat on a stand.



Assembly drawing of the CESR-c superferic wiggler magnets, vital for charm conversion.

radiation source, the luminosity in CESR in the charm-threshold region approached  $2 \times 10^{31} \text{ cm}^{-2} \text{ s}^{-1}$ , which is already above luminosities achieved at other colliders in this energy range. The final luminosity with all wigglers installed will be around  $3 \times 10^{32} \text{ cm}^{-2} \text{ s}^{-1}$ .

Six wigglers, representing 8 m of the 18 m required, have already been built and will be installed during a machine shutdown from March through June. For cooling, these wigglers will use the cryogenic facilities in place for CESR's superconducting RF cavities. Space in the ring is being created by removing two dipole bending magnets, in the third of the circumference closest to the central lab, and increasing the field of adjacent magnets.

Other hardware changes are minor, such as using thinner windows in injection lines, improving the regulation of the power supply, and optimizing the superconducting RF field control for higher-field and lower-beam

loading. The modifications of the CLEO detector are also modest. The main upgrade is replacing the silicon vertex detector with a small drift chamber.

Because of the lower beam energy, synchrotron-radiation users will no longer be able to run in parallel with high-energy physics operation. Dedicated periods of operation with beam energies above 5 GeV will serve the needs of X-ray users. The higher-energy running also benefits the beam lifetime for high-energy physics operations by keeping the vacuum chamber clean thanks to the action of the higher-energy synchrotron radiation photons.

CESR will operate in the charm-threshold region during the second half of 2003, after a period of commissioning and synchrotron-radiation running. At the same time the remaining wiggler units will be built and tested, ready for installation when convenient, so that full-intensity operation for high-energy physics can follow shortly afterwards.



## OPTICAL AMPLIFIER

### Example 1.

For  $N \cong 10^{10}$ ,  $l_B \cong 15cm$ ,  $M = 2.5$ ,  $(\Delta E / E) \cong 10^{-3}$ ,  $\gamma \cong 500$  (250 MeV),  $\lambda \cong 1\mu m$ , optical amplifier must be able to have amplification about 300, peak power about 5 kW, average power about 25 W with repetition rate  $f$  of the order of 10 MHz. Number of the particles in the bandwidth  $N_s \cong 3 \cdot 10^5$  defines the number of the turns and the damping time  $\tau_c \cong N_s / f \cong 30ms$ . Emittance reduction  $\varepsilon_f / \varepsilon_0 \cong 1 / \alpha N_s \cong 10^{-3}$ .

### Example 2.

For  $N \cong 10^8$ ,  $l_B \cong 5cm$ ,  $M = 2.5$ ,  $(\Delta E / E) \cong 10^{-4}$ ,  $\gamma \cong 500$  (250 MeV),  $\lambda \cong 1\mu m$ , optical amplifier must be able to have amplification about 100, peak power about 225 W, average power about 0.075 W with repetition rate of 2 MHz. Number of the particles in the bandwidth  $N_s \cong 2 \cdot 10^3$  defines the number of the turns and the damping time  $\tau_c \cong N_s / f \cong 1ms$ . Emittance reduction  $\varepsilon_f / \varepsilon_0 \cong 1 / \alpha N_s \cong 7 \cdot 10^{-2}$ .

### Ti:Al<sub>2</sub>O<sub>3</sub> amplifier

For Titanium Sapphire  $\tau_L \cong 3.5 \mu s$  ,  $\sigma_{01}(490nm) \cong 10^{-19} cm^2$  ,  $\sigma_{10}(790nm) \cong 3 \cdot 10^{-19} cm^2$  ,  $n_0 \approx 10^{20} cm^{-3}$  . Absorption length value becomes  $l_{ab} \cong 1 / (n_0 \sigma_{01}) \cong 0.1 cm$  , the pumping area  $S_{pump} \cong \lambda \cdot l_{ab} \cong 7 \cdot 10^{-6} cm^2$  . Saturation power density becomes  $P_{sat} \cong \frac{\hbar \omega n_0 l_{ab}}{\tau_L} \leq 1 MW / cm^2$  and the power of radiation required to pump the Ti:Al<sub>2</sub>O<sub>3</sub> becomes  $I = P_{sat} \cdot S_{pump} \cong 7W$  . Amplification can be calculated as  $\kappa \cong \exp[\sigma_{10}(\lambda) \cdot n_1 \cdot l] \approx \exp(\sigma_{10} / \sigma_{01}) \approx 20$  for the length  $l \cong l_{ab}$  . So two stages can give a resulting amplification up to  $20^2 = 400$  . For pumping the Argonne laser can be used here.

In conclusion of this section we can say, optical amplifier must be able to give amplification about 1000 a peak power about 1 *kW*, average power about 10*W*. Repetition rate must be of the order of few MHz. Some estimation made for Dye, Titanium Sapphire.

Interesting investigation done by F.X. Kärtner,

“ *Amplifier Development for Optical Stochastic Cooling*”, Research Laboratory for Electronics LARP Meeting, Jefferson Port, October 25, 2006. The conclusions are:

An ultra-broadband optical amplifier for optical stochastic cooling can be built using PPLN and OPA at  $2\ \mu\text{m}$ .

Dispersion in this wavelength range is low and group delay can be kept minimal.

Pump laser concepts:

Directly pumped OPA using a high power laser

Cavity enhanced OPA using a medium power laser.

Total optical delay in amplifier within 10 mm ( $>2\text{mm}$ )

# CONCLUSION

Coming to conclusion, there are no limitations in testing OSC with relatively low investment.

The profits might be significant, however, if applied to proton machines or to machine with multiple-charged ions.

Cornell can deliver two wigglers with 40 cm period, seven poles. For experiment with electrons these can be feed at room temperature. For operation with protons/ions wigglers can operate been cooled with liquid Helium.

Optical amplifier within achievable parameters.

# Emittance Exchange at FNPL

Ray Filler for Tim Koeth

November 28<sup>nd</sup>, 2006

# Overview

- Motivation & Overview
- Planned Experiment
- Present Status
  - Beam line design
  - Beam line simulation
  - $TM_{110}$  RF cavity
- Timeline

# Motivation

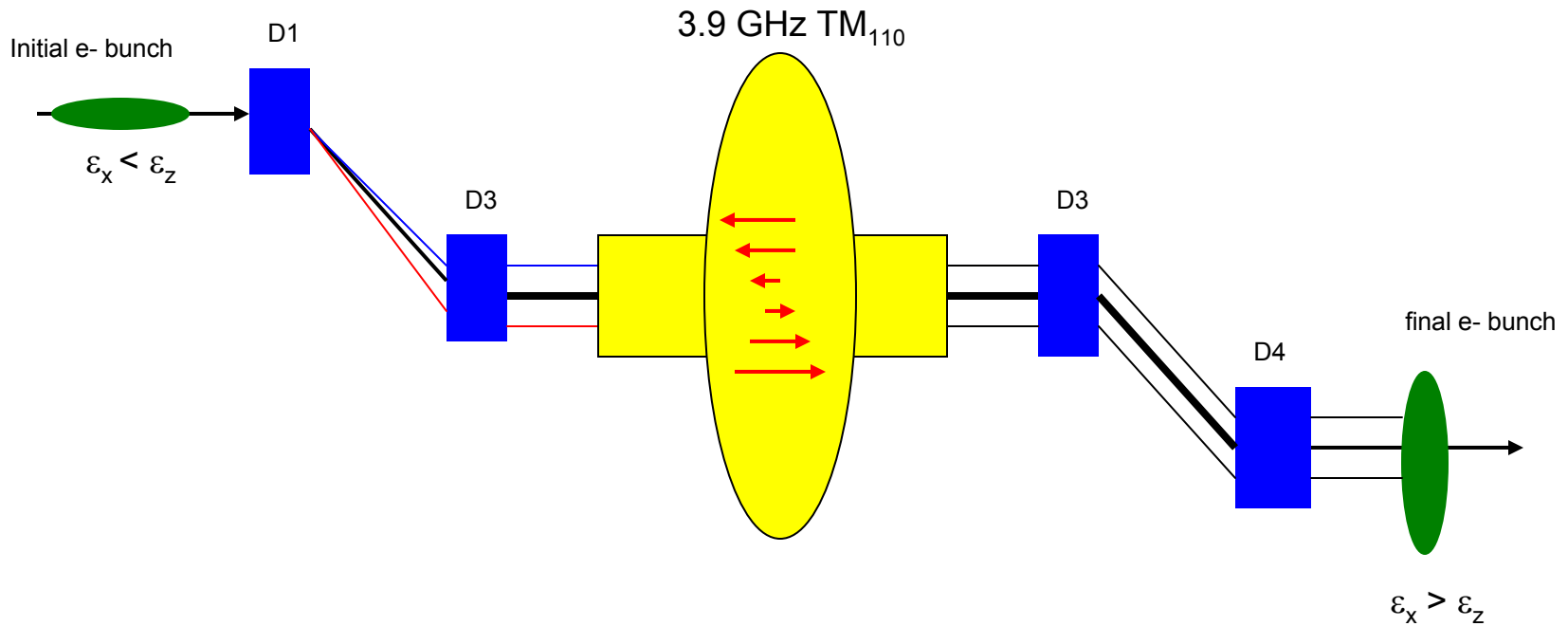
For FEL applications it is desirable to have a small transverse emittance and high brightness. A longitudinal to transverse emittance exchange has been proposed to achieve this goal. \*

The A0 Photo Injector wishes to show a proof of principle of the emittance exchange.

\* M. Cornacchia, P. Emma, Phys. Rev. ST Accel. Beams 5, 084001 (2002)

# Emittance Exchange

Place a 3.9 GHz  $TM_{110}$  cavity between two dog-leg bends to reduce the momentum spread, thereby reducing the longitudinal emittance. This comes at the cost of introducing a transverse betatron amplitude, thus an increase in transverse emittance. A complete longitudinal to transverse emittance exchange should be observed

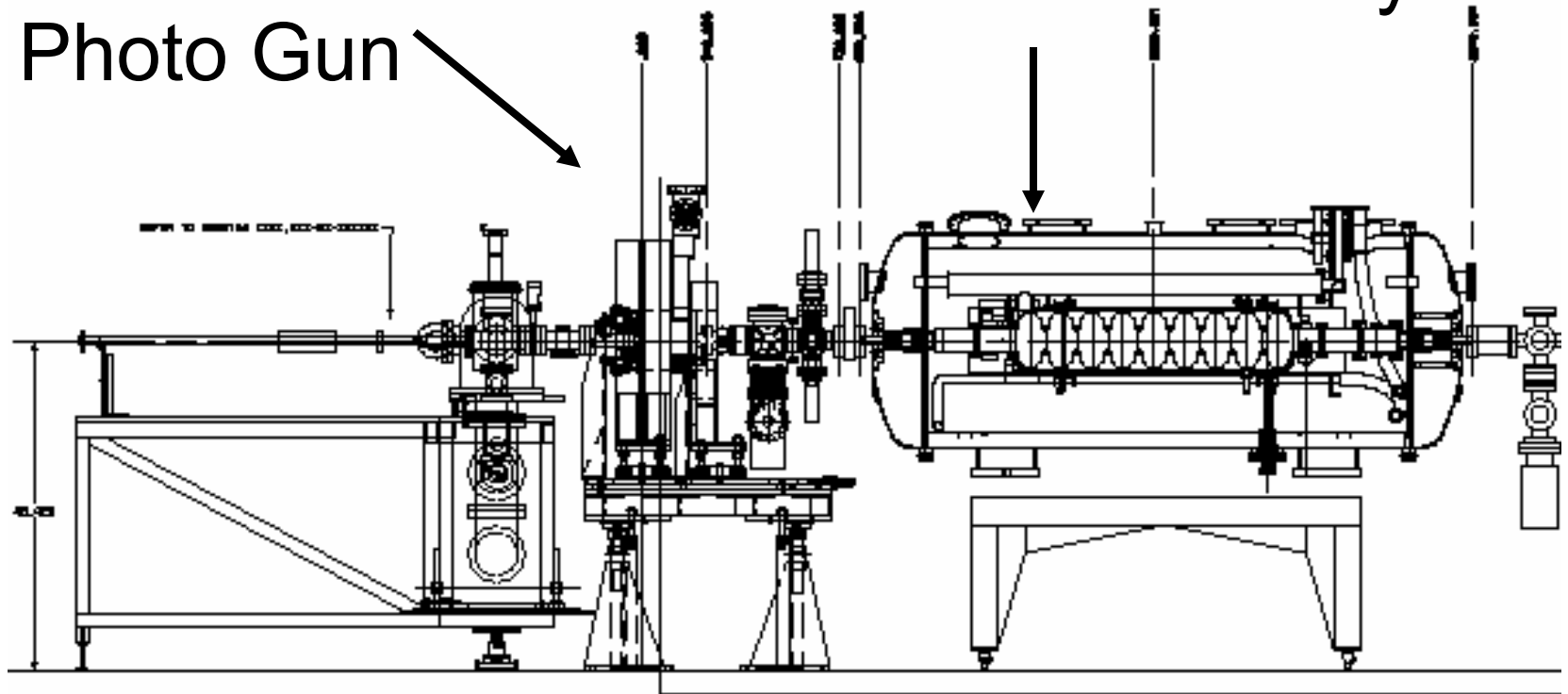




# The A0 PhotoInjector

1.5 Cell Cu  
Photo Gun

SC 9-Cell Cavity



Nominal operating values for round beam after the 9-cell:

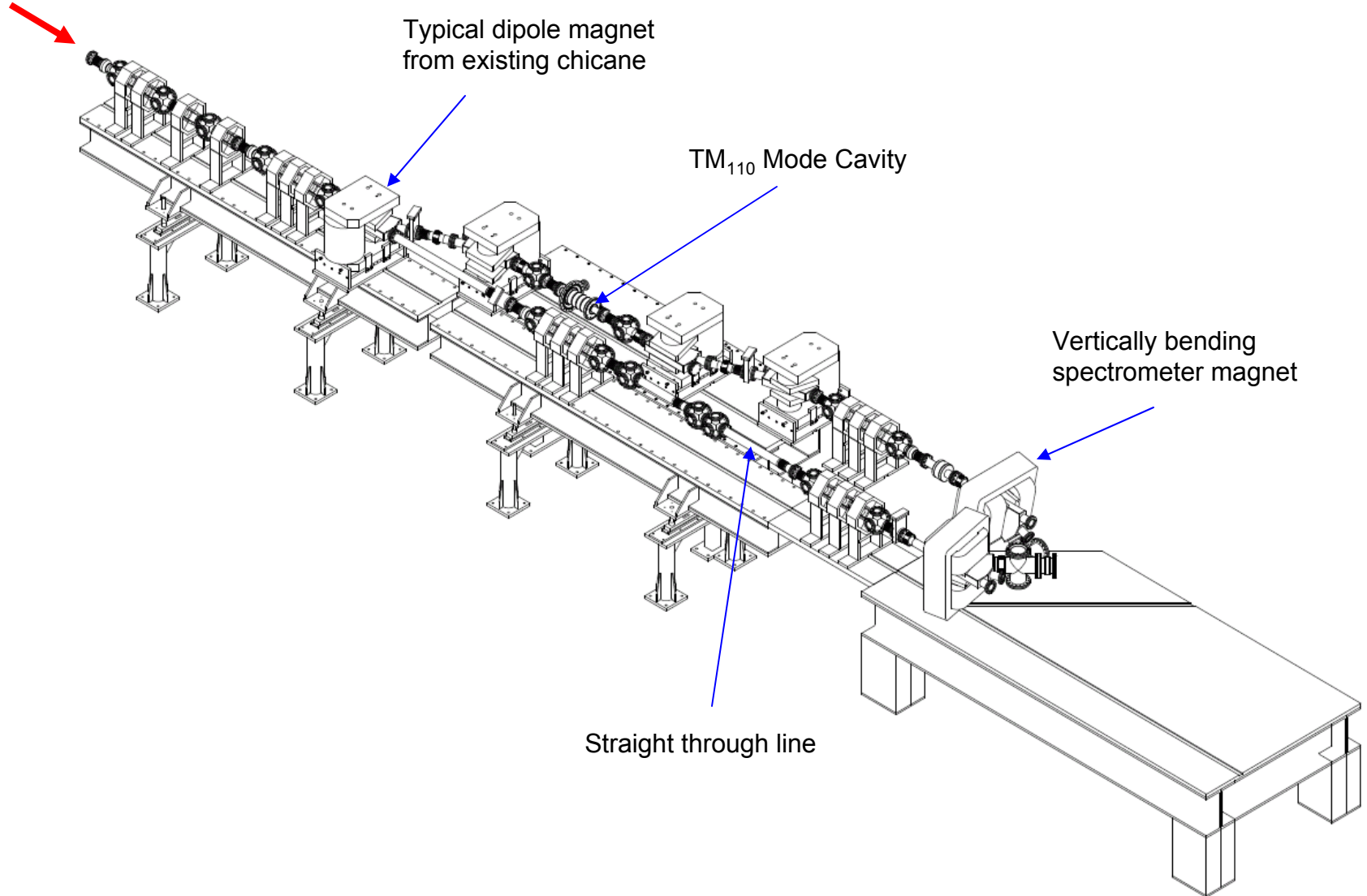
1nC/bunch (typically 10 bunches), nominal energy: 15MeV

$\epsilon_{\text{rms-x}}$  &  $\epsilon_{\text{rms-y}} \sim 3 \text{ mm mrad}$  (measured & from ASTRA)

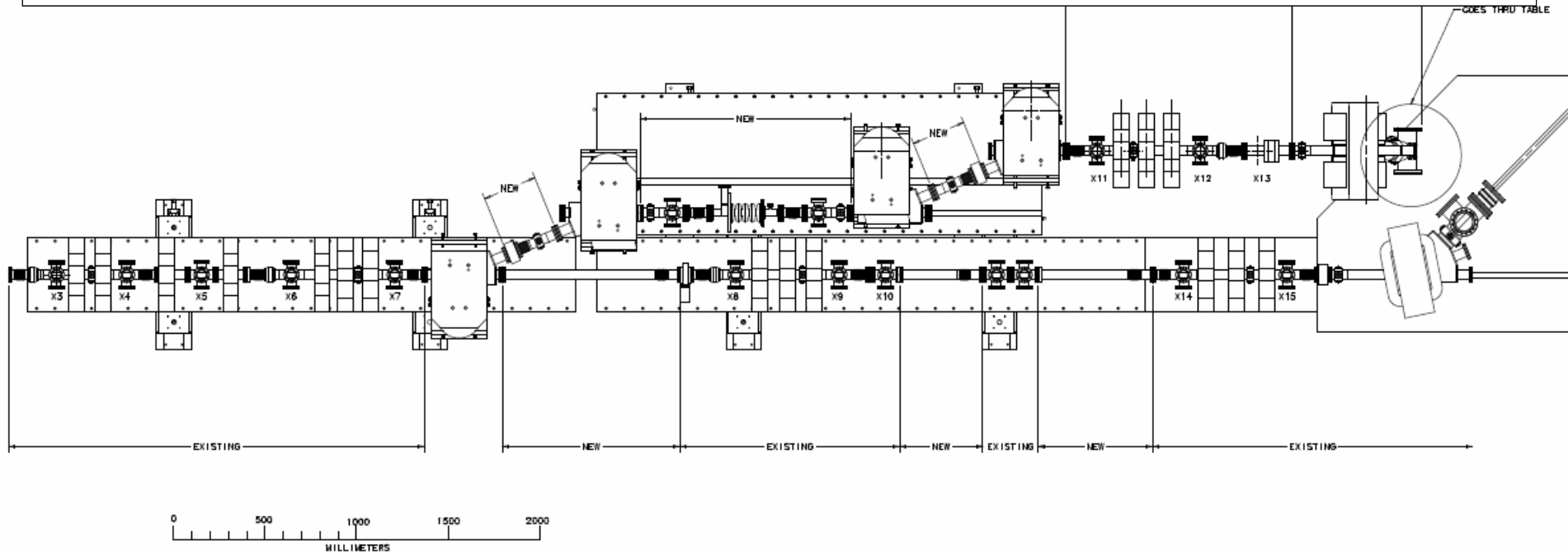
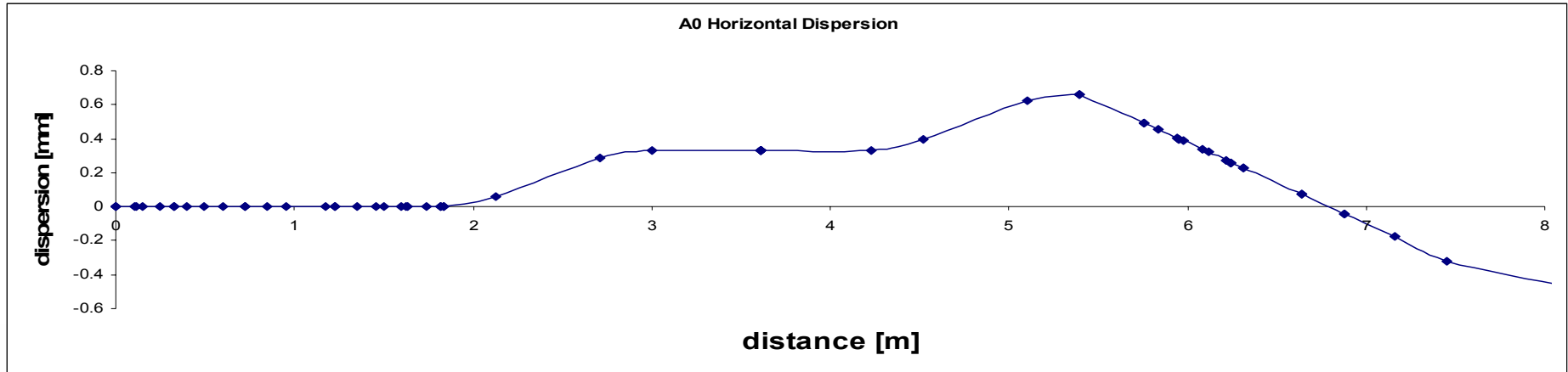
$\epsilon_{\text{rms-z}} = 23 \text{ mm mrad}$  (from ASTRA)

# A0 Beam Line Layout

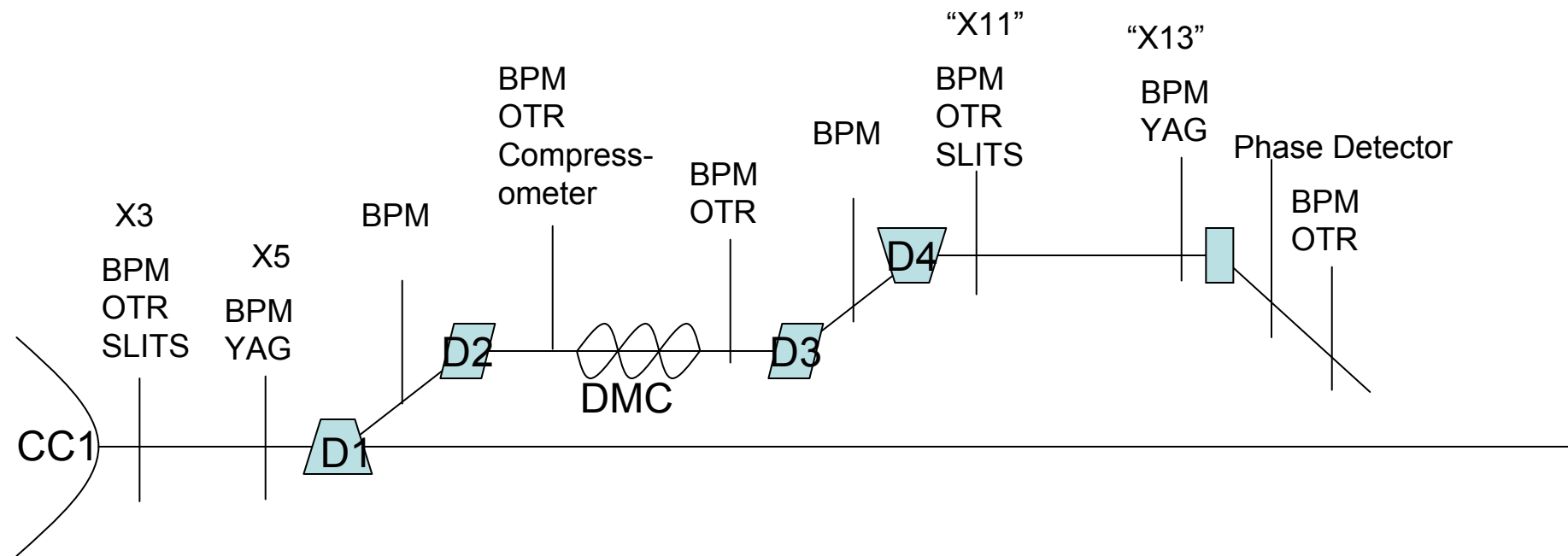
15 MeV beam from 9-cell



# Beam Line Layout

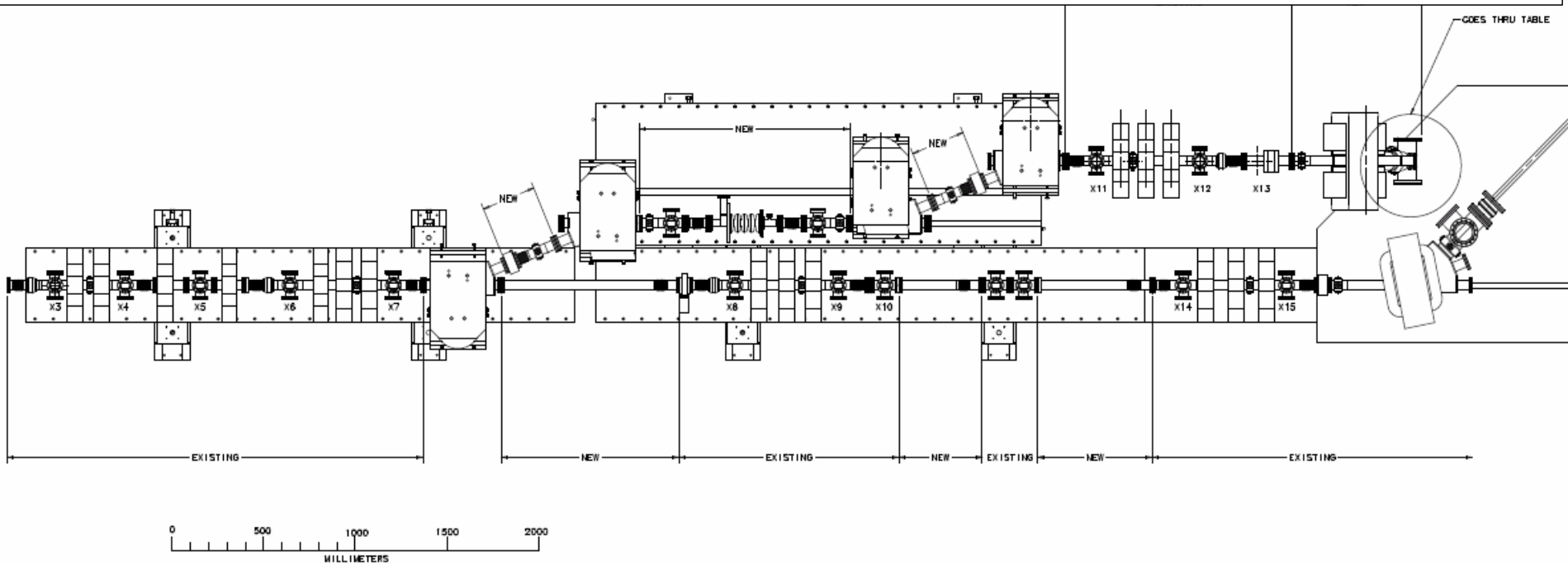
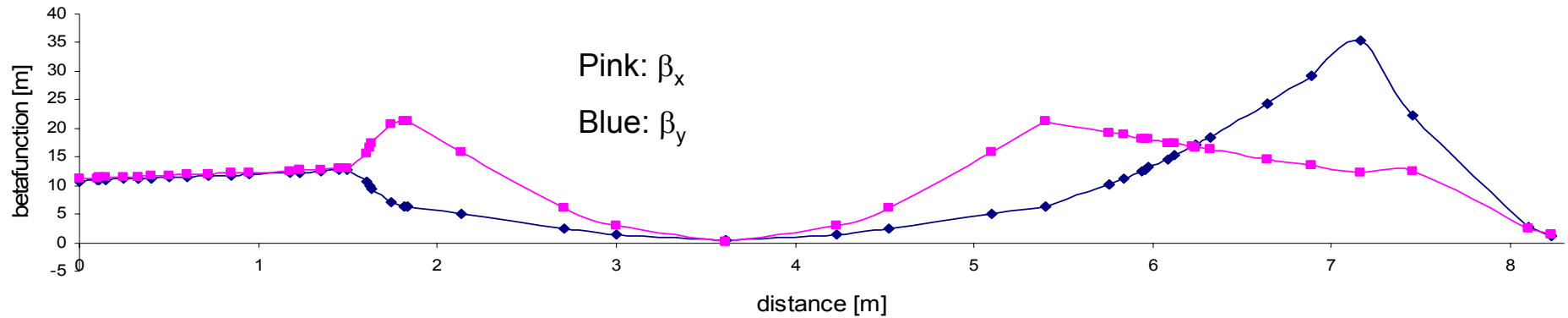


# Beam Line Diagnostics



# Twiss Parameters

Beta Functions

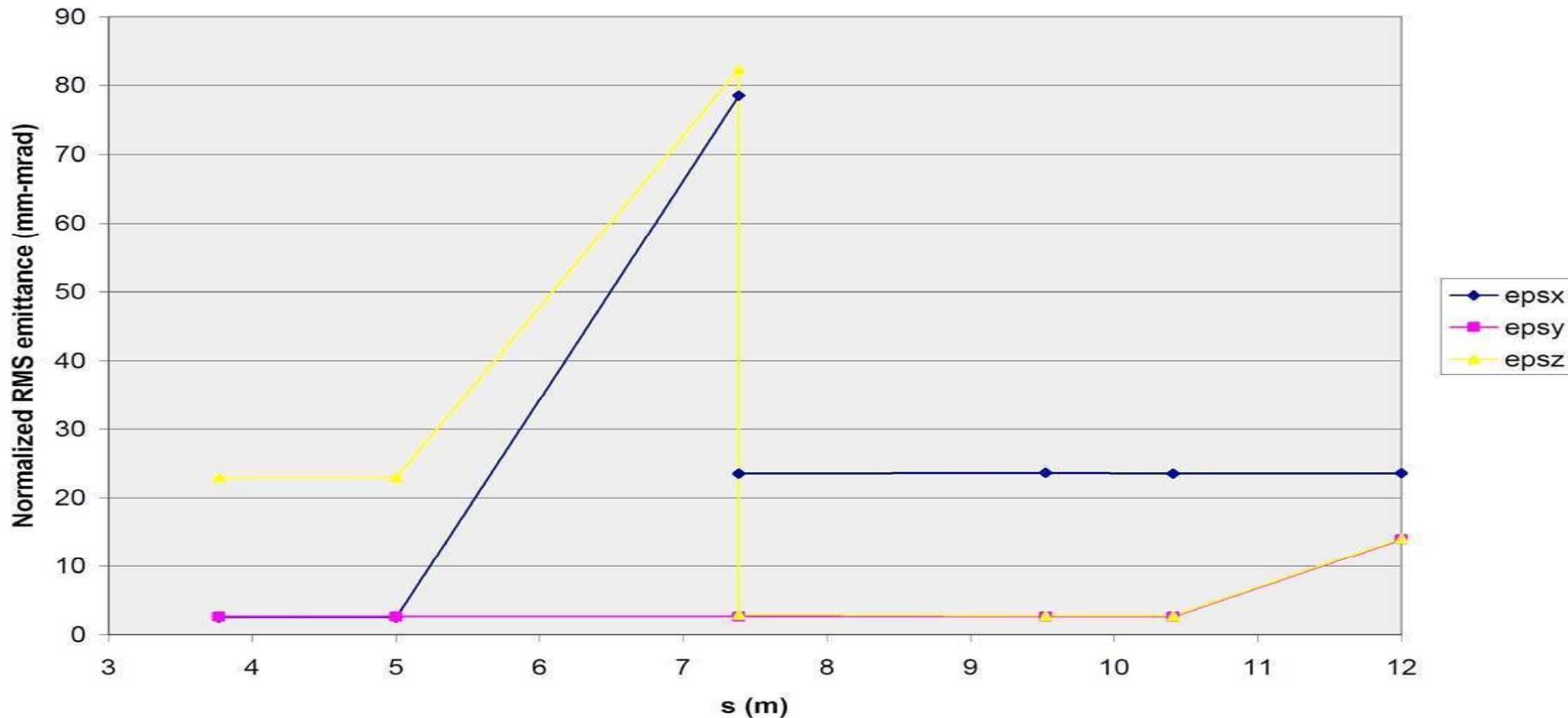


# Beam Line Simulations

ASTRA models the beam line from the cathode to the exit of the 9 cell superconducting cavity.

ELEGANT is used from the output of the 9-cell to the dump.

**Emittance Along Beamline**



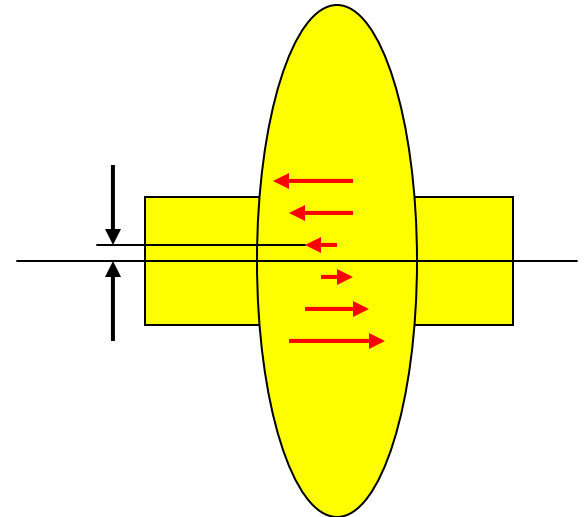
# Required off axis Longitudinal E-Field

$$\frac{\Delta E}{E_o} \approx \frac{\Delta p}{p} \qquad \Delta X_{disp} = D \frac{\Delta p}{p}$$

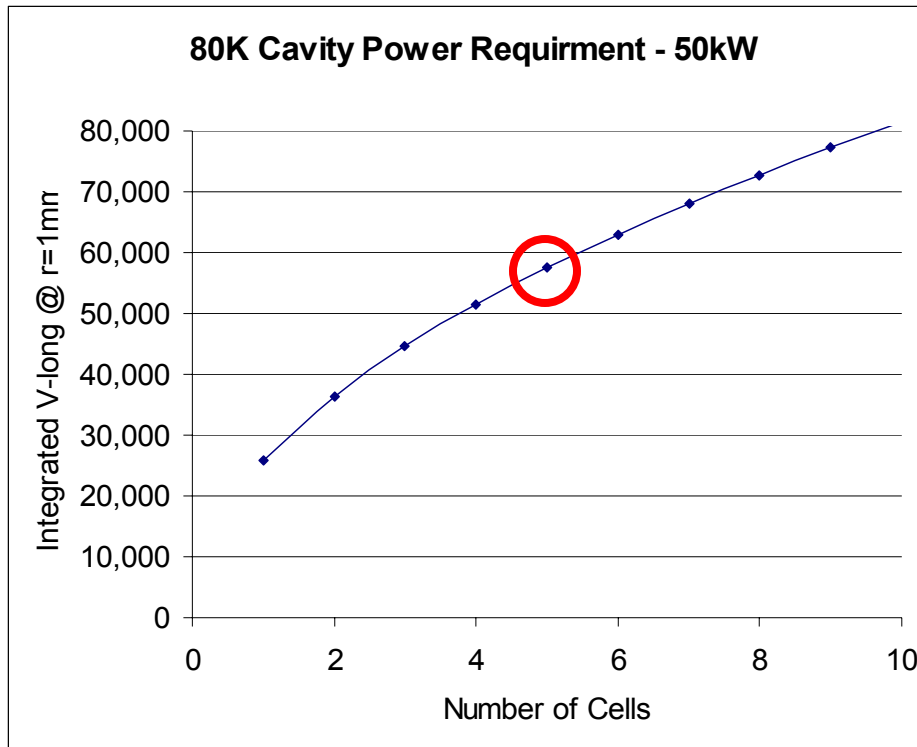
$$\frac{\Delta E}{\Delta x} = \frac{\partial E}{\partial x} = \frac{E_o}{D}$$

Where  $E_o$  is 15MeV and  $D = 0.330m$

$$\frac{\partial E}{\partial x} = \frac{15MeV}{0.33m} = 45.5keV / mm$$



# 3.9 GHz Power Requirements



80K Q of 36,000 shows 50 kW is fine

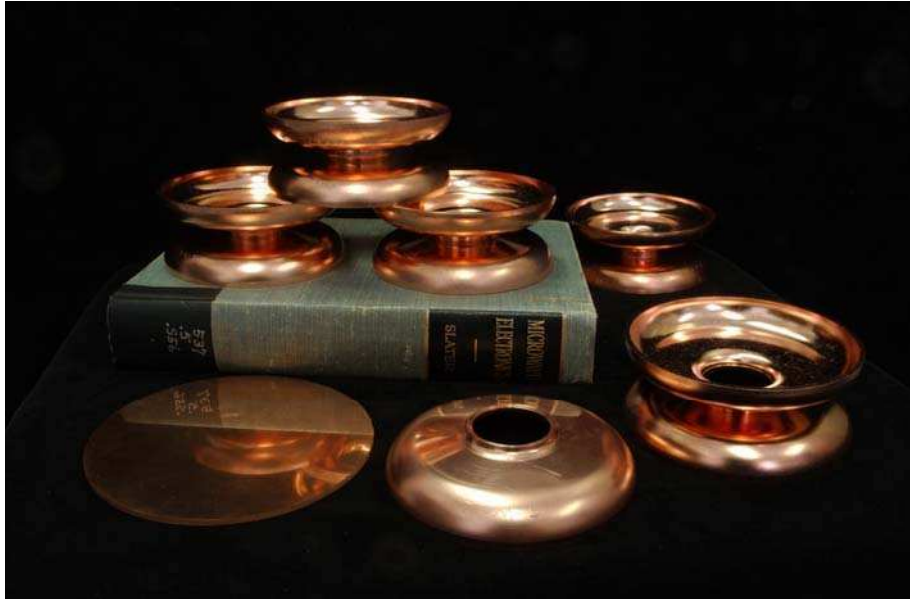
(We will be using an existing 3<sup>rd</sup> harmonic input coupler)

An 80 kW 3.9 GHz klystron is being installed in A0 for 3<sup>rd</sup> Harmonic Input Coupler Processing. We will use this for our cavity. Commissioning of the klystron is beginning next week !





# TM<sub>110</sub> Copper Cavity



Half cells were punched from 0.093" copper disks at AES.

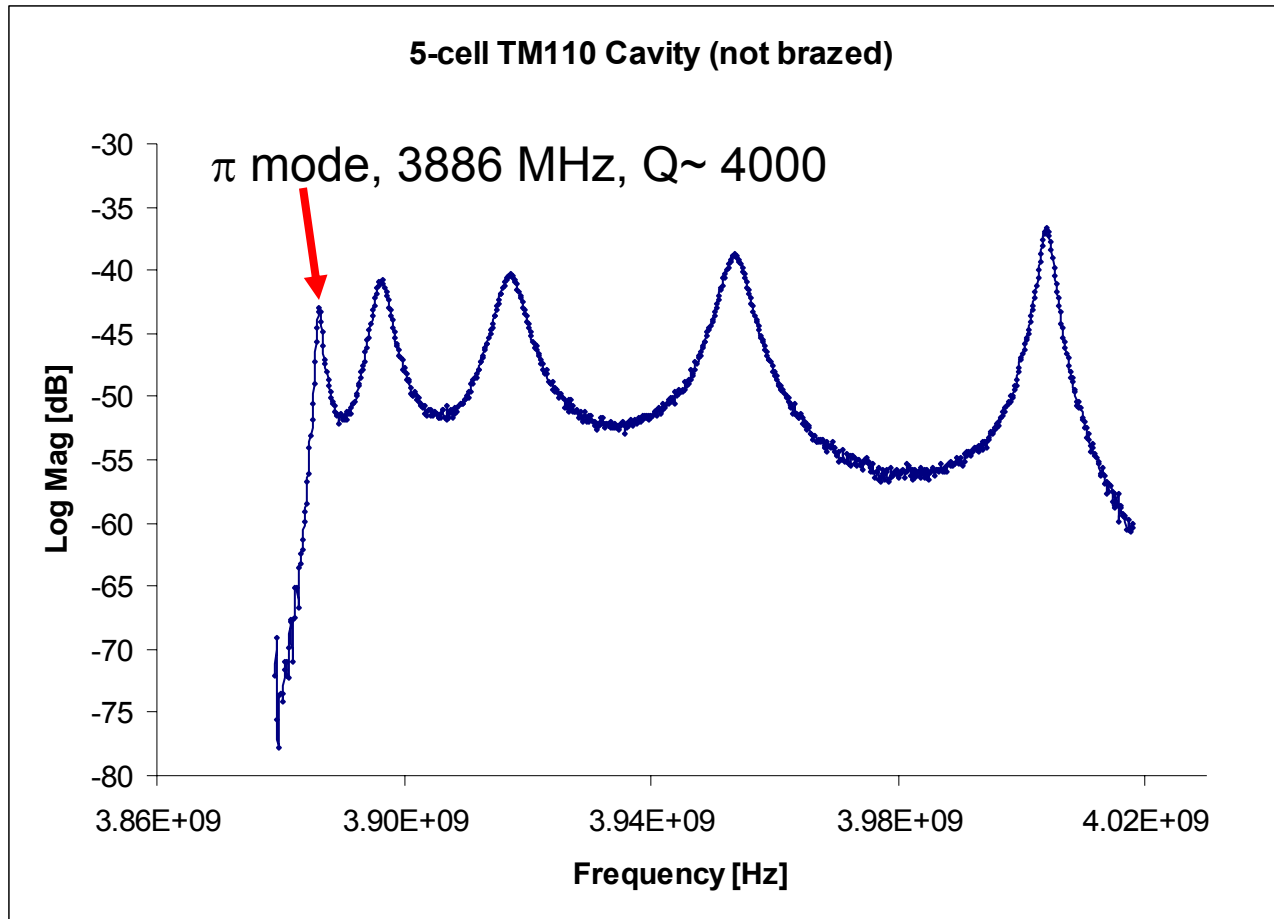
Half cells are 1<sup>st</sup> brazed at iris to form dumbbells.

Measure dumbbells & trim to freq.

There is close proximity of one end cell, input coupler, and LN2 tank flange. Therefore these parts were machined from a copper block.

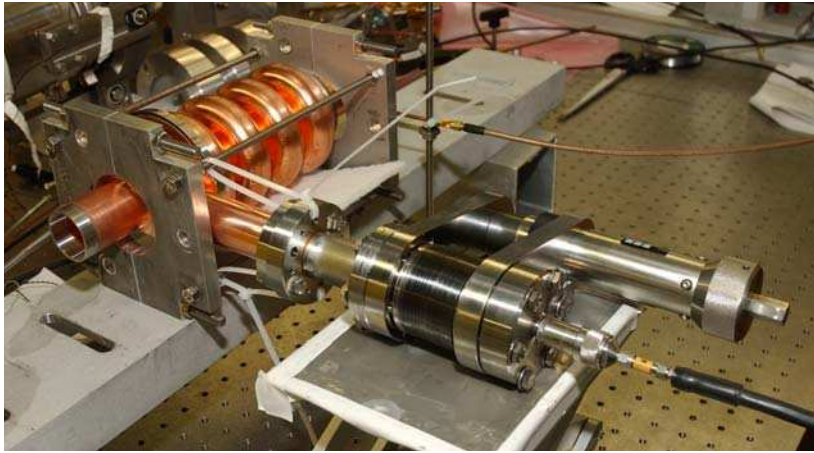


# Measure Stacked Dumbbells



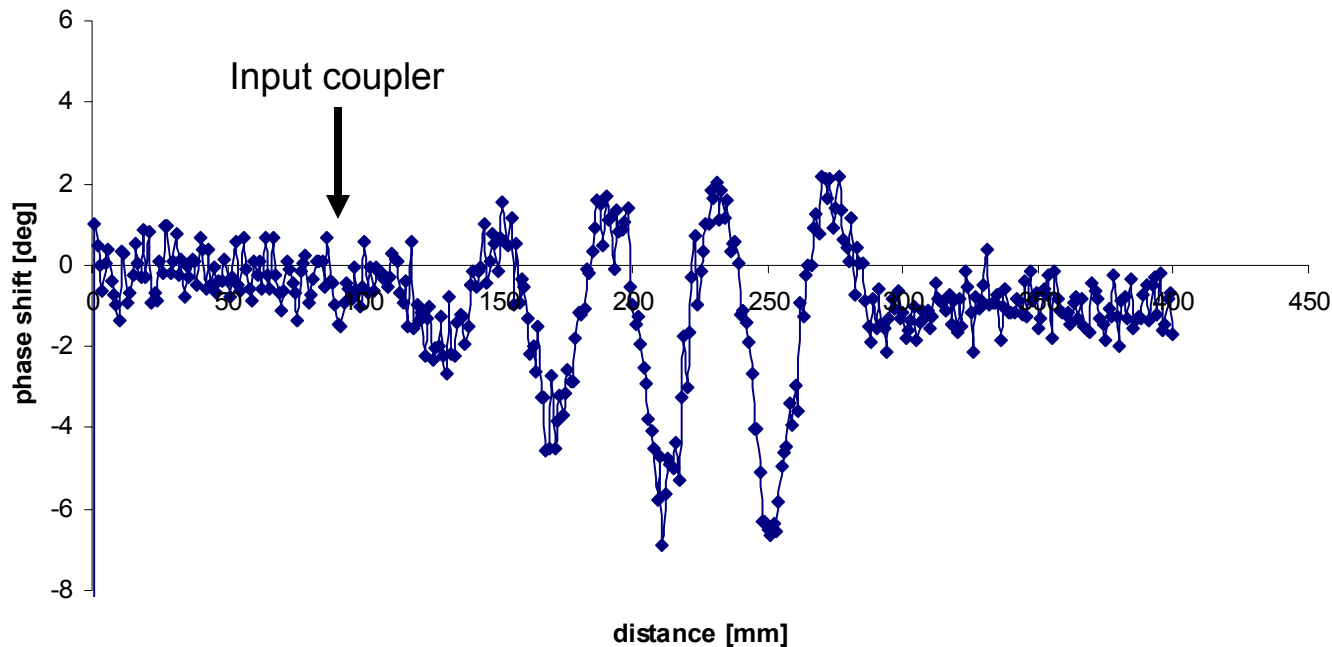
Shows why 5 cells is the upper limit – from mode spacing.

# Bead Pull for Field Flatness



Initial bead pull shows that “solid” input coupler end cell frequency is higher than the others.

5-cell bead pull (not brazed)



# Problems:

Input Coupler End (ICE) machined 0.168mm too short (3MHz too high)

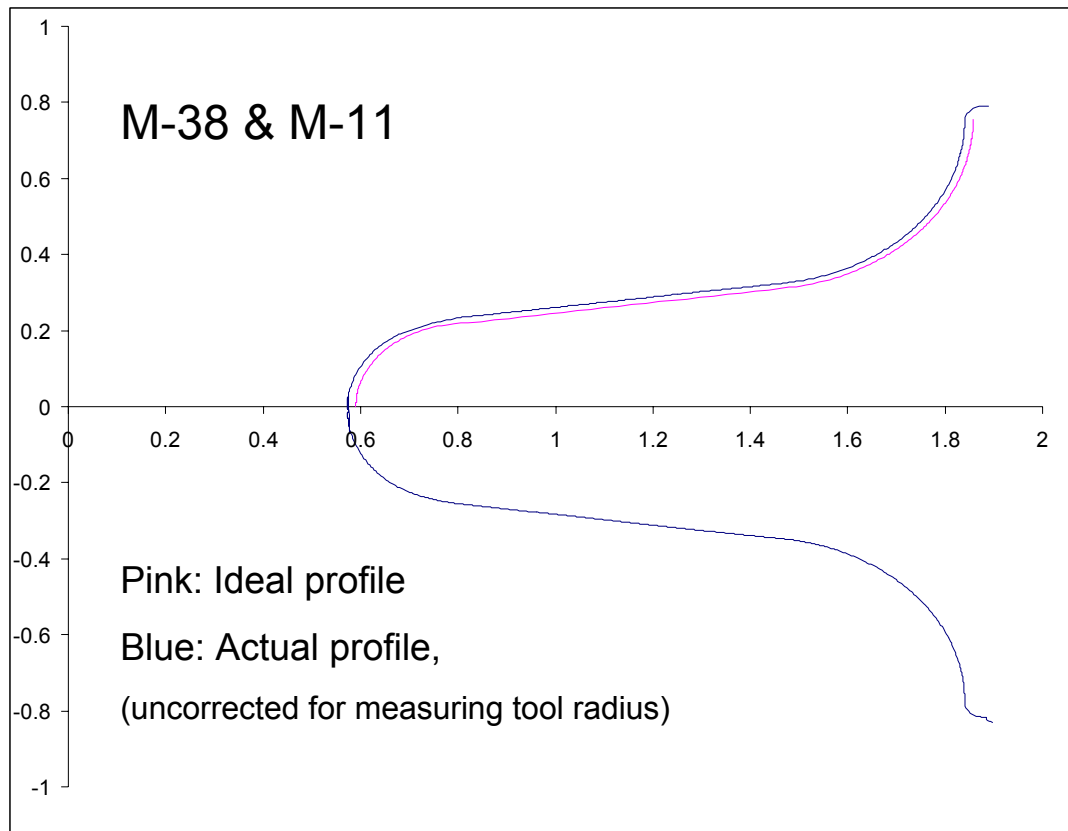
Dumbbells shrinkage due to vacuum leak check (0.022 inches, ~ 10MHz low)

Restored initial length, but frequency did not follow

0.014 inches too much trimmed (3MHz too high)

Dumbbells are physically too long by ~ 1mm.

Cavity profile in question → CMM'ing First data taken Monday:



Four radial profiles taken (90 deg increments) on dumbbell M38-M11.

Needs analysis....

Rest are being scanned.

# Highlights of Time Line

| ID | Task_Name                                  | Duration    | Start_Date   | Finish_Date  | Predecessors          | Resource_Names |
|----|--------------------------------------------|-------------|--------------|--------------|-----------------------|----------------|
| 1  | <b>Preparation</b>                         | 95.63 days? | Thu 11/16/06 | Thu 3/22/07  |                       |                |
| 7  | Remaining Optical design of Beamline       | 2 wks       | Thu 11/16/06 | Thu 11/30/06 |                       |                |
| 9  | Design Beamline Vacuum                     | 3 days      | Wed 12/6/06  | Fri 12/8/06  | 8                     |                |
| 10 | Aquire BPM buttons                         | 4 mons      | Mon 11/27/06 | Fri 3/9/07   |                       |                |
| 25 | Aquire vacuum components for Tim's Line    | 6 wks?      | Wed 12/6/06  | Wed 1/17/07  | 7,8                   |                |
| 26 | Aquire vacuum components for straight line | 6 wks?      | Wed 12/6/06  | Wed 1/17/07  | 7,8                   |                |
| 27 | <b>Installation Phase I</b>                | 23 days?    | Wed 1/17/07  | Wed 2/14/07  | 3,26,20               |                |
| 28 | Break Vacuum                               | 1 day?      | Wed 1/17/07  | Wed 1/17/07  |                       |                |
| 31 | Modify A0 Beamline                         | 2 wks?      | Mon 1/22/07  | Fri 2/2/07   | 29                    |                |
| 32 | Install Dogleg Dipole 1                    | 1 day?      | Fri 2/2/07   | Mon 2/5/07   | 31                    |                |
| 36 | Commission new A0 Beamline                 | 2 days      | Thu 1/25/07  | Mon 1/29/07  | 35                    |                |
| 37 | <b>Installation Phase II</b>               | 32 days?    | Thu 3/22/07  | Tue 5/1/07   | 12,25,24,7,8,19,20,22 |                |
| 38 | Break Vacuum                               | 1 day?      | Thu 3/22/07  | Thu 3/22/07  |                       |                |
| 39 | Install RF cavity                          | 3 days      | Fri 3/23/07  | Tue 3/27/07  | 38                    |                |
| 41 | Close vacuum                               | 3 days      | Fri 4/13/07  | Tue 4/17/07  | 40                    |                |
| 44 | Commission Tim's Cavity                    | 2 wks?      | Tue 5/1/07   | Mon 5/14/07  | 37                    |                |
| 45 | Commission new beamline                    | 7 days      | Tue 5/1/07   | Wed 5/9/07   | 37                    |                |
| 46 | Commission new interlocks                  | 1 day       | Tue 5/1/07   | Wed 5/2/07   | 37                    |                |
| 47 | Rad Safety Clearance                       | 1 day?      | Wed 5/9/07   | Thu 5/10/07  | 46,37,45              |                |
| 48 | Make Measurment                            | 4 mons      | Mon 5/14/07  | Tue 8/21/07  | 47,44                 |                |
| 49 | Tim Writes Thesis                          | 6 mons      | Tue 8/21/07  | Thu 1/17/08  | 48                    |                |
| 50 | Tim Graduates                              | 0 days      | Thu 1/17/08  | Thu 1/17/08  | 49                    |                |



# ***Keep alive e<sup>+</sup> source for the ILC***

*Wei Gai, Wanming Liu*

**ANL**

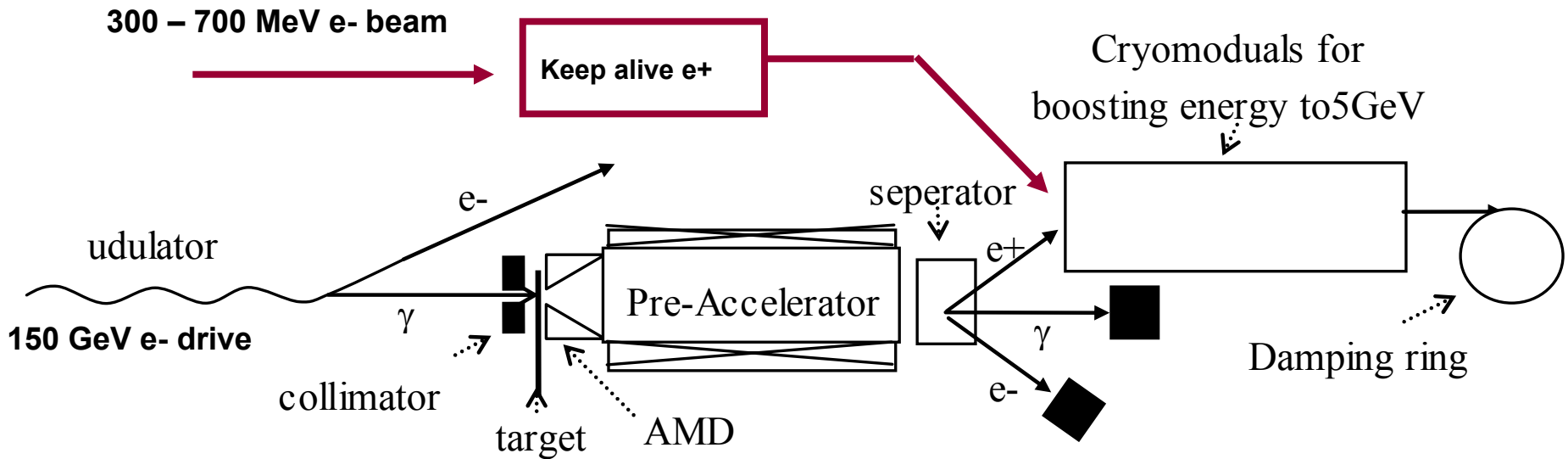
***Argonne National Laboratory***



A U.S. Department of Energy  
Office of Science Laboratory  
Operated by The University of Chicago

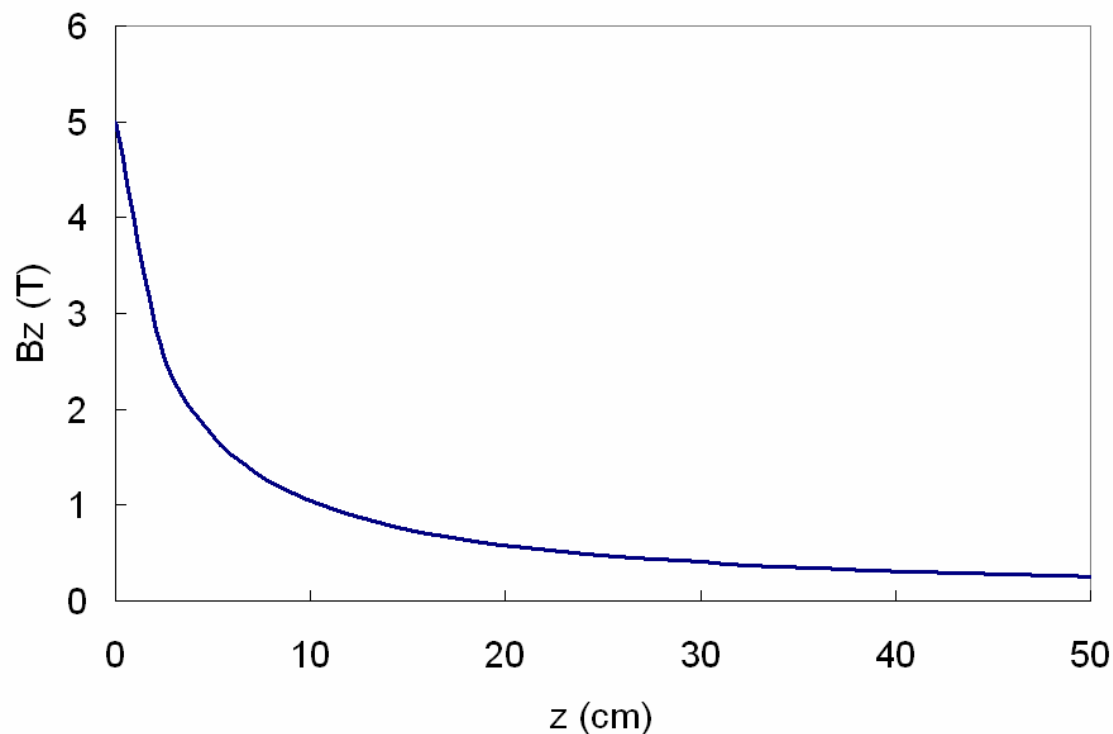


# Complete modeling of undulator based $e^+$ source\*



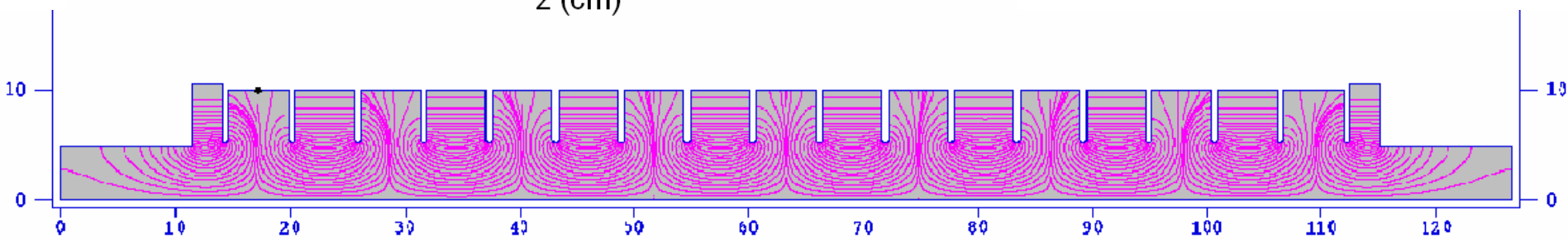
\*Working with collaborators (SLAC/DESY/CCRL)

# AMD profile and PreAccelerator Filed Map



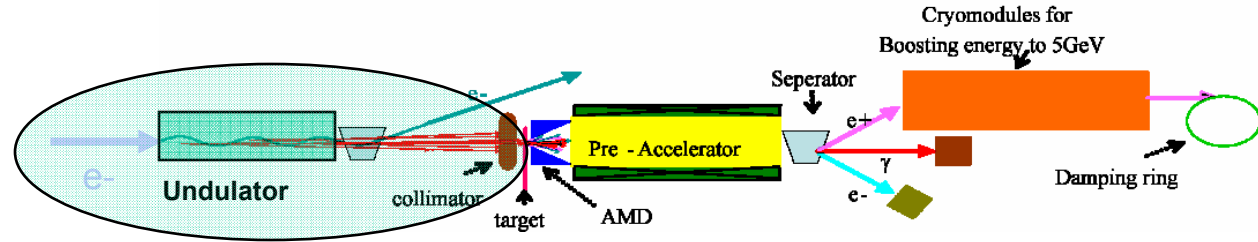
AMD field: 5T-0.25T in 50cm

Accelerating gradient in  
preaccelerator: 12MV/m





# Photon Spectrum and Polarization of ILC baseline undulator



Results of photon number spectrum and polarization characteristic of ILC undulator are given here as examples. The parameter of ILC undulator is  $K=1$ ,  $\lambda_u=1\text{cm}$  and the energy of electron beam is  $150\text{GeV}$ .

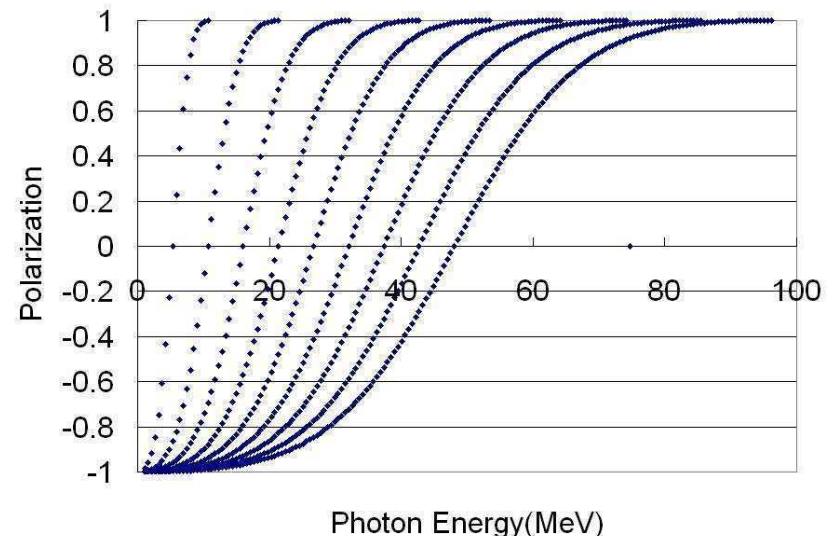
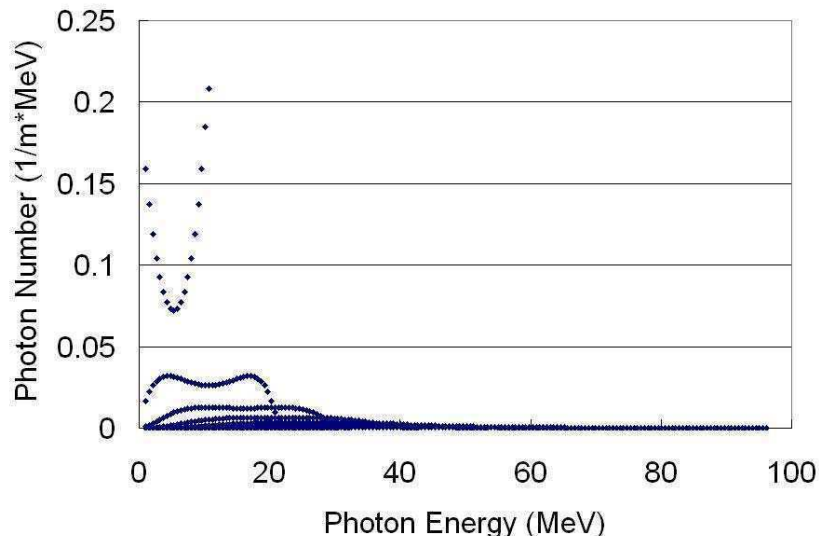
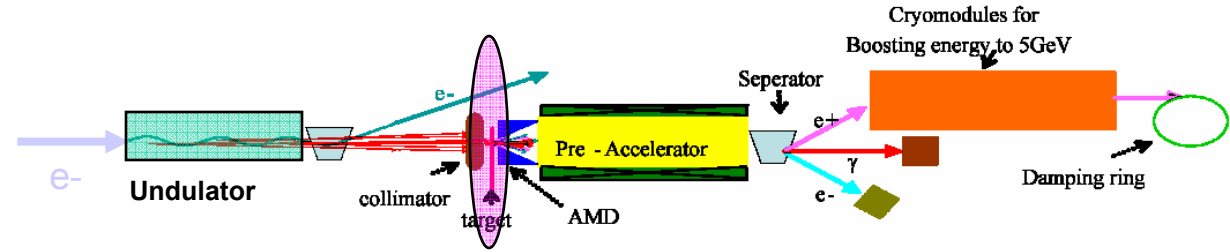
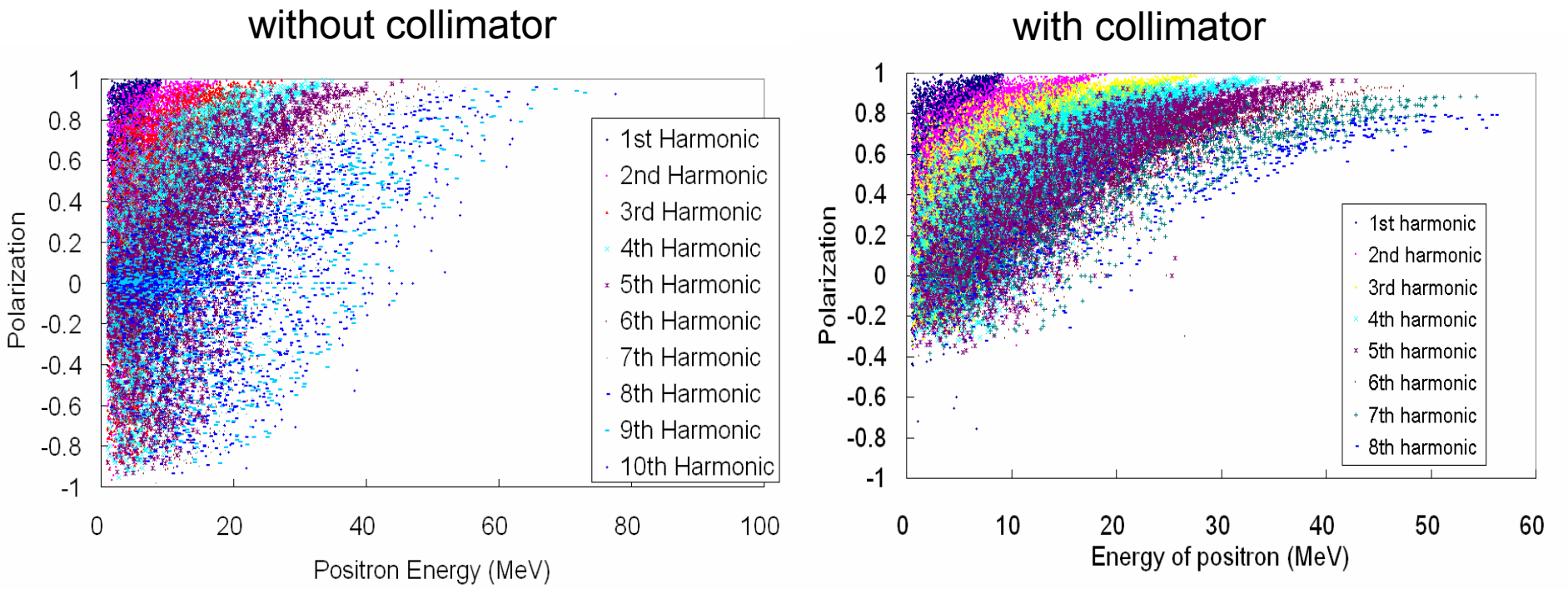


Figure1. Photon Number spectrum and polarization characteristics of ILC undulator up to the 9<sup>th</sup> harmonic

# Comparison of the generated positron polarization spectrum: with/without collimator.

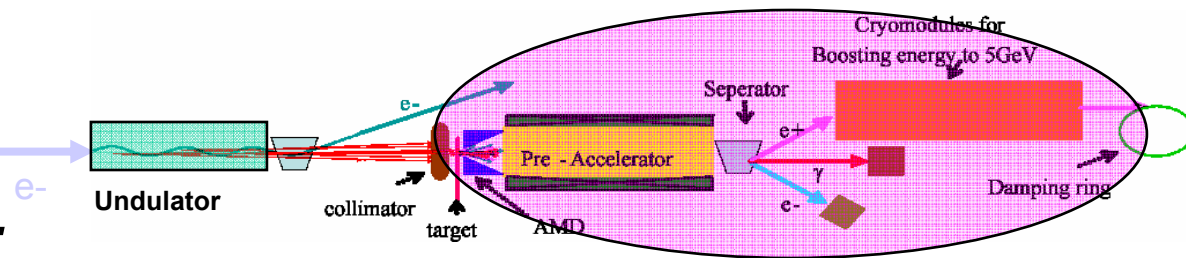


## Initial distribution of polarization of positrons



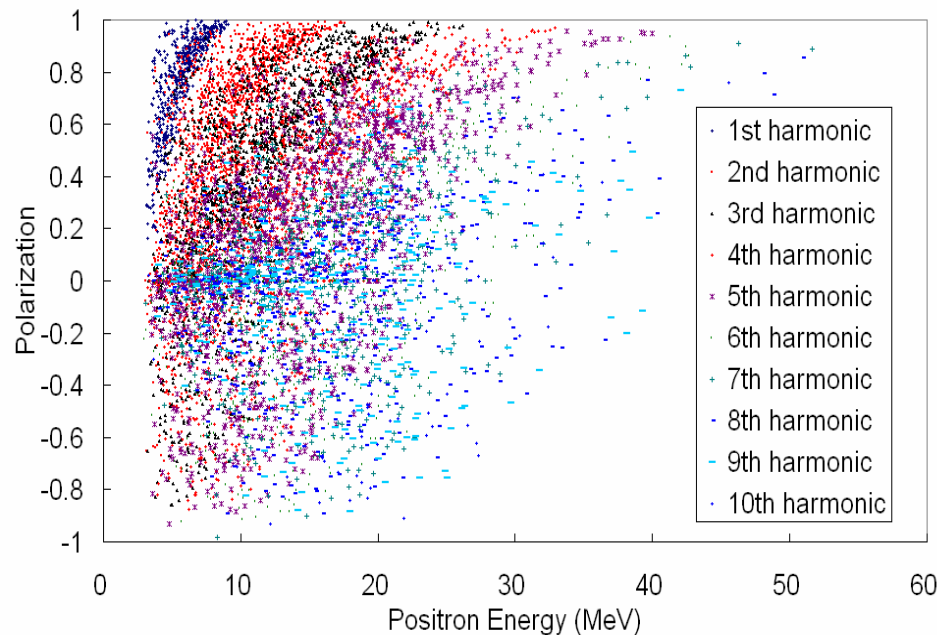
The collimator is 2.5mm in radius and is 700m away from the end of a 100m long undulator. Photons are radiated uniformly along the undulator. For the case without collimator, the photon source is treated as a point source. The collimator screened out those photon with lower polarization and thus improved the positron polarization.

# Comparison of the captured positron polarization spectrum: with/without collimator.

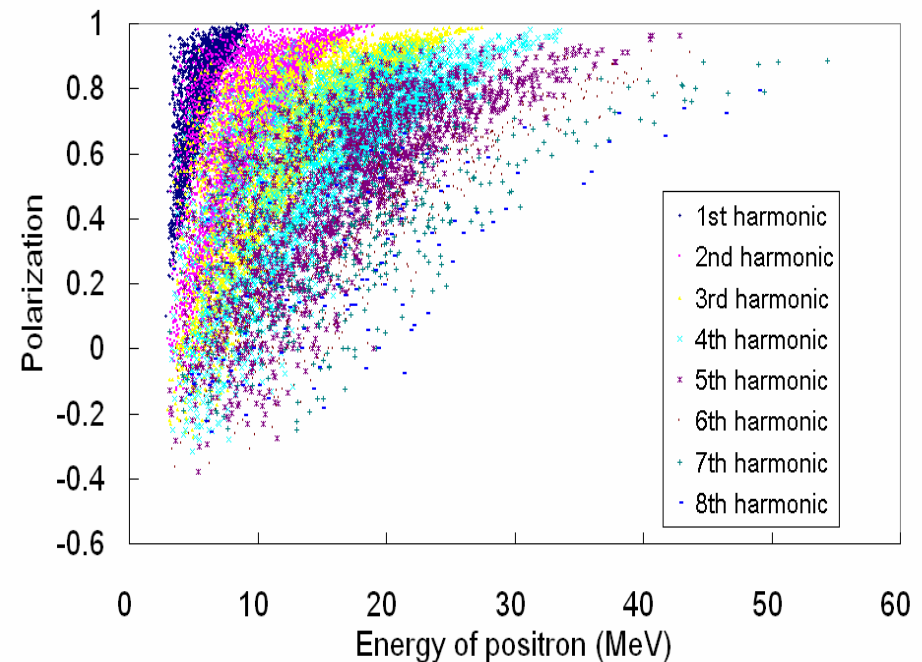


Initial Polarization vs energy of those captured positrons

Without collimator



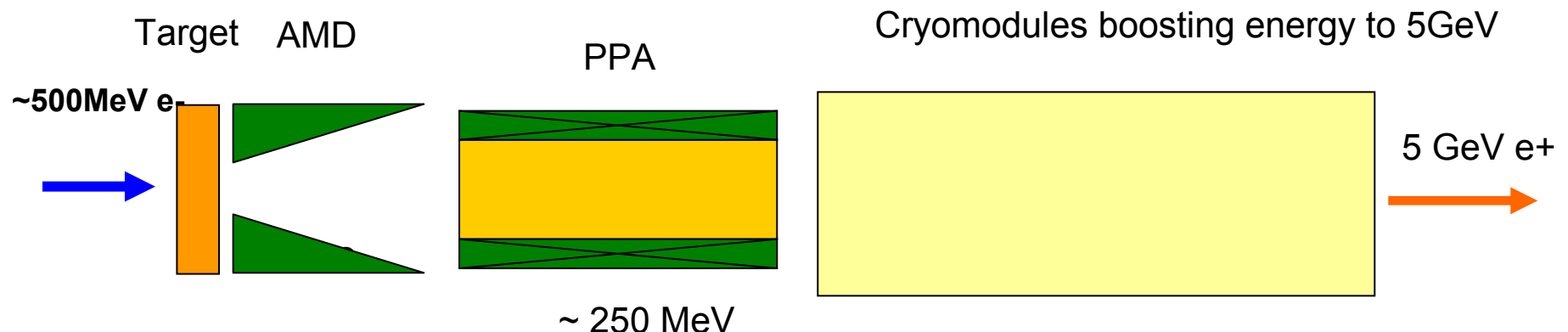
With collimator



The capturing optics are the same for both with and without collimator. The collimator screened out those photons with lower polarization and thus improved the polarization of resulting positron beam. The polarization of captured positron beam is about 30% without collimator and 63% with the collimator setting used here.

# Keep alive positron source

- Functions as a backup/commissioning  $e^+$  source when undulator based  $e^+$  not available.
- From GDE: a 0.3 nC  $e^+$  beam keep alive source from a conventional target with drive beam energy of  $\sim 500$  MeV and maximum intensity of  $\sim 4 \times 10^{10} e^-$
- Identical beam line for polarized positron source is used. When AMD is off, the AMD field is replaced by a uniform  $B_z$  field of 0.25T.
- Damping ring acceptance: 1% energy spread and  $\gamma A_x + \gamma A_y < 0.09$  m-rad.
- The positron yield is normalized to per incident electron.



## Comparison between different target configure

| Target             | e- Beam size | e- Energy     | Raw Yield     | Emittance    | Capture Yield | AMD        |
|--------------------|--------------|---------------|---------------|--------------|---------------|------------|
| <b>0.2 r.l. Ti</b> | <b>1mm</b>   | <b>500MeV</b> | <b>0.0375</b> | <b>0.007</b> | <b>0.011</b>  | <b>ON</b>  |
| <b>0.4 r.l. Ti</b> | <b>1mm</b>   | <b>500MeV</b> | <b>0.126</b>  | <b>0.011</b> | <b>0.031</b>  | <b>ON</b>  |
| <b>4.0 r.l. W</b>  | <b>1mm</b>   | <b>500MeV</b> | <b>1.327</b>  | <b>0.021</b> | <b>0.216</b>  | <b>ON</b>  |
| <b>0.2 r.l. Ti</b> | <b>1mm</b>   | <b>500MeV</b> | <b>0.0375</b> | <b>0.007</b> | <b>0.0034</b> | <b>OFF</b> |
| <b>0.4 r.l. Ti</b> | <b>1mm</b>   | <b>500MeV</b> | <b>0.126</b>  | <b>0.011</b> | <b>0.008</b>  | <b>OFF</b> |
| <b>4.0 r.l. W</b>  | <b>1mm</b>   | <b>500MeV</b> | <b>1.327</b>  | <b>0.021</b> | <b>0.029</b>  | <b>OFF</b> |

Energy deposition for recommended e- energy(500MeV) and intensity( $4e^{10}$ ) are:

- 0.2 rl Ti: 0.0336(J)
- 0.4 rl Ti: 0.0757(J)
- 4.0 rl W: 1.17 (J)

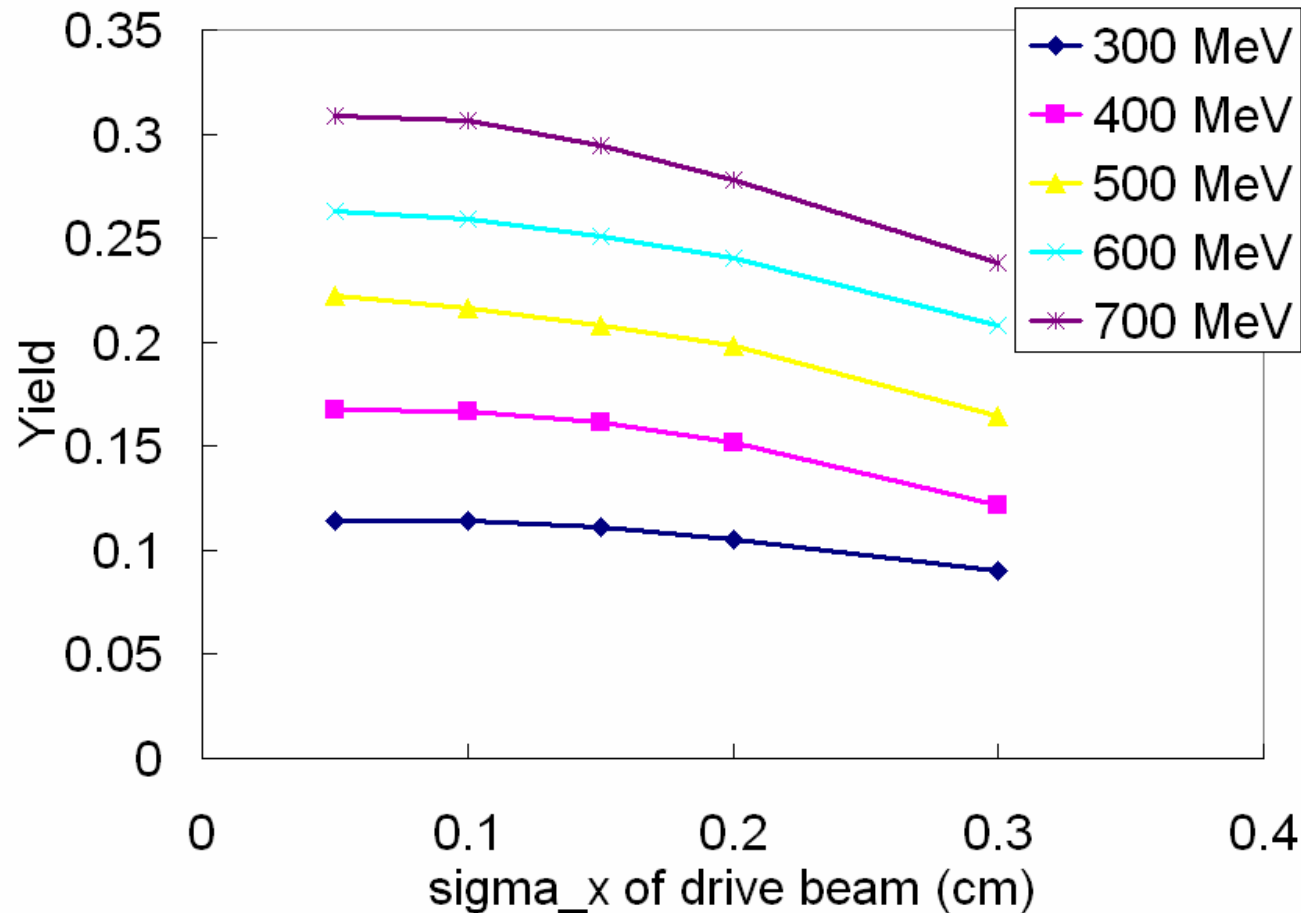
# Minimum requirements

| Target            | e- Beam size | e- Energy                          | Raw Yield    | Capture Yield   | AMD        |
|-------------------|--------------|------------------------------------|--------------|-----------------|------------|
| <b>4.0 r.l. W</b> | <b>2mm</b>   | <b>300MeV</b>                      | <b>0.717</b> | <b>0.105</b>    | <b>ON</b>  |
| <b>4.0 r.l. W</b> | <b>0.5mm</b> | <b>700MeV*</b><br><b>Double e-</b> | <b>1.908</b> | <b>&gt;0.05</b> | <b>OFF</b> |

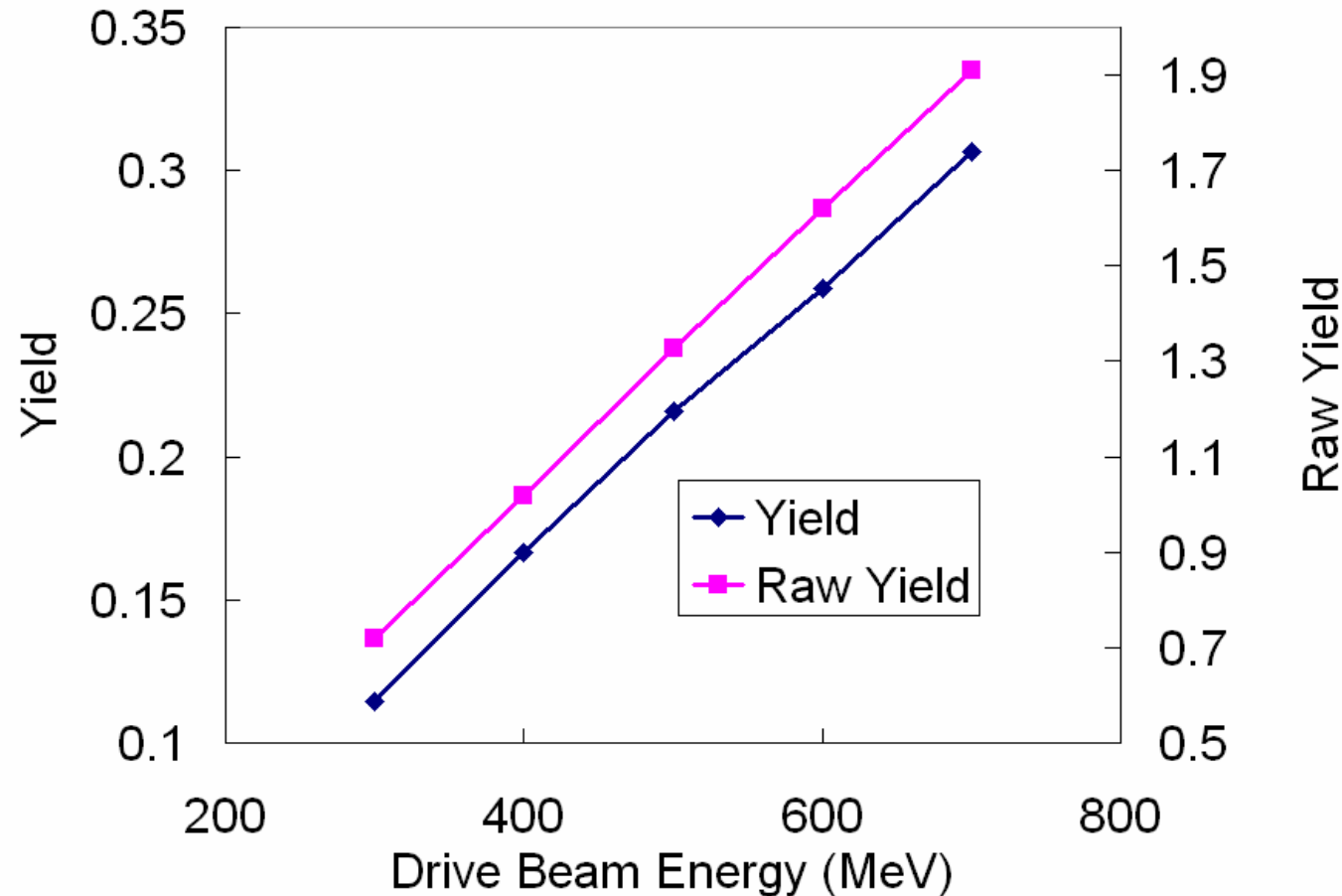
NOTE: The captured yield for 4 rl W when AMD off is estimated with assumption of bunch compressing in beamline (it was shown by Roger, Juwen and Klauss that compression could enhance the yield by 20 – 30%).

# ***Captured Yield vs drive beam spot size***

## ***Target: 4rl, W, AMD on***



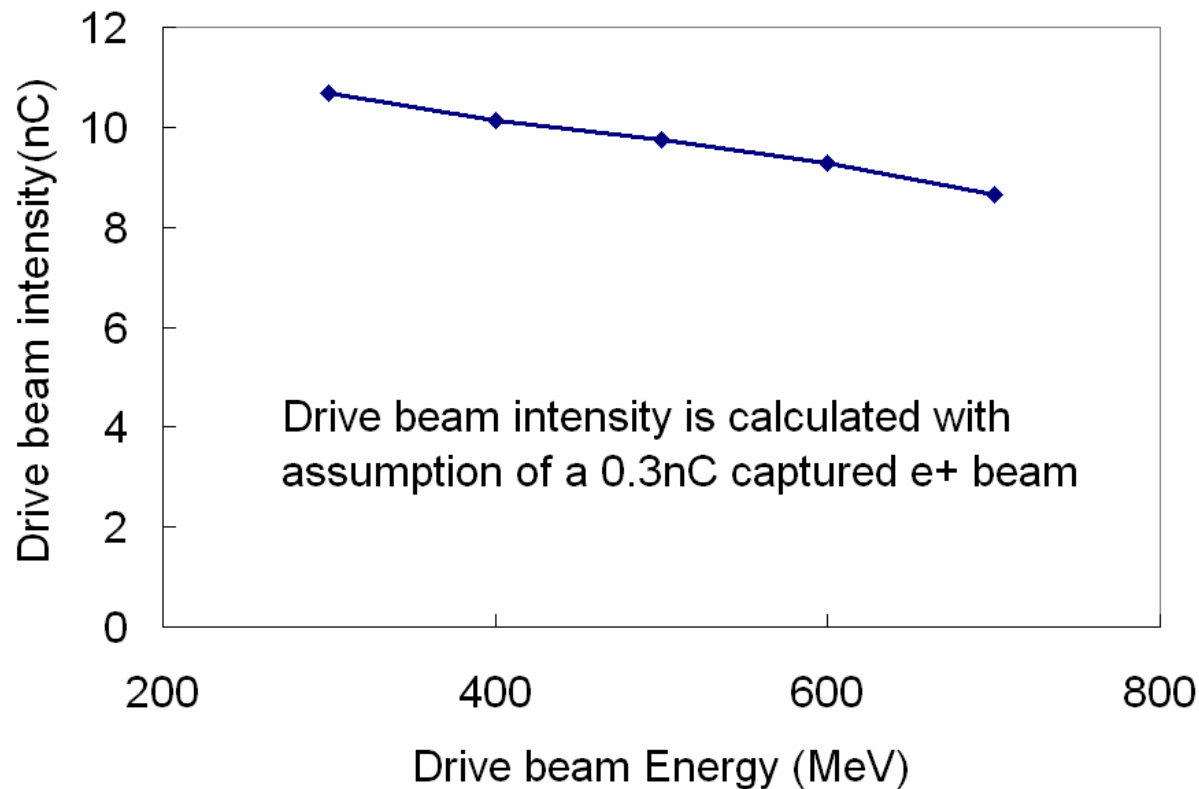
# ***Captured Yield and Raw yield vs drive beam energy, Target: 4rl, W***





# ***Drive beam intensity required to generate 0.3nC captured e<sup>+</sup> beam, target: 4rl, W, AMD off***

Drive beam size:  $\sigma=1\text{mm}$



# Summary

- The keep-alive source can be made with 300 – 700 MeV drive beam.
- The capturing schemes need to be improved for no AMD option.
- The ILCTA can be a place to test some of the capturing components.





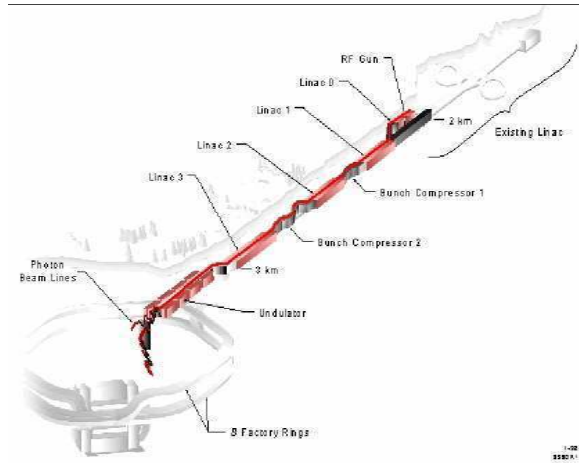
# EO sampling Experiment in ILCTA

---

Jinhao Ruan  
A0 Photon Injector  
Fermi lab

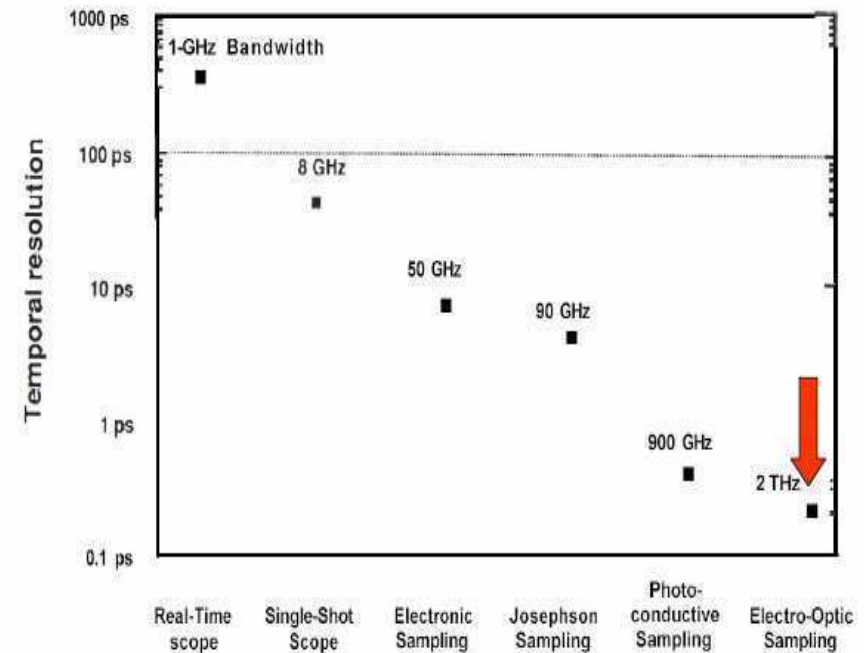
# Motivation

- o LCLS: 200 fs FWHM @ 15 GeV



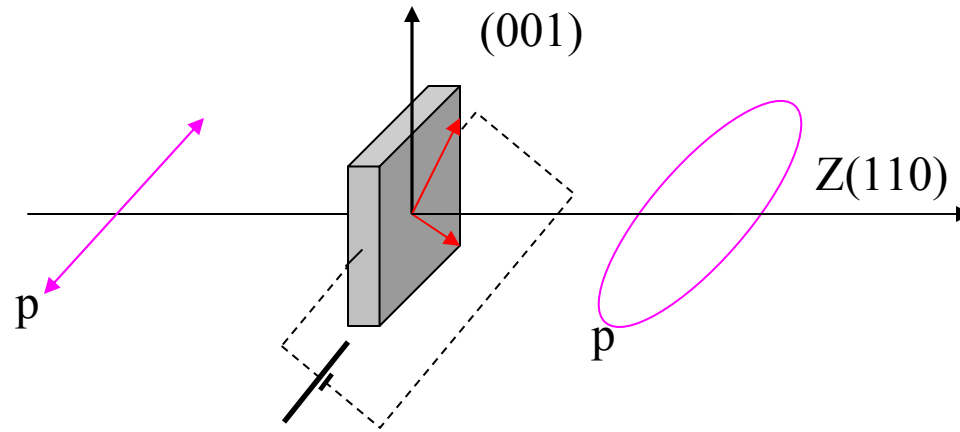
- o LUX: 30 fs FWHM @ 3 GeV
- o ILCTA: < 1 ps rms

## *Impact of Optics on Ultrafast Electronics*

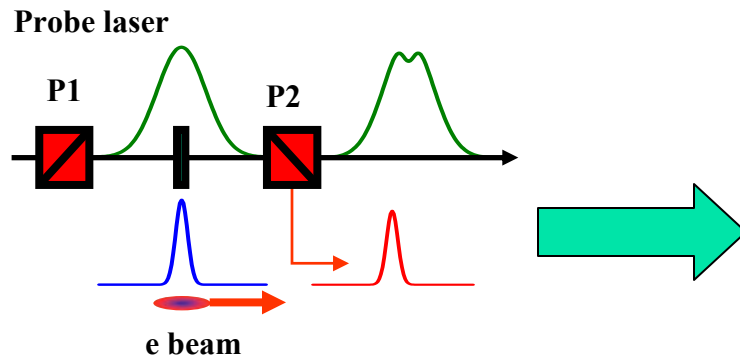


# Principle of EOS

## Pockel's effect (ZnTe)



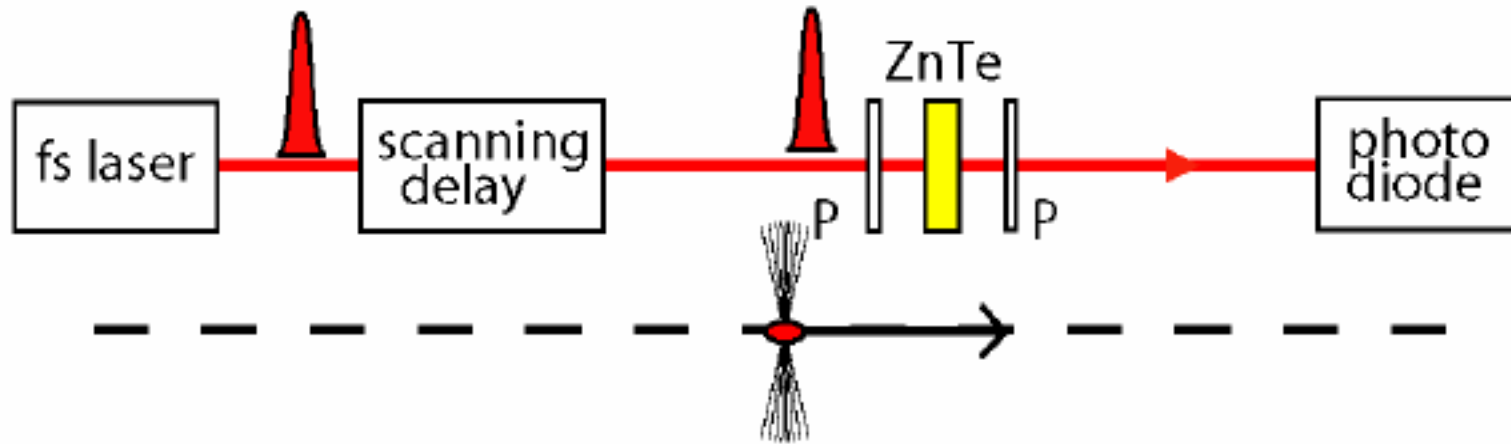
By detecting this phase shift we will know the electrical field



- Scanning Delay sampling
- Spectral decoding
- Temporal decoding
- Spatial decoding

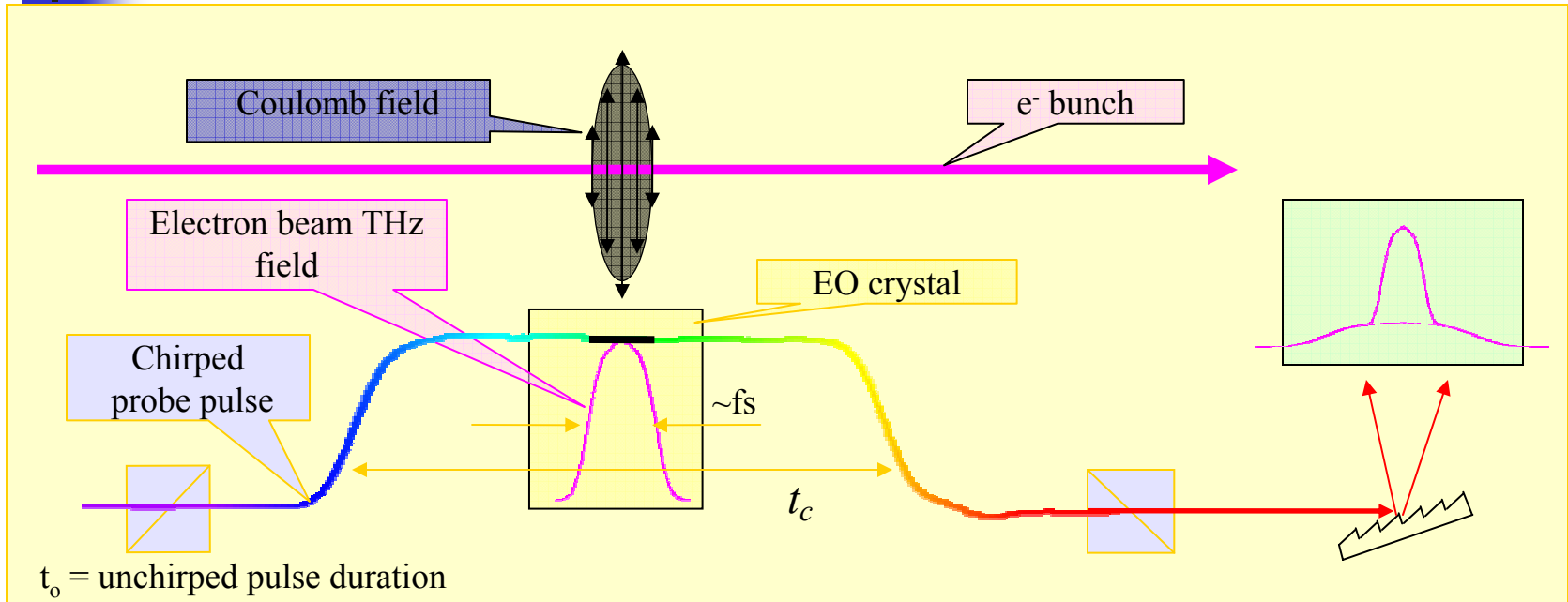
By detecting the optical pulse we are hoping to get electron bunch information

# Scanning Delay (SD) sampling



- The bunch profile is sampled by changing the delay between e-bunch and a femtosecond laser pulse
- Commonly used in THz spectroscopy (pump probe)
- Technically simple, highest resolution

# Spectral Decoding

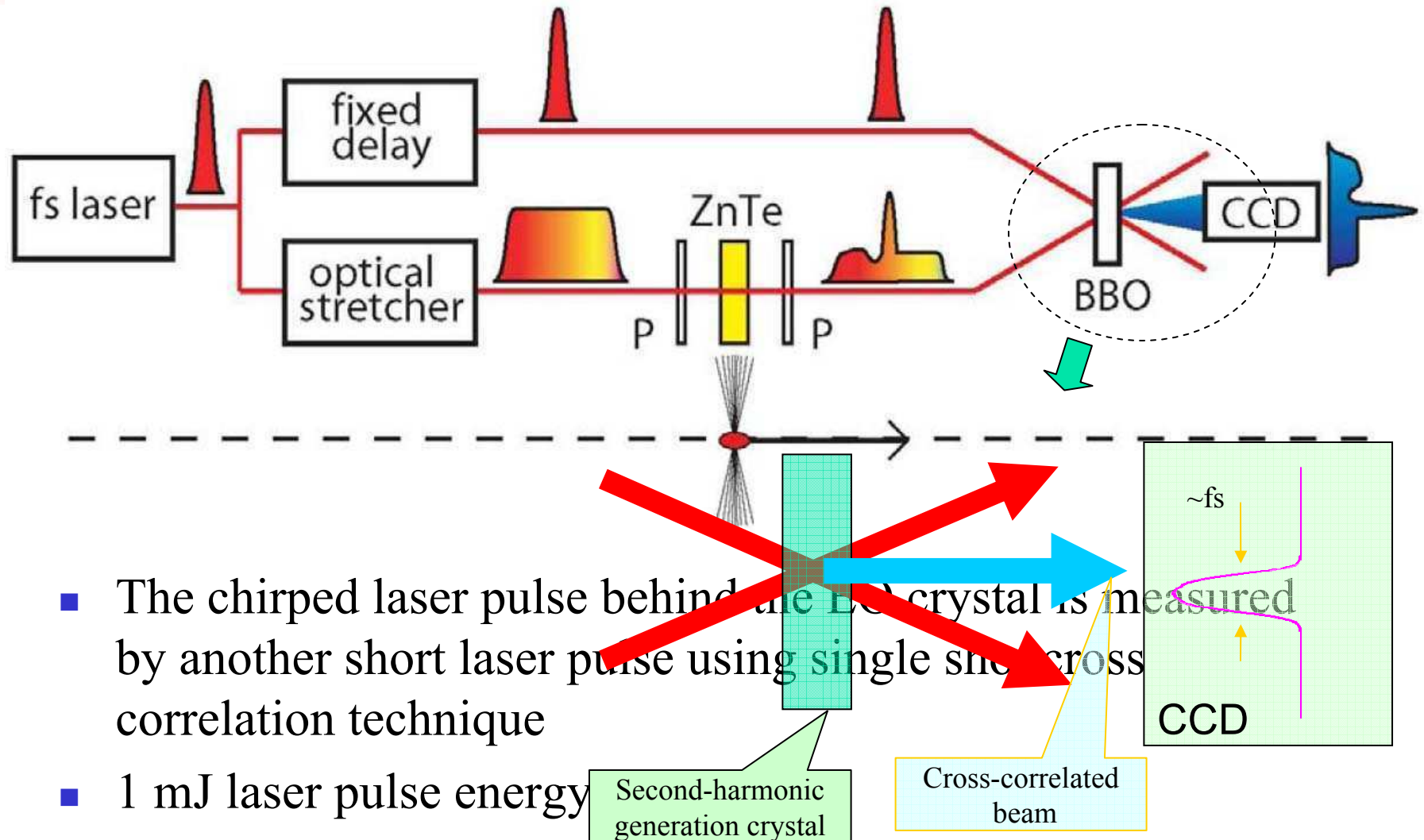


- The laser pulse is stretched spectrally (chirped), the longitudinal structure is therefore encoded in the spectrum
- Single shot experiment
- The instantaneous bandwidth of the chirped pulse needs to be sufficient to represent the e-bunch structure

$$\tau_{\text{lim}} \propto \sqrt{\tau_0 \tau_c}$$

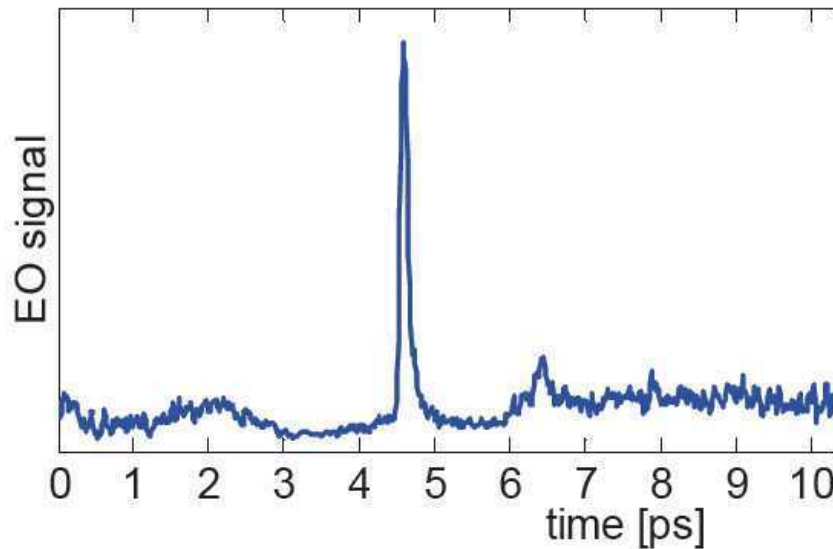
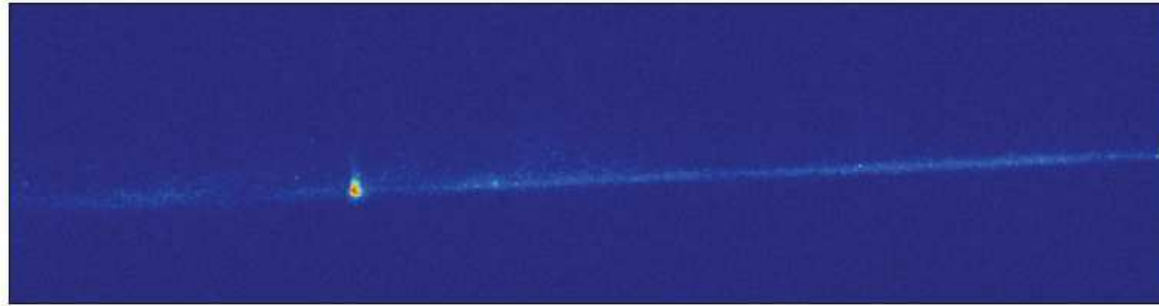
I. Wilke et al PRL 88, 124801, 2002

# Temporal Decoding

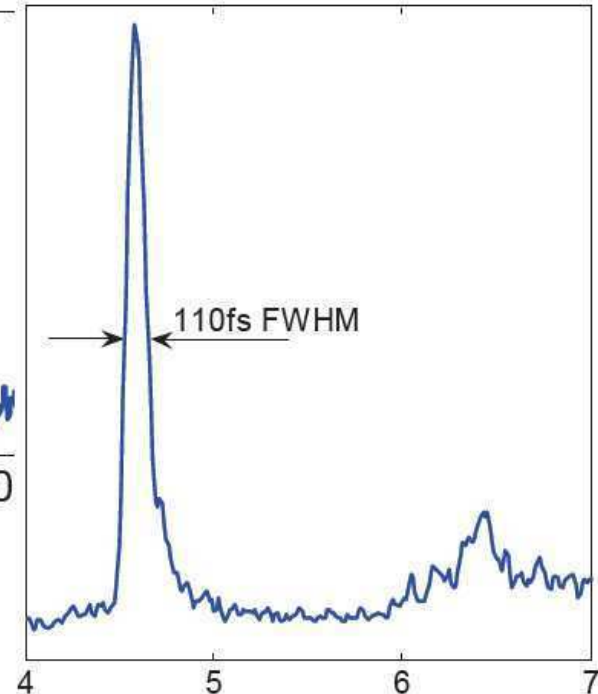




# Temporal Decoding

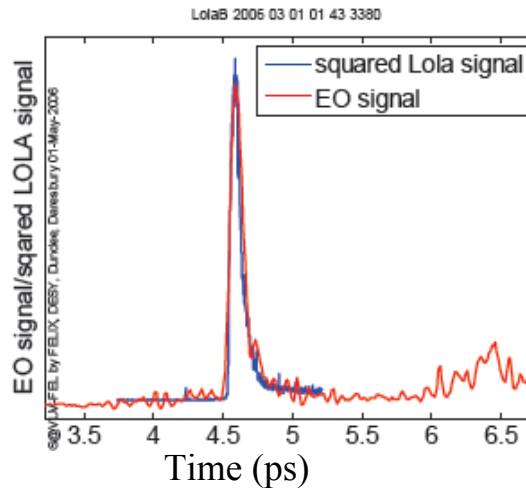


Shortest EO signals seen: 110 fs (FWHM)  
including optical resolution limits

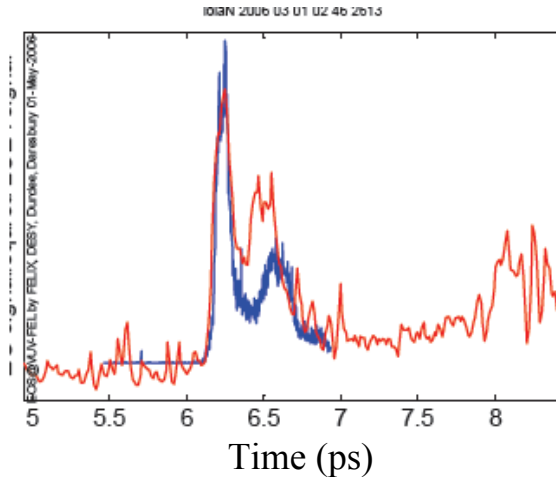


# Temporal Decoding

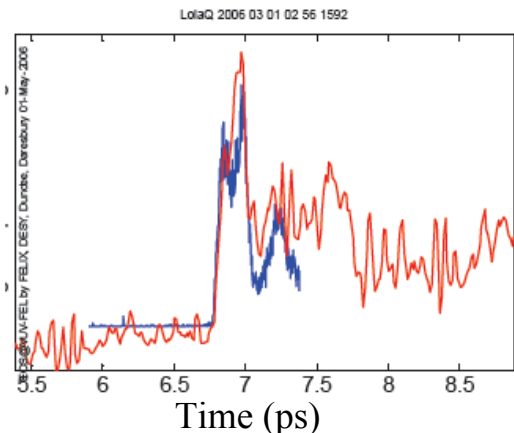
EO at first bunch and LOLA at second bunch



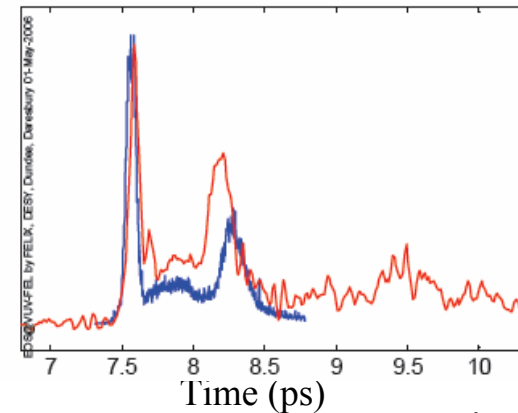
Compressed



ACC 1° overcompression



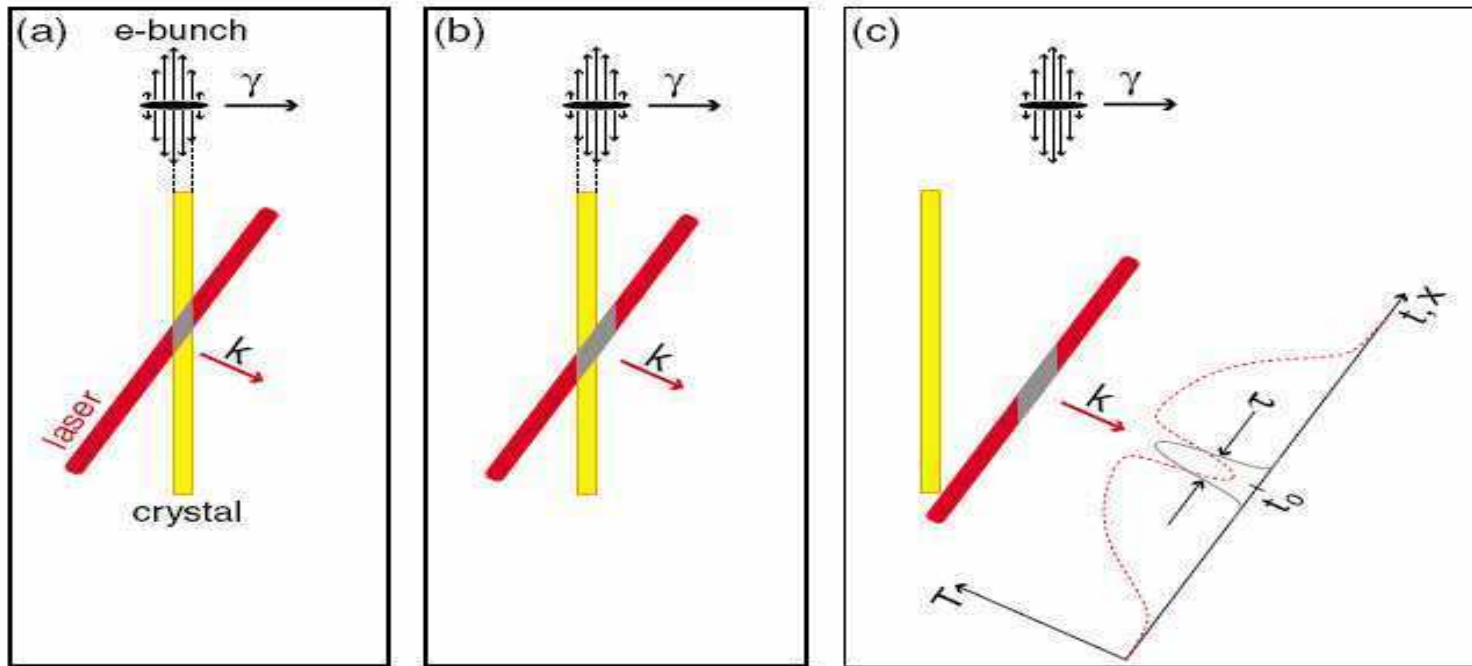
ACC 2° overcompression



ACC 3° overcompression

Preliminary unpublished data by G. Steffen in DESY

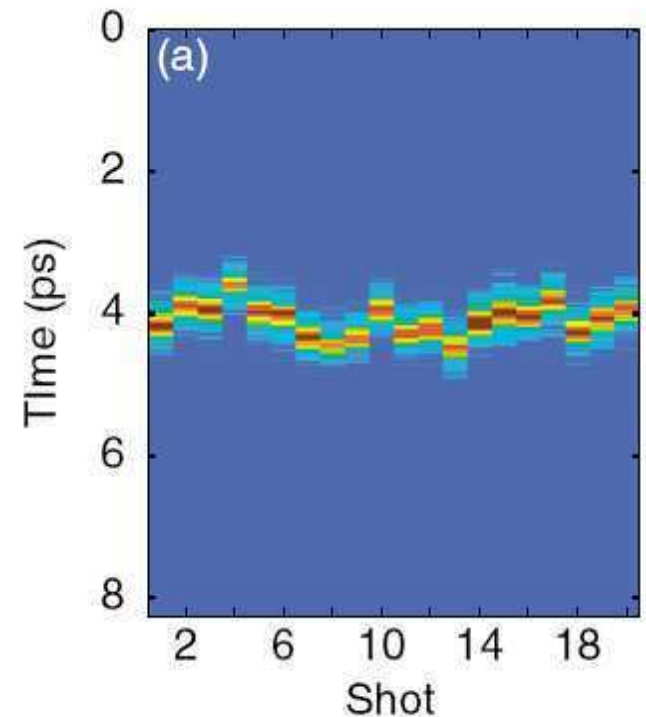
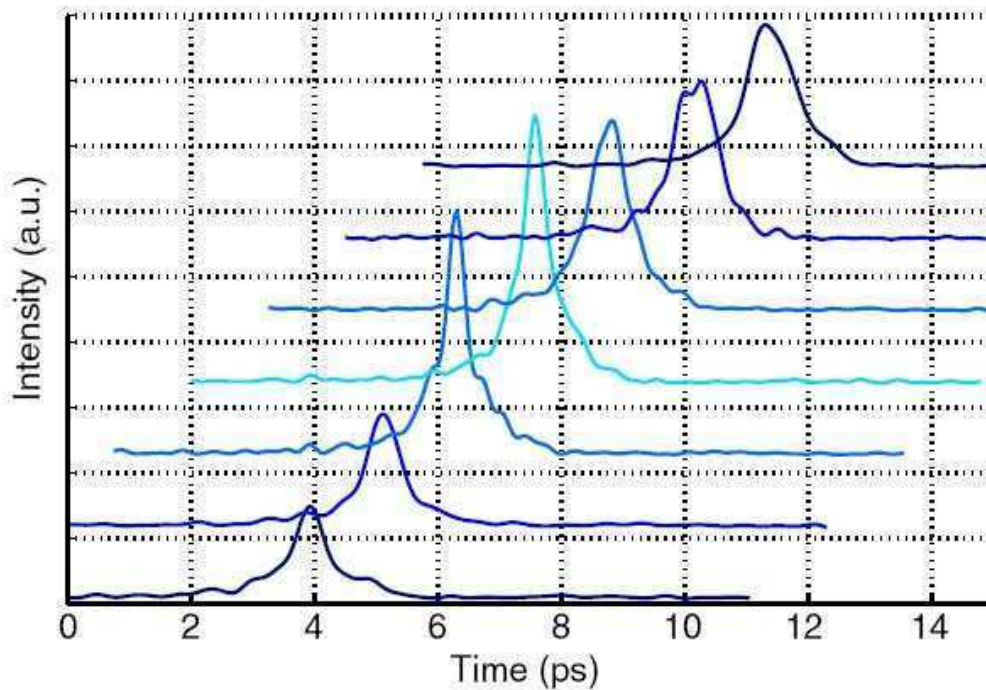
# Spatial Decoding



- The femtosecond laser pulse is focused as a line image to the crystal and passes the crystal at an angle
- The bunch length is transferred to the spatial structure of the laser

A. J. Cavalieri et al PRL 94, 114801, 2002

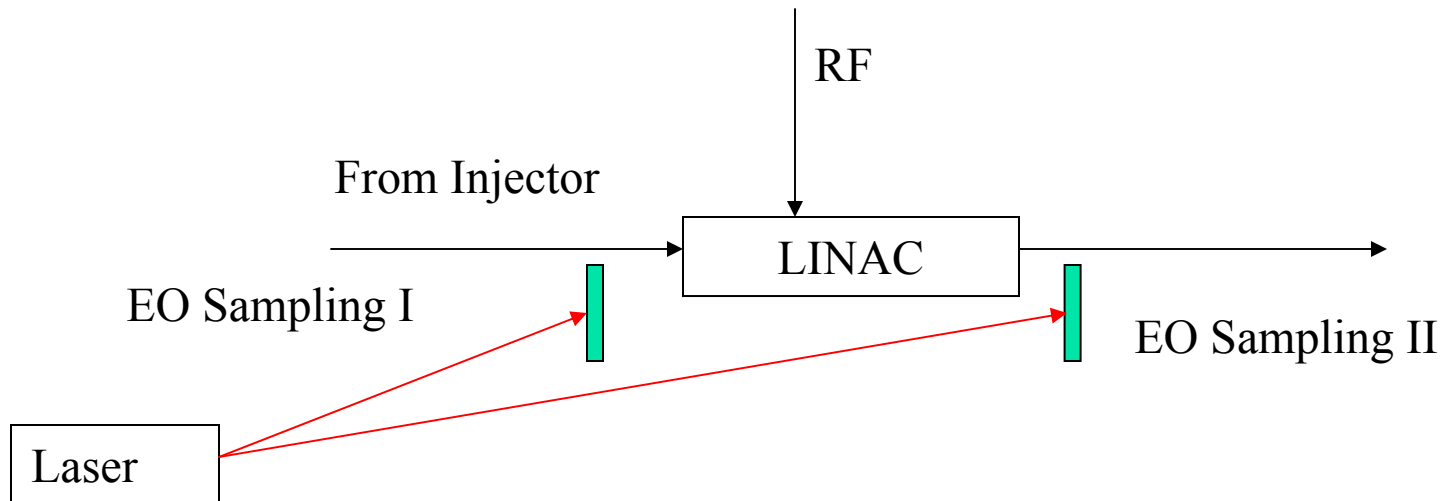
# Spatial Decoding



A. J. Cavalieri et al PRL 94, 114801, 2002

# Applications in ILCTA

## ■ Jitter measurement



EO station 1 will give us the jitter caused everything before LINAC

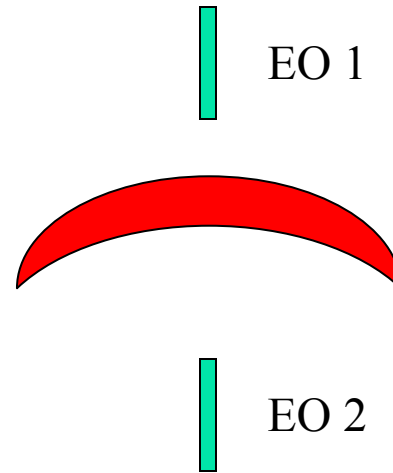
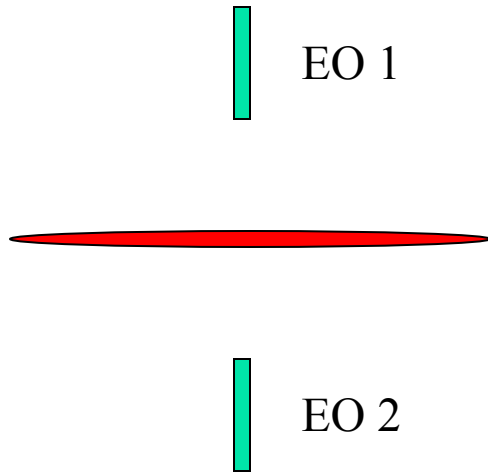
EO station 2 will give us the jitter caused everything before LINAC plus LINAC



# Applications in ILCTA

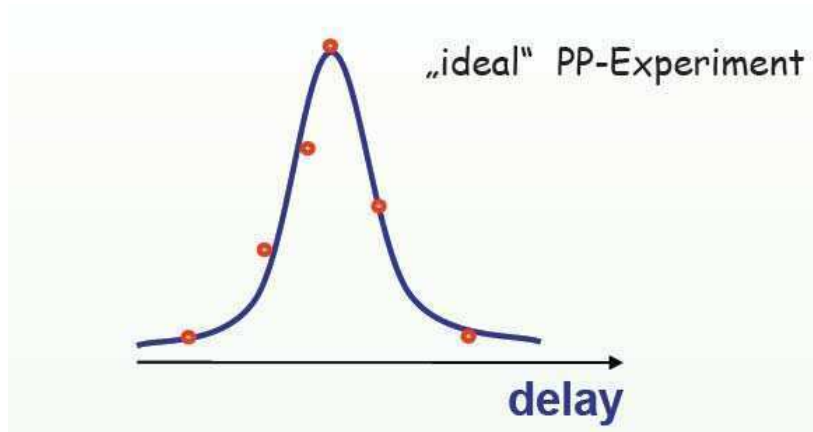
---

- Real-time beam shape Monitor



# Applications in ILCTA

- Timing pump-probe measurement



# *Electron beam diagnostics*

Yuelin Li

*Accelerator Systems Division, Argonne National Laboratory*

*ylli@aps.anl.gov*



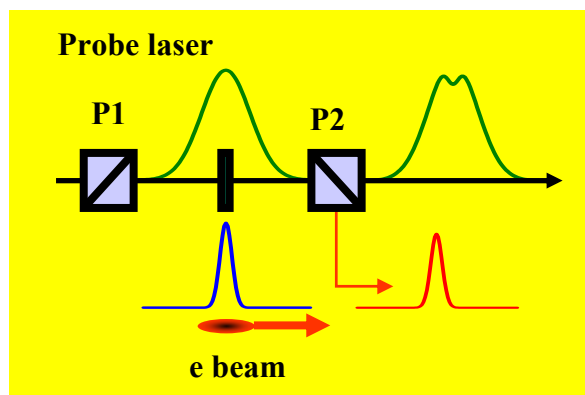
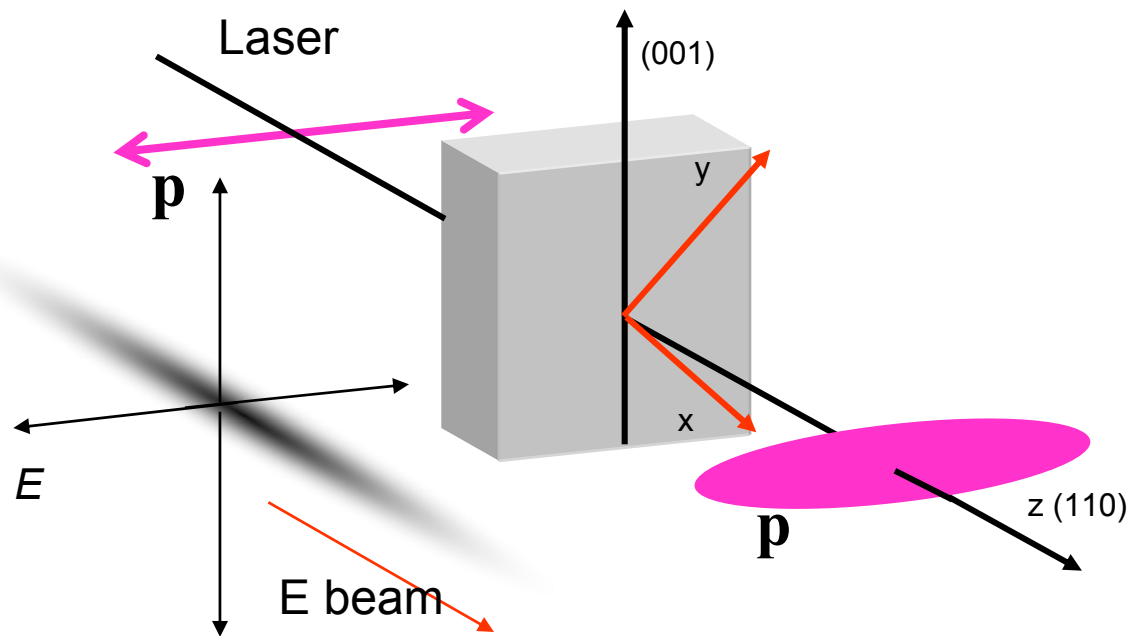
*Argonne National Laboratory is managed by  
The University of Chicago for the U.S. Department of Energy*



## Content

- Electron optical sampling
  - Mechanism and limit
  - Goal: Bunch structure and timing jitter measurement, 10 fs?
  - Local experience
    - *APS experience*
    - *On going collaboration among APS, AWA, FNAL, NIU*
- Optical replica for electron beam structure
  - Mechanism
  - Setup and real estate requirement
  - Local experience
    - *Laser experience at APS, AWA, FNAL, NIU*
    - *APS FEL FROG measurement*
- Discussion

## Mechanism of electron optical sampling



$$n_{x,y} = n \pm \frac{1}{2} n^3 E r_{41}$$

$$\delta = \frac{2\pi n^3 E r_{41} l}{\lambda} \sim 7.27 \times 10^{-4} El$$

$$I_{\perp} = I_p [1 - \cos(\delta_r + \delta)],$$

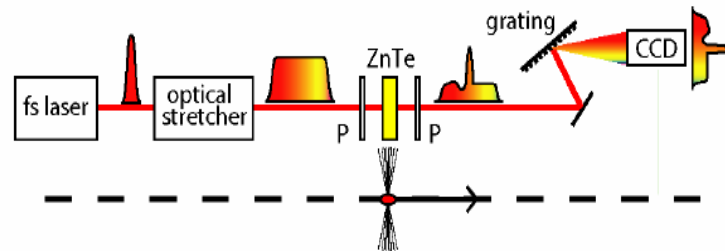
$$I_{\parallel} = I_p [1 + \cos(\delta_r + \delta)].$$

$\delta_r$ : crystal residual or bias birefringence.

## Overview of EO geometries

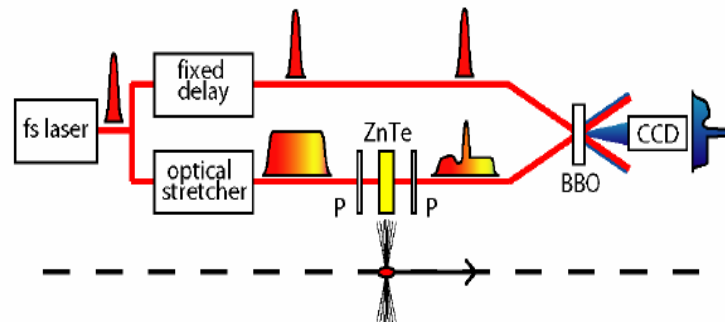
### Spectral Decoding:

- + simple (laser) system
- + high repetition rate
- limited resolution (**500fs**)
- distorted signal for e-bunches < 200fs



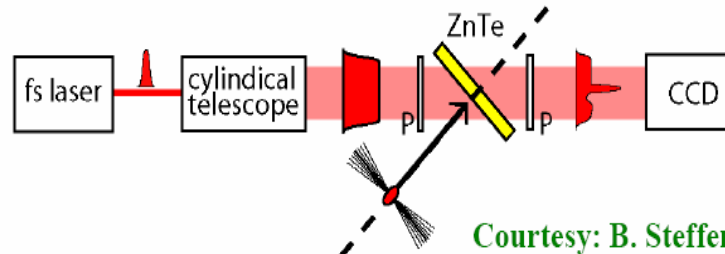
### Temporal Decoding:

- + large time window
- + high resolution (**120fs, GaP**)
- mJ laser pulse energy
- low repetition rate



### Spatial Decoding:

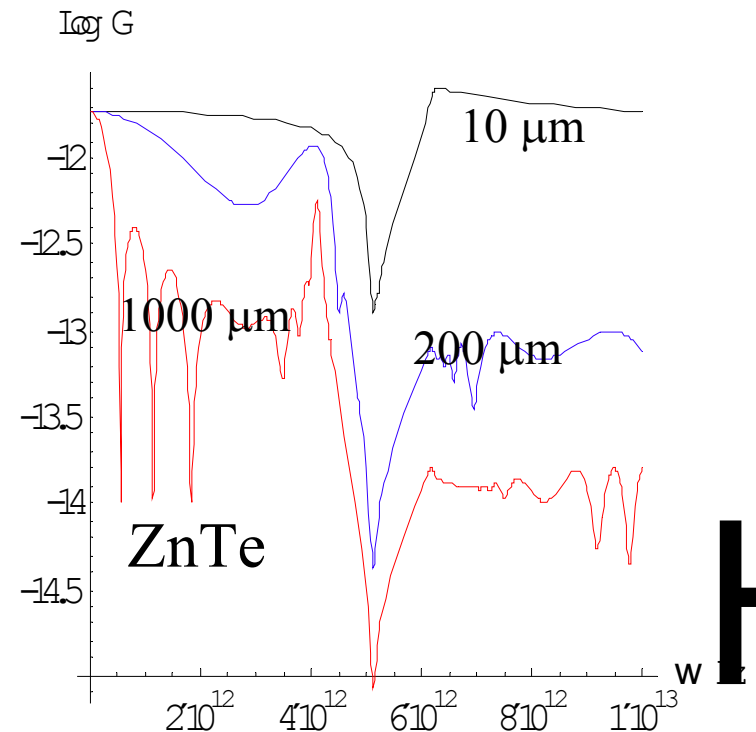
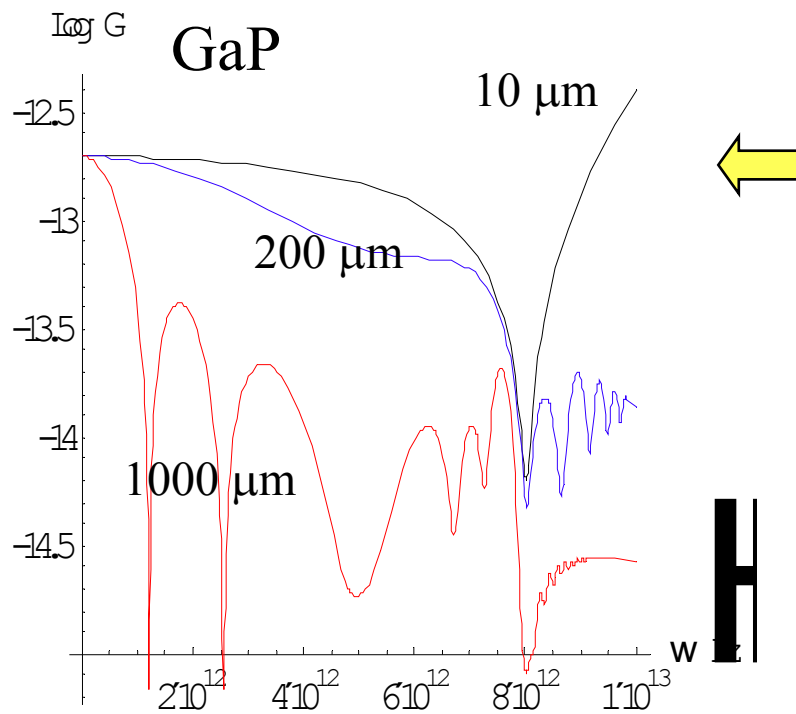
- + simple laser system
- + high repetition rate
- + high resolution (**170fs, ZnTe**)
- more complex imaging optics



Courtesy: B. Steffen et al

H. Schlarb, DESY

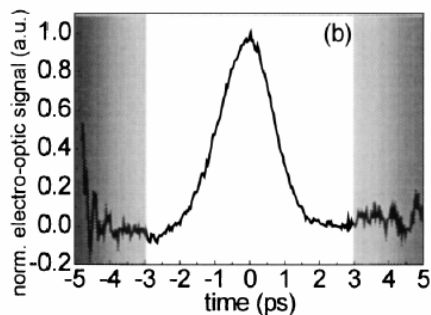
## EO characteristics Broad Band Crystal response



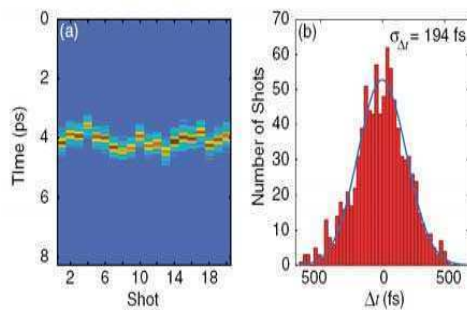
## EO Electron beam measurement

### ■ Beam profile

- 1999, Laser-THz measurement: 128 THz  $\rightarrow$  <10 fs
- 2000, FELIX, 2 ps;
- 2003, FELIX, 0.3 ps;
- 2005, SLAC, 0.3 ps;
- 2006, DESY, 0.15 ps;
- Future, FNAL, 10 fs

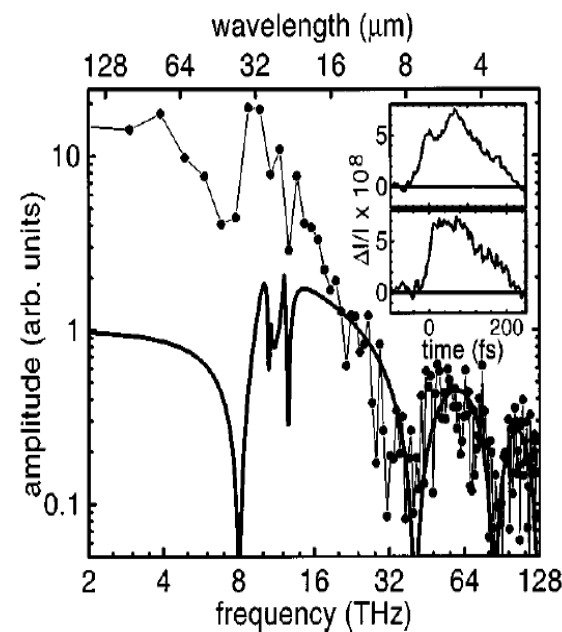


FELIX results: Yan et al., PRL 85, 3404 (2000); 2 ps



FELIX Results: Berden et al. PRL 93, 114802 (2004), 300 fs

SLAC SPPS result: Cavalieri et al., PRL 94, 114801 (2005), 300 fs



Any possibility to do better? This is a laser measurement, 4 fs

Leitenstorfer et al. Appl. Phys. Lett., Vol. 74, 1517 (1999)

## *Advantage and goal*

### ■ Advantages

- Non interceptive
- Single shot
- Potential high temporal resolution: sub 20 fs: main challenge
- Relatively cheap

### ■ Issues

- Can we do <20 fs resolution?
  - *Need a 20 fs structure in source: ILC TC?*
- Survivability under extreme beam conditions
  - *Take the CTR radiations from a bend?*
  - *Direct beam field?*
- High rep rate single shot capabilities
  - *Survivability under extreme beam conditions*

## Loca experience 1

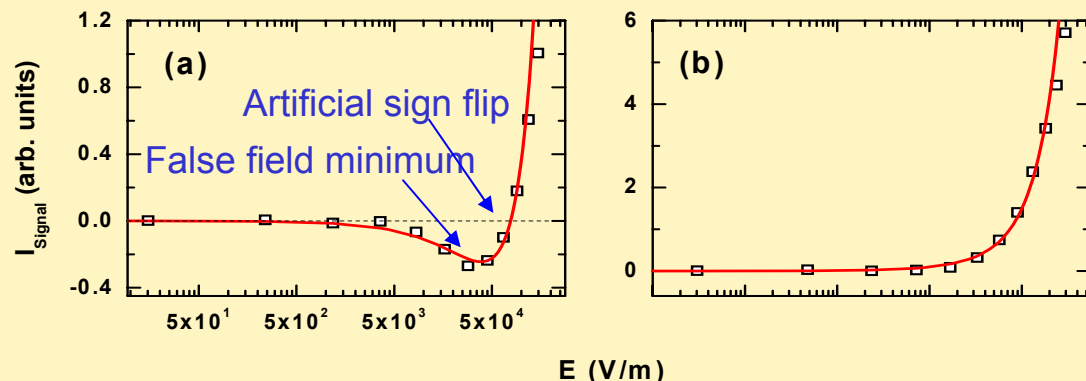
### APS off line EO testing Signal distortion

- Use laser generated THz as phantom electron signal
- Explore distortion under high field
- Explore high temporal resolution possibility
- Application to laser plasma and conventional accelerators
- Continuing in collaboration with FNAL, NIU

EO sampling signal as a function of the field strength under investigation

(a) Field anti-parallel to the residual birefringence

(b) Field parallel to the residual birefringence



Li et al., Appl. Phys. Lett. 88, 251108 (2006)

## Local experience 2

### ANL, FNAL, NIU collaboration at AWA

#### FNAL

- Jinhao Ruan (A0)
- Jamie Santucci (A0)
- Cheng-yan Tan (AD)
- Vic Scarpine (Instrumentation)
- Randy Thurman-Keup (Instrumentation)

#### ANL

- Yuelin Li (APS)
- John Power (AWA)

#### NIU

- P. Piot
- Tim

| Stage | Plan                                                                                                                                                                                  | Time      | How                                                                                     | Major concern                                                                                                                    | Goal                                                             |
|-------|---------------------------------------------------------------------------------------------------------------------------------------------------------------------------------------|-----------|-----------------------------------------------------------------------------------------|----------------------------------------------------------------------------------------------------------------------------------|------------------------------------------------------------------|
| 1     | <ul style="list-style-type: none"> <li>■ Background study;</li> <li>■ optical layout;</li> <li>■ Purchase</li> <li>■ Safety training</li> </ul>                                       | 1 month   | Email communication                                                                     | <ul style="list-style-type: none"> <li>■ Expenses</li> <li>■ Detail of experiment need to be considered</li> </ul>               | Everything ready for EO experiment                               |
| 2     | Reproduce Yuelin's setup in AWA laser room using laser generate THz as a phantom beam                                                                                                 | 2-3 month | Jinhao, John, Yuelin, Tim : 1-2d per week in AWA<br>Others: 1 day per week if necessary | <ul style="list-style-type: none"> <li>■ Insert Pockel cell to pick up Ti:Sa pulse</li> <li>■ Setup the EO experiment</li> </ul> | EO experiment successful done on <b>laser induced THz signal</b> |
| 3     | <ul style="list-style-type: none"> <li>■ Getting Ti-sa pulse into cave in AWA</li> <li>■ EO experiment on OTR signal</li> <li>■ EO experiment on e-beam (out side the Vac)</li> </ul> | 2-3 month | Jinhao, John, Tim : 1-2d per week in AWA<br>Others: 1 day per week if necessary         | Getting Ti-sa pulse into cave in AWA                                                                                             | EO experiment done for <b>e-beam outside the vacuum</b>          |



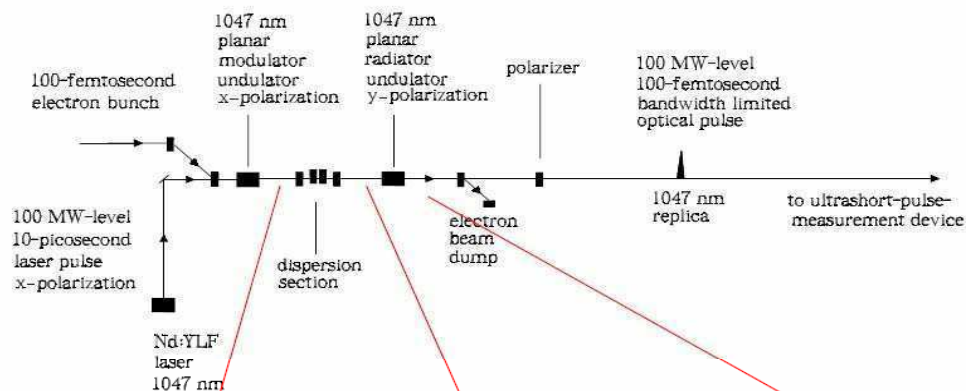
## Content

- Electron optical sampling
  - Mechanism and limit
  - Goal: Bunch structure and timing jitter measurement, 10 fs?
  - Local experience
    - *APS experience*
    - *On going collaboration among APS, AWA, FNAL, NIU*
- Optical replica for electron beam structure
  - Mechanism
  - Setup and real estate requirement
  - Local experience
    - *Laser experience at APS, AWA, FNAL, NIU*
    - *APS FEL FROG measurement*
- Discussion

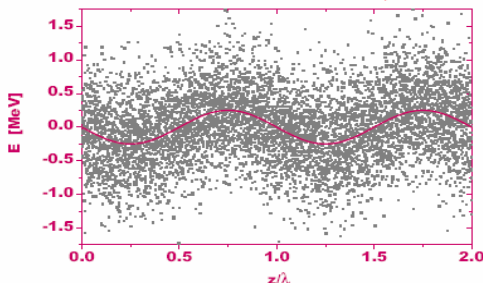
## The idea of optical replica



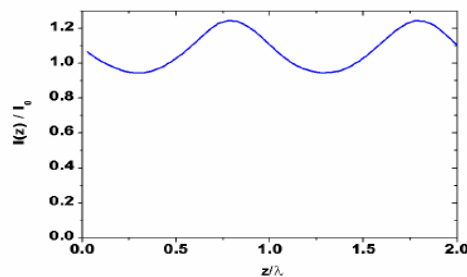
The optical replica synthesis through optical modulation of electron bunch and coherent radiation in the output undulator



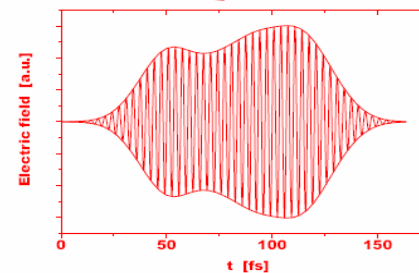
$$E(t) = F(I(t), \epsilon_n(t), \Delta\mathcal{E}(t)) = I(t)f(\epsilon_n(t), \Delta\mathcal{E}(t))$$



Energy modulation



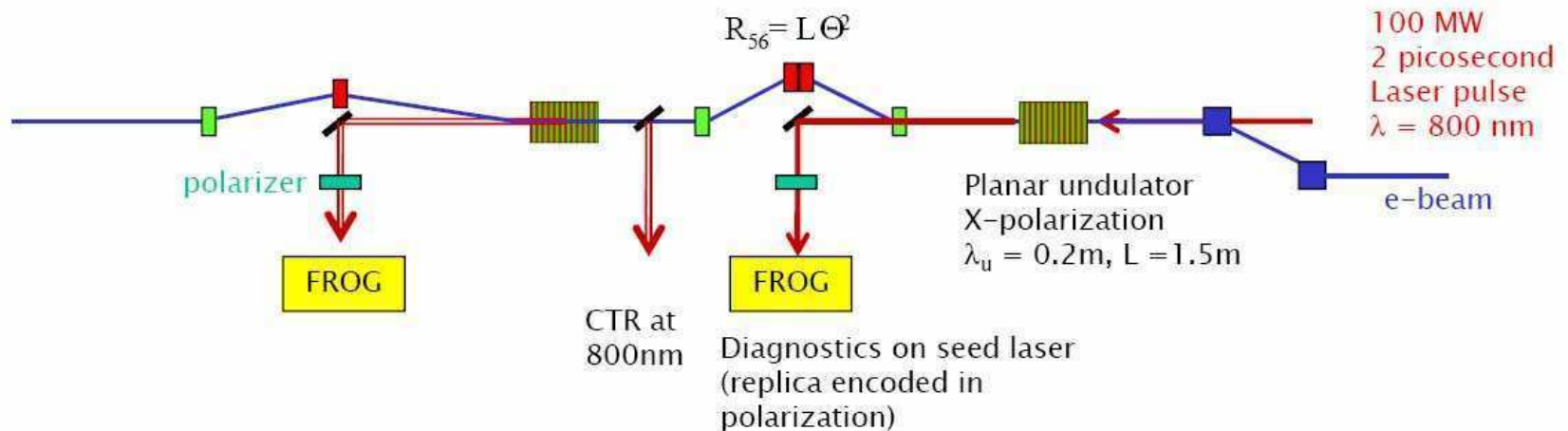
Density modulation



Optical replica

## More on the mechanism

- First: Energy modulation via (v.E) coupling
- Second: Longitudinal density modulation in chicane
- Third: coherent emission of light pulse in radiator that mimics the longitudinal shape of the electron bunch (optical replica)
- Fourth: radiation detected by optical method (FROG, resolution up to a few fs)



H. Schlarb, DESY

## *DESY undulator for optical replica*

- DESY is going full steam on this, and is expecting result in a year

|                             |                                 |
|-----------------------------|---------------------------------|
| Type                        | Electromagnetic                 |
| Number of undulator         | 1-2 (vert + horiz)              |
| Gap                         | 40 mm                           |
| Period length               | 200 mm                          |
| Pole length/width           | 50/100 mm                       |
| Number of full periods      | 5                               |
| Number of poles             | 14                              |
| Nominal field               | 0.31 T                          |
| Nominal K-Value             | 5.7                             |
| Maximal field               | 0.42 T                          |
| Maximum K-Value             | 7.7                             |
| Iron yoke length            | 1400 mm                         |
| Overall length incl. coils  | < 1500 mm                       |
| Ampere-turns per coil       | to be decided                   |
| Number of turns             | to be decided                   |
| Maximal current             | < 400 A, better < 100 A         |
| Number of basic / end coils | 10 main, 4 end coils            |
| Vacuum chamber diameter     | 35 mm                           |
| First field integral        | $5 \times 10^{-5} \text{ Tm}$   |
| Second field integral       | $2 \times 10^{-4} \text{ Tm}^2$ |

## *Advantages and limitation*

### ■ Pros

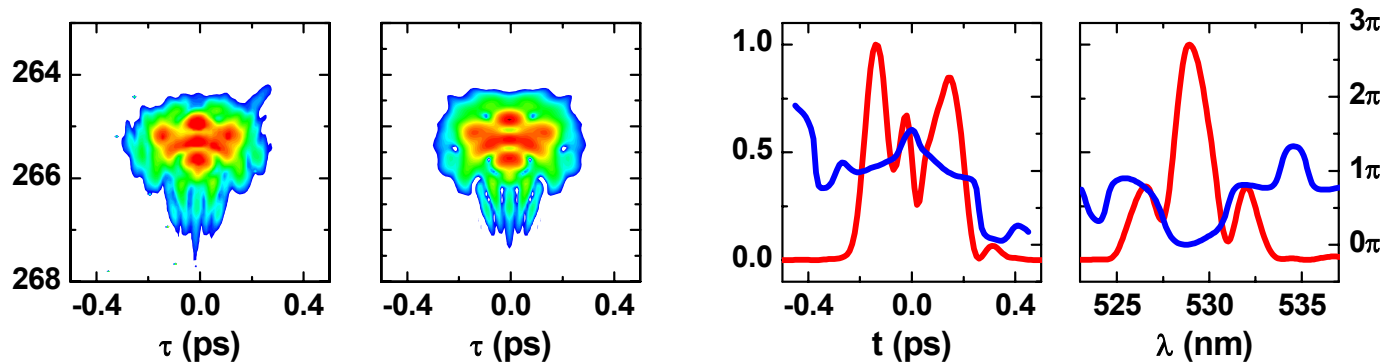
- Single shot
- Non interceptive
- Guaranteed resolution of  $<20$  fs (limited by slippage length, or number of oscillation in undulator multiplies to radiation wavelength, in DESY case 15 fs,  $5 \times 2.75$  fs)
- Accurate

### ■ Con

- Expensive: laser, chicane, and two undulators
- Large real estate
- May be complicated by slice emittance

## Local experience

- First FROG measurement on undulator radiation (SASE FEL at LEULT)



Y. Li et al., PRL 89, 234801 (2002); 91, 243602 (2003)

SV Milton, et.al., Science 292, 2037-2041 (2001).

- Local experience on lasers: ANL (CHM, AWA, APS), FNAL, NIU

## *EO vs. Optical Replica*

|             | EO                                                                                                         | Optical replica                                                               |
|-------------|------------------------------------------------------------------------------------------------------------|-------------------------------------------------------------------------------|
| Resolution  | 150 fs demonstrated for beam<br>128 THz bandwidth demonstrated in THz (10 $\mu$ m crystal)<br><20 possible | 50 fs demonstrate in SASE measurement<br>5 fs demonstrate in optics<br><20 fs |
| Real estate | small                                                                                                      | huge                                                                          |
| Cost        | Inexpensive<br>Synchronized laser<br>Crystal chamber or mirror station                                     | Expensive<br>Synchronized laser<br>Two undulators<br>Chicane                  |
| Complexity  | Relatively low                                                                                             | High                                                                          |
|             |                                                                                                            |                                                                               |
|             |                                                                                                            |                                                                               |
|             |                                                                                                            |                                                                               |
|             |                                                                                                            |                                                                               |
|             |                                                                                                            |                                                                               |



*... for a brighter future*



U.S. Department  
of Energy

UChicago ►  
Argonne<sub>LLC</sub>



A U.S. Department of Energy laboratory  
managed by UChicago Argonne, LLC

# ***Possible ODR Imaging Diagnostics for ILCTA***

***Alex H. Lumpkin***

***ASD Diagnostics Group and Argonne Accelerator Institute***

***Advanced Photon Source***

***FNAL ILC Test Accelerator Workshop***

***November 28, 2006***

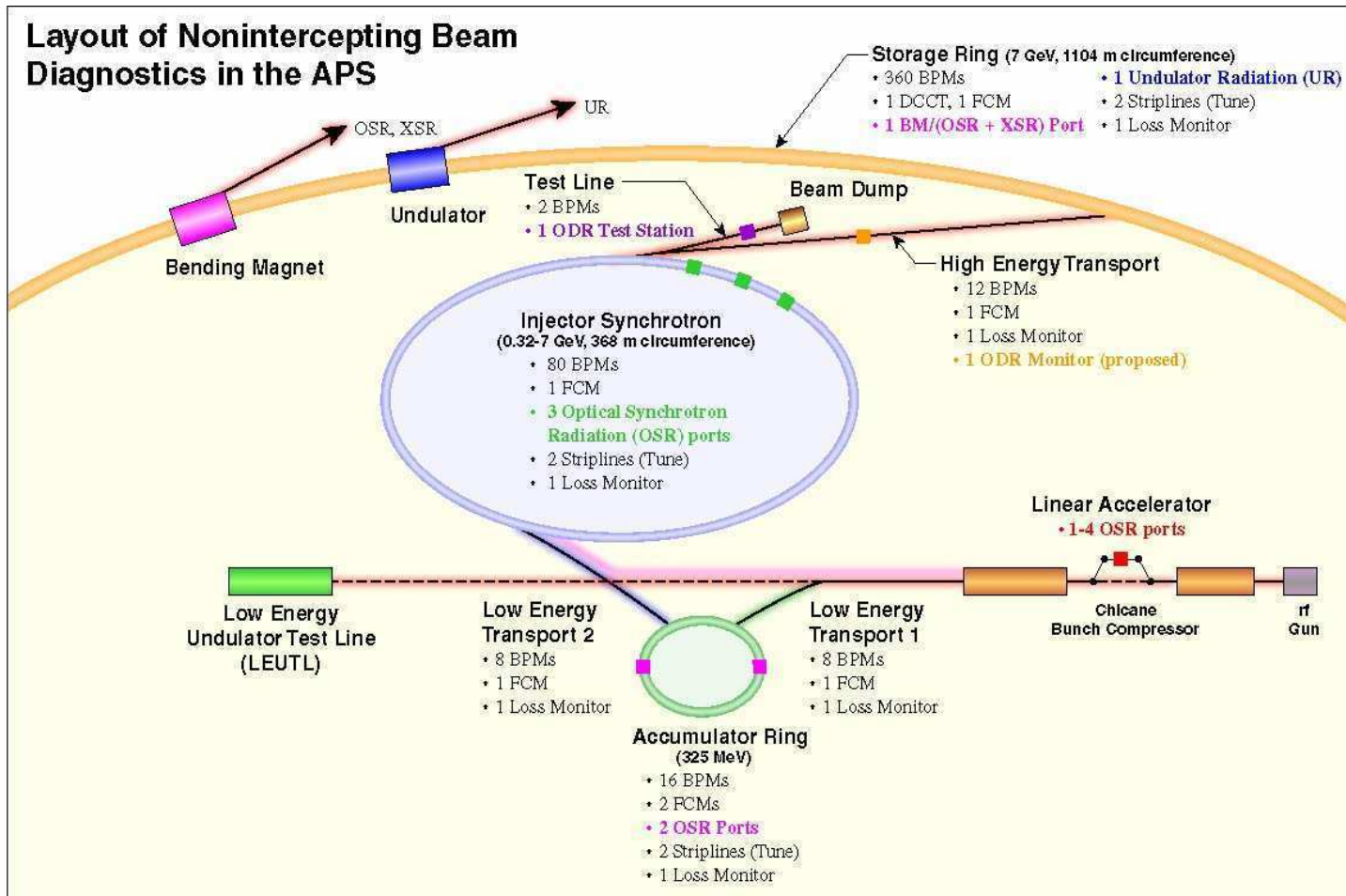


# OUTLINE

- Introduction
- Optical Diffraction Radiation (ODR) Background
- Optical Diffraction Radiation Experimental Results
- Potential Applications of ODR to ILCTA
- Summary

# The APS Facility has Provided Sources for Developing Time-Resolved, NI Diagnostics

- Beam Energies from 50 MeV to 7 GeV are available for tests.



# *Development of Imaging Diagnostics for Multi-GeV Beams*

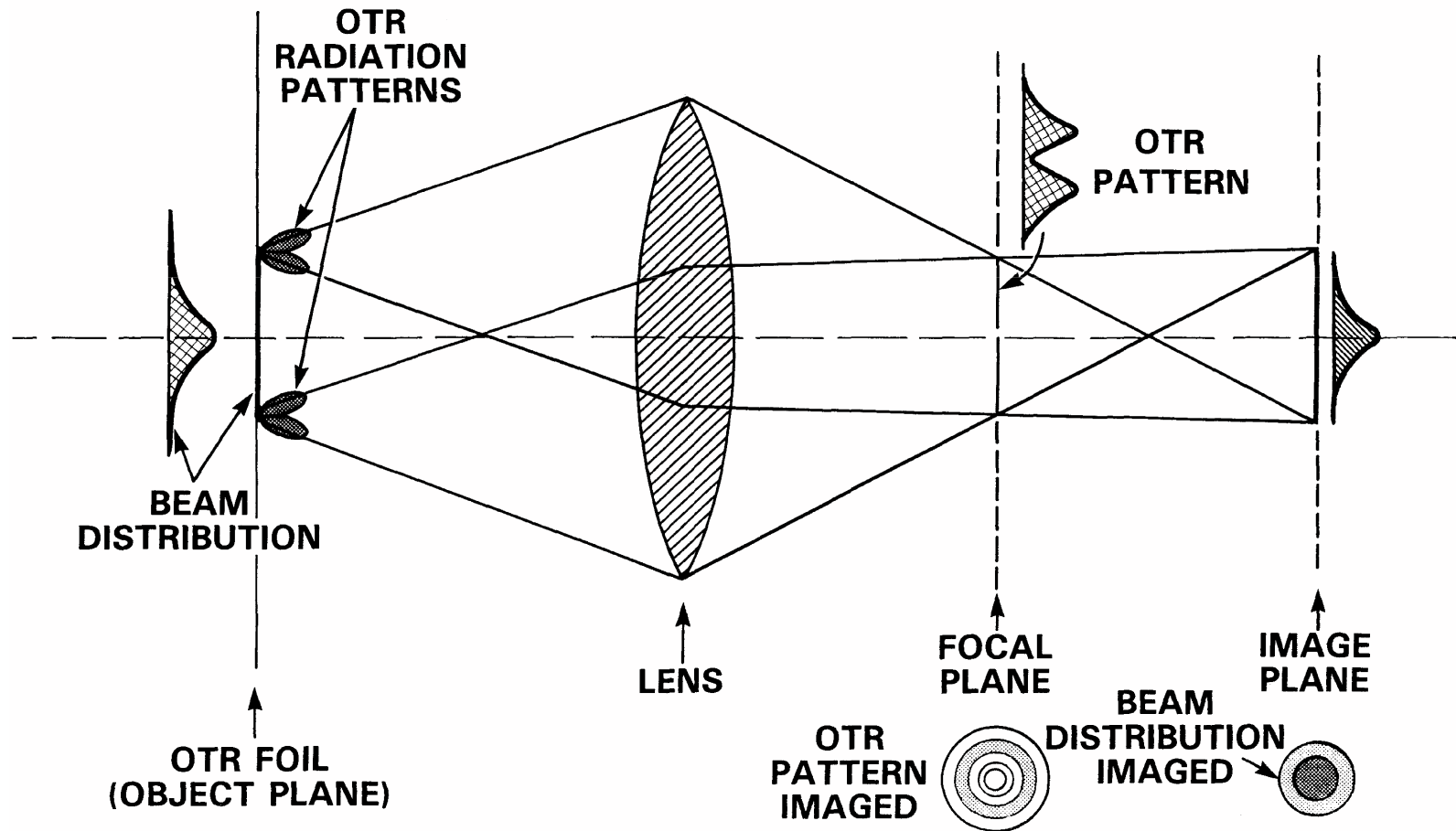
- Diagnostics of bright beams continue to be a critical aspect of present and future accelerators.
- Beam size, divergence, emittance, and bunch-length measurements are basic to any facilities involving bright beams.
- Nonintercepting (NI) characterizations of multi-GeV beam parameters are of particular interest in rings and high-current applications. These can be addressed by optical and x-ray synchrotron radiation (OSR and XSR, respectively) in rings.
- The development of optical diffraction radiation (ODR) as an NI technique for relative beam size, position, and divergence measurements in linear transport lines has occurred in the last few years at KEK and APS.
- Results from the APS transport line for 7-GeV beam will be discussed.
- Relevance to new and proposed projects such as x-ray FELs, energy recovering linacs (ERLs), and the International Linear Collider (ILC) will be addressed.
- Relevance to ILCTA will be suggested at sub-GeV energy, but high current.

## Strategy (Can we extend to ODR?)

Convert particle-beam information to optical radiation and take advantage of imaging technology, video digitizers, and image processing programs. Some reasons for using OTR are listed below:

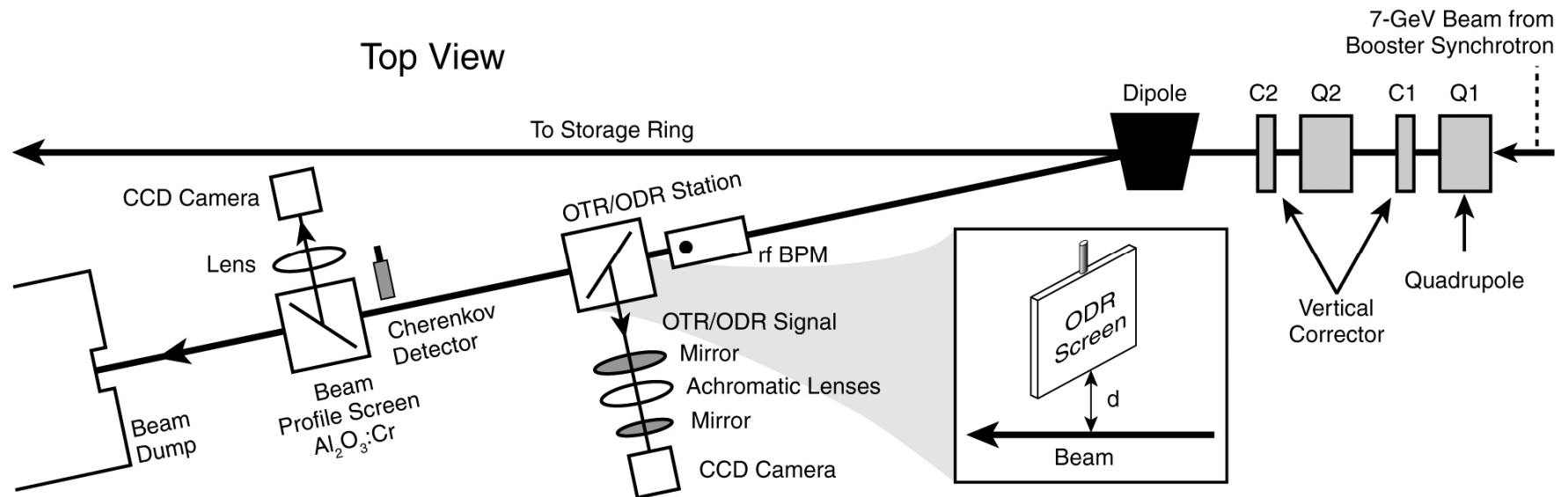
- The charged-particle beam will transit thin metal foils to minimize beam scattering and Bremsstrahlung production.
- These techniques provide information on
  - Transverse position
  - Transverse profile
  - Divergence and beam trajectory angle

# Optical Ray Diagram for OTR/ODR Imaging

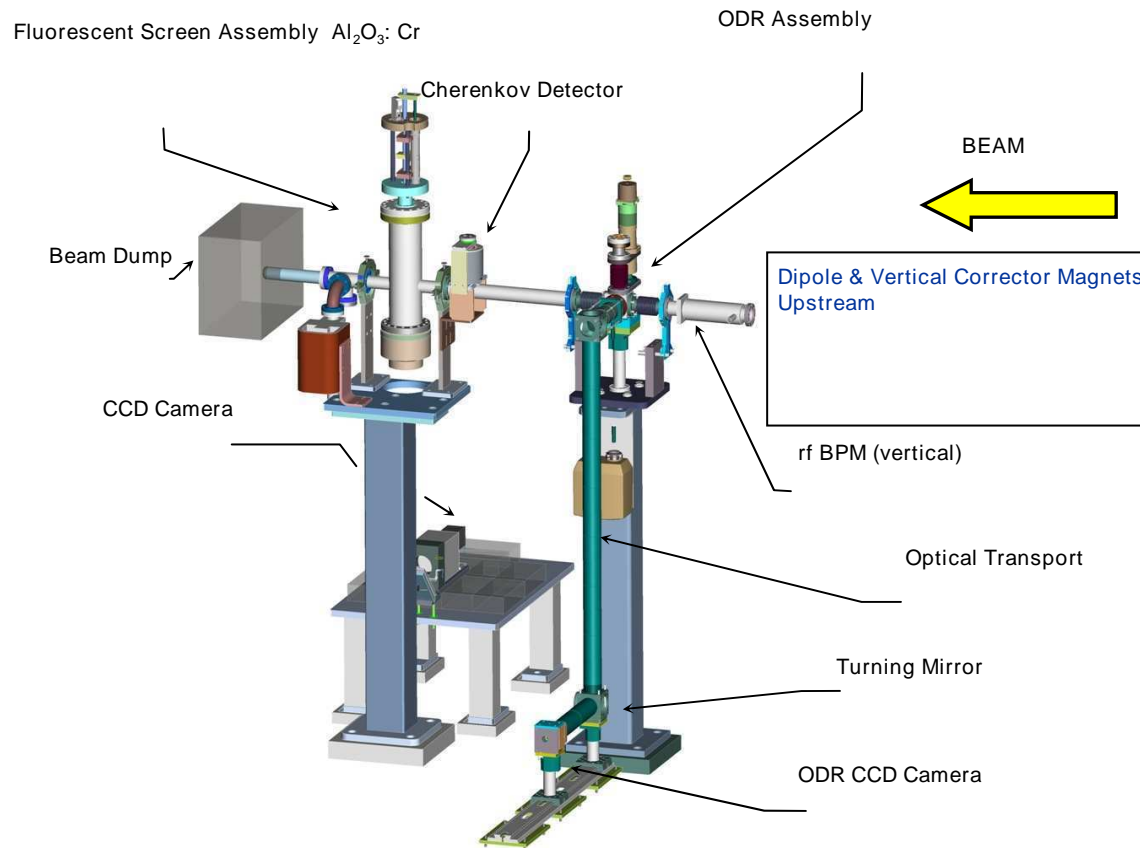


# Schematic of the OTR/ODR Test Station on the BTX Line at APS

- Test station includes the rf BPM, metal blade with stepper motor control, imaging system, Cherenkov detector, and downstream beam profile screen. The dipole is 5.8 m upstream of the ODR converter screen.

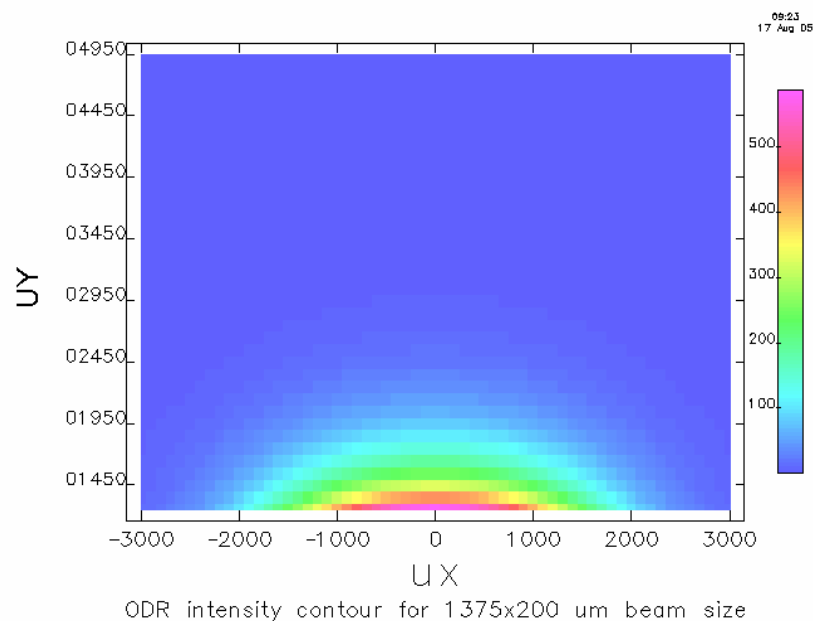
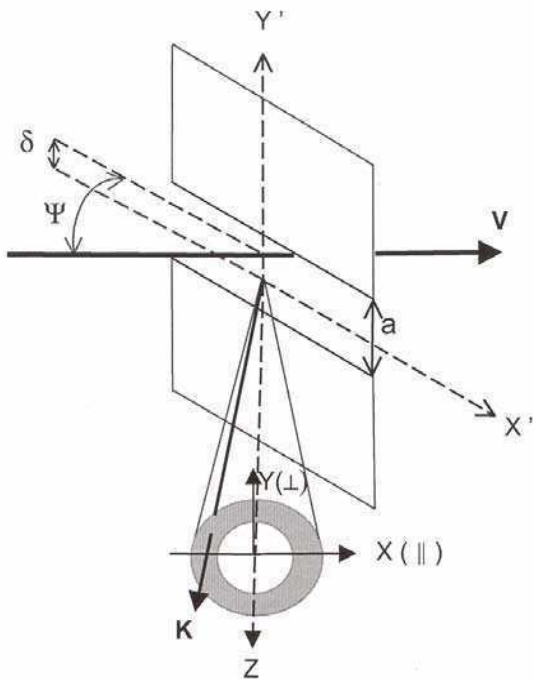


# An OTR/ODR Test Station was Developed on the BTX Line for 7-GeV Beams



# ODR is a Potential Nonintercepting Diagnostic for Multi-GeV Beams

- At left, schematic of ODR generated from two vertical planes (based on Fig. 1 of Fiorito and Rule, NIM B 173, 67 (2001). We started with a single plane.
- At right, calculation of the ODR light generated by a 7-GeV beam for  $d=1.25$  mm in the optical near field based on a new model (Rule and Lumpkin).





## *An Analytical Model has been Developed by D. Rule for ODR Near-Field Distributions Based on the Method of Virtual Quanta*

- We convolved the electron beam's Gaussian distribution of sizes  $\sigma_x$  and  $\sigma_y$  with the field expected from a single electron at point  $P$  in the metal plane (J.D. Jackson)

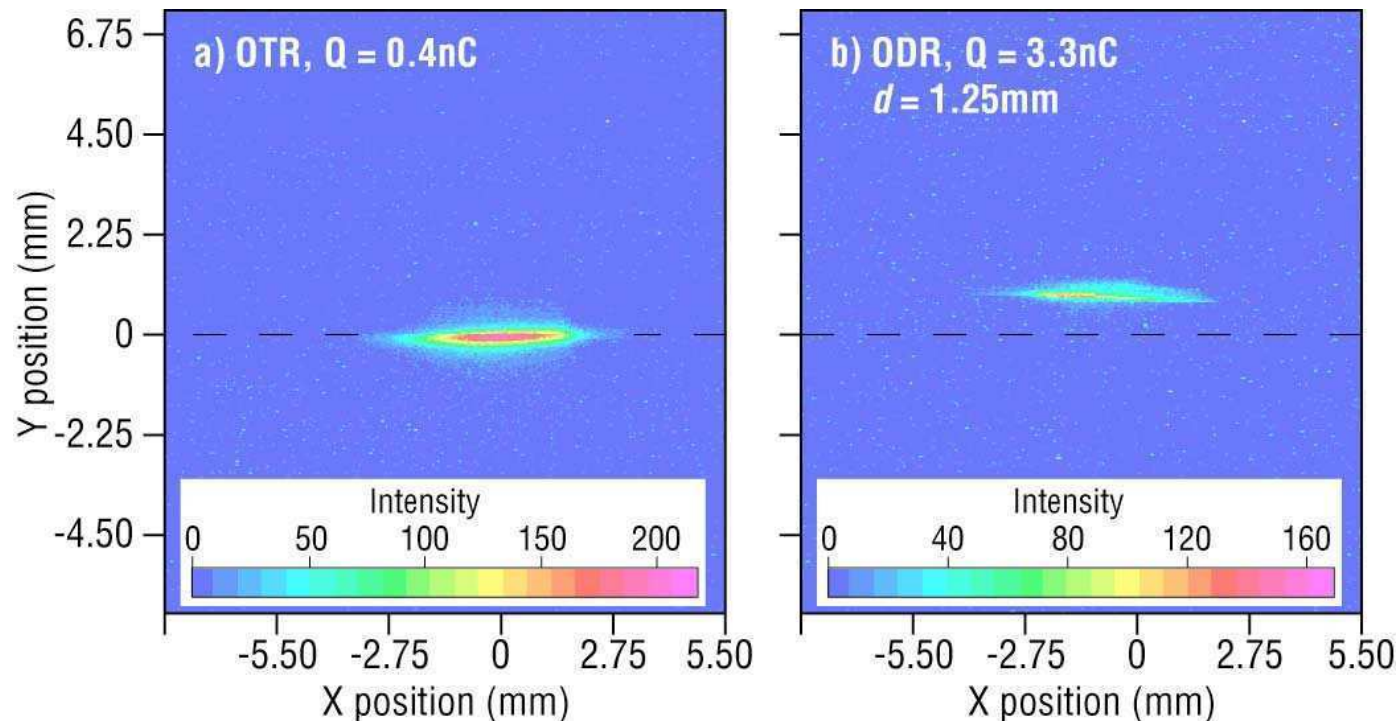
$$\frac{dI}{d\omega}(\mathbf{u}, \omega) = \frac{1}{\pi^2} \frac{q^2}{c} \left( \frac{c}{v} \right)^2 \alpha^2 N \frac{1}{\sqrt{2\pi\sigma_x^2}} \frac{1}{\sqrt{2\pi\sigma_y^2}} \times$$

$$\iint dx dy K_1^2(\alpha b) e^{-\frac{x^2}{2\sigma_x^2}} e^{-\frac{y^2}{2\sigma_y^2}},$$

where  $\omega$  = radiation frequency,  $v$  = electron velocity  $\approx c$  = speed of light,  
 $q$  = electron charge,  $N$  is the particle number,  $K_1(ab)$  is a modified Bessel function with  $\alpha = 2\pi/\gamma\lambda$ , and  $b$  is the impact parameter.

# Investigations of Optical Diffraction Radiation on 7-GeV Beams at APS are Relevant to GeV Beams

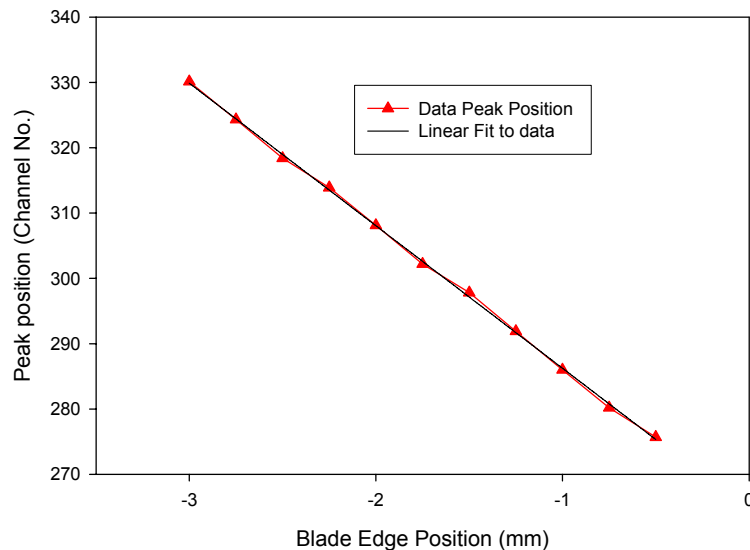
■ ODR offers the potential for nonintercepting, relative beam-size monitoring with near-field imaging. This is an alternate paradigm to far-field work at KEK.



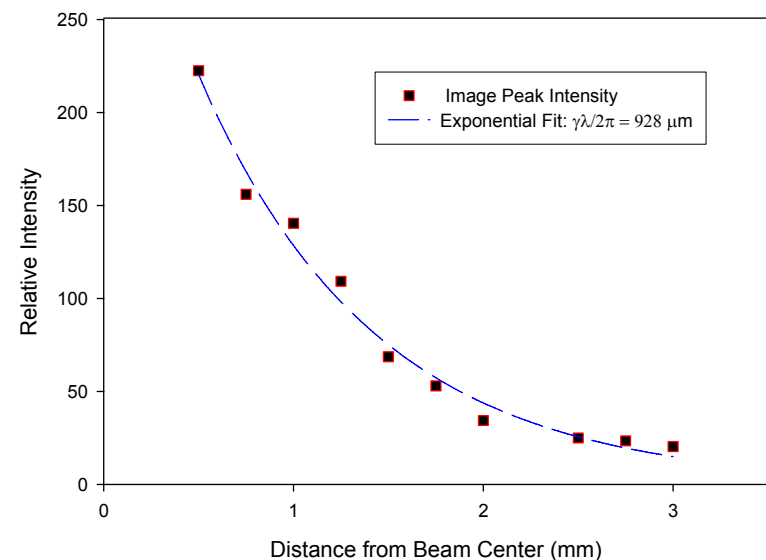
Submitted to Phys. Rev.

# Observed Signal Position and Intensity are Dependent on Impact Parameter Magnitude

Signal Peak Position versus Blade Edge Position  
(10-08-04)



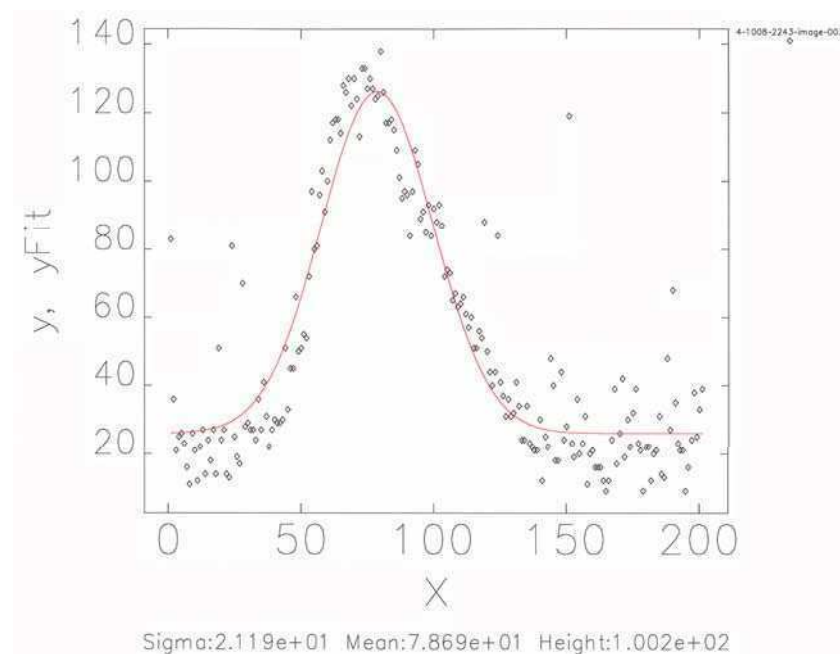
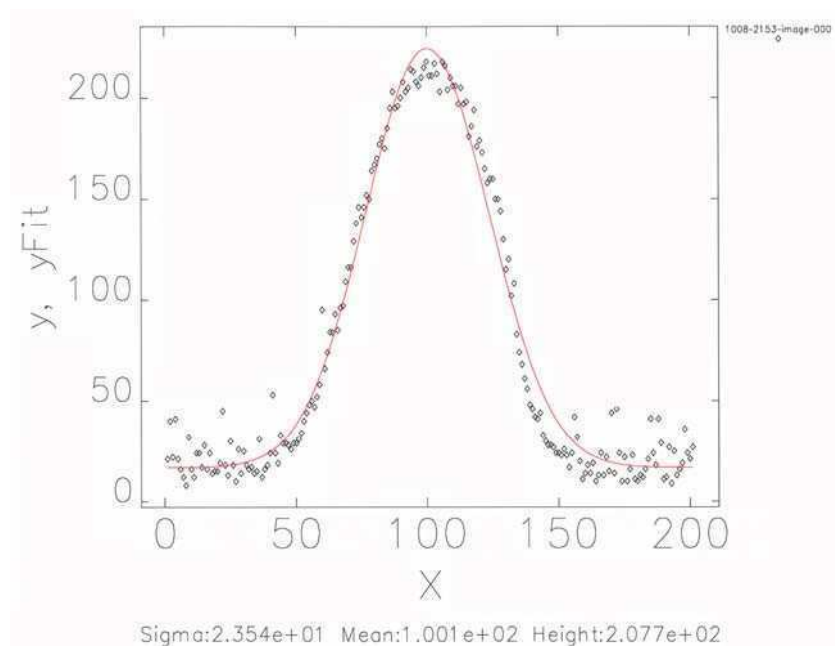
Signal Peak Intensity versus Blade Edge Position  
(10-08-04)



# OTR and ODR Images Recorded by Online Video Digitizer and Processed

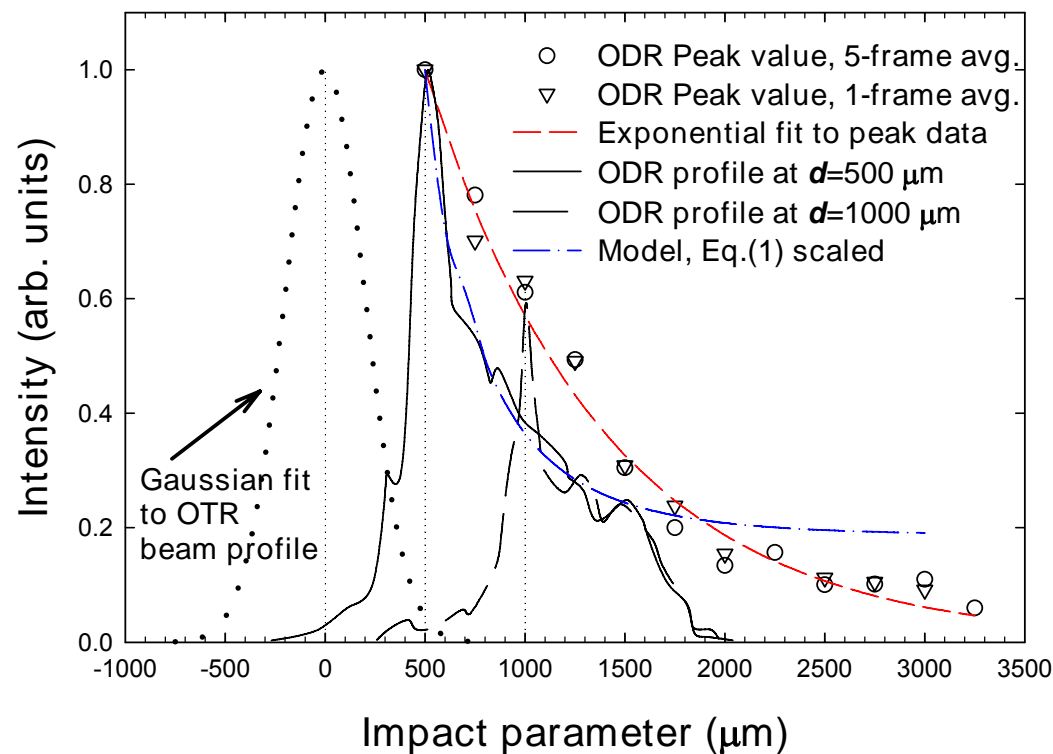
■ OTR profile,  $Q=0.4$  nC

ODR profile,  $Q=3.2$  nC  
 $d=1.25$  mm



# Analytical Model Addresses Main Features of Vertical Profiles from ODR Near-field Images

- Comparison of OTR beam profile and ODR vertical profile data. The peak intensity has an exponential behavior with impact parameter while the total profile has the modified Bessel function effect.



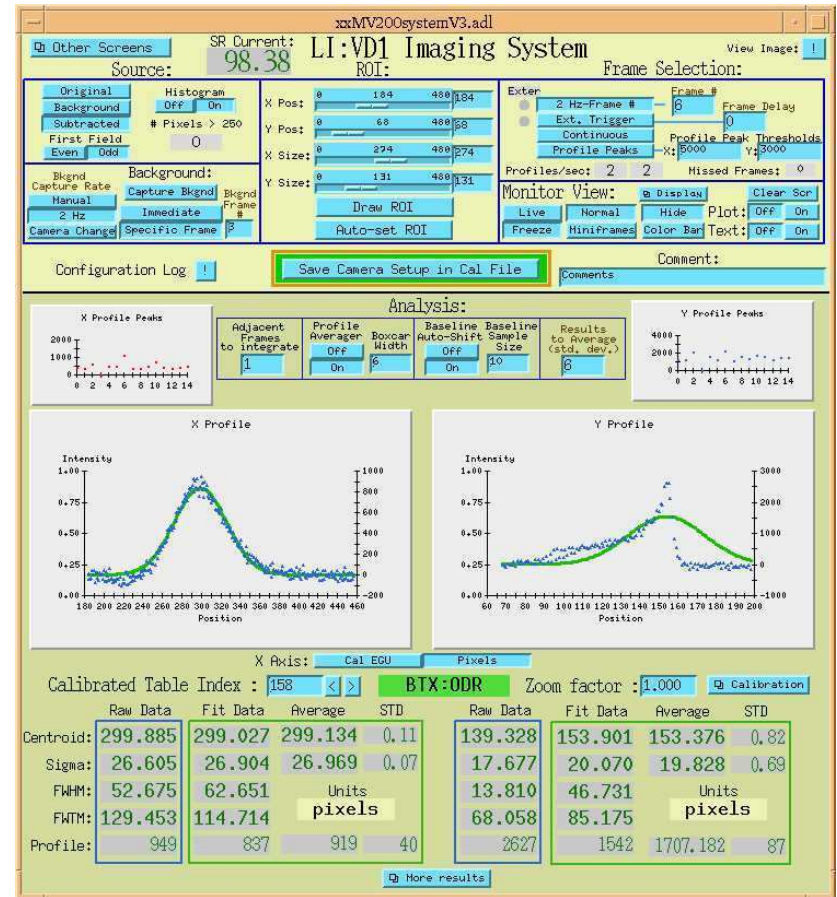
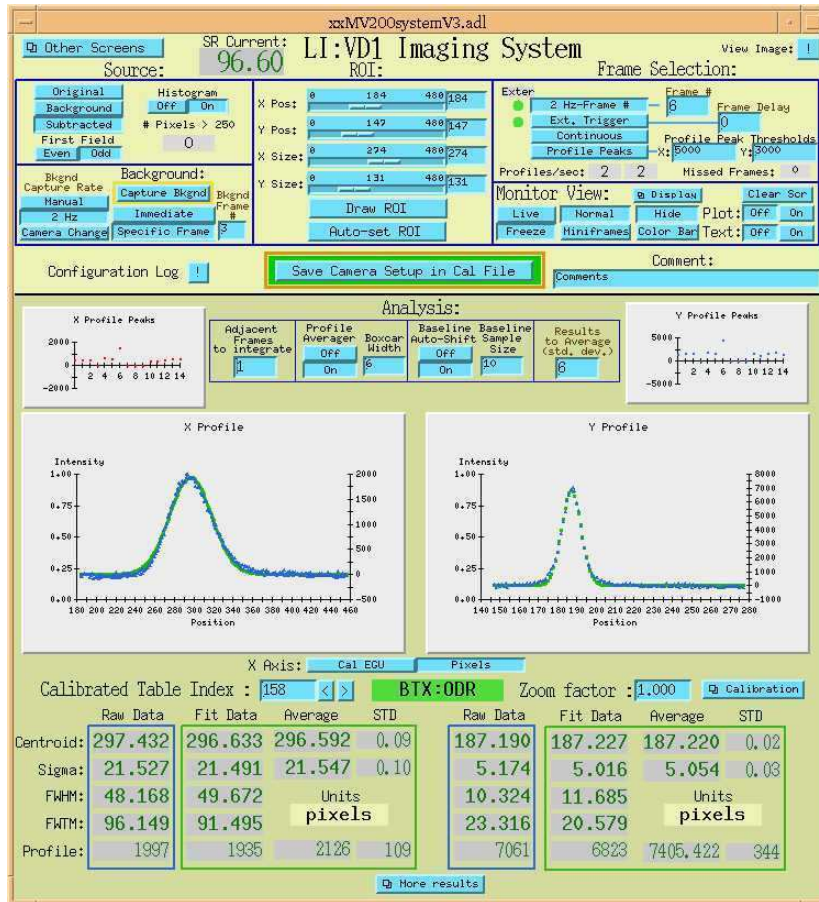
Submitted to Phys. Rev.



# Online Image Processing Shows OTR and ODR Results

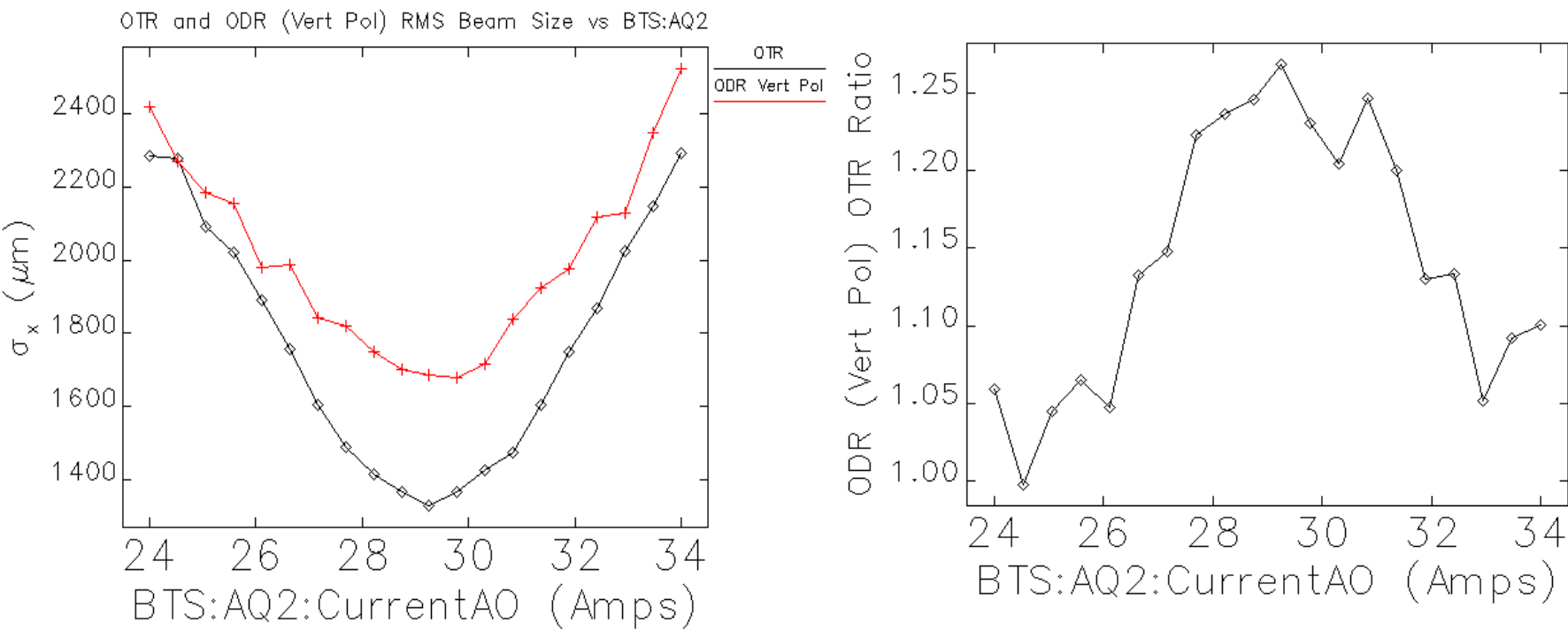
## OTR Profiles

## ODR Profiles (Vert. Pol.)



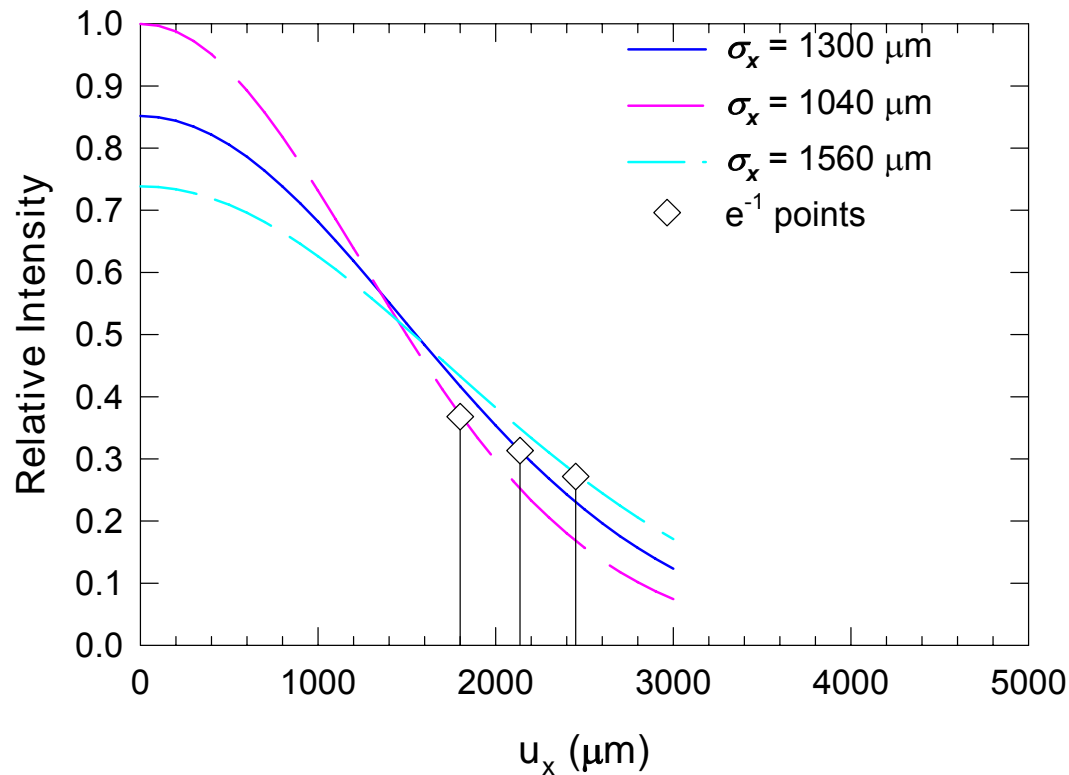
# Orthogonal ODR Polarization Component (Vertical in this case) Useful for Horizontal Beam Size Measurement

- Vertical Polarization component of ODR gives more direct representation of horizontal beam size than the sum of ODR polarization components.



# Analytical Model Indicates Beam-size Sensitivity on x Axis

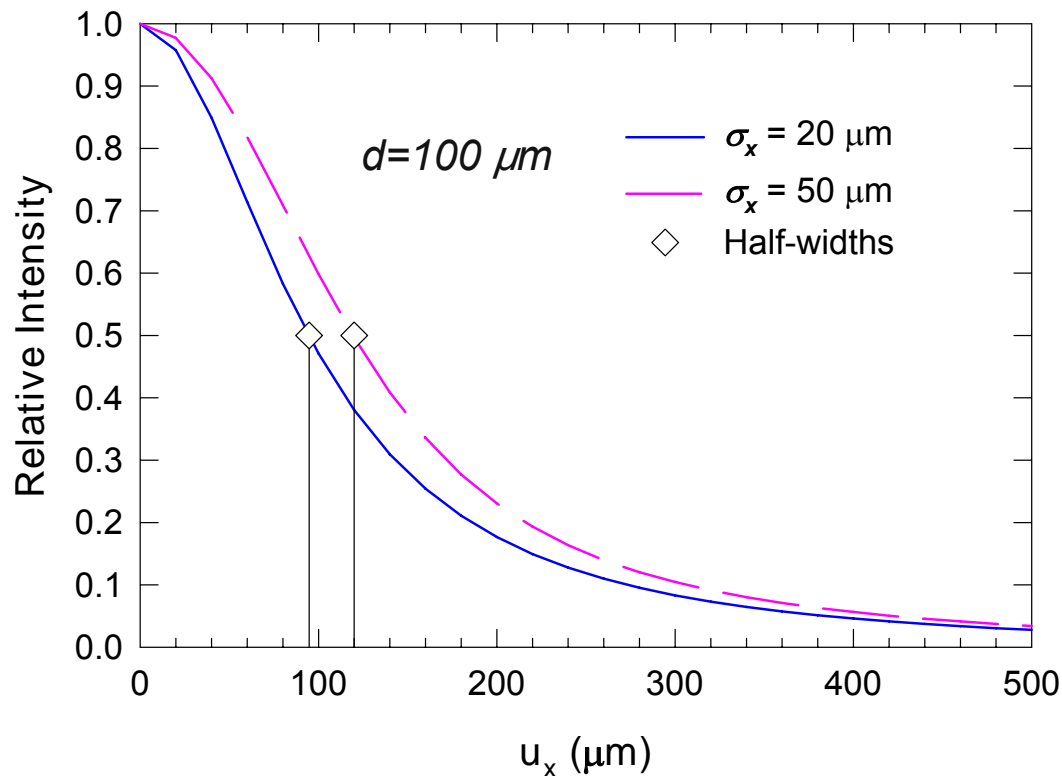
- Beam size varied  $\pm 20\%$  around 1300- $\mu\text{m}$  value to show change in ODR profile detectable with  $d=1000\text{ }\mu\text{m}$  and  $\sigma_y=200\text{ }\mu\text{m}$ .





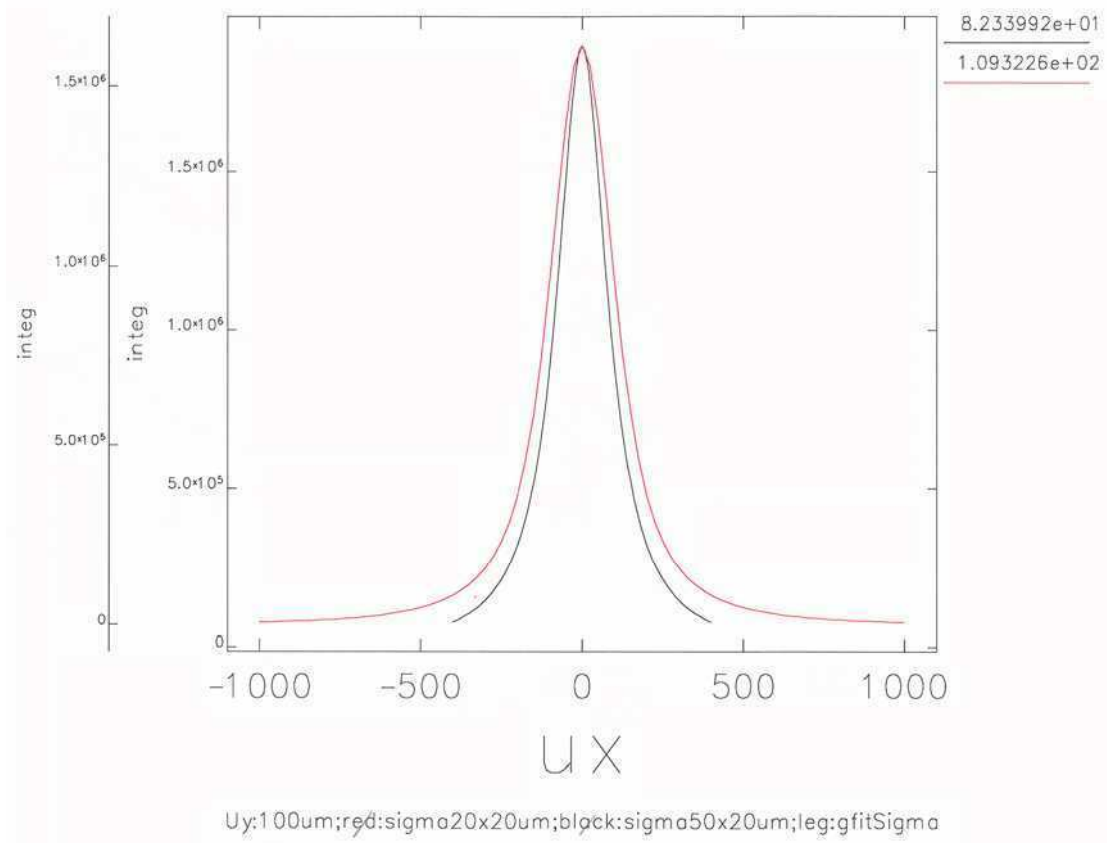
# Analytical Model Indicates Beam-size Effect in New Regime at 20-50 $\mu\text{m}$ for 7-GeV Beam (XFEL, ERL, ILC)

- ODR model shows new regime possible even without polarization selection for fixed  $\sigma_y = 20 \mu\text{m}$ .



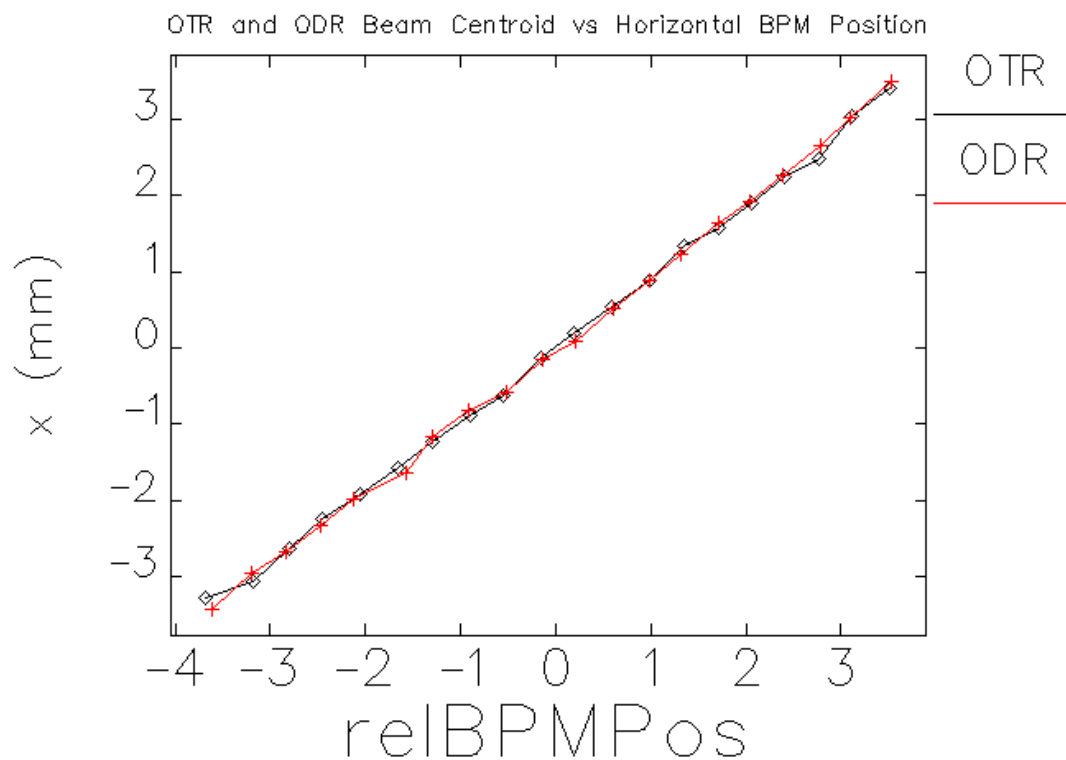
# ODR Model Predicts Sensitivity to Beam Sizes at 20-50 $\mu\text{m}$ Level for 7-GeV Beam (X-ray FELs, ILC, LWFA)

- ODR image profile changes with horizontal beam size for fixed  $\sigma_y$  of 20  $\mu\text{m}$  at  $d = 100 \mu\text{m}$ .



## ODR Also Has Good NI Beam-Position Sensitivity Using Orthogonal Polarization Component

- OTR and ODR image centroids versus horizontal rf BPM values are linear.

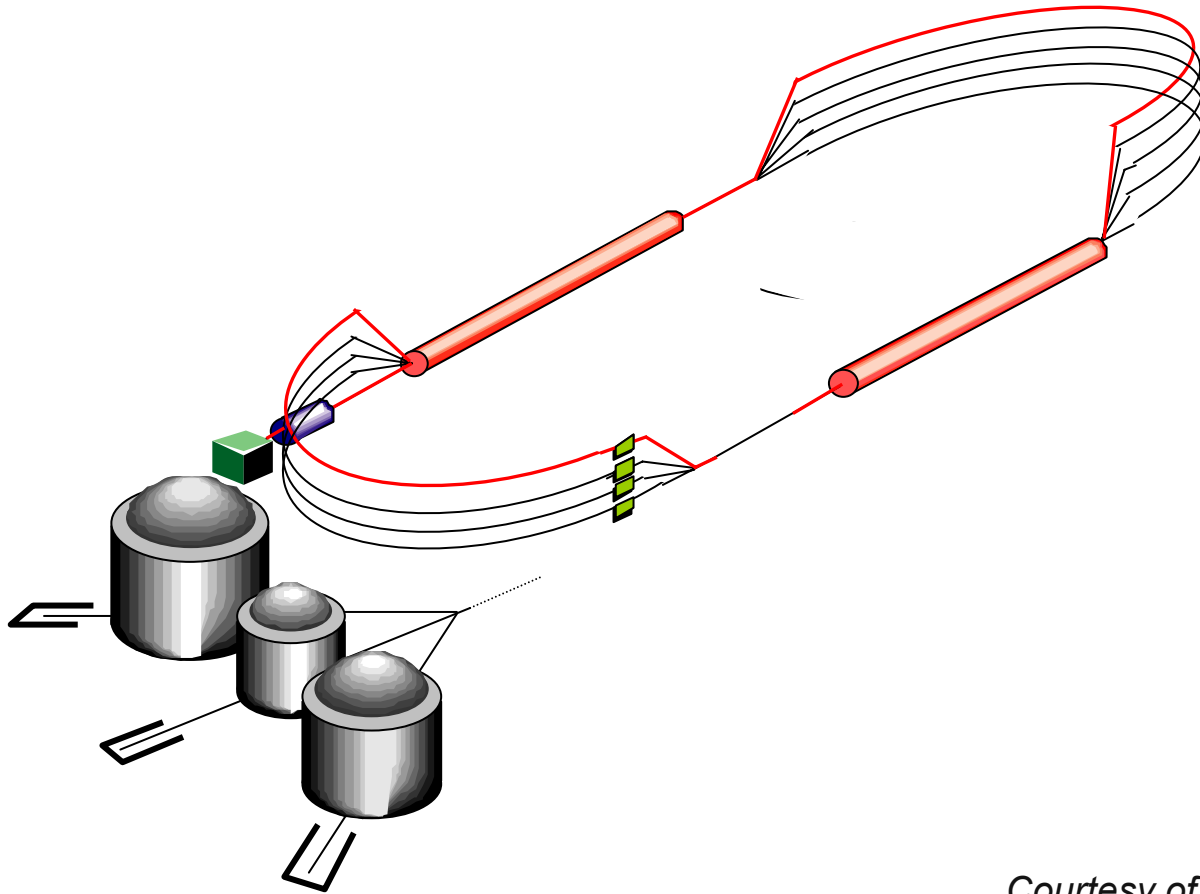


## *ODR Near-field Techniques can Address the e-beam Parameters in Proposed Projects on x-ray FELs, ERLs, ILC, and Future LWFAs*

- Nominal beam sizes in LCLS undulator diagnostics locations are  $\sigma_{x,y} = 30$   $\mu\text{m}$  for 14- and 4.5-GeV beams. NI aspect of ODR relative beam size monitor is important to minimize beam scattering to protect permanent magnets. Could use the OTR station optics with sensitive camera.
- ERLs for light sources involving high average currents (100 mA) for 5-7 GeV beams (Cornell and APS Upgrade).
- The ILC beam after the damping ring is projected to be flat with  $\sigma_x = 50$   $\mu\text{m}$  and  $\sigma_y = 5$   $\mu\text{m}$  at 5 GeV with high average current. Tests of ODR at higher energies would be useful for main linac application. (SABER?).
- The beam sizes for ILCTA in round and flat mode are ILC prototypical. Use OTR for reference low-intensity beam size.
- Polarization aspects are very useful for beam-size tracking.
- Wakefield question should be checked, but the conducting screen/plane can be retractable and the impact parameter adjusted.

# CEBAF 5-GeV Recirculating Linac

- 100  $\mu$ Amps CW beam extracted at 1, 2, 3, 4, or 5 GeV



*Courtesy of Alex Bogacz, JLAB*

## *ILC-TA Beam Offers Extended Parameter Space to Test and ODR Offers an NI Beam-size Monitor for Operations*

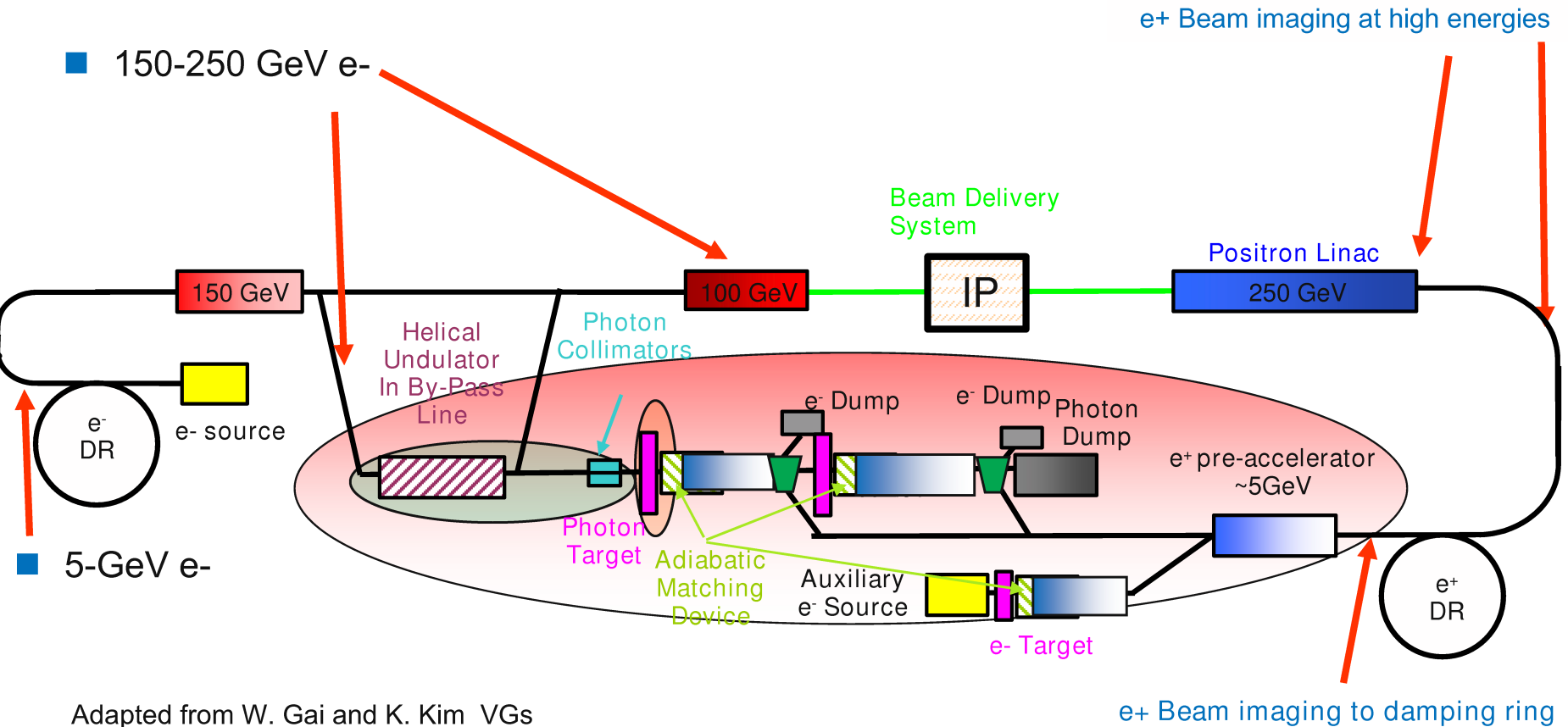
- CEBAF beam size is 10 times smaller and the charge is 1000 times greater than APS case. ILCTA beam sizes are nearly ILC prototypical.

| <u>Parameter</u>                              | <u>APS</u> | <u>CEBAF</u> | <u>ILCTA</u> |
|-----------------------------------------------|------------|--------------|--------------|
| <i>Energy (GeV)</i>                           | 7          | 1- 5         | 0.5-0.7      |
| <i>X Beam size (<math>\mu\text{m}</math>)</i> | 1300       | 30-50        | 12, 4        |
| <i>Y Beam size (<math>\mu\text{m}</math>)</i> | 200        | 30-50        | 12,36        |
| <i>Current (nA)</i>                           | 6          | 100,000      | 50,000       |
| <i>Charge/ 33 ms (nC)</i>                     | 3          | 3,000        | 10,000       |

## *Sub-GeV Beam with 10 $\mu\text{C}$ Should Give ODR Image*

- ILCTA beam sizes provide prototypical test of ILC parameters.
- ODR image intensity scales in exponential argument as  $-4\pi d/\gamma\lambda$ .
- If energy is reduced by 10, then can reduce  $d$  if beam is smaller. Also increase charge integrated in image by 3000 compared to APS case.
- Alternately, use intensified or cooled camera to extend sensitivity range.
- Can look at FIR, but imaging sensors may limit resolution.
- Modeling should be extended to lower energies. Orthogonal polarization components should be evaluated.

# Schematic of ILC Shows Potential $\text{NI}$ Imaging Applications to $e^-$ and $e^+$ Beams





# SUMMARY

- *A new NI relative beam size monitor based on ODR has been proposed to support APS top-up operations.*
- *The ODR near-field imaging techniques also have relevance to x-ray FELs, ERLs, the proposed ILC, APS upgrade, and emerging LWFAs.*
- *The ODR techniques also appear applicable to NI monitoring of the CEBAF 5-GeV beam at 100  $\mu$ A before the experiment hall.*
- *The ODR techniques appear applicable to ILCTA for sub-GeV beam with high-average current.*

# ACKNOWLEDGMENTS

- Collaborators: W. Berg, N. Sereno, C.-Y. Yao, B.X. Yang, ASD/APS/ANL; D.W. Rule, NSWC-Carderock Division
- Previous publications on ODR near-field imaging results at APS in ERL05, PAC05, FEL05, BIW06, and FEL06 proceedings.
- Previous publications by KEK on far-field imaging to deduce beam size in PRL (10-minute angle scan) and PAC05 (dephased planes).



# Possible P<sub>lasma</sub> W<sub>ake</sub> F<sub>ield</sub> A<sub>cceleration</sub> Experiment

**Patric Muggli**  
**University of Southern California**  
[muggli@usc.edu](mailto:muggli@usc.edu)



## *E-167 Collaboration:*

I. Blumenfeld, F.-J. Decker, P. Emma, M. J. Hogan, R. Iverson, R. Ischebeck, N.A. Kirby, P. Krejcik, R.H. Siemann, D. Walz

*Stanford Linear Accelerator Center*

D. Auerbach, C. E. Clayton, C. Huang, C. Joshi, K. A. Marsh, W. B. Mori, W. Lu, M. Zhou

*University of California, Los Angeles*

T. Katsouleas, E. Oz, P. Muggli

*University of Southern California*

*and E-157/162/164/164X Collaborations*

Work supported by US DoE

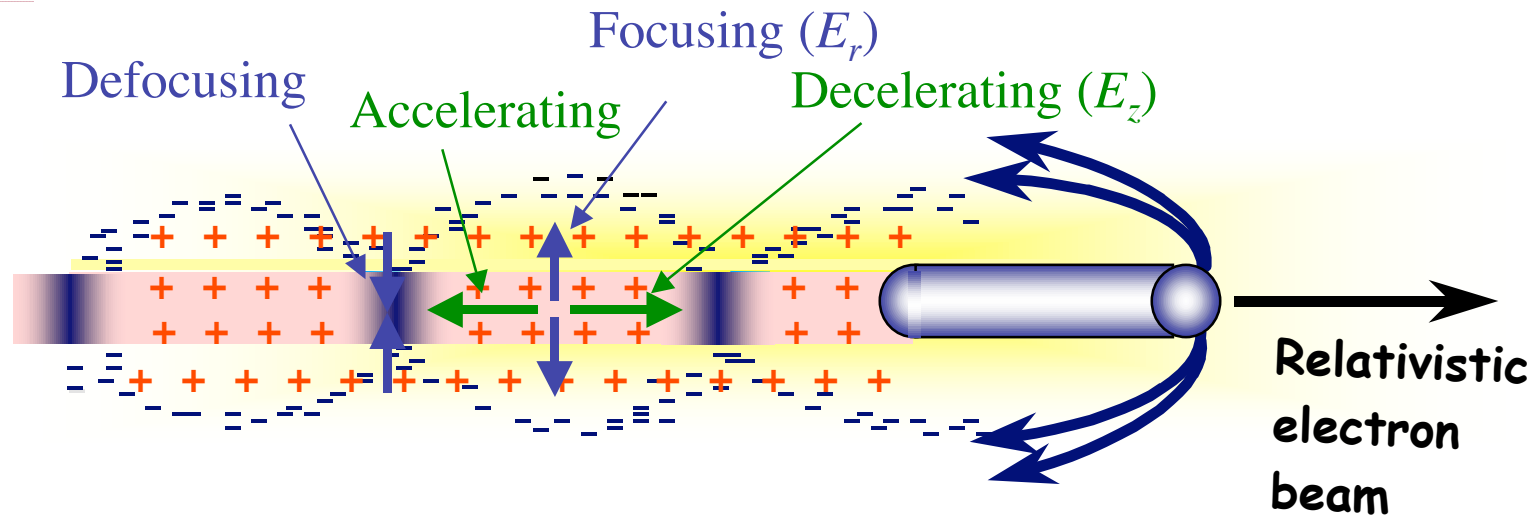




# OUTLINE

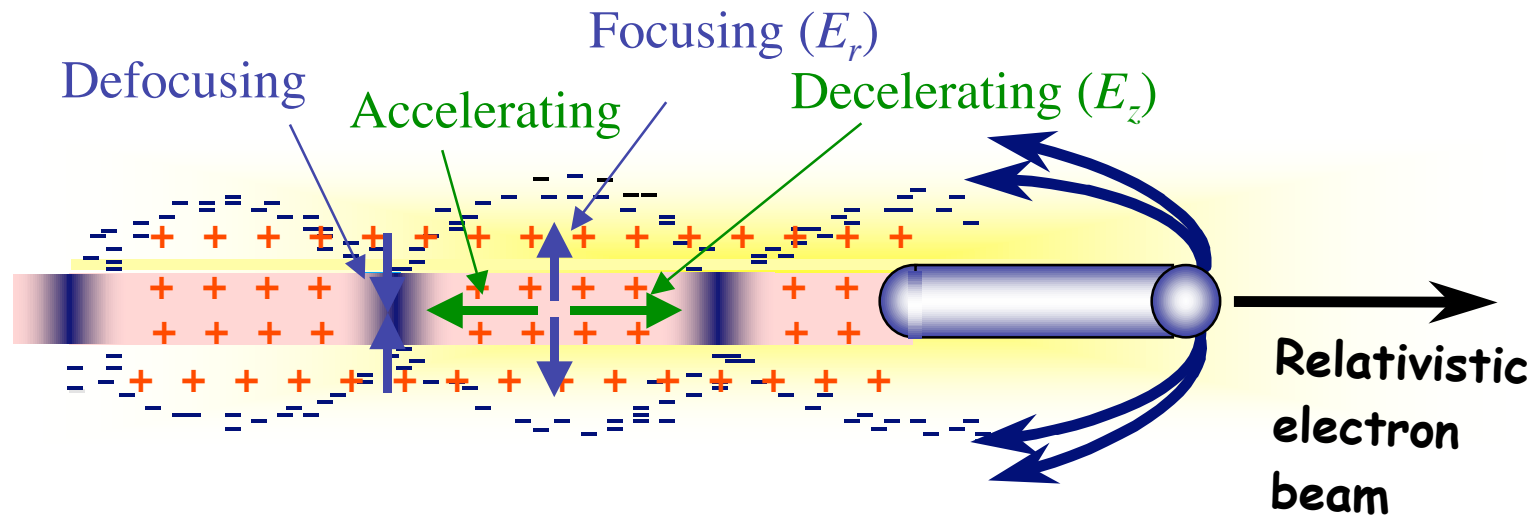
- ➡ The Plasma Wakefield Accelerator (PWFA)
- ➡ SLAC PWFA experiment
- ➡ Energy gain in the SLAC experiment
- ➡ Possible PWFA experiment @ ILCTA
- ➡ Summary/Conclusions

# PLASMA WAKEFIELD ( $e^-$ )



- Plasma wave/wake excited by a relativistic particle bunch
- Plasma  $e^-$  expelled by space charge forces  $\Rightarrow$  energy loss + focusing
- Plasma  $e^-$  rush back on axis  $\Rightarrow$  energy gain
- Plasma Wakefield Accelerator (PWFA) = energy transformer, 2-beam accelerator

# PLASMA WAKEFIELD ( $e^-$ )



- PWFA: high-frequency, high-gradient, strong focusing beam-driven accelerator

- Linear scaling: 
$$E_{acc} \cong 110 (MeV / m) \frac{N/2 \times 10^{10}}{(\sigma_z / 0.6 mm)^2} \approx 1/\sigma_z^2 \text{ (and indep. of } E_0\text{!)} \\ @ k_{pe} \sigma_z \approx \sqrt{2} \text{ or } n_e \approx 10^{14} cm^{-3} \text{ (with } k_{pe} \sigma_z \ll 1)$$

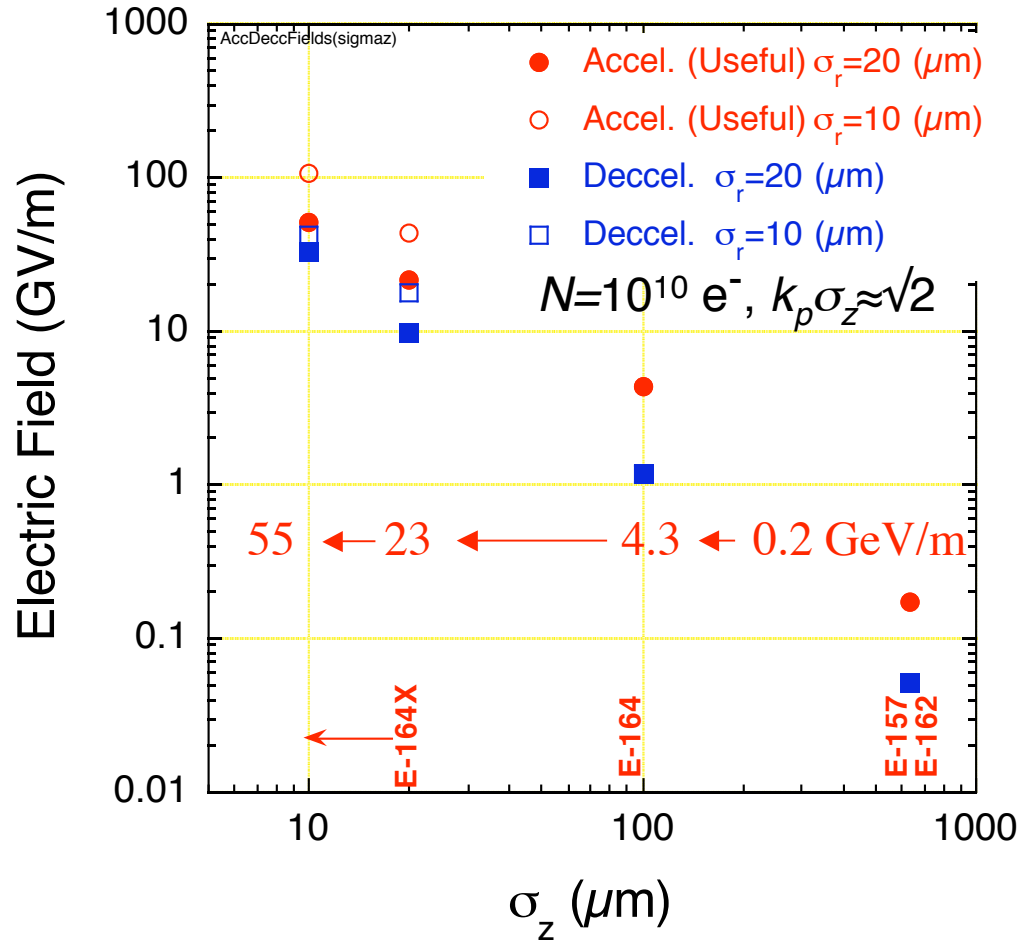
- Focusing strength: 
$$\frac{B_\theta}{r} = \frac{1}{2} \frac{n_e e}{\epsilon_0 c} = 3kT / m \times n_e (10^{14} cm^{-3})$$

- Single bunch: particles fill all the phases of the accelerating bucket

# NUMERICAL SIMULATIONS $e^-$



Gradient Increases when  $\sigma_z$  decreases ( $N=\text{cst}$ )

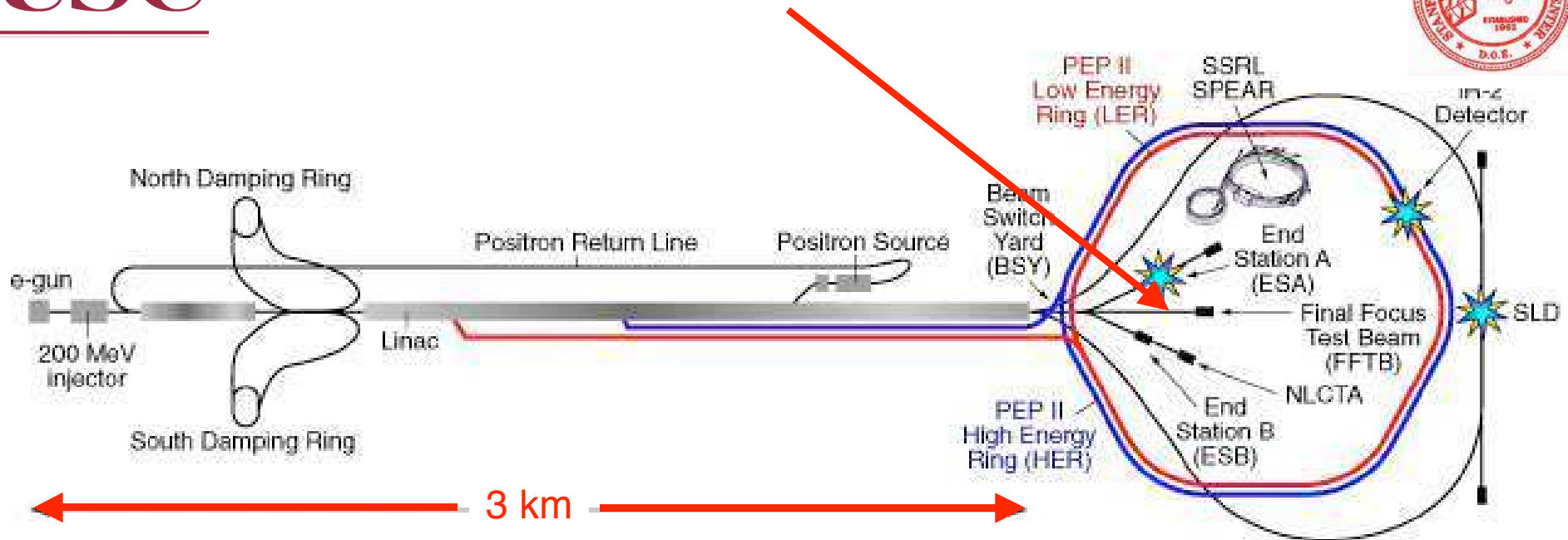


- E-167:  $\sigma_z=20-10 \mu\text{m}$ :  $>10$  GV/m gradient! ( $\sigma_r$  dependent!  $k_p\sigma_r \approx 1$ )
- $n_e \approx 1.4 \times 10^{17} \text{ cm}^{-3}$  for  $k_p\sigma_z \approx \sqrt{2}$  and  $\sigma_z=20 \mu\text{m}$

6



# PWFA EXPERIMENTS @ SLAC



## Long-bunch Experiments

$e^-/e^+$  28.5 GeV  
 $N \approx 1.2-1.8 \times 10^{10}/\text{bunch}$   
 $\sigma_z \approx 700 \mu\text{m}$   
 $\sigma_r \approx 30 \mu\text{m}$   
 $n_e \approx 2 \times 10^{14} \text{ cm}^{-3}$   
 $L_p \approx 1.4 \text{ m}$   
 Pre-ionized

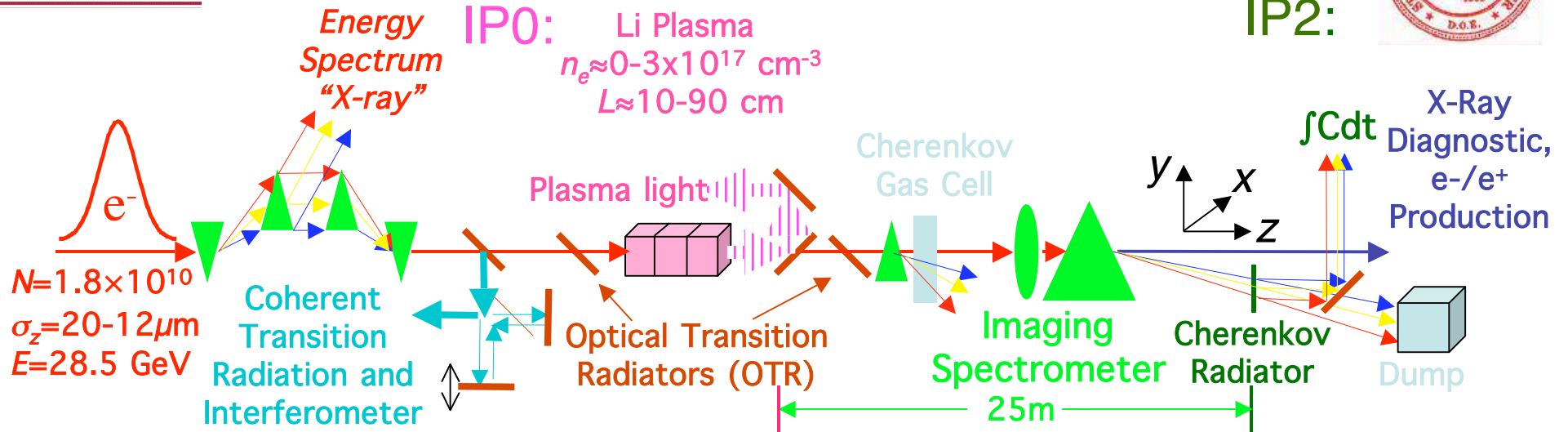
## Short-bunch experiments

$e^-$  28.5, 42 GeV  
 $\sigma_z \approx 30-20 \mu\text{m}$   
 $\sigma_r \approx 10 \mu\text{m}$   
 $n_e \approx 2-3 \times 10^{17} \text{ cm}^{-3}$   
 $L_p \approx 10, 20, 30, 60, 90, 120 \text{ cm}$   
 Field-ionized

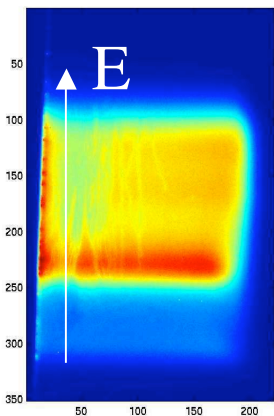
$$k_{pe} \sigma_z \approx \sqrt{2}$$

$$0.1-10 \text{ GV/m}$$

# EXPERIMENTAL SET UP (GENERIC)



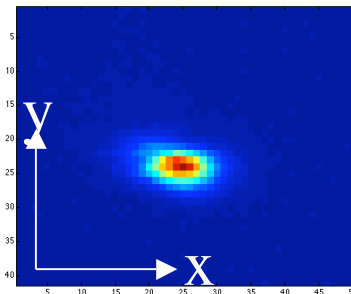
• X-ray  
Chicane



-Energy  
resolution  $\approx 60$  MeV

• Coherent Transition  
Radiation (CTR)  
- CTR Energy  $\approx I_{\text{peak}} \approx 1/\sigma_z$

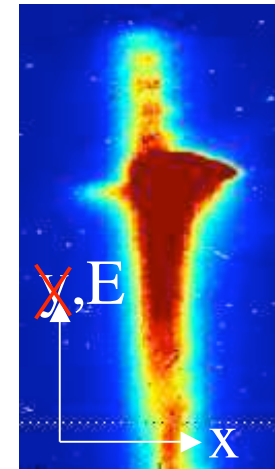
• OTR



-Spatial  
-resolution  $\approx 9 \mu\text{m}$

• Cherenkov (aerogel)

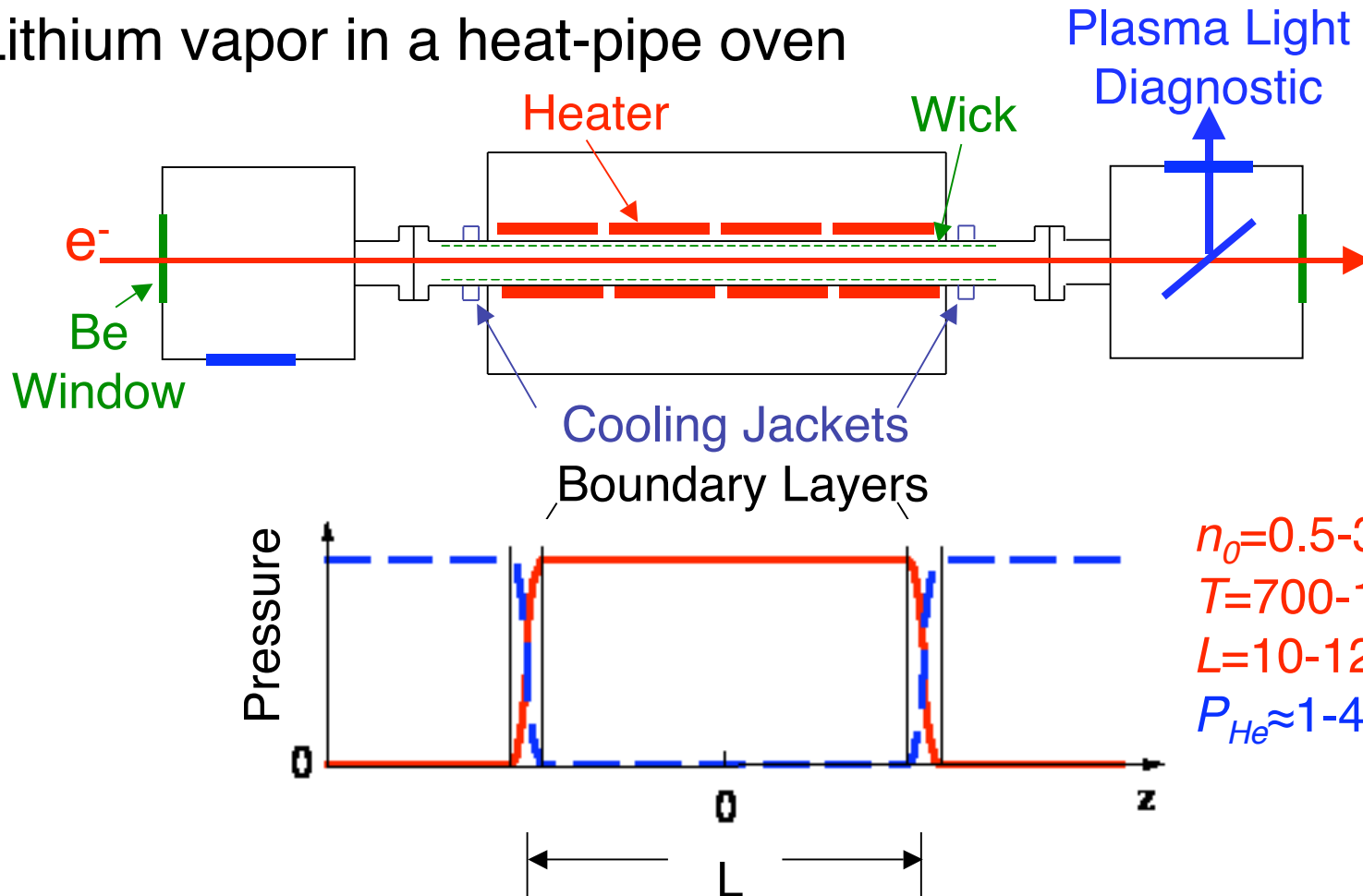
- Spatial resolution  $\approx 100 \mu\text{m}$   
- Energy resolution  $\approx 30$  MeV



# “PLASMA SOURCE”



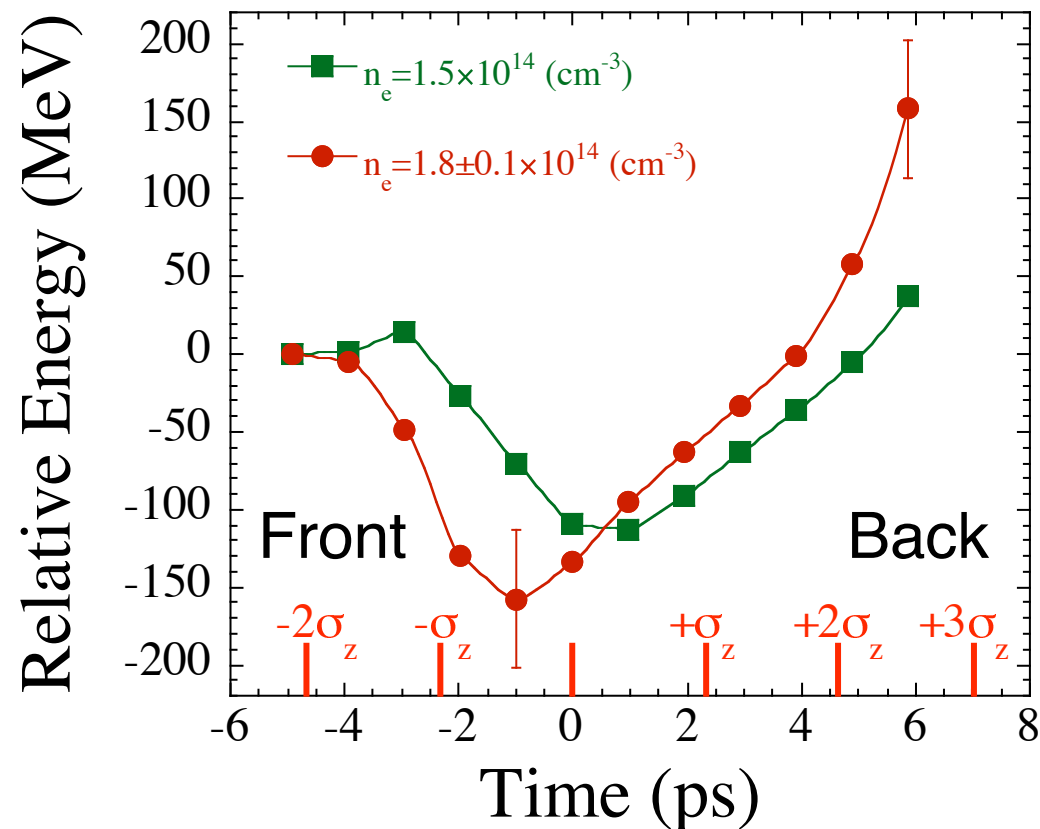
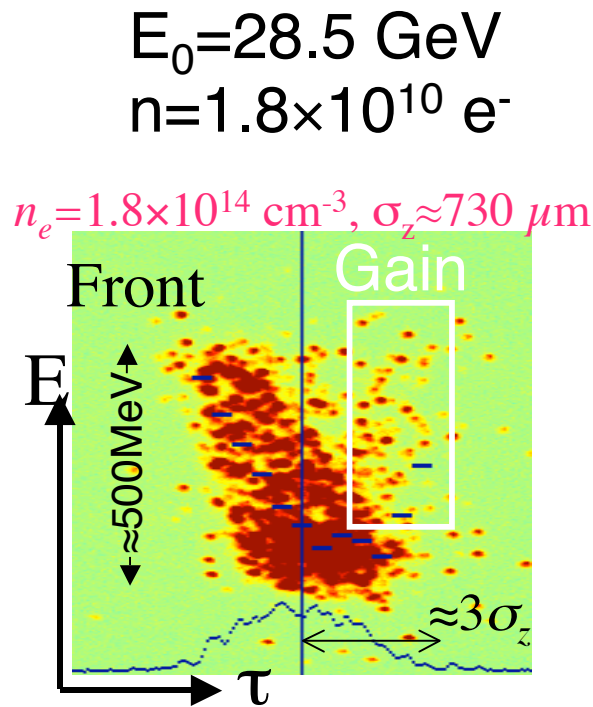
- Lithium vapor in a heat-pipe oven



- ➔ Extremely simple and cheap, high-gradient accelerator
- ➔ UV-laser photo-, pre-ionization or beam induced tunnel-ionization

# SLICE ANALYSIS RESULTS

## PRE-IONIZED, LONG BUNCH ( $\sigma_z \approx 730 \mu\text{m}$ )



- ➡ Energy gain smaller than, hidden by, incoming energy spread
- ➡ Time resolution needed, shows the physics
- ➡ Peak energy gain: 279 MeV,  $L = 1.4 \text{ m}$ ,  $\approx 200 \text{ MeV/m}$

Bunch Field:

$$E_{r,peak}(r \approx 1.6\sigma_r, z = 0) \approx 5.2 \times 10^{-10} \frac{N}{\sigma_r \sigma_z}$$

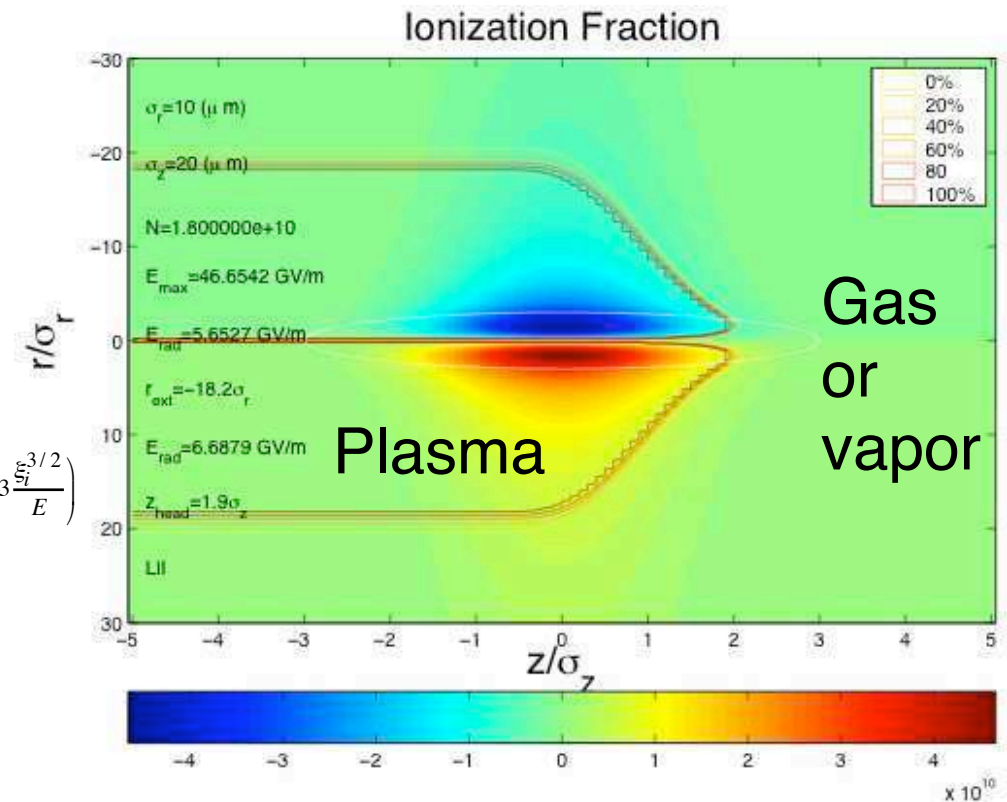
Tunneling ionization rate  
(ADK model):

$$W[s^{-1}] \cong 1.52 \times 10^{15} \frac{4^{n^*} \xi_i}{n^* \Gamma(2n^*)} \left( 20.5 \frac{\xi_i^{3/2}}{E} \right)^{2n^*-1} e^{\left( -6.83 \frac{\xi_i^{3/2}}{E} \right)}$$

$\xi_i$  = ionization potential = 5.45 eV for LiI

$E(t)$  = electric field in GV/m

$n^*$  = effective quantum number  $\approx 3.68 Z / \xi_i^{1/2}$



➔ Need  $E_r > 6$  GV/m for LiI,  $\sigma_r = 10 \mu\text{m}$ ,  $\sigma_z = 20 \mu\text{m}$ ,  $N = 1.8 \times 10^{10} e^-$   
or  $I_{\text{peak}} \approx 6$  kA

➔ The bunch creates its own plasma (fully ionized)



Latest energy gain results removed until they appear in  
Nature

Until then, please contact me ([muggli@usc.edu](mailto:muggli@usc.edu)) for  
questions and enquiries!



# ILCTA PARAMETERS

**Table 1: Specified nominal beam parameters out of the photoinjector and anticipated range.**

| Parameter                           | Symbol                   | Nominal      | Expected Range | Units         |
|-------------------------------------|--------------------------|--------------|----------------|---------------|
| charge per bunch                    | $Q$                      | 3.2          | 0.1 – 10       | nC            |
| number of bunch/macropulse          | $N_b$                    | 2850         | 1 – 3000       | -             |
| Bunch repetition rate               | $f_b$                    | 3            | 1-3            | MHz           |
| macropulse repetition rate          | $f_{mac}$                | 5            | 1-5            | Hz            |
| beam total energy                   | $E$                      | 40-50        | 40-50          | MeV           |
| rms transverse normalized emittance | $\epsilon_x, \epsilon_y$ | 4-5 (3.2 nC) |                | $\mu\text{m}$ |

$$\sigma_z \approx 390 \mu\text{m} (1.3 \text{ ps})$$

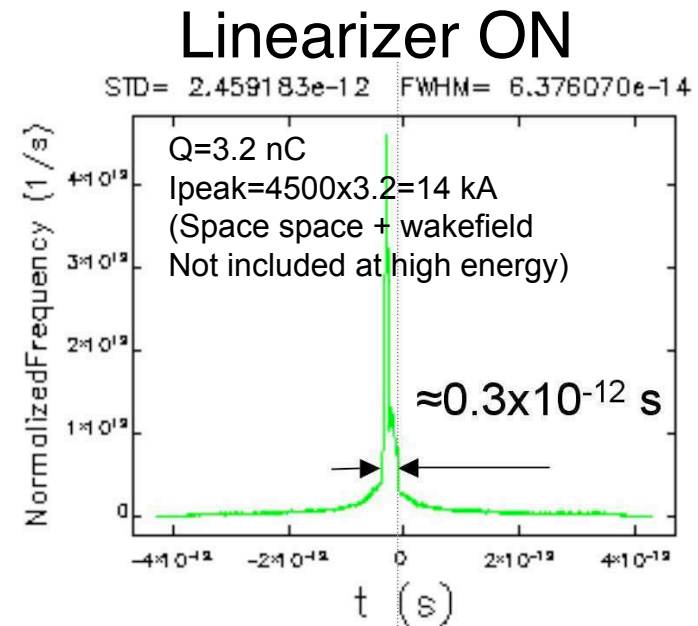
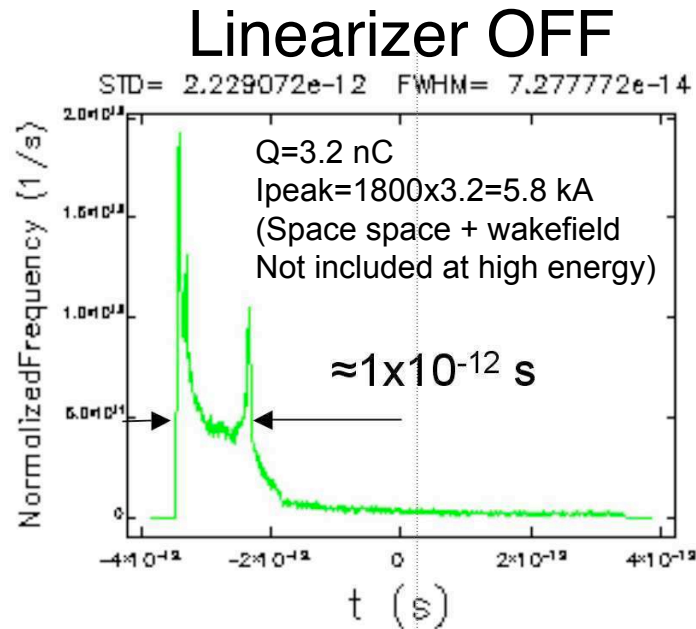
PWFA linear theory:  
 $k_p \sigma_z \approx \sqrt{2}$ ,  $n_e \approx 3.8 \times 10^{14} \text{ cm}^{-3}$   
 $n_b \approx 3.7 \times 10^{15} \text{ cm}^{-3}$ ,  $n_b/n_{pe} > 1$

**Table 2: Anticipated beam parameters at the interaction point for 3.2 nC**

| Parameter                                                           | Autumn 07      | Autumn 08      | FY 09          | Units         |
|---------------------------------------------------------------------|----------------|----------------|----------------|---------------|
| maximum total energy                                                | 280            | 520            | 760            | MeV           |
| Beta functions at IP                                                | 0.1            | 0.1            | 0.1            | m             |
| rms transverse normalized emittance (round)                         | 4-5            | 4-5            | 4-5            | $\mu\text{m}$ |
| Beam sizes at IP (round)                                            | 30             | 22             | 18             | $\mu\text{m}$ |
| rms transverse normalized emittance (flat) $\epsilon_x, \epsilon_y$ | $\sim 0.5, 50$ | $\sim 0.5, 50$ | $\sim 0.5, 50$ | $\mu\text{m}$ |
| Beam sizes at IP (flat) $\sigma_x, \sigma_y$                        | $\sim 10, 95$  | $\sim 7, 70$   | $\sim 6, 58$   | $\mu\text{m}$ |
| Peak current                                                        | $\sim 2.5$     | $\sim 2.5$     | $\sim 2.5$     | kA            |

➡ Parameters very similar to SLAC E-162 parameters:  
 $\approx 200 \text{ MV/m}$  measured in meter-long, pre-ionized plasma

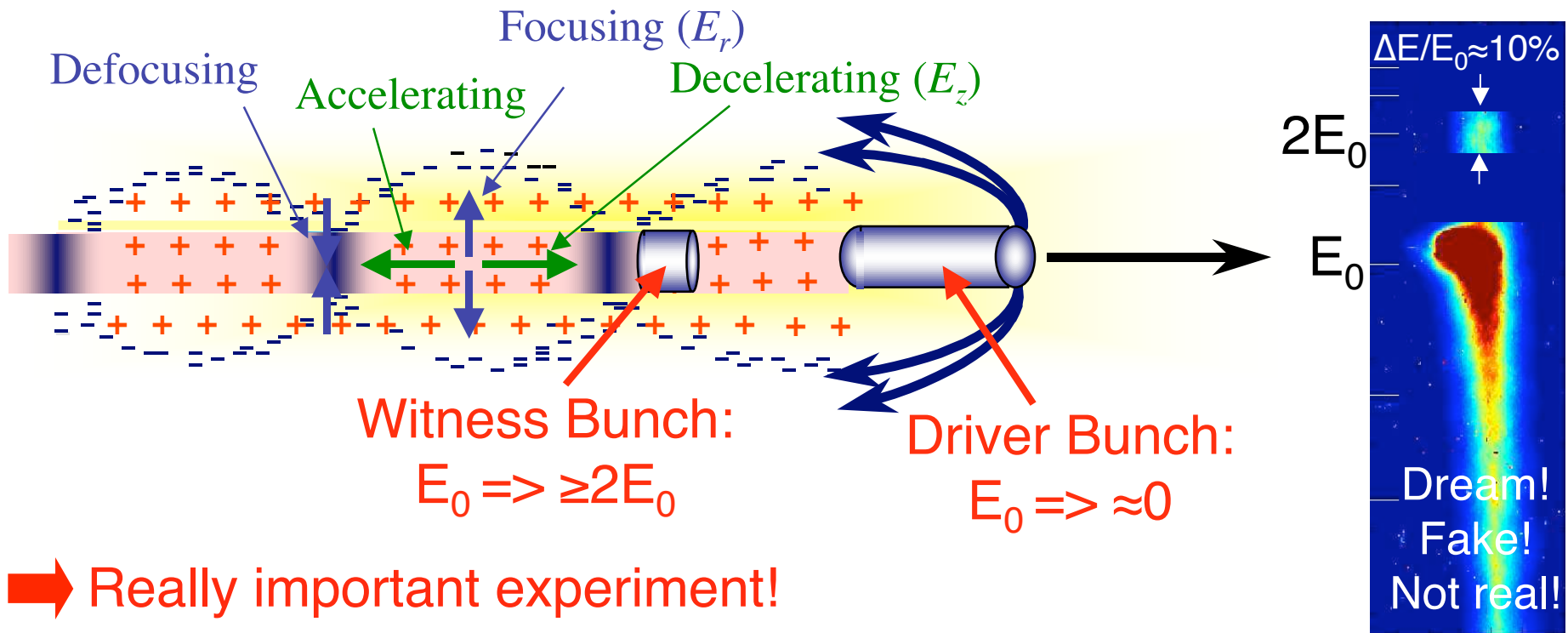
# ILCTA PARAMETERS



- ➡ With these parameters ( $\sigma_z \approx 90 \mu\text{m}$ ,  $I_{\text{peak}} \approx 14 \text{ kA}$ ), ionization of Lil and multi-GV/m gradient possible (similar to short bunch SLAC experiment!)
- ➡ Plasma source (pre- or tunnel-ionized, length) and energy gain are strong functions of the beam parameters!



# 2-BUNCH PWFA



➡ Really important experiment!

➡ Driver bunch: high-charge ( $3N$ ), modest emittance, shaped?

➡ Witness bunch: lower charge ( $N$ ), good emittance, shorter  
beam loading for  $\Delta E/E \ll 1$

## 2-BUNCH PWFA @ ILCTA

Possible parameters (need to be verified!)

Drive bunch:  $N_D = 6 \times 10^{10} \text{ e}^-$  (10 nC),  $\sigma_{zD} \approx 90 \mu\text{m}$

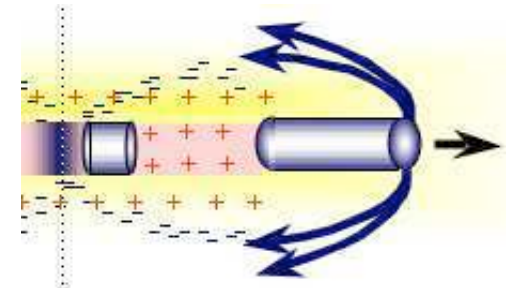
Witness bunch:  $N_W = 0.2 \times 10^{10} \text{ e}^-$ ,  $\sigma_{zW} \leq 90 \mu\text{m}$

Bunches spacing:  $\approx 300 \mu\text{m}$

Plasma density:  $n_e \approx 1 \times 10^{16} \text{ cm}^{-3}$

Accelerating gradient  $> 1\text{-}10 \text{ GV/m}$

Plasma length:  $L_p \approx 1 \text{ m}$  (tunnel-ionized Li?)



► First demonstration of high-gradient beam acceleration with ILC-like beams!!

@ 1.3 GHz,  $90 \mu\text{m} \Leftrightarrow 0.14^\circ$  of phase

$300 \mu\text{m} \Leftrightarrow 0.46^\circ$  of phase

► Producing the two bunches is a beam/accelerator physics challenge

## SUMMARY & CONCLUSION

- ➡ “Feel” for PWFA experiments
- ➡ High beam energy is not necessary for relevant PWFA experiments
- ➡ Bunch length and current are important ( $E_{\text{acc}} \approx N/\sigma_z^2$ )  
Small beam emittances are desirable ( $k_p \sigma_r < 1$ )
- ➡ Most important plasma experiments:
  - ❖ 2-bunch, beam PWFA:  $\Delta E/E \ll 1$
  - ❖ Emittance preservation, beam loading, ...
  - ❖ Plasma ions motion study and mitigation (J. Rosenzweig)
- ➡ Low rf frequency, high-charge ILCTA beam suitable for 2-bunch generation?

# Radiation Sources

Geoff Krafft  
Jean Delayen (presenter)

Jefferson Lab and  
Old Dominion University

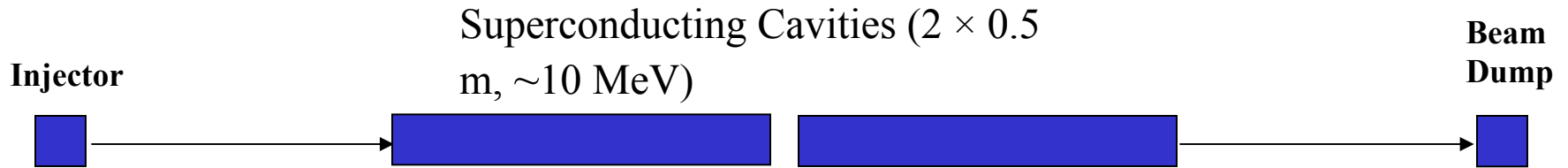
# Outline

FERMI Talk  
Nov. 28, 2006

- **CW SRF Beam Test Facility**
- **THz Source**
- **Compton X-ray Source**
- **Compton X-rays from ILC Test Accelerator**
- **Conclusions**

# CW SRF Test Facility

FERMI Talk  
Nov. 28, 2006



**Fits in existing test cave at JLAB!**

# Coherent Synchrotron Radiation

FERMI Talk  
Nov. 28, 2006

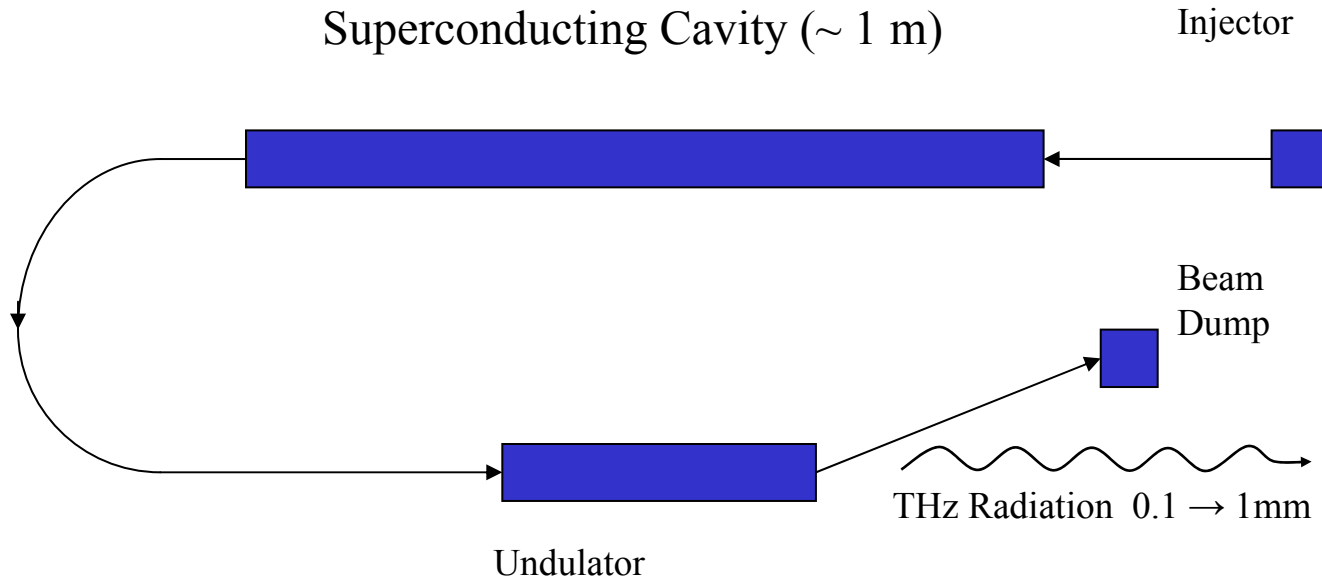
- Coherent synchrotron radiation (CSR) is electromagnetic energy radiated from the “bunch-as-a-whole” at wavelengths longer than the bunch length.
- The radiation from the individual electrons occurs at the same phase. Coherent superposition increases the output power level. Goes as bunch charge squared. Not unique to synchrotron radiation (e.g., transition and undulator radiations)
- Nodvick and Saxon (in more modern notation)

$$\frac{d^2 E}{d\omega d\Omega}(\omega) = N_e \frac{d^2 E}{d\omega d\Omega} \Big|_{1e} \left( 1 + (N_e - 1) |S(\omega)|^2 \right)$$

- First observed in electron linacs (Nakazato, *et al.*)
- Not observed in rings originally because the damped bunch length in the rings exceeded the transverse beam pipe size yielding “shielding” of the coherent emission
- Recently observed in low  $\alpha$  rings, at reduced efficiency (coherent enhancement  $< 1000$ ), because the full bunch does not radiate coherently

# Compact THz Source

FERMI Talk  
Nov. 28, 2006



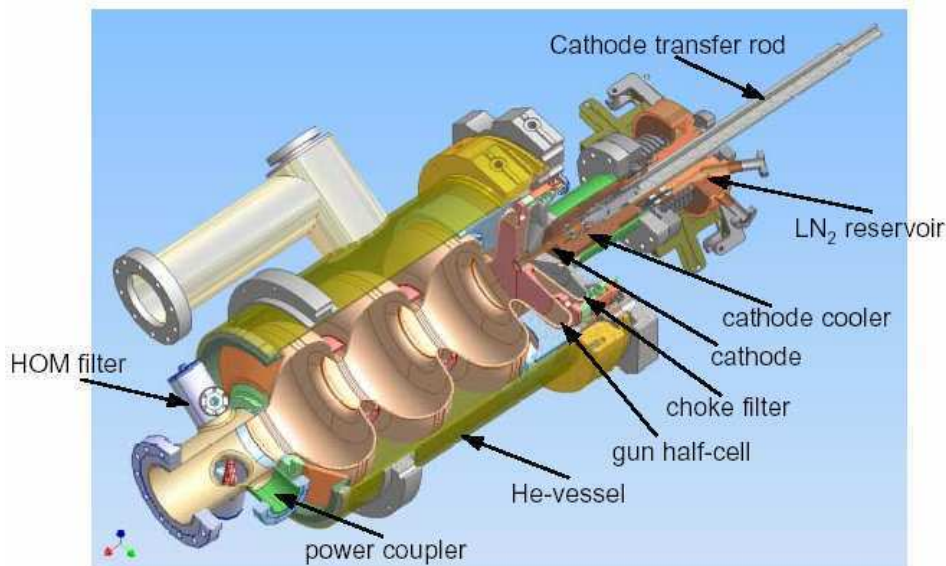
U. S. Patent 6,753,662 assigned to Jefferson Lab



# SRF photoinjectors

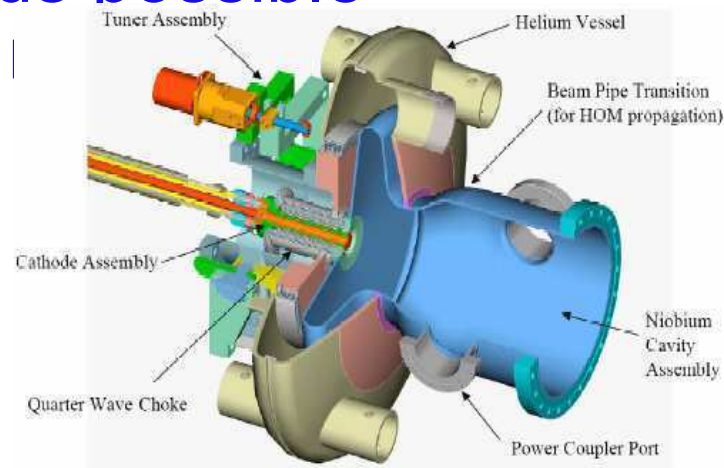
FERMI Talk  
Nov. 28, 2006

- High CW RF fields possible
- Significant R&D



**Rossendorf proof of principle experiment:**

1.3 GHz, 10 MeV  
77 pC at 13 MHz and 1 nC at  
< 1 MHz



**BNL/AES/JLAB development:**  
1.3 GHz  $\frac{1}{2}$ -cell Nb cavity at 2K  
Test diamond amplified cathode

**AES/BNL development:**  
703.75 MHz  $\frac{1}{2}$ -cell Nb photoinjector

# Source Parameters

FERMI Talk  
Nov. 28, 2006

TABLE I THz source accelerator parameters.

| Quantity                      | Value    | Unit                   |
|-------------------------------|----------|------------------------|
| Beam energy                   | 3.1–9.9  | MeV                    |
| Average beam current          | 100      | $\mu\text{A}$          |
| Charge per beam bunch         | 12       | pC                     |
| Bunch repetition rate         | 8.3      | MHz                    |
| Normalized rms beam emittance | 5        | mm mrad                |
| Longitudinal rms emittance    | 10       | keV degrees            |
| rms bunch length at wiggler   | 300 (90) | fsec ( $\mu\text{m}$ ) |

TABLE II THz source undulator and calculated optical parameters.

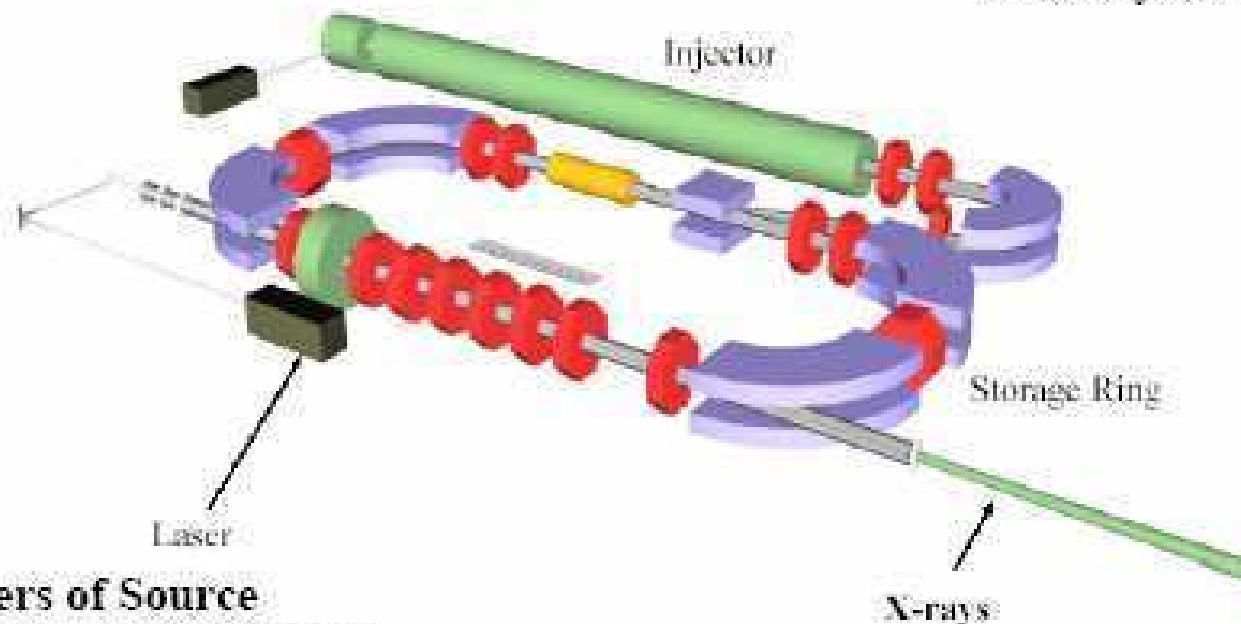
| Quantity                                    | Value                                       | Unit                                                            |
|---------------------------------------------|---------------------------------------------|-----------------------------------------------------------------|
| Undulator                                   |                                             |                                                                 |
| Period length                               | 5                                           | cm                                                              |
| Period number                               | 3, 25                                       |                                                                 |
| Field strength, $K = eB\lambda_0/2\pi mc^2$ | 1                                           |                                                                 |
| Wavelength at 5.7 MeV                       | 0.3                                         | mm                                                              |
| Fundamental optical power                   | 0.7, 5.9                                    | W                                                               |
| Fundamental flux                            | $0.9 \times 10^{18}$ , $7.3 \times 10^{18}$ | photon/s in 0.1% bandwidth                                      |
| Fundamental brilliance                      | $1.6 \times 10^{13}$ , $2.8 \times 10^{14}$ | photon/(s mm <sup>2</sup> mrad <sup>2</sup> ) in 0.1% bandwidth |
| Optical pulse length ( $N\lambda$ )         | 0.9, 7.5                                    | mm                                                              |

## Lyncean Technologies Compact Source Concept

### A Conceptual Picture of the CLS

(The 30 cm ruler in the middle is shown for scale.)

Courtesy of Ron Ruth

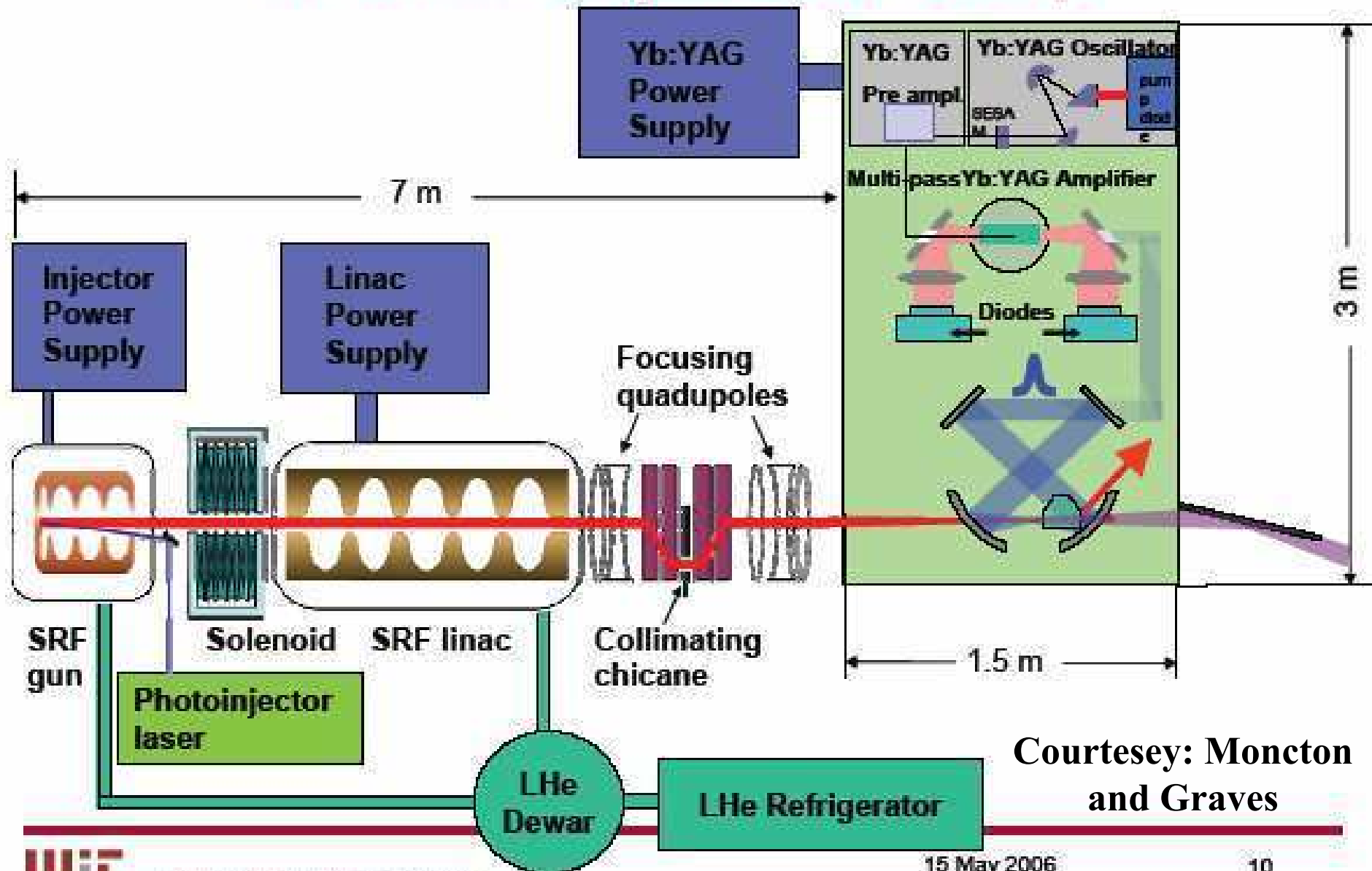


#### Parameters of Source

|              |                       |
|--------------|-----------------------|
| Average flux | $10^{12}$ photons/sec |
| Source size  | 100 microns           |

"This is not a good time now for us to present results because we are in the middle of tune up"—5/11

## MIT Inverse Compton Source Concept



Courtesy: Moncton and Graves

# Compton/Thomson Scattering at ILCTA

FERMI Talk  
Nov. 28, 2006

$$E_{scattered} \approx 2 - 4 \gamma^2 E_{laser}$$

$$\dot{n}_X = \frac{N_e N_p f}{4\pi\sigma^2} \frac{8\pi r_e^2}{3}$$

**During macropulse,  $\dot{n}_X \sim 10^{10} \text{ sec}^{-1}$**

# Conclusions

FERMI Talk  
Nov. 28, 2006

- SRF beam acceleration systems have been successfully developed and used in a wide variety of accelerators.
- Recent development of superconducting cavities has enabled CW operation at energy gains in excess of 20 MV/m.
- We at JLAB would like to develop “compact” radiation sources on SRF technology. This development might complement nicely the work at FERMILAB.
- A laser similar to the MIT proposal, producing back-scattered photons from the test accelerator, yields a hard X-ray source with very high average flux within the macropulse.

# Dual Applications of Laser- Compton Scattering

K. Chouffani

*Idaho Accelerator Center, Idaho State University, Pocatello,  
ID 83209.*

# Laser-Compton Scattering (LCS)

- Interaction of high-energy electron with photon  
 $\Rightarrow$  electron scatters low energy photon to higher energy at the expense of the electron kinetic energy.
- Similar to channeling/Undulator radiation
- Emission of highly directed (direction of e- beam), mono-energetic, and tunable X-ray beams with divergence on the order of  $1/\gamma$ .



Relativistic electron bunch  
 $\gamma = E_e / m_e c^2 = 10 - 60$

Scattered photons are  
upshifted in energy  
 $h\nu_{\text{scat}} = 4\gamma^2 h\nu_{\text{laser}}$   
and emitted in a forward  
cone with angle  $\sim \frac{1}{\gamma}$

Scattered photon speed  
and direction

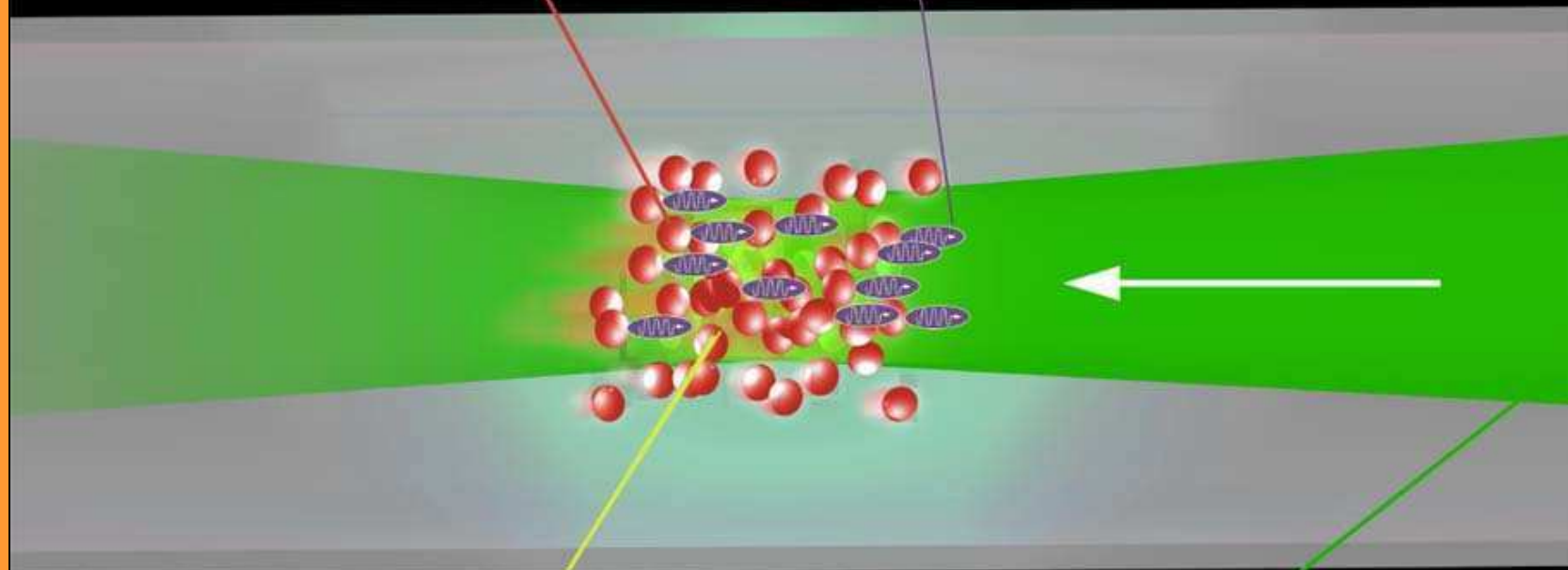


Laser speed and direction

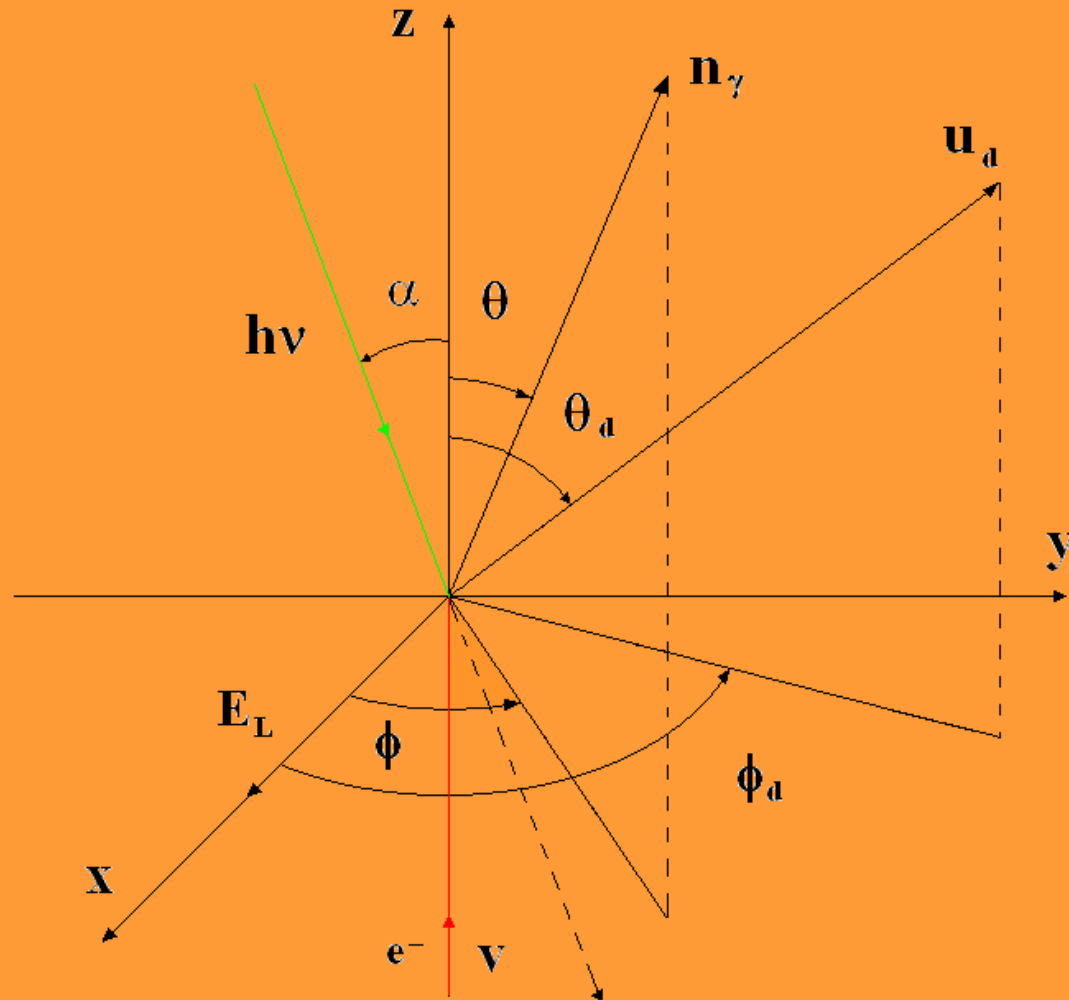


Compton scattering of laser  
photons by relativistic electrons

Incident  
laser pulse



# Orientation



- Compton x-ray energy (from energy momentum conservation):

$$E_{\gamma} \approx \frac{E_L (1 + \beta \cos \alpha)}{1 - \beta \cos \theta}.$$

- $E_{\gamma}$  = x-ray energy,  $E_L$  = Laser photon energy
- For collision geometries where  $\alpha \approx 0$  and for emission angles close to the electron beam direction:

$$E_{\gamma} \approx E_M / (1 + \gamma^2 \theta^2).$$

- Where  $E_M = 4 \gamma^2 E_L$  is the maximum energy generated in the forward direction for a head-on collision (Highest gain in energy, twice Doppler shifted).

# LCS Spectrum:

Derived from Klein-Nishina differential Compton cross section (for an incident linearly polarized wave):

$$\frac{dN_\gamma}{dE_\gamma} = \int_{d\Omega_d} \frac{dN_\gamma}{d\Omega_d dE_\gamma} d\Omega_d,$$

$$\begin{aligned} \frac{dN_\gamma}{d\theta_{x,d} d\theta_{y,d} dE_\gamma} &= L \frac{d\sigma}{d\theta_{x,d} d\theta_{y,d} dE_\gamma} \\ &= \frac{L 2r_0^2}{(2\pi)^{3/2} \sigma_x \sigma_y \sigma_e} \int_0^\infty \int_0^{2\pi} \frac{(1+\beta)}{E_M} \left[ (\cos 2\varphi + 1) \frac{E_\gamma}{E_M} \left( \frac{E_\gamma}{E_M} - 1 \right) + 1/2 \right] \\ &\quad \times \exp\left(-\frac{(\gamma' - \gamma)^2}{2\sigma_e^2}\right) \exp\left(-\frac{(\theta_{x,d} - \theta_x)^2}{2\sigma_x^2}\right) \exp\left(-\frac{(\theta_{y,d} - \theta_y)^2}{2\sigma_y^2}\right) d\varphi d\gamma'. \end{aligned}$$

$$\begin{aligned} d\Omega_d &= d\theta_{x,d} d\theta_{y,d}, \quad \theta_{x,d} \approx \theta_d \cos\varphi_d, \quad \theta_{y,d} \approx \theta_d \sin\varphi_d, \quad \theta_x \approx \theta \cos\varphi, \\ \theta_y &\approx \theta \sin\varphi, \quad E_M = 4\gamma'^2 E_L \quad \text{and} \quad \theta \approx \sqrt{1 - E_M/E_\gamma} / \gamma'. \end{aligned}$$

$L$ : single collision luminosity in the case of head-on collision.

$$L = c(1 + \beta) \iiint \rho_e(x, y, z, t) \rho_L(x, y, z, t) dx dy dz dt$$

Simplifications:

Assume transverse and longitudinal spatial distributions are Gaussians:

$$\rho_e = \frac{N_e}{(2\pi)^{3/2} x_\sigma(z) y_\sigma(z) z_\sigma} \exp\left(-\frac{x^2}{2x_\sigma^2(z)} - \frac{y^2}{2y_\sigma^2(z)} - \frac{(c\beta t - z)^2}{2z_\sigma^2}\right),$$

$$\rho_L = \frac{N_L}{(2\pi)^{3/2} \sigma_w^2(z) \sigma_L} \exp\left(-\frac{x^2}{2\sigma_w^2(z)} - \frac{y^2}{2\sigma_w^2(z)} - \frac{(ct + z)^2}{2\sigma_L^2}\right).$$

If transverse rms widths are independent of longitudinal coordinate

$$L = N_e N_L / 2 \pi \sqrt{x_\sigma^2 + \sigma_w^2} \sqrt{y_\sigma^2 + \sigma_w^2}$$

Number of LCS X-rays/burst:

$$N_{LCS} = L \sigma_\Omega$$

$\sigma_\Omega$  = Cross section within cone of solid angle  $\Omega$ .

# LCS x-ray energy and energy spread (FWHM) depend on

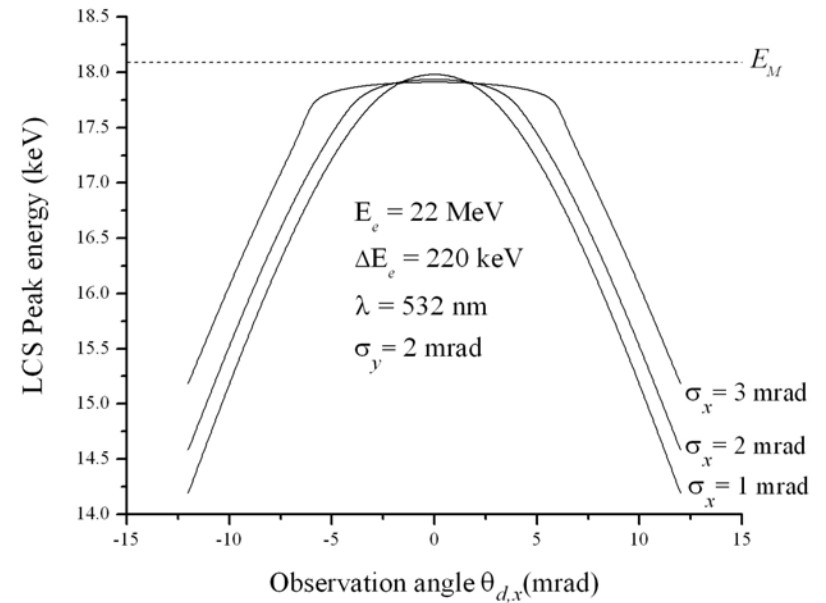
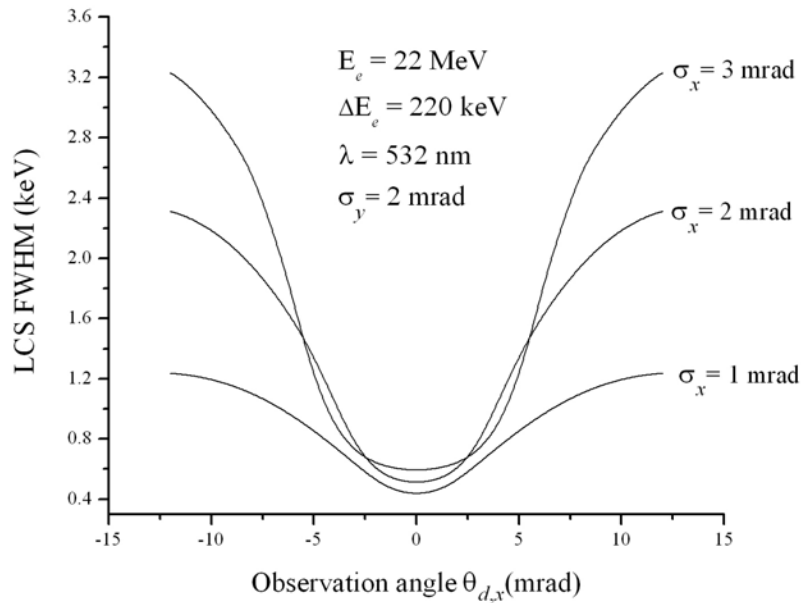
- Laser frequency bandwidth.
- Electron beam energy and energy deviation.
- e- beam angular spread.
- Electron beam direction.
- Finite detector collimation.
- Finite interaction length.

# Potential applications of LCS

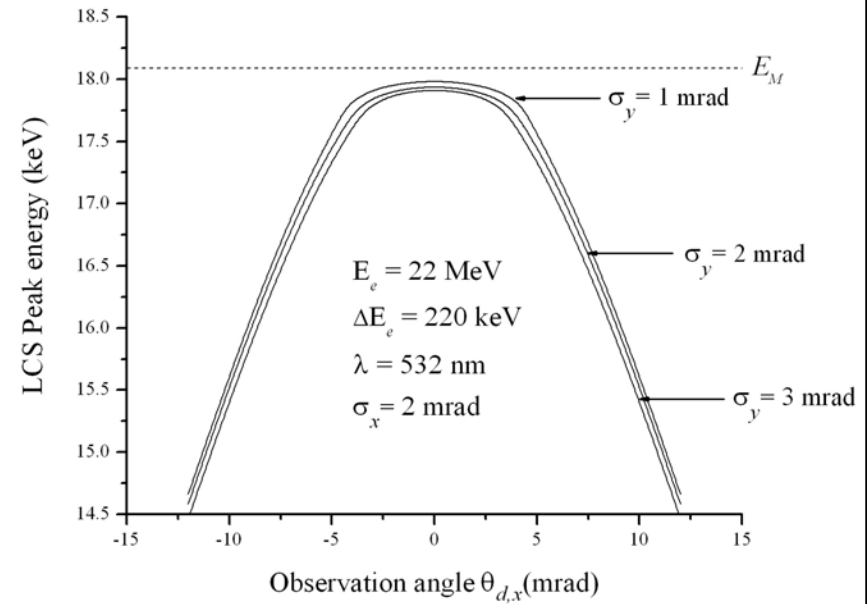
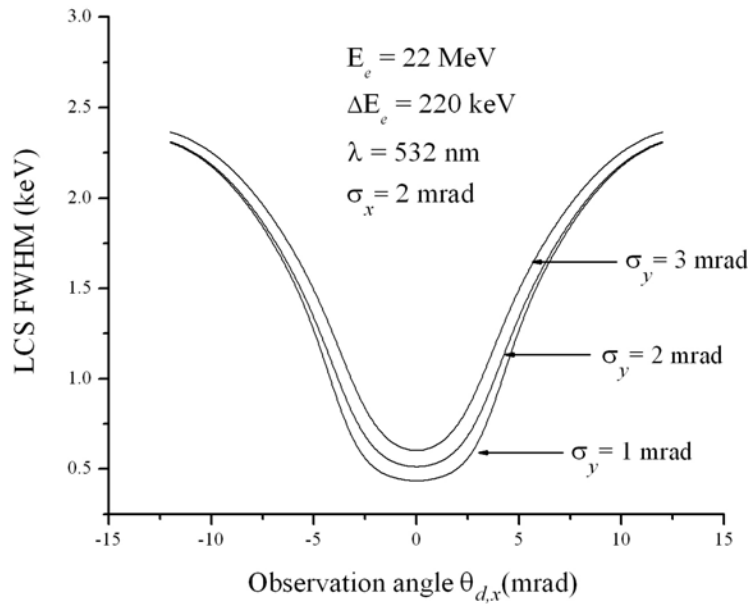
- LCS x-ray pulse durations:
  - 180° geometry:  $\tau_x \approx \tau_e$
  - 90° geometry:  $\tau_x =$  transit time
- 90° LCS geometry: scanning laser across e-beam spot size (nm range).
- Electron beam emittance, energy, energy spread and direction.



# LCS energy and FWHM dependence on beam divergence $\sigma_x$ for scan along x-direction



# LCS energy and FWHM dependence on beam divergence $\sigma_y$ for scan along x-direction

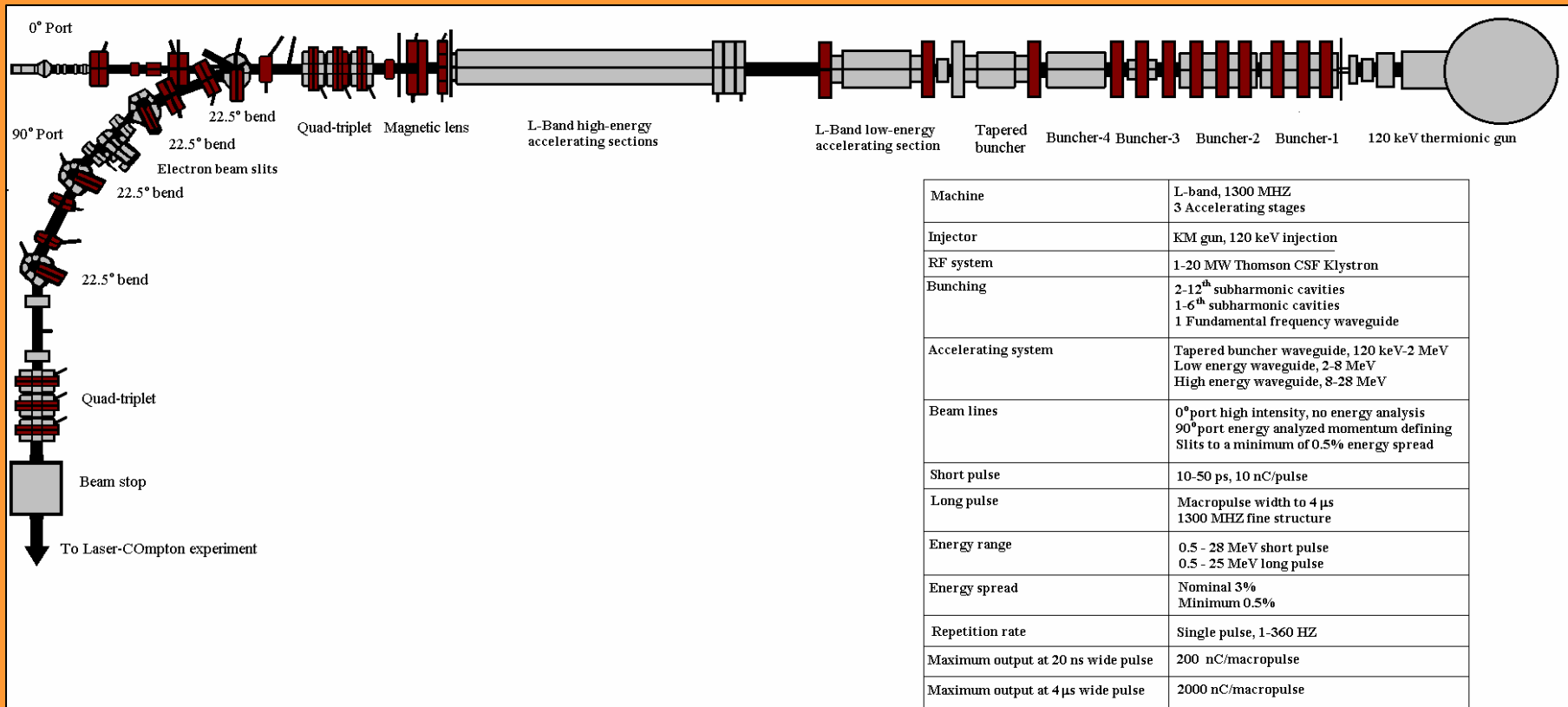


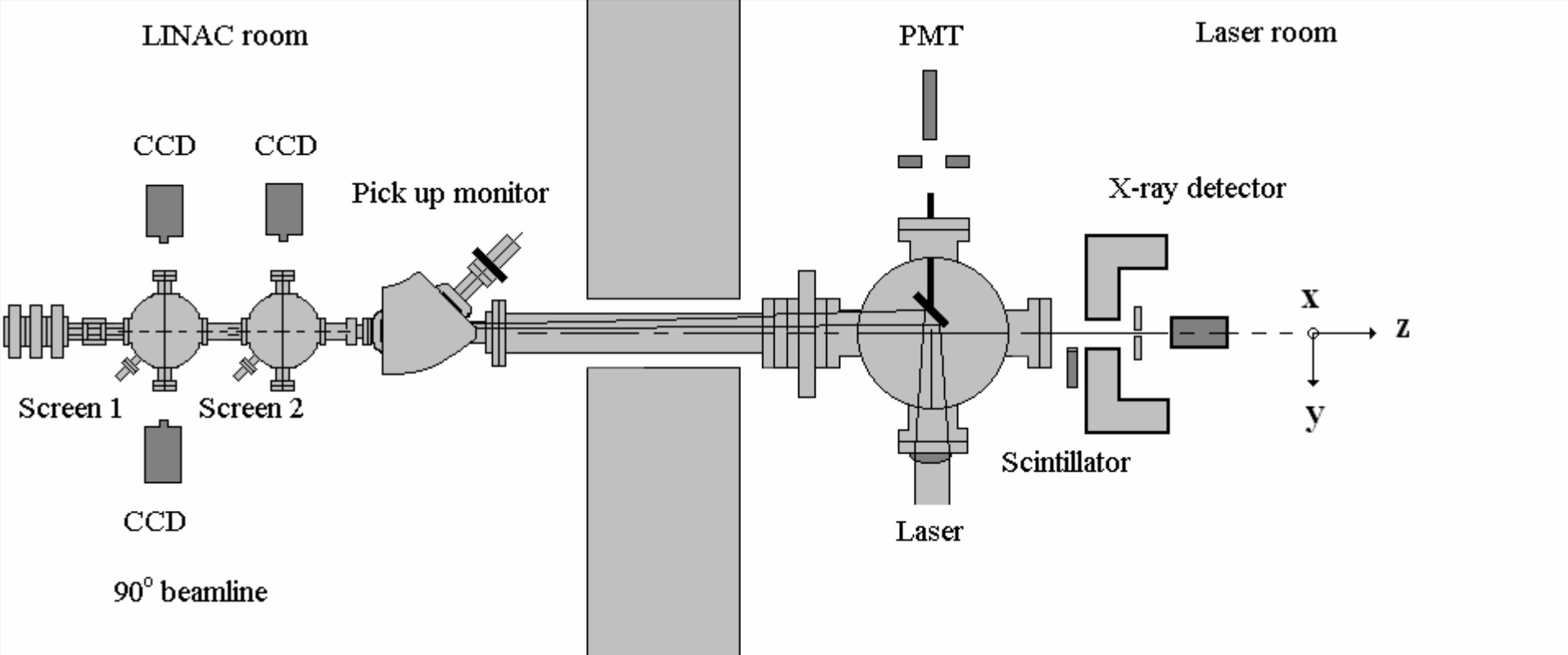
# Electron beam and laser parameters (LCS-Experiment)

- Electron beam:
- Beam energy:  
20-25 MeV
- Pulse length: 5 ns
- Charge/macro-bunch:  
 $\leq 0.9$  nC
- Rep. Rate = 10 HZ

- YAG-Laser:
- $\lambda_1 = 1064$  nm
- $\lambda_2 = 532$  nm
- Pulse length = 7-10 ns
- Energy( $\lambda_1$ ) = 0.75 Joule
- Energy( $\lambda_2$ ) = 0.25 Joule
- Rep. Rate = 10 HZ

# IAC LINAC Layout

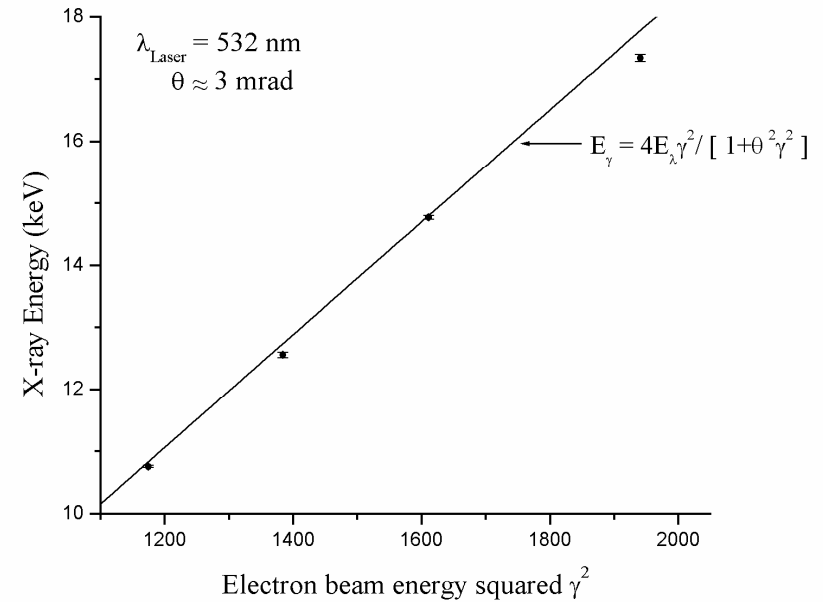
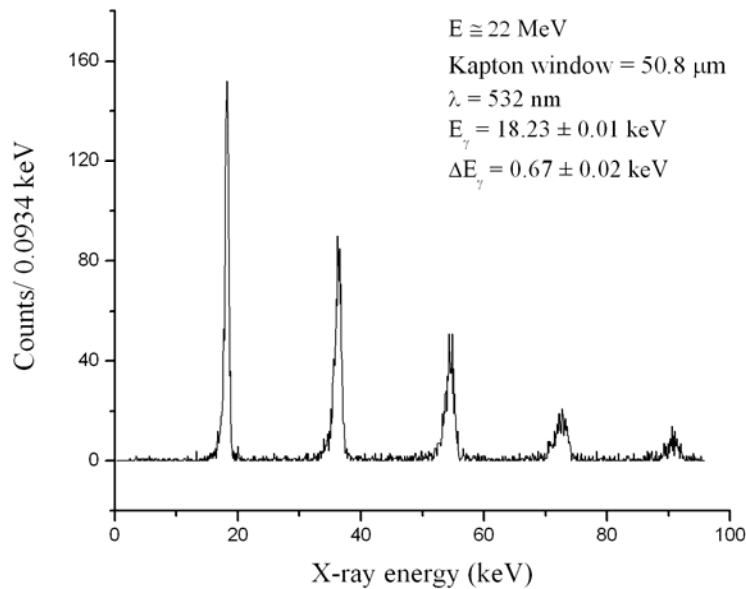




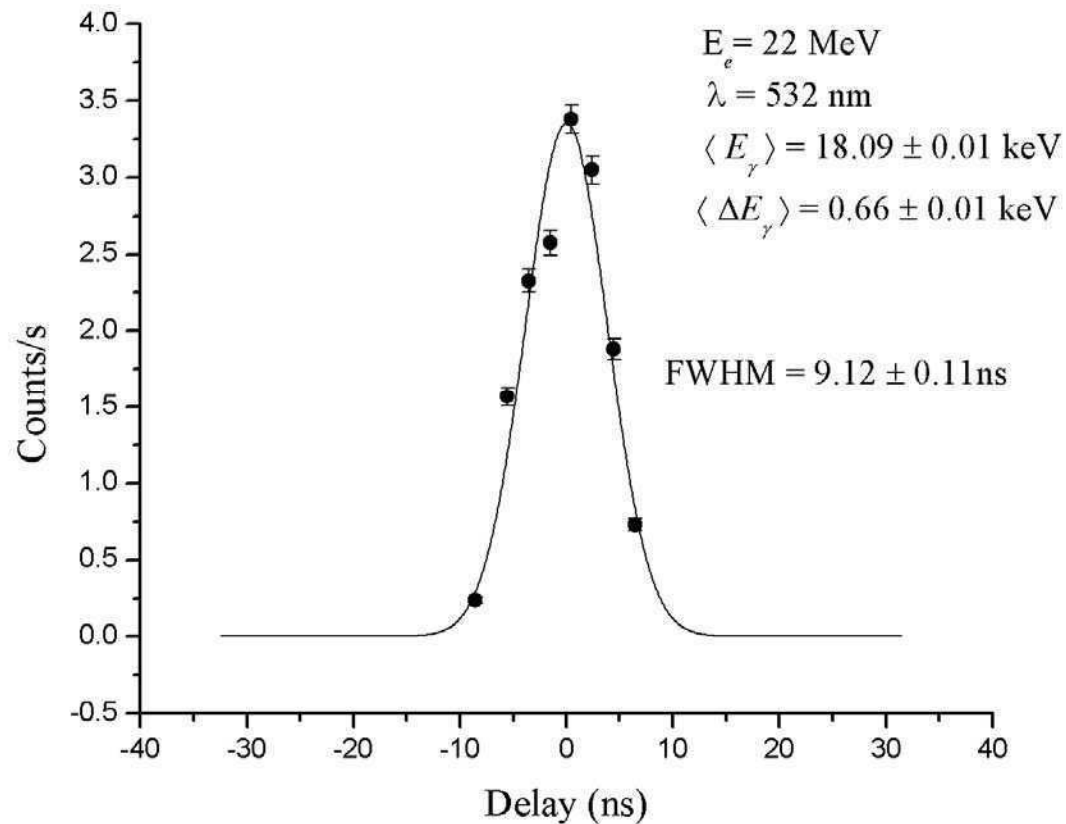
- Laser-beam line angle:  $\alpha \cong 6.2$  mrad.
- Solid angle:  $d\Omega_\gamma \cong 0.6$   $\mu$ sr.
- 1064 nm-Pol:  $\pi$ , 532 nm-Pol:  $\sigma$
- Injection seeded:

$$\Delta\nu = 90 \text{ MHz @ } 1064 \text{ nm}, \Delta\nu = 127 \text{ MHz @ } 532 \text{ nm}$$

# LCS spectrum from interaction of e-beam and laser beams and energy tunability



# Time delay between laser and electron beam pulses, SM = 90



# Angular measurements

- Scan across x-ray cone along horizontal and vertical directions to locate spectrum with maximum energy and minimum FWHM.

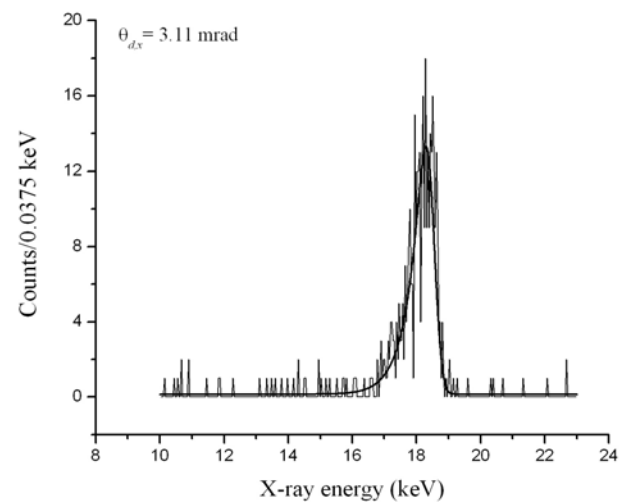
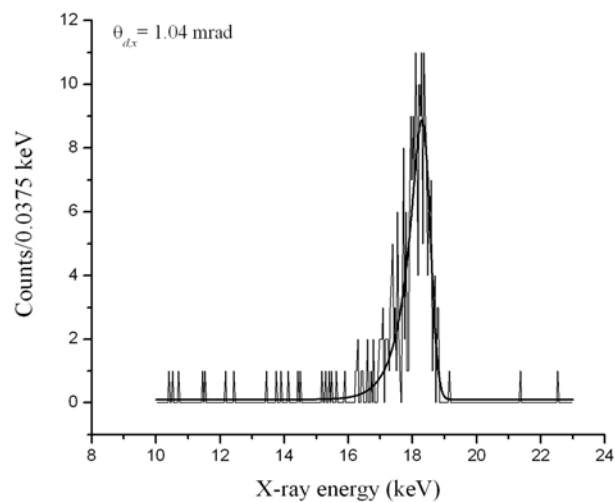
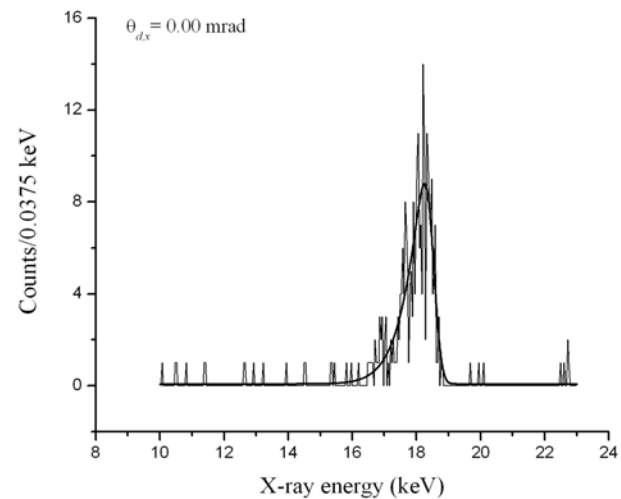
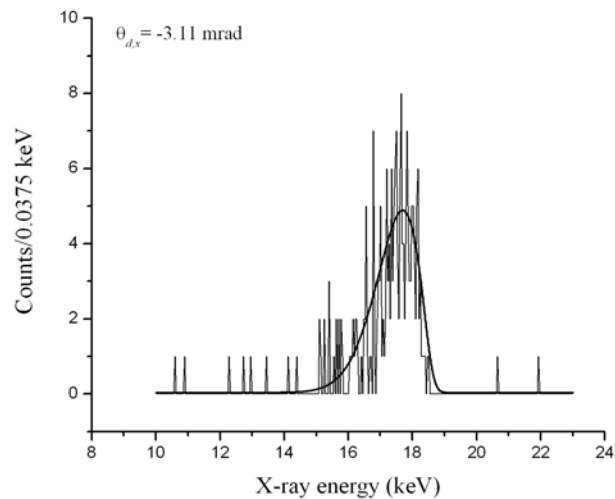
Minimization method:

- Common fit to spectra to determine common e-beam Parameters from several responses *i.e.* spectra.
- Minimization of det  $\{V_{i,j}\}$

$$\{V_{i,j}\} = \sum_k \frac{(y_{i,k} - f_{i,k})}{\sigma_{i,k}} \frac{(y_{j,k} - f_{j,k})}{\sigma_{j,k}}$$



# Angular scan (15 Spectra), SM = 200



# Measured beam parameters with minimization method

With 15 spectra:

$$E = 22.27 \pm 0.04 \text{ MeV}$$

$$\Delta E = 0.21 \pm 0.07 \text{ MeV}$$

$$\sigma_x = 2.08 \pm 0.13 \text{ mrad}$$

$$\sigma_y = 3.05 \pm 0.5 \text{ mrad}$$

$$\theta_b = -2.12 \pm 0.32 \text{ mrad.}$$

With energy and FWHM  
(E and  $\Delta E$  fixed)

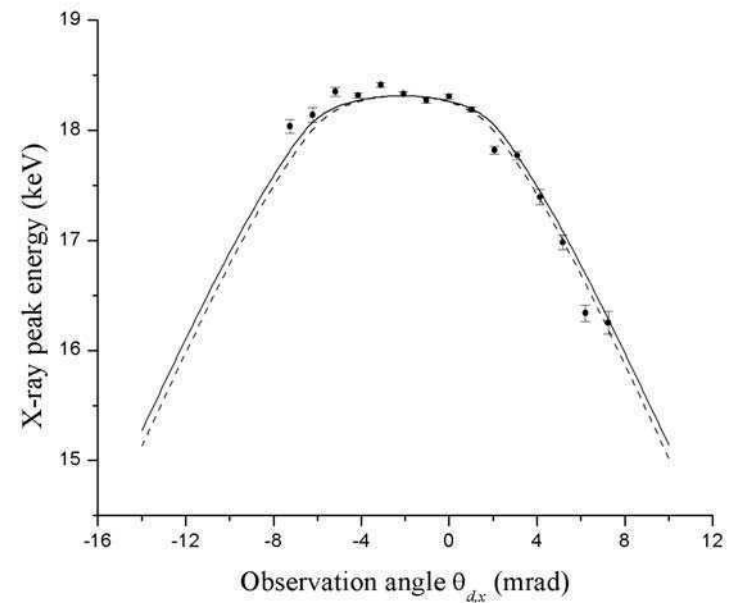
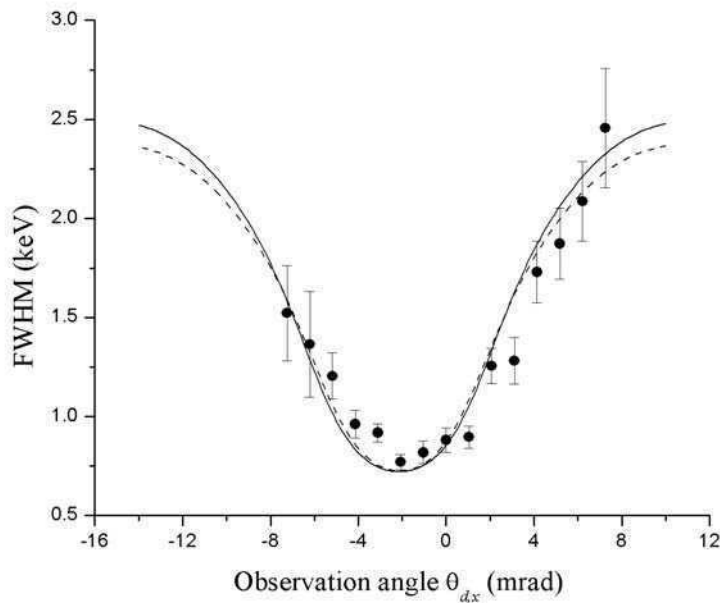
$$\sigma_x = 2.23 \pm 0.11 \text{ mrad}$$

$$\sigma_y = 2.81 \pm 0.5 \text{ mrad}$$

$$\theta_b = -2.15 \pm 0.5 \text{ mrad.}$$

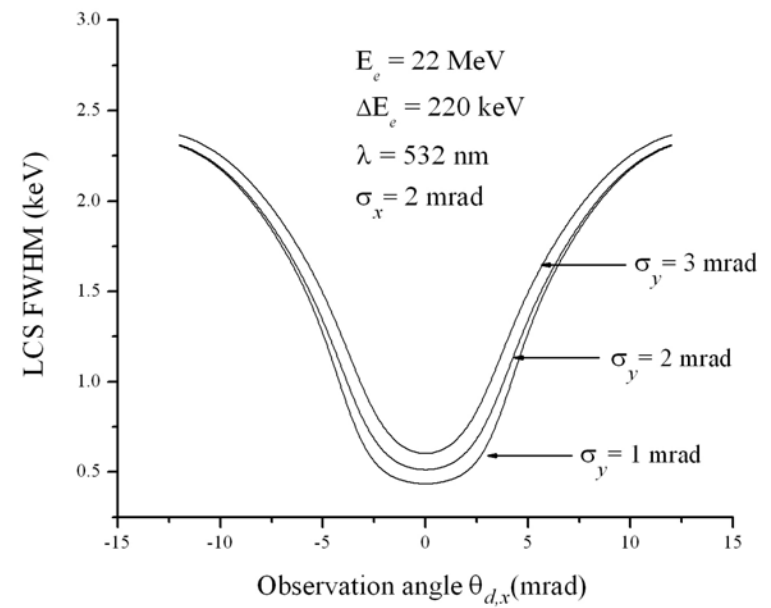
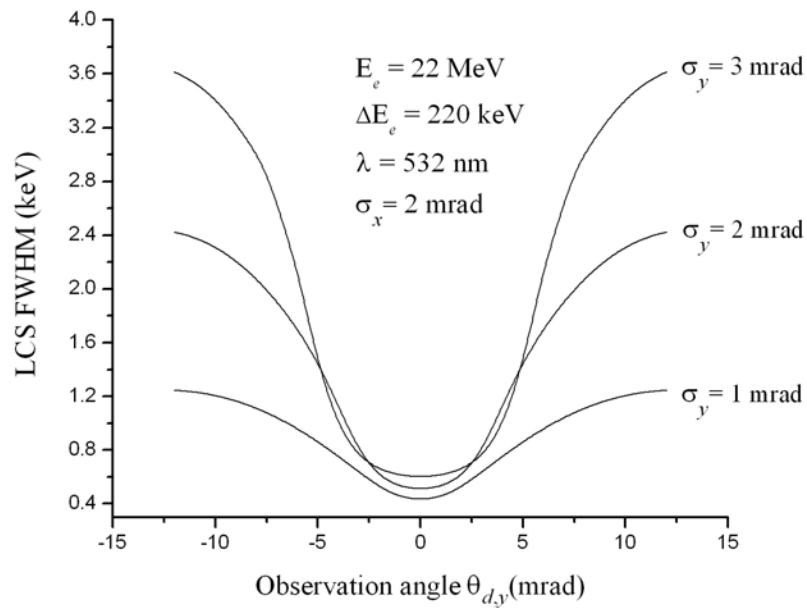
k. Chouffani *et al.* Phys. Rev. Spec. Top. AB 9, 050701 (2006).

# LCS Energy, FWHM VS Observation angle

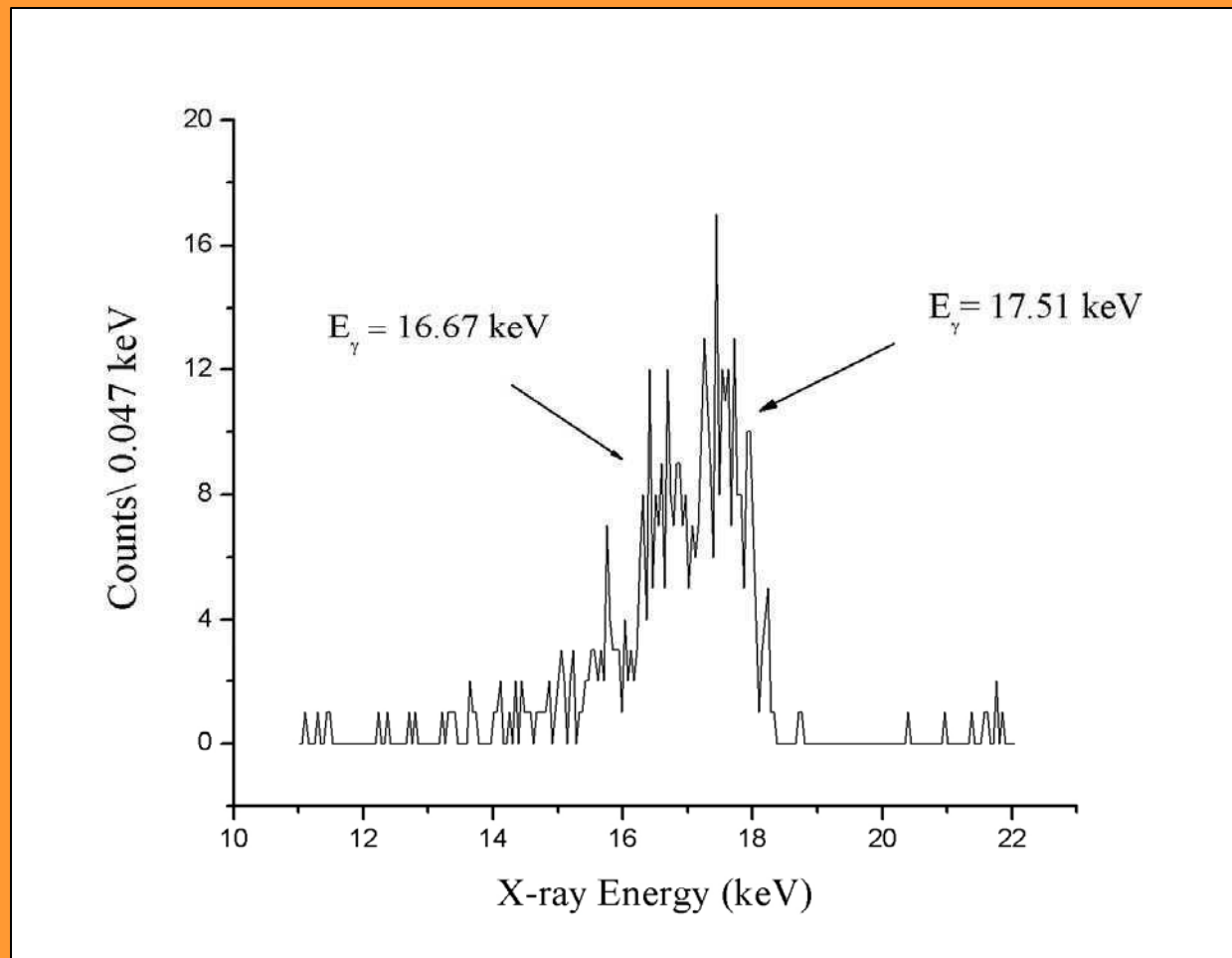


K. Chouffani *et al.* Laser Part. Beams 24, (2006) 411.

# Scan perpendicular to electric field



# Method susceptible to beam instabilities



# Bio-Medical Imaging

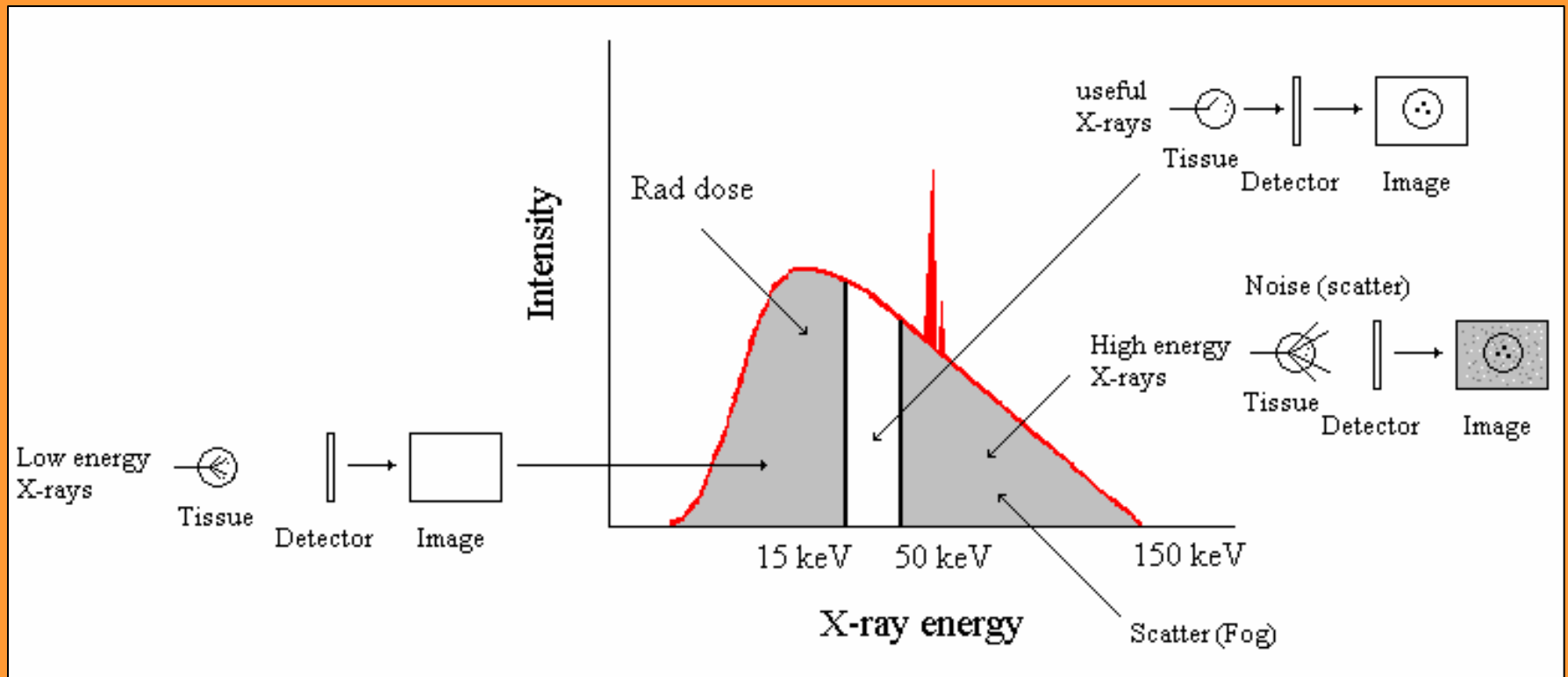
Production of high-quality images of soft tissue while reducing dose .

K-edge subtraction angiography.

Phase contrast imaging (DEI, X-ray interferometry).

X-ray protein crystallography.

# Conventional X-ray source



# Single pulse imaging



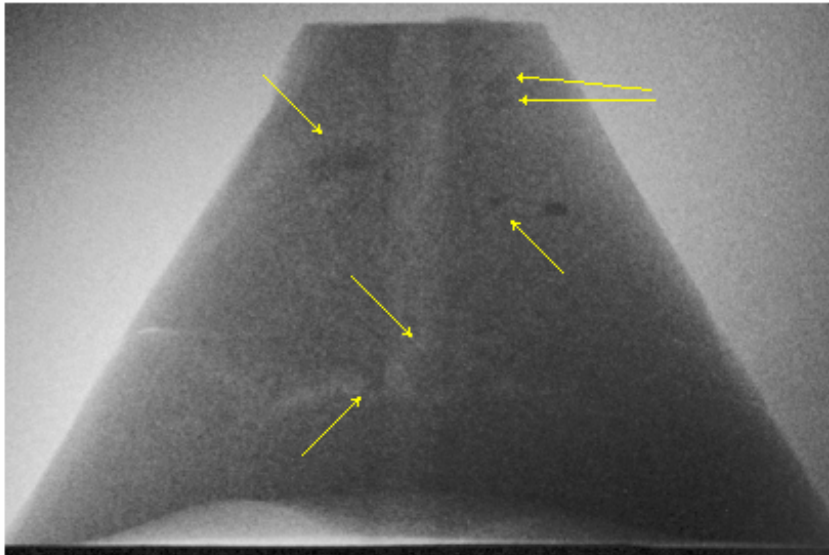
19 keV LCS  
X-ray



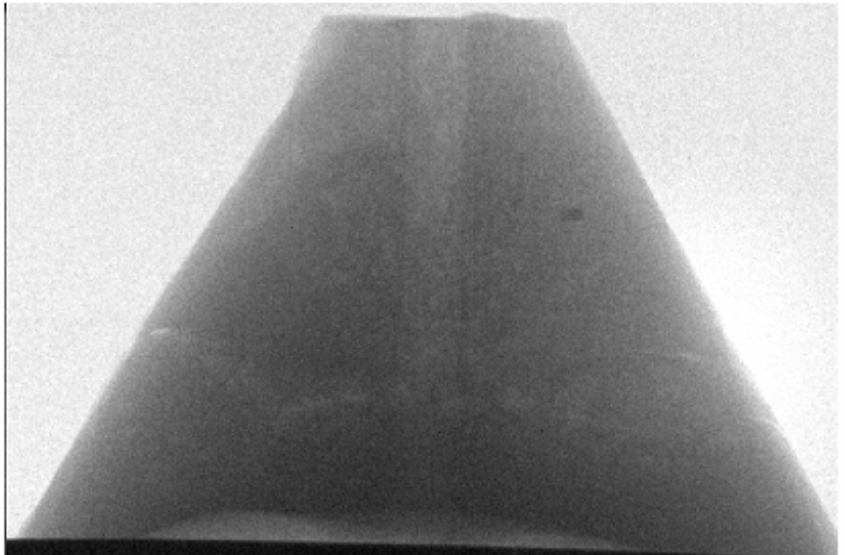
29 keV LCS  
X-ray



# LCS vs Polychromatic source



Tunable, LCS X-rays  
at 23 keV



Polychromatic  
X-ray beam

# LCS as e- beam monitor

Ability to determine electron beam divergence and beam spread with angular measurements.

Determination of electron beam direction and energy and pulse length.

Arrays of PIN X-ray detectors would enable faster angular measurements.

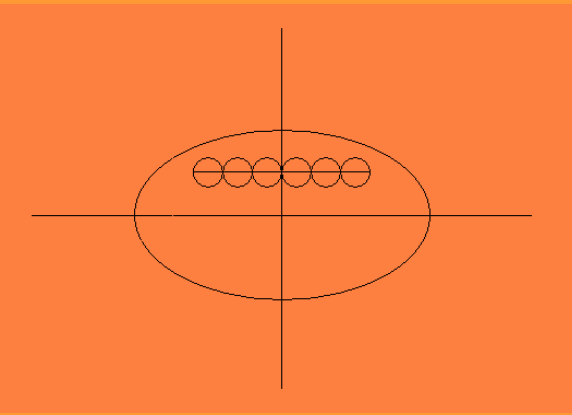
# Future goals

- Comparison of LCS and OTRI.

OTRI:  $\sigma \approx 0.01/\gamma$

Limitation: Low energy e-beams and high quality e- beams due to scattering in first foil.

- $(x, x')$  e<sup>-</sup> mapping



# Conclusion

- LCS bright, tunable and monochromatic x-ray source for broad range of applications.

- With Nd:YAG laser (newly acquired):

4 GW, 60Hz, 1J/pulse @1064 nm.

Expected average intensity:

$10^9$  photons/s emitted in cone of half angle  $1/\gamma$ .

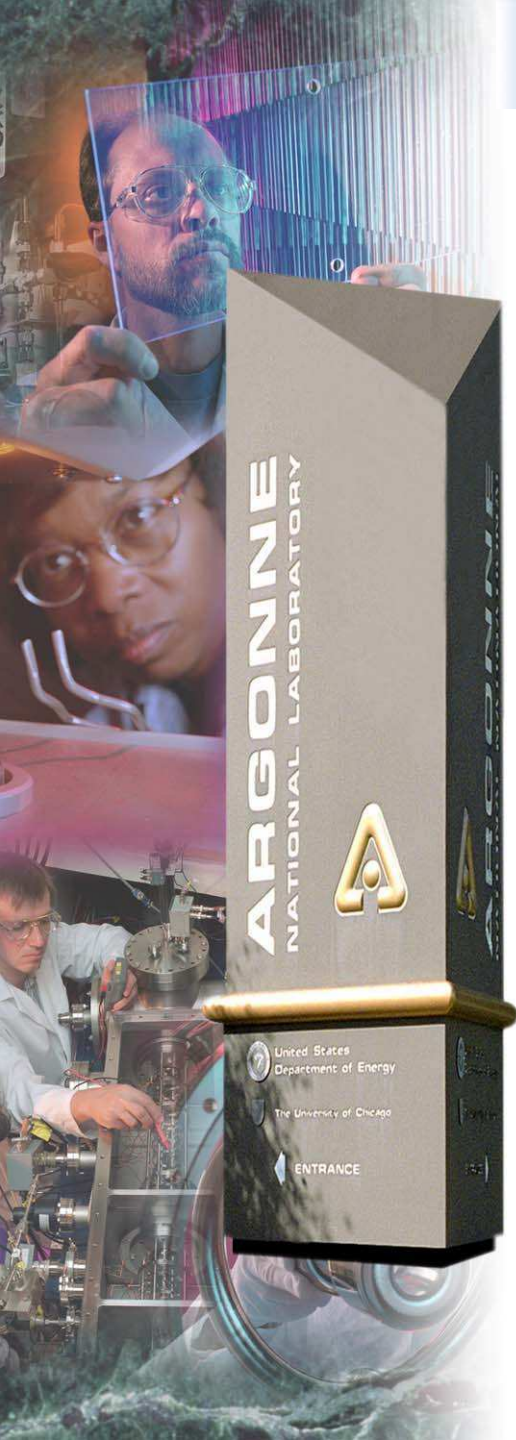
- x-ray energies from 15 –60 keV for  $E \cong 20$ -40 MeV.

# *Short X-ray, Gamma ray, and positron beam generation*

Yuelin Li

*Accelerator Systems Division, Argonne National Laboratory*

*[ylli@aps.anl.gov](mailto:ylli@aps.anl.gov)*



THE UNIVERSITY OF  
CHICAGO



*Argonne National Laboratory is managed by  
The University of Chicago for the U.S. Department of Energy*

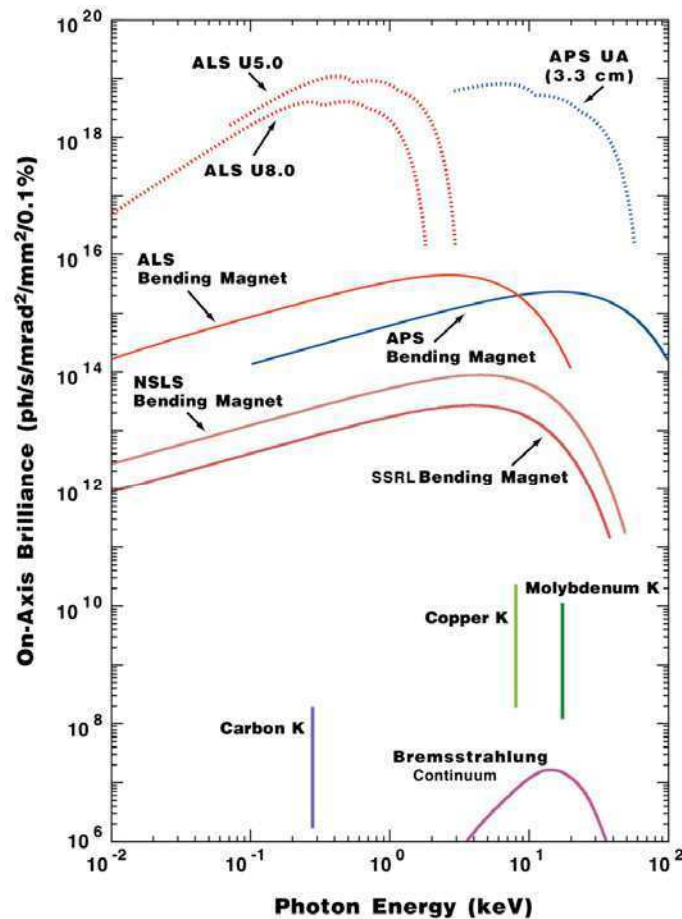
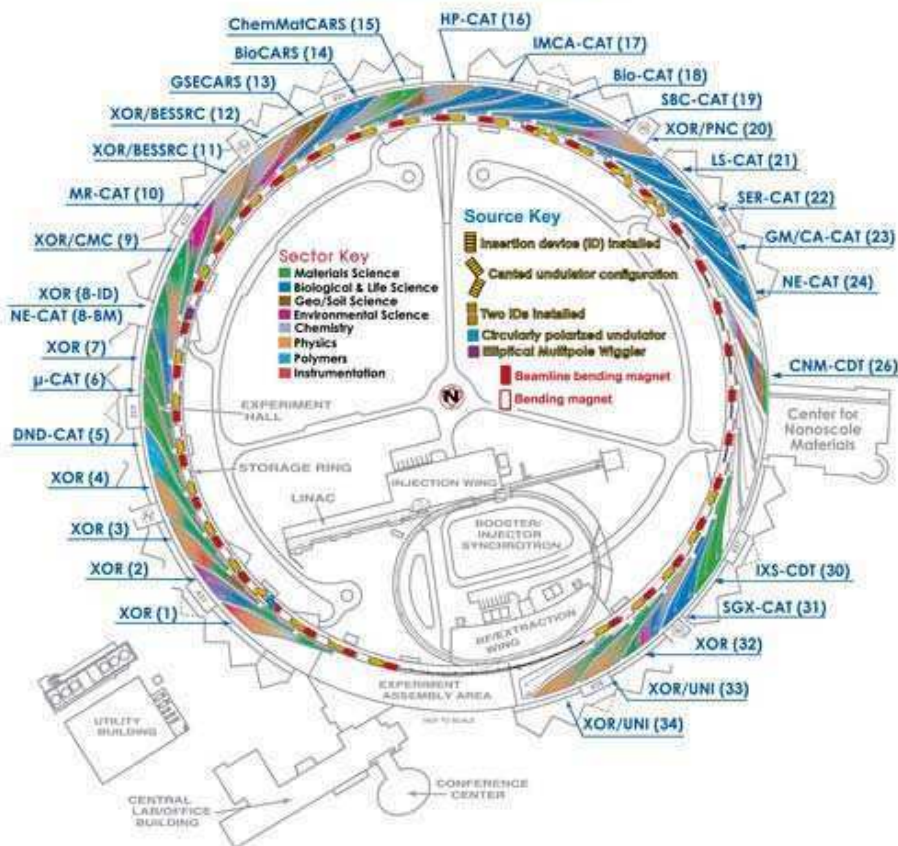
## Content

- Short pulse X-ray sources
  - Laser plasma X-ray sources and beam based X-ray source
  - Small angle Thomson scattering
    - *Short pulse capability*
    - *Tunability*
  - Real estate
- Short pulse Positron beam
  - Short pulse Gamma Ray
  - Short pulse positron
- Discussion

# The Advanced Photon Source



## THE ADVANCED PHOTON SOURCE Sector Allocations & Disciplines Source Configuration

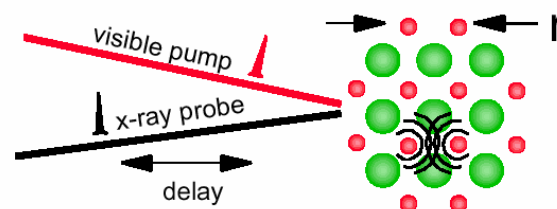
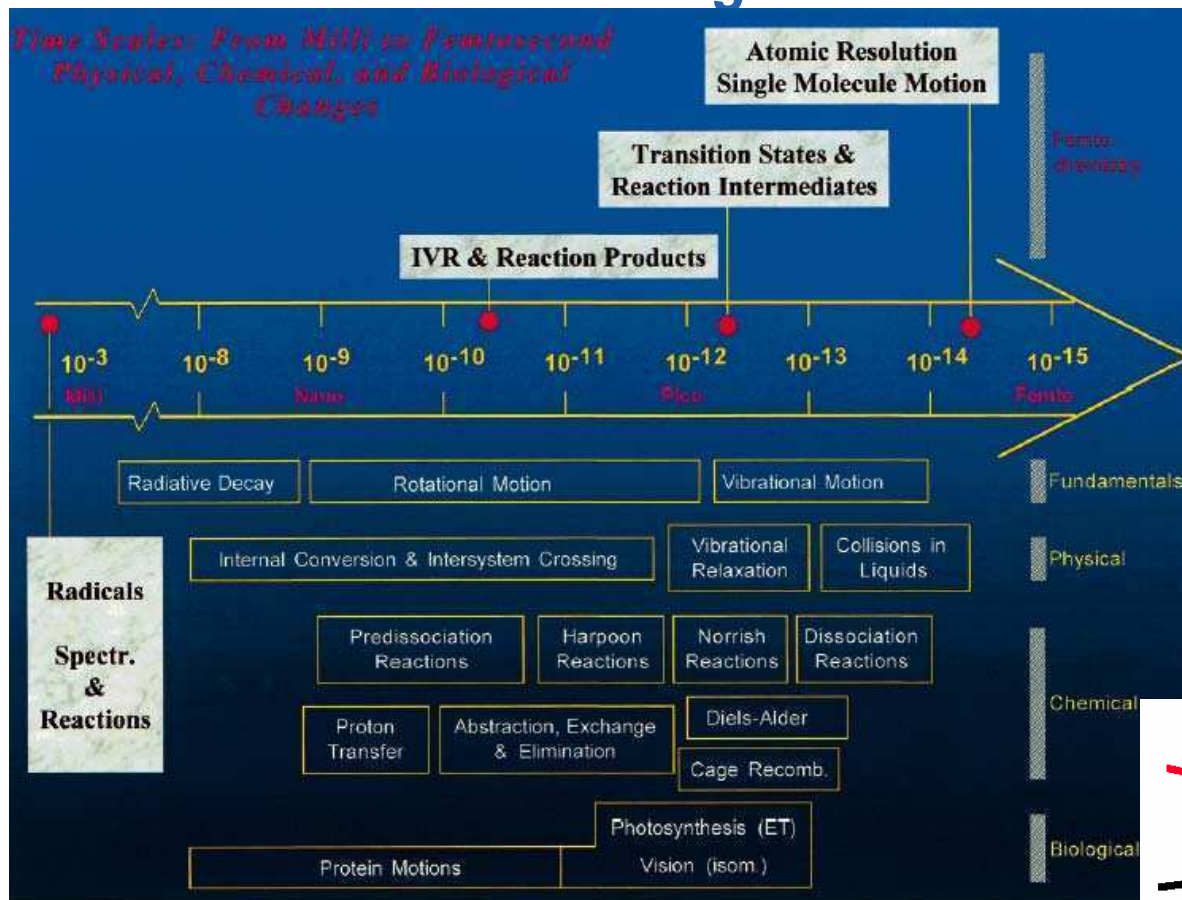


10.97

Pulse duration: 100 ps FWHM



## Someone need something faster: 100 fs

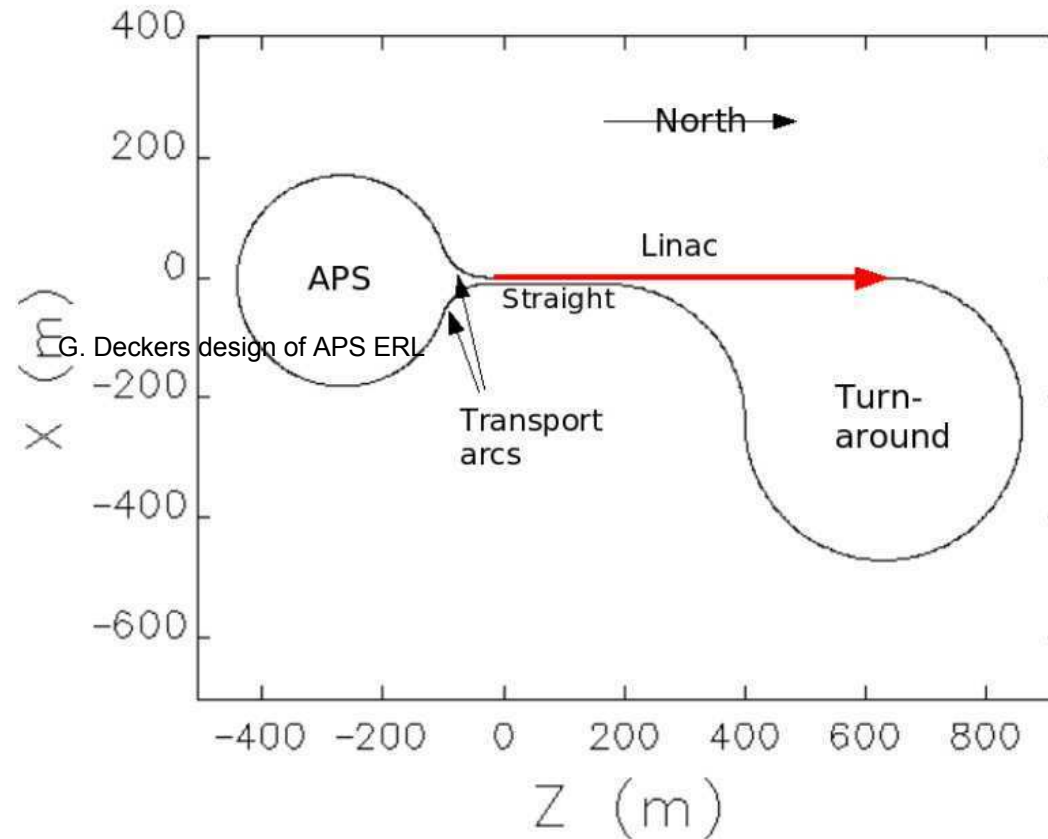


Ahmed H. Zewail, *J. Phys. Chem. A* **104**, 5660 (2000)

Schoenlein et al.



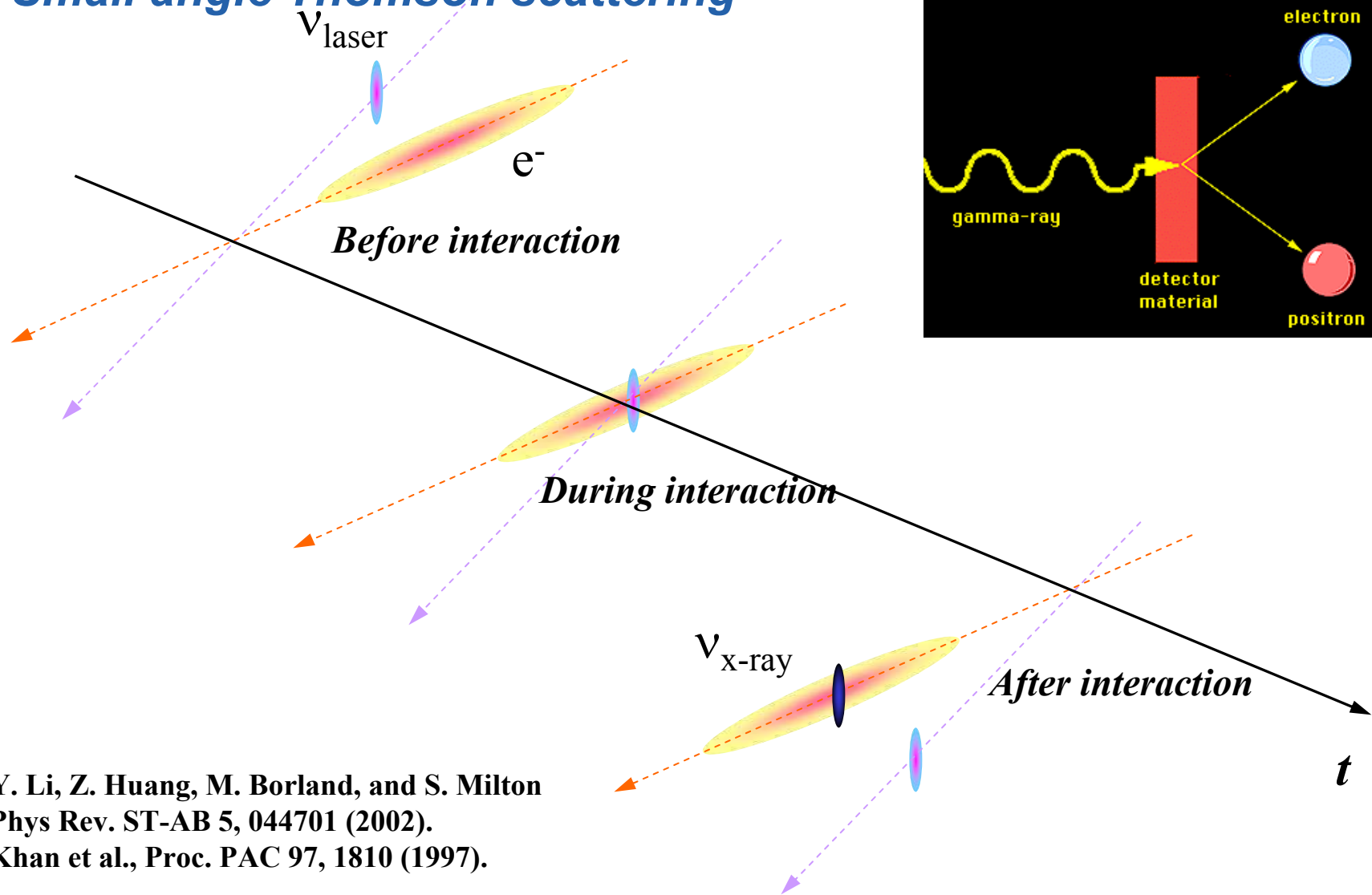
***Large scale:  
the APS upgrade option: energy recovery linac (ERL)  
Free electron laser (LCLS, TESLA, etc)***



## *Radiation source generation*

- Free electron lasers
  - Temporal pulse measurement (Y. Li et al., PRL 89, 234801 (2002); 91, 243602 (2003))
- Small angle Thomson scattering for short pulse X-ray (Li et al, PRST-AB 5, 044701 (2002), )
  - duration determined by laser pulse duration
  - No limitations on electron bunch length
- Short pulse positron generation (Li et al, Appl. Phys. Lett. 88, 021113 (2006))
  - Low energy, short pulse Gamma generating using small angle Thomson scattering from any storage ring with an off-the shelf fs laser
  - Gamma-ray to generate the positrons

## Small angle Thomson scattering



Y. Li, Z. Huang, M. Borland, and S. Milton  
Phys Rev. ST-AB 5, 044701 (2002).  
Khan et al., Proc. PAC 97, 1810 (1997).

## Small angle scattering: X-ray pulse duration=laser pulse duration

### X-ray pulse duration estimate

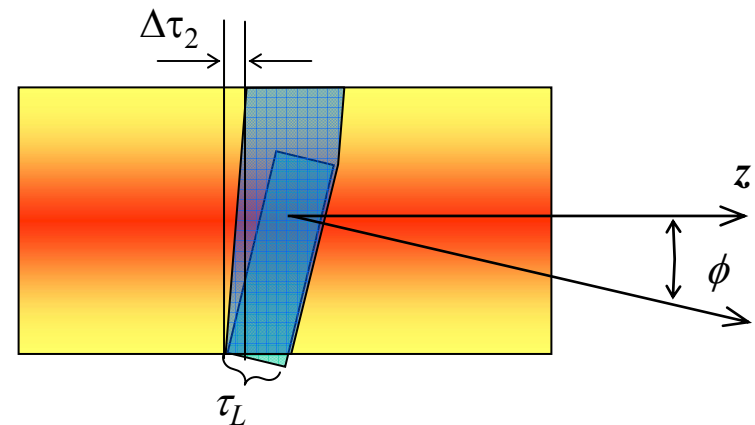
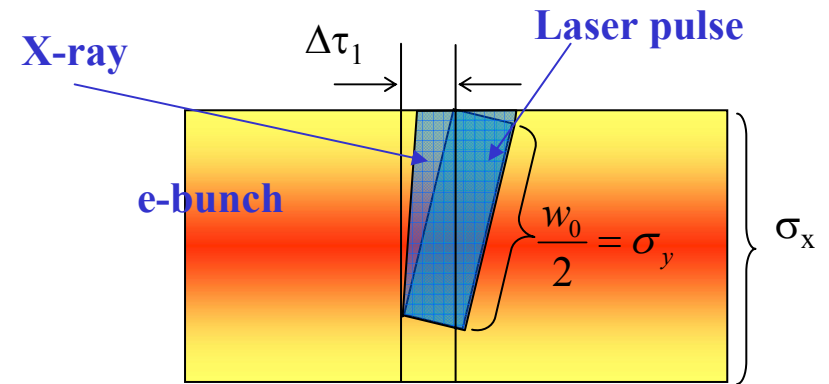
$$\Delta\tau_1 = (1 - \cos\phi) \frac{w_0 \cos\phi}{2c \sin\phi} - \frac{w_0 \sin\phi}{2c} \approx -\frac{w_0}{4c} \phi$$

$$\Delta\tau_2 = (1 - \cos\phi) \frac{\sigma_x}{c \sin\phi} \approx -\frac{\sigma_x}{2c} \phi$$

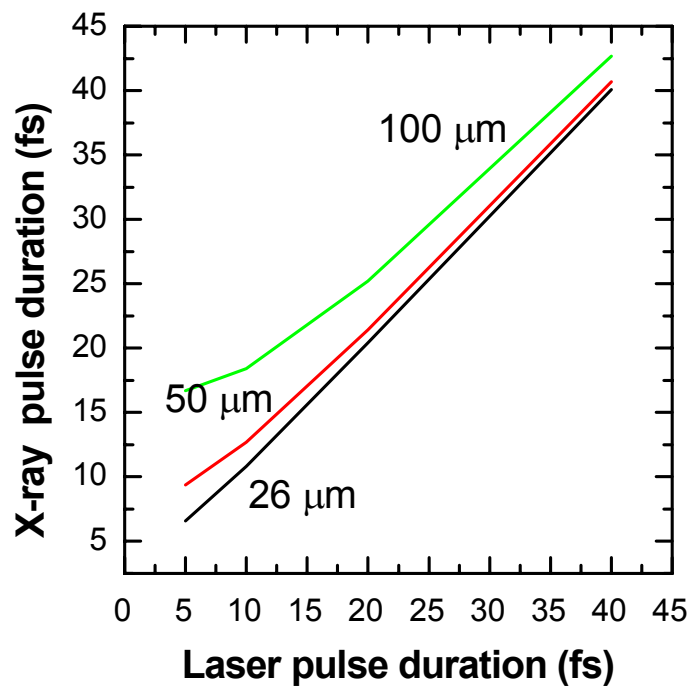
$$\tau = \left( \frac{\tau_L^2}{\cos^2\phi} + \Delta\tau_1^2 + \Delta\tau_2^2 \right)^{1/2}$$

$$= \tau_L \left[ 1 + \left( 1 + \frac{\sigma_x^2 + \sigma_y^2}{4\tau_L^2 c^2} \right) \phi^2 \right]^{1/2}$$

$$\tau \approx \tau_L$$

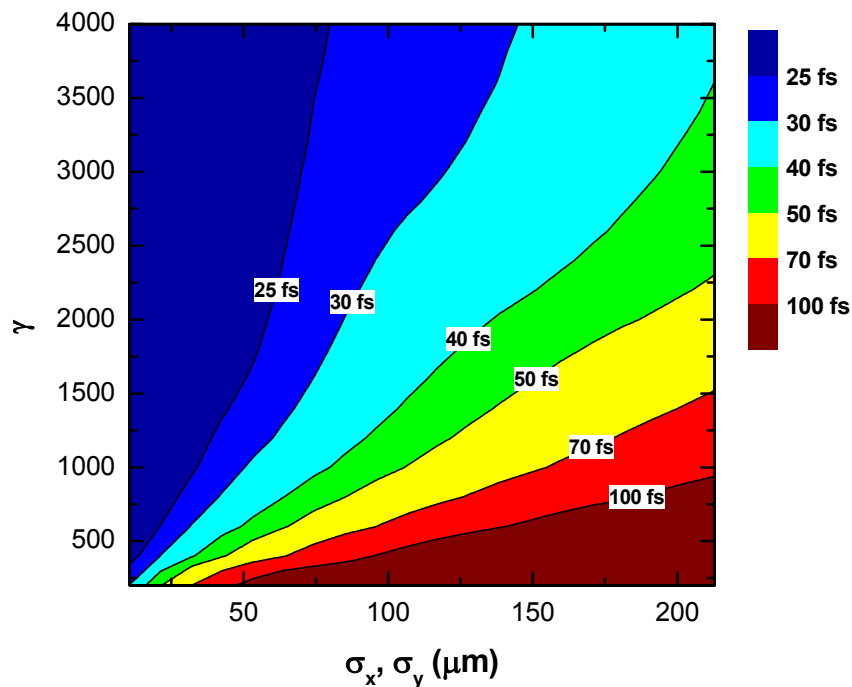


## X-ray pulse duration: Simulation: pulse duration



Photon energy

8-keV



Photon energy

8-keV

Bunch energy

650 MeV

$\lambda_L$

800 nm

$\Phi$

60 mrad

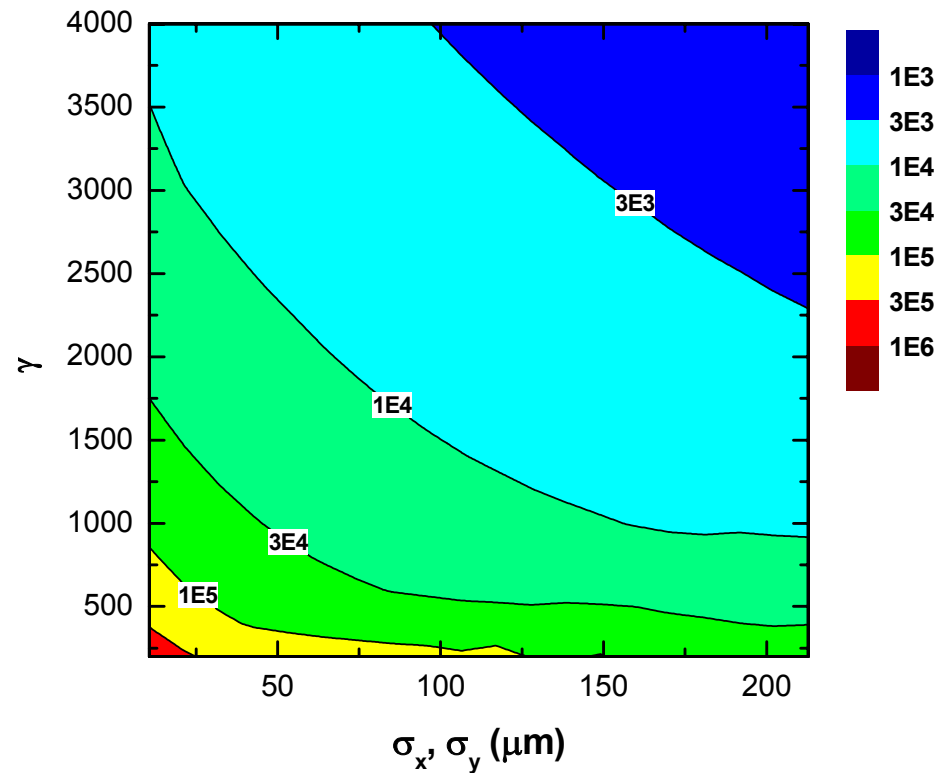
## X-ray photon flux

$$\begin{aligned}
 F &\approx \frac{1}{2\pi} \frac{n}{\tau} \frac{\delta_{BW}}{(\frac{\Delta E}{E})_{\text{int}}} \\
 &\approx \frac{\Sigma_0}{4\pi} \frac{N_p N_e}{\sigma_z \tau_L} \frac{\delta_{BW}}{\lambda_L} \phi^2 \\
 &\approx \frac{\Sigma_0}{4\pi} \frac{N_p N_e}{\sigma_z \tau_L} \frac{\delta_{BW}}{\lambda} \frac{1}{\gamma^2}
 \end{aligned}$$

Where we used

$$\phi = \frac{1}{\gamma} \sqrt{\frac{E}{E_L}} = \frac{1}{\gamma} \sqrt{\frac{\lambda_L}{\lambda}}$$

## X-ray photon flux (photons s<sup>-1</sup> 0.1% bandwidth)



## X-ray spectral brightness

$$B = \frac{F}{(2\pi)^2 \phi_x \phi_y s_x s_y}$$

$$\approx \frac{\sqrt{2} \Sigma_0}{16\pi^3} \frac{N_p N_e}{\sigma_x \sigma_y \sigma_z \tau_L} \frac{\delta_{BW}}{\lambda}$$

### Parameters

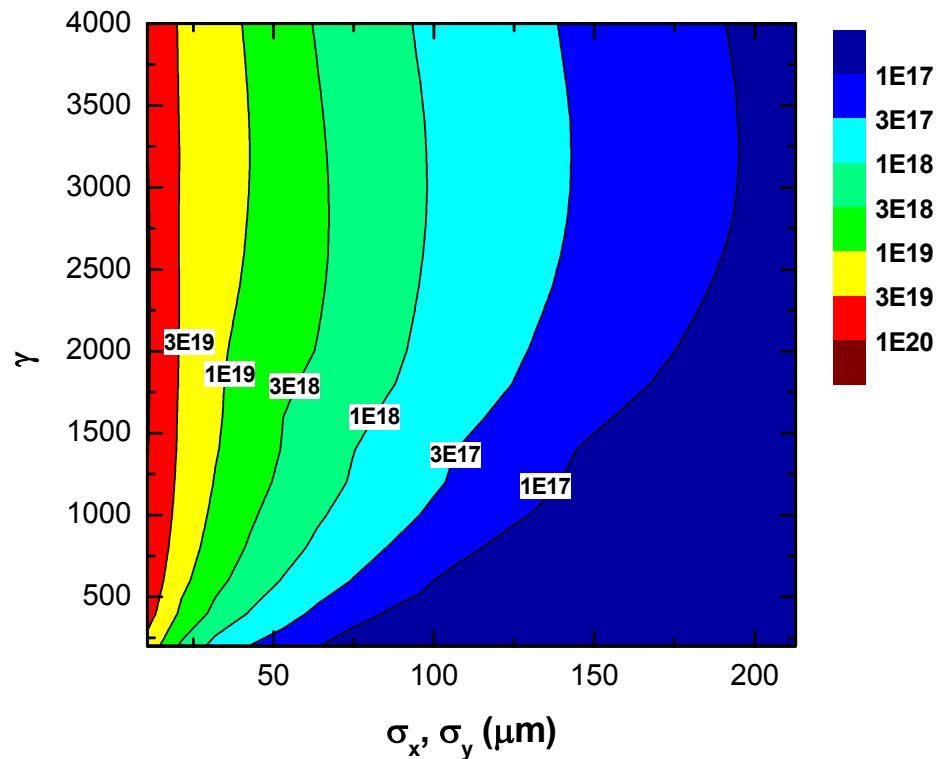
$\sigma_z = 0.212$  ps  
 $\epsilon_n = 10^{-5}$  m rad  
 1 nC charge

$\tau_L = 8.6$  fs (FWHM 20)  
 $\lambda_L = 800$  nm  
 2 J per pulse

E=8 keV

## Peak spectral brightness

Photons  $\text{s}^{-1} \text{mm}^{-2} \text{mrad}^{-2}$  per 0.1% BW



## Content

- Short pulse X-ray sources
  - Laser plasma X-ray sources and beam based X-ray source
  - Small angle Thomson scattering
    - *Short pulse capability*
    - *Tunability*
  - Real estate
- Short pulse Positron beam
  - Short pulse Gamma Ray
  - Short pulse positron
- Discussion



## Generation of ultrafast Gamma ray from the APS

**Table 1 Advanced Photon Source Beam parameters, and the laser pulse parameters**

|                         | <i>Beam</i>                            | <b>Laser</b>                           |
|-------------------------|----------------------------------------|----------------------------------------|
| Particles per pulse     | $10^{11}$ (15 nC)                      | $2 \times 10^{16}$ (5 mJ)              |
| Electron, photon energy | 7 GeV                                  | 1.55 eV                                |
| Energy spread (rms)     | 0.1%                                   | 0.5%                                   |
| Pulse duration          | 45 ps                                  | 0.1-1 ps                               |
| Repetition rate         | 6.528 MHz                              | 4 kHz                                  |
| RMS beam size           | $92 \mu\text{m} \times 26 \mu\text{m}$ | $26 \mu\text{m} \times 26 \mu\text{m}$ |

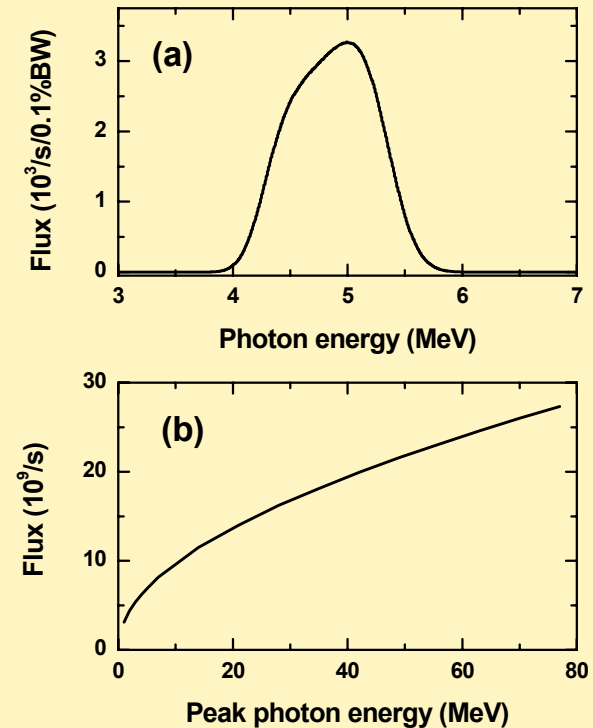
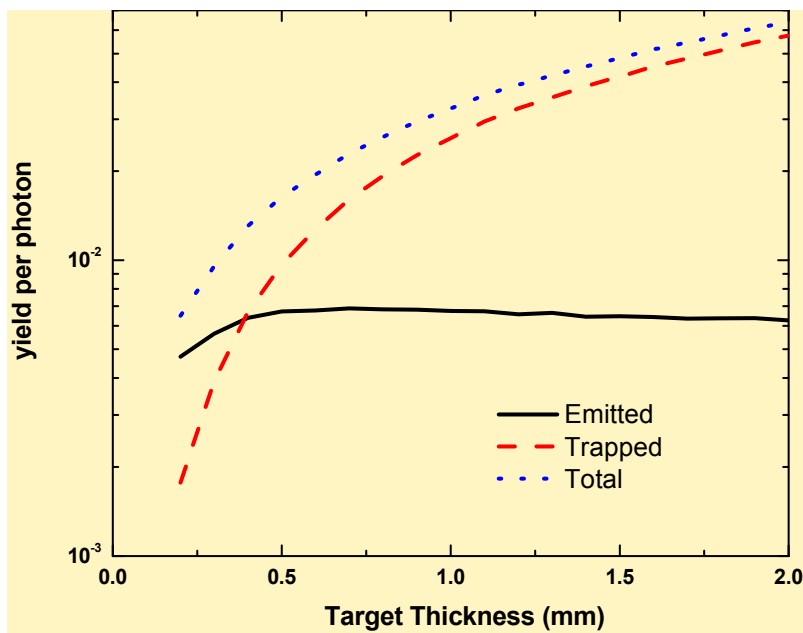
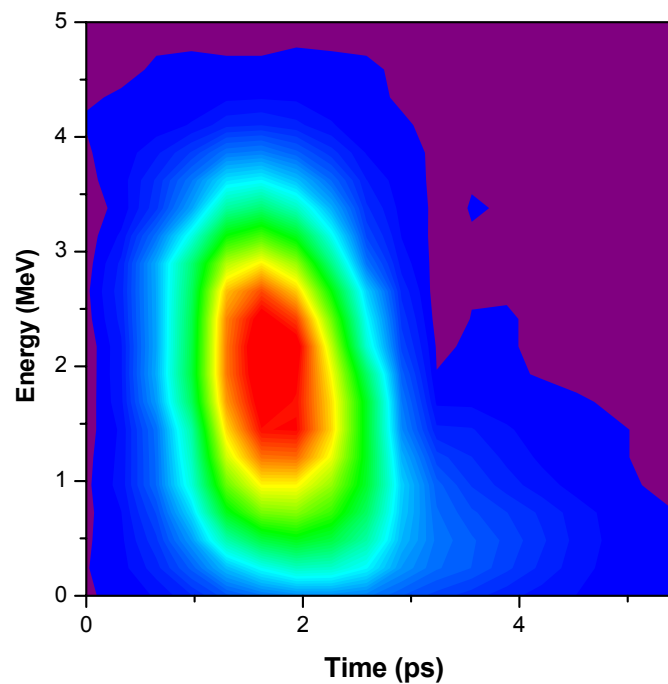


FIG. 1 (a) A  $\gamma$ -ray spectrum peaked at 5 MeV; (b) the total flux as a function of the peak photon energy. An acceptance angle of  $1/\gamma$  is used in the calculation, where  $\gamma$  is the relativistic factor of the beam. In (b), the peak photon energy is tuned by changing the interaction angle between the laser and the electron beam. Here a laser repetition rate of 4 kHz and an optical cavity with a quality factor of 1000 at 6.52 MHz is considered.

## Positron generation



Total, trapped, and emitted positron yield per photon as a function of target length by EGS4 Monte Carlo simulation.



Positron spectrum as a function of time, calculated by EGS4 Monte Carlo simulation with a 1-mm tungsten target.

## *Summary*

- Beam energy around 500 MeV is good for short pulse x-ray generation with duration down to 20 fs
- Higher beam energy can be using for generating short low energy short gamma ray burst
- The short gamma ray burst can be useful for short positron bunch generation

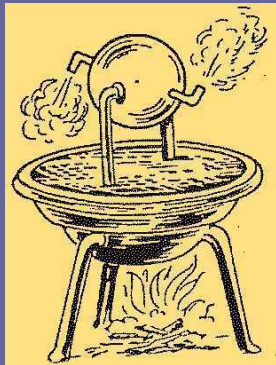
FERMILAB, November 28, 2006

# LASER ACCELERATION WITH SWEEPED LASER BURST

*Mikhailichenko, Cornell University, LEPP, Ithaca NY 14853*

Based on talks given at PAC2005 and EPAC 2006

Lot of technologies existed but not requested at a time

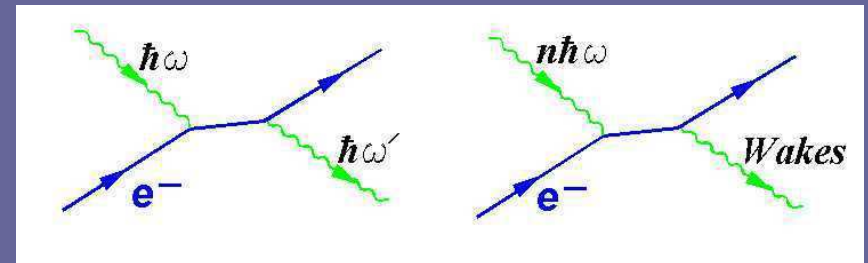


Such new technology appears to be nanofabrication

Situation with RF acceleration of charged particles might be a good example for all these ideas represented above.

Acceleration is a process of energy absorption from RF fields. This means that particle acquires *many* RF photons during the acceleration process. In principle one can imagine the energy exchange between single high energy photon (having TeV scale), but in this case the source of these photons in quantities required will be a much more difficult problem, however.

The possibility to accelerate charged particles of any sign of charge is a vital component for High energy physics.



This second photon is crucial agent in all business. Presence of this (radiated) photon allows, for example, particle acceleration by the plane wave; the process is going while particle re-radiates. In terms of photon absorption, the cross section of this process decreases with energy preventing usage of this method at high energy.

Looks like plasma-methods are missing importance of positron acceleration.  
Also it is not shown where this second photon hidden in theirs methods, however.

Experiments done show that the limit to damage is strongly dependent of the time of illumination; shorter the illumination time—higher density is allowable. Reported density measured  $6 \text{ J/cm}^2$  for  $1 \text{ ps}$  pulse duration and  $10 \text{ J/cm}^2$  for  $0.3 \text{ ps}$  pulse.

From the other hand for  $3 \text{ cm}$  long structure the pass-time to be  $100 \text{ ps}$ .

We proposed in [1994] a method on how to arrange this local excitation with the help of sweep of focused laser radiation along the accelerating structure and called this procedure Travelling Laser Focus (TLF).

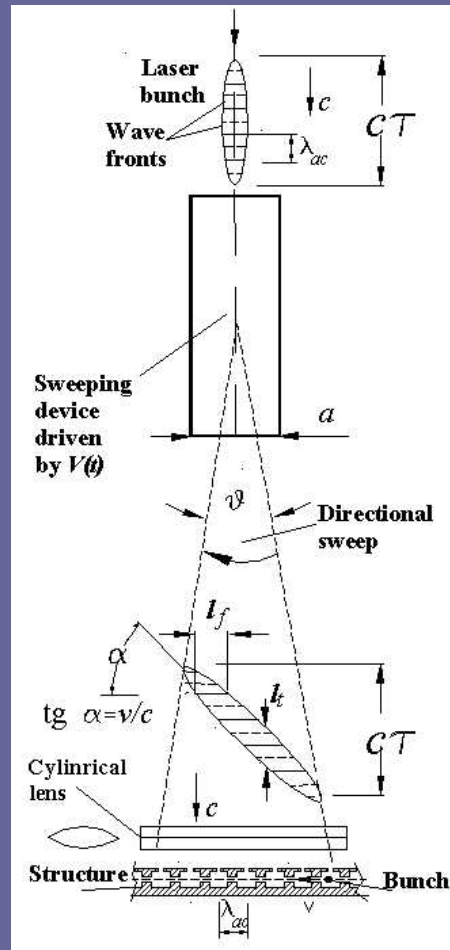
Laser radiation applied to every point of structure during  $t = l_t / a_c$ ,

The number of accelerating cells excited simultaneously is  $\sim l_f / c$

The focal point is following the beam *in average*.

Phase of the laser radiation is synchronized once with the particle's bunch motion.

Accelerating cells in a structure separated in longitudinal direction with distance  $l_{ac}$ , so an electromagnetic field is in phase inside each cell.



Sweeping device could be characterized by deflection angle  $q$  and by the angle of natural diffraction –

$$q_d = l/a,$$

where  $a$  – is the aperture of the sweeping device which is of the order of the transverse laser beam size. The ratio of deflection angle to diffraction angle is fundamental measure of the quality for any deflecting device. This ratio defines the number of resolved spots (pixels) placed along the structure. The last number is an invariant under optical transformations.

$$N_R = q/q_d$$

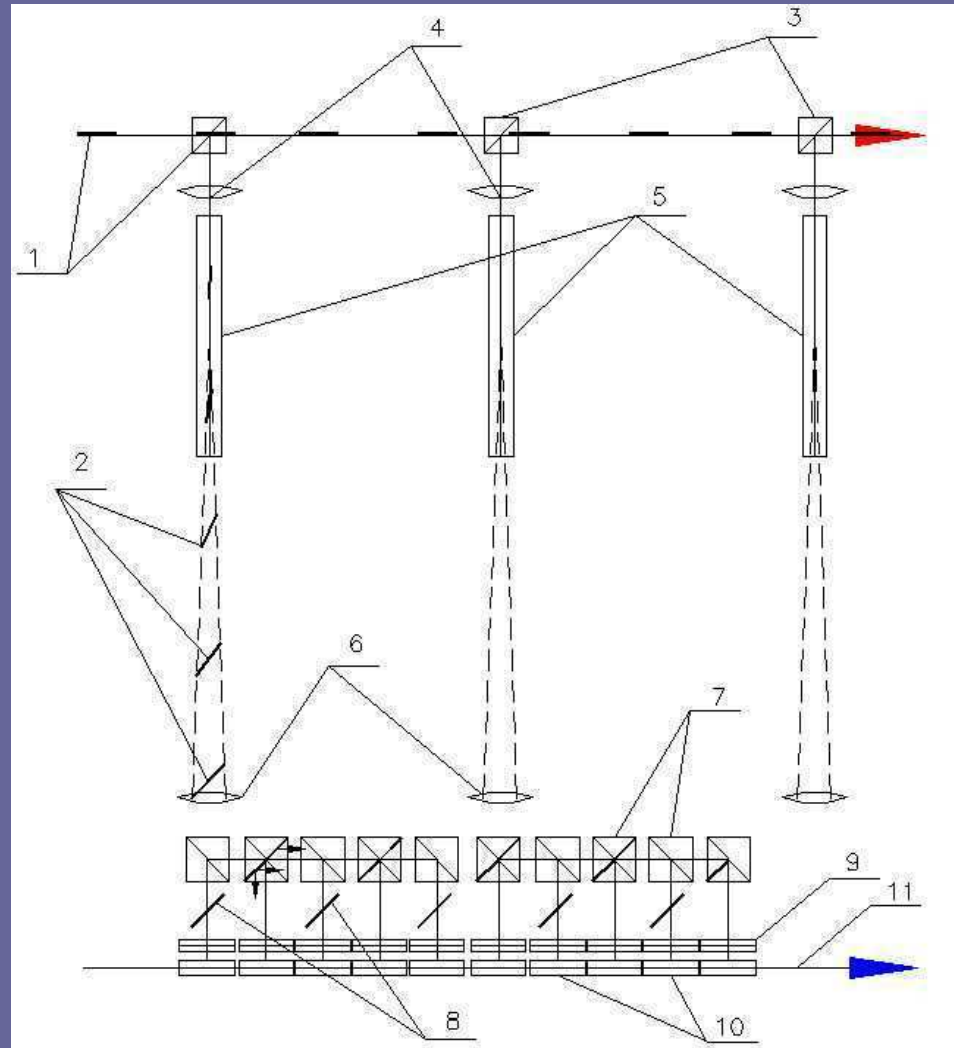
A cylindrical lens serves for the focusing of laser radiation in a transverse to the motion direction.

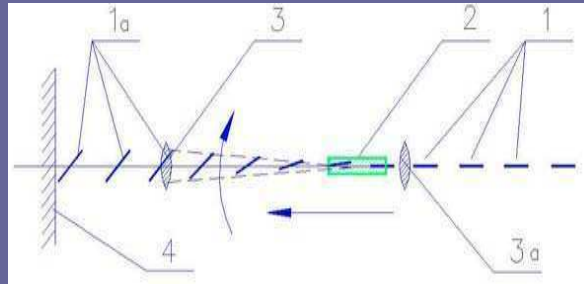
Illumination time  $t=0.3 \text{ ps}$  . Laser density =  $0.3 \text{ J/cm}^2$  for  $E=10 \text{ GeV/m}$

## Sweeping device serves for few accelerating structures.

Laser bunch train, 1 coming from the left and passing sequentially power splitters 3. By 2 marked locations and configuration of the swept laser bunches. Lenses 4 installed a prior to the sweeping devices 5 having focal plane at location of lens 6. By 7 marked power splitters and mirrors allowing feed few structures from single sweeping device. Even number of reflections (basically two), bring the slope to the proper tilt shown by 8. This system also equipped by cylindrical lenses 9 which have transverse focus on the openings of accelerating structures. Structures marked by 10. Accelerated bunches are running to the right 11 inside structures.

**We expect that this can be done for 5-10 structures.**

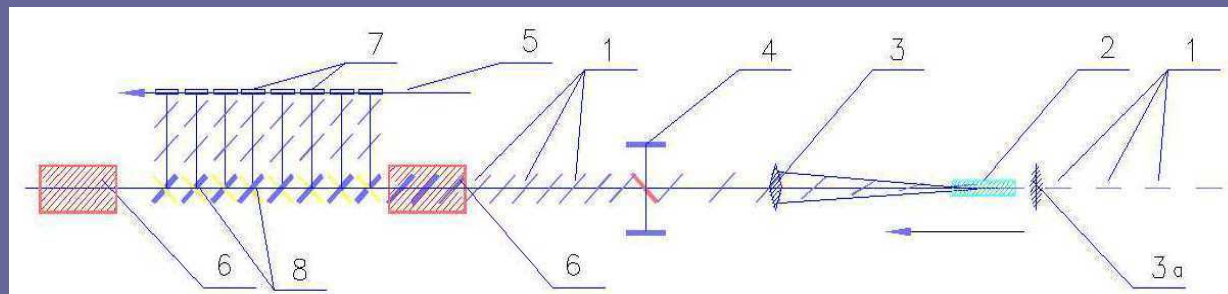




- Dynamics of laser bunch sweeping; a look from the side. 1—shows laser bunch configuration at the entrance, 1a— is a bunch after second lens, 2—is a sweeping device, 3 and 3a— are the focusing lenses. 4 —is an image plane, where accelerating structure located. Beam is moving from the bottom of this Fig. to the top.

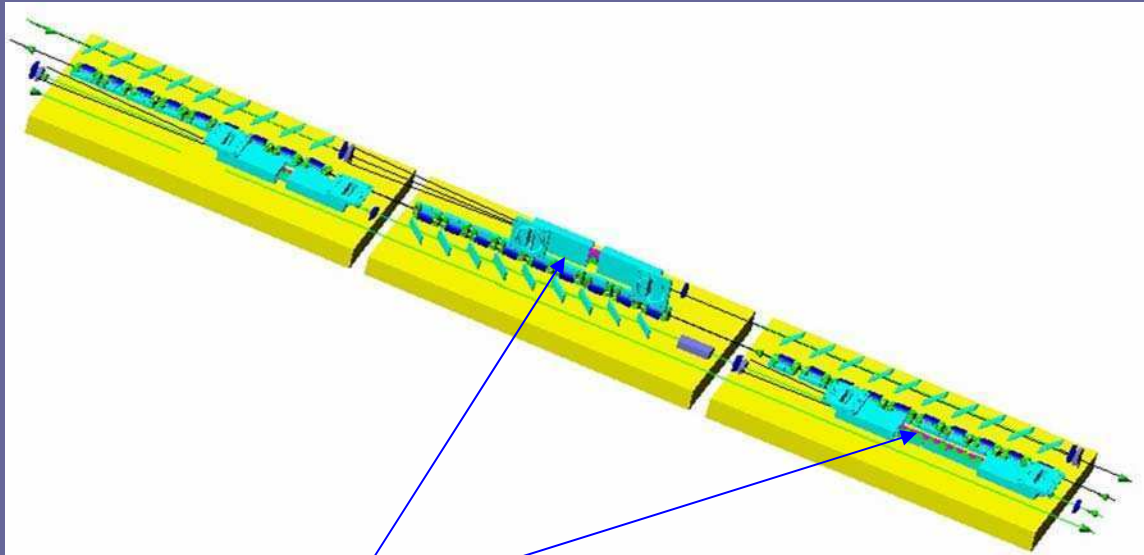
Additional lens 3 has a focal point located in effective sweeping center. After this lens laser bunches have no angular divergence. Lens 3a has focal point located at the accelerating structure, what is the plane marked 4. So the sweeping device 2 located between lenses 3a and 3.

- Direction of sweep defines the laser bunch slope. For practical applications second lens 3 can be combined with cylindrical lens.
- Optimization of sweeping device shows, that its length must be  $2/3$  of distance from lens 3a to the lens 3,

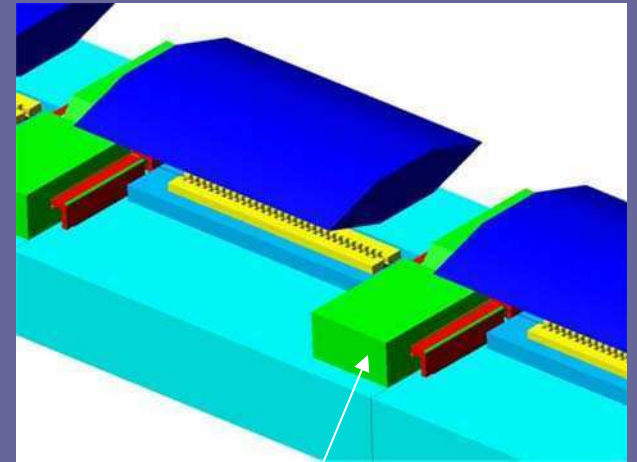


Extended scheme with single sweeping device. 1—shows laser bunch configuration at different locations, 2—is a sweeping device, 3—focusing lens, 4—laser bunch doubler, 5—accelerated bunch, 6—optical amplifier, 7—accelerating structures, 8—power splitters (semi-transparent mirrors).

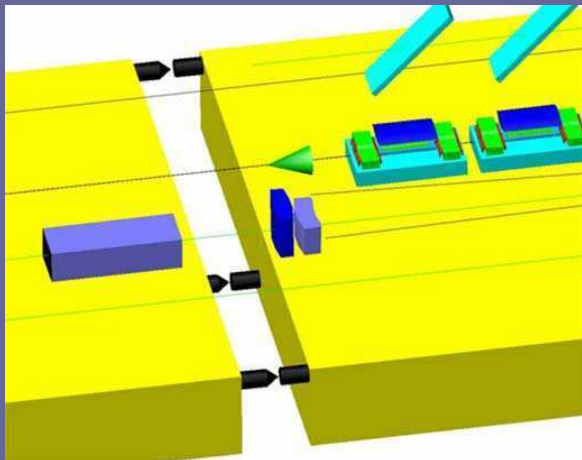




Sweeping device



Quadrupole lens



Alignment of blocks arranged with the help of tunneling probes

# SWEEPING DEVICE

For a prism-based device, change in refraction index yields the change in deflection angle. To arrange such a change, the basements of the prism must be covered by metallic foils and a high voltage applied to them.

The deflecting angle is defined by the phase delay across the laser beam front arising from differences in the path lengths in material of the prism having a refractive index  $n$ ,

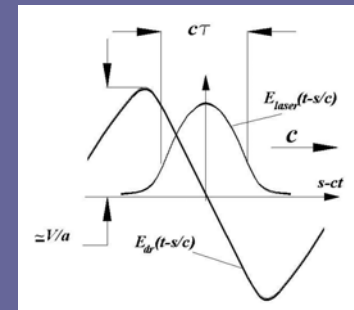
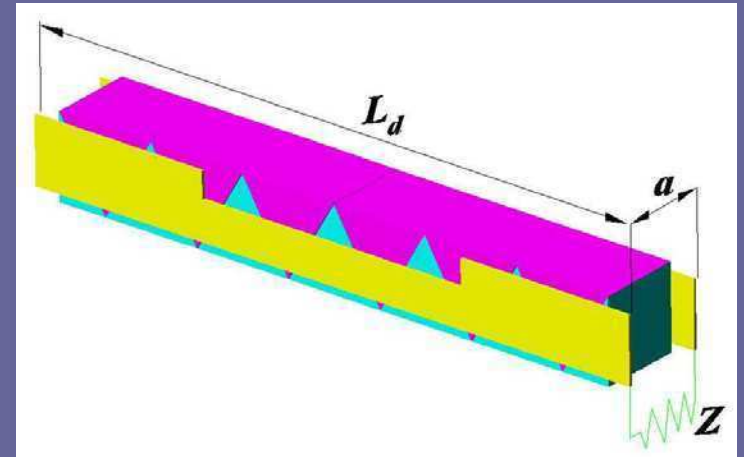
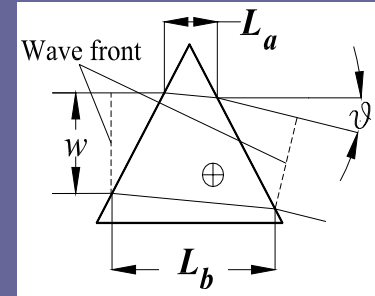
$$\Delta\vartheta \cong n \frac{(L_a - L_b)}{w}$$

At the right- prisms with *oppositely directed optical axes* installed in series between two parallel strip-line electrodes, Electromagnetic pulse propagates with laser bunch to the right as traveling wave.

In this case the full length of this device is working for deflection.

The deflection angle and the number of resolved spots for such device become

$$\Delta\vartheta \cong \Delta n(t) \frac{L_d}{w} \quad N_R \cong \frac{|\Delta\vartheta|_{\max}}{\lambda / w}$$



Tensor  $r_{ij}$  links refraction index change and applied electrical field

$$1/n_i^2 = 1/n_{0i}^2 + \sum_j r_{ij} \cdot E^j$$

$$\Delta n_i \cong (\partial n_i / \partial E_j) E^j(t)$$

$$\partial n_i / \partial E_j = -n_{0i}^3 r_{ij} / 2$$

$$\begin{pmatrix} \Delta(1/n_1^2) \\ \Delta(1/n_2^2) \\ \Delta(1/n_3^2) \\ \Delta(1/n_4^2) \\ \Delta(1/n_5^2) \\ \Delta(1/n_6^2) \end{pmatrix} = \begin{pmatrix} r_{11} & r_{12} & r_{13} \\ r_{21} & r_{22} & r_{23} \\ r_{31} & r_{32} & r_{33} \\ r_{41} & r_{42} & r_{43} \\ r_{51} & r_{52} & r_{53} \\ r_{61} & r_{62} & r_{63} \end{pmatrix} \times \begin{pmatrix} E_x \\ E_y \\ E_z \end{pmatrix}$$

**GaAs**

$$(r)_{ij} = \begin{pmatrix} 0 & 0 & 0 \\ 0 & 0 & 0 \\ 0 & 0 & 0 \\ 1.5 & 0 & 0 \\ 0 & 1.5 & 0 \\ 0 & 0 & 1.5 \end{pmatrix} \times 10^{-12} [m/V]$$

**KDP**

$$(r)_{ij} = \begin{pmatrix} 0 & 0 & 0 \\ 0 & 0 & 0 \\ 0 & 0 & 0 \\ 8.8 & 0 & 0 \\ 0 & 8.8 & 0 \\ 0 & 0 & 10.5 \end{pmatrix} \times 10^{-12} [m/V]$$

Materials for 1um: KDP, DKDP, ADP, KDA, LiNbO<sub>3</sub>

Materials for 5um: LiNbO<sub>3</sub>, LiTaO<sub>3</sub>, CuCl

Materials for 10um: GaAs, ZnTe, ZnS, CdS, CuCl

$$\Delta \theta \cong \Delta n(t) \frac{L_d}{w} \cong \frac{L_d}{a^2} n_0^3 \cdot r_{ij} \cdot V(t)$$

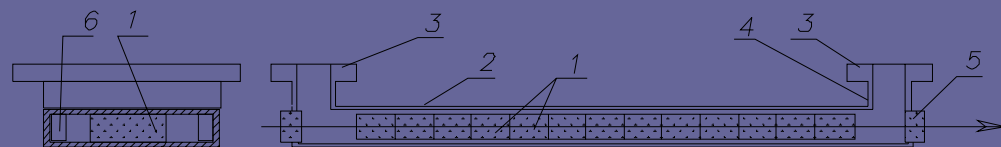
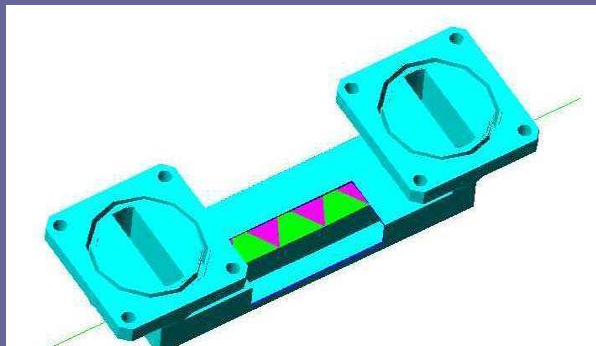
$$N_R \cong \frac{|\Delta \theta|_{\max}}{\lambda / w} = |\Delta n|_{\max} \frac{2L_d}{\lambda} = \frac{L_d}{\lambda} n_0^3 r_{ij} |\Delta V|_{\max}$$

For  $L_d = 25cm$ ,  $a = 0.5 cm$ , deflection angle is  $\Delta \theta \cong 10^{-2}$   
 $N_R = 200$  for  $\lambda \cong 1\mu m$

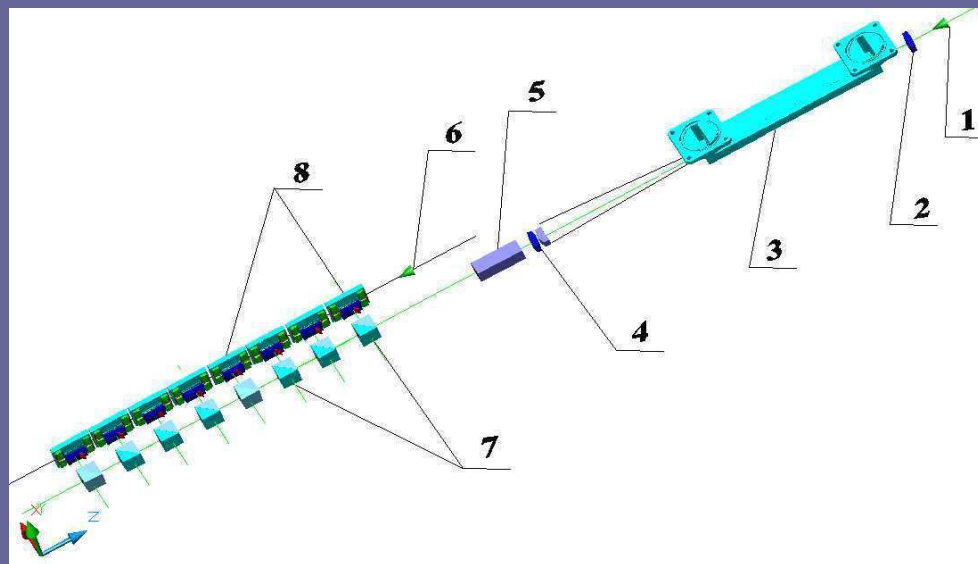
Such devices can be manufactured routinely



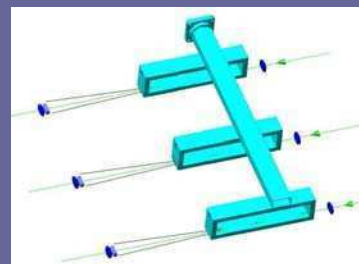
# Waveguide sweeping device



Multi-prism traveling wave sweeping device in a waveguide. 1—is electro-optical crystals, positioned in a waveguide 2, having bends 4 with flanges 3. 5—is an optical window. 6 —is a matching dielectric.

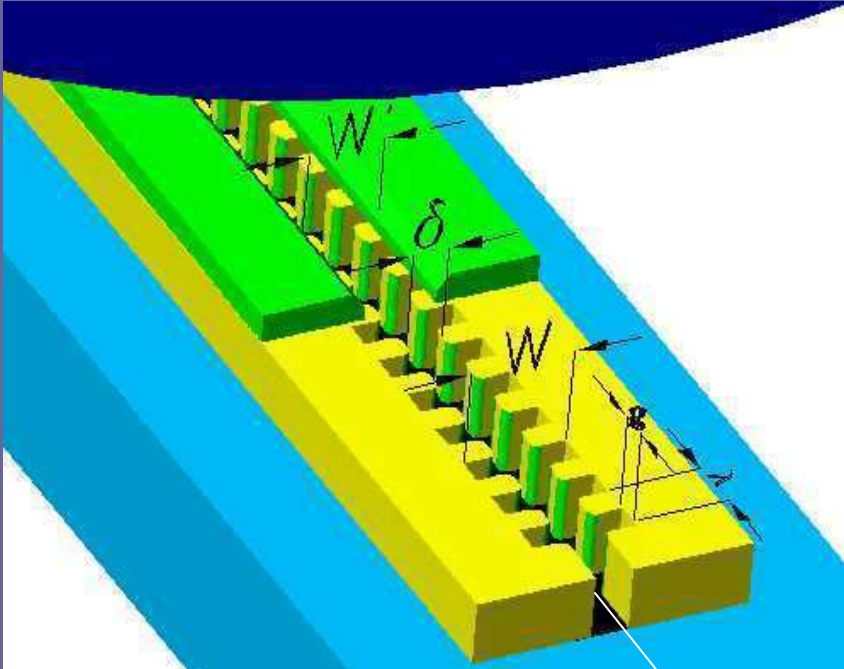


1 —is the laser beam, 2—focusing lens, 3—waveguide sweeping device, 4—lens, 5—optical amplifier, 6—particle beam under acceleration, 7—laser power splitting devices, 8—accelerating structures with beam focusing elements.

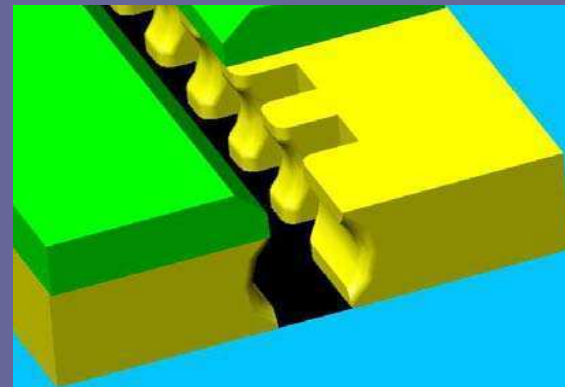
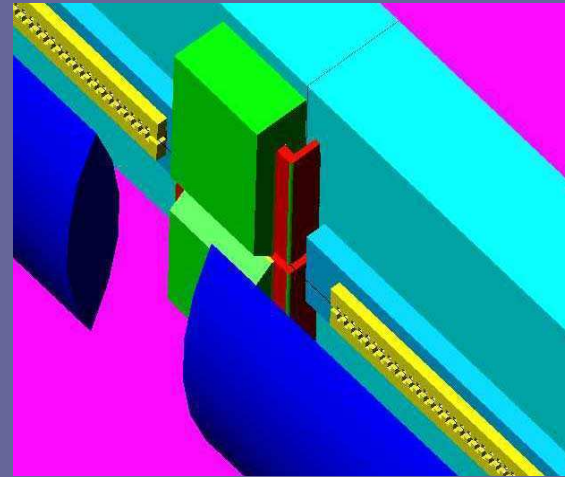


Power required ~1 MW , losses are minimal

# ACCELERATING STRUCTURE



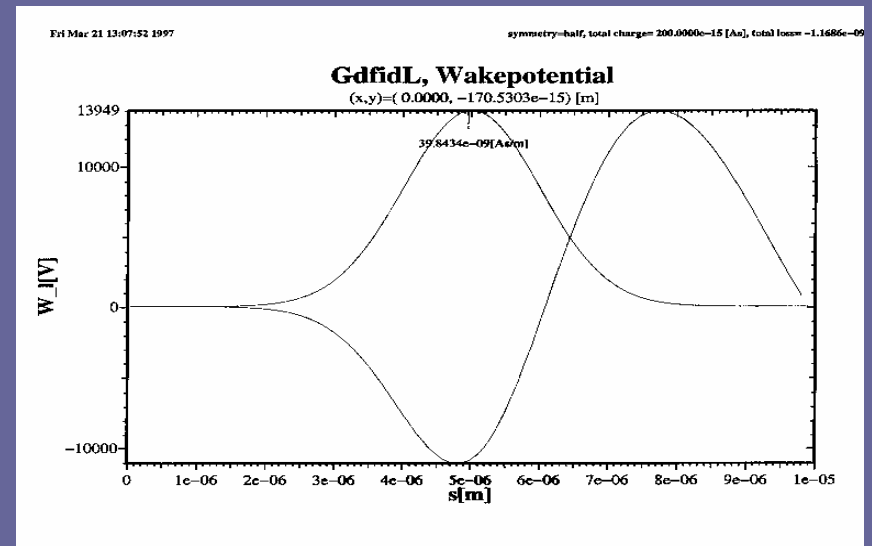
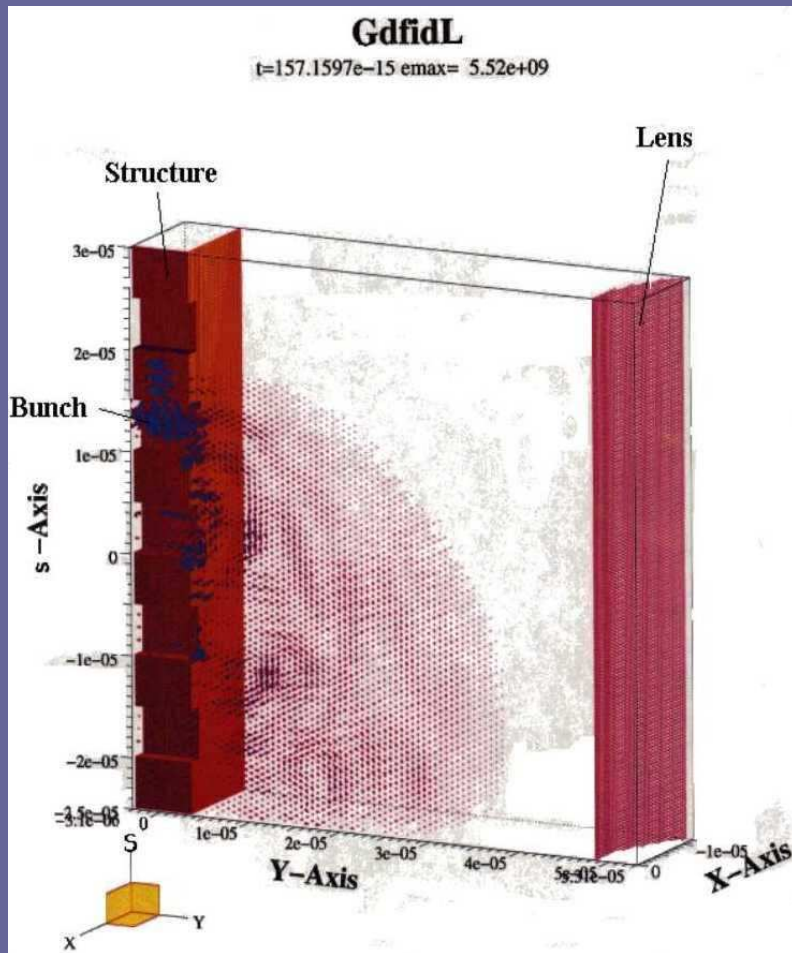
Beam is going inside the structure



$$k_x = -\frac{1}{pc} \frac{\partial \langle F_x \rangle}{\partial x} \cong -\frac{e \lambda_{ac} E_m}{mc^2 \gamma W^2} \sin \phi \approx 4 \cdot 10^5 \cdot \sin \phi [m^{-2}]$$



# WAKES

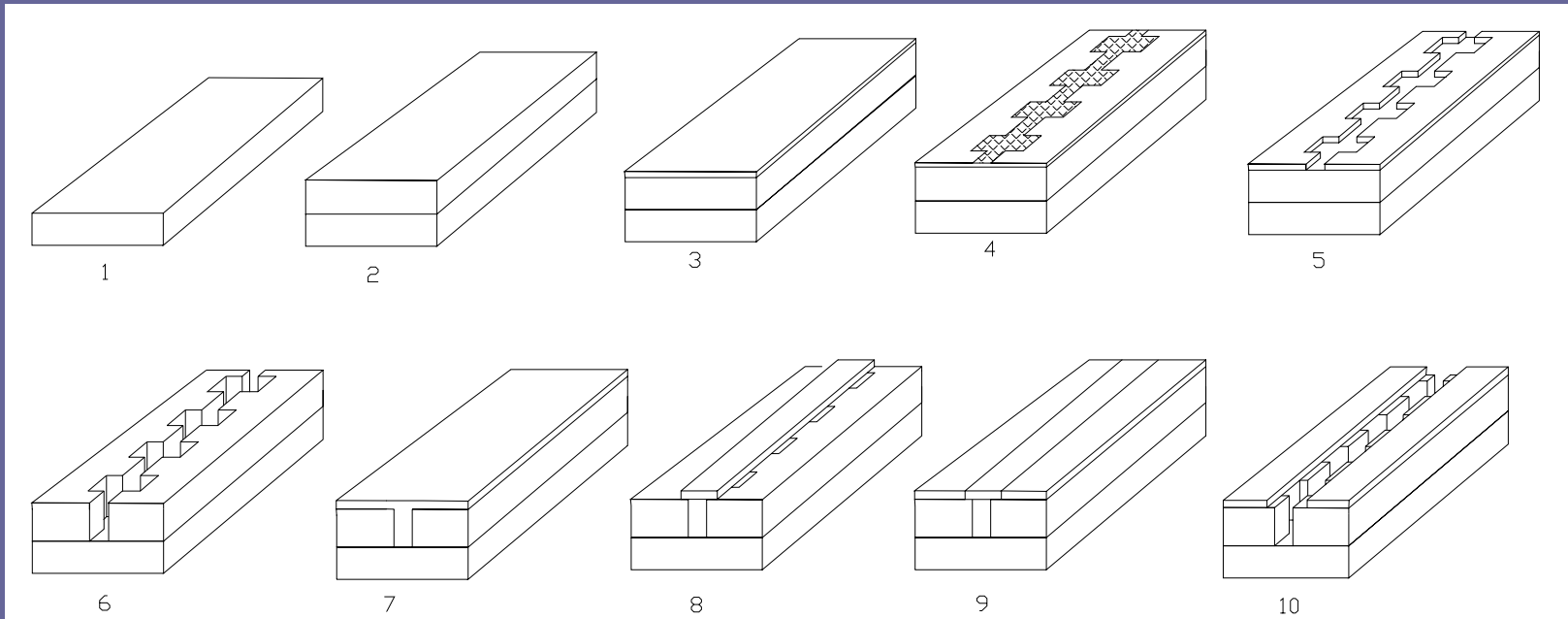


$$W_{\parallel} \cong -7kV / pC \quad W_{\perp} \cong 2.2 \cdot 10^2 V / pC / \mu m$$

$$N \cong 310^5 \quad eN \cong 4.8 \cdot 10^{-14} C = 0.048 pC$$

Wakes/Acceleration  $\sim 4\%$ ,

# FABRICATION

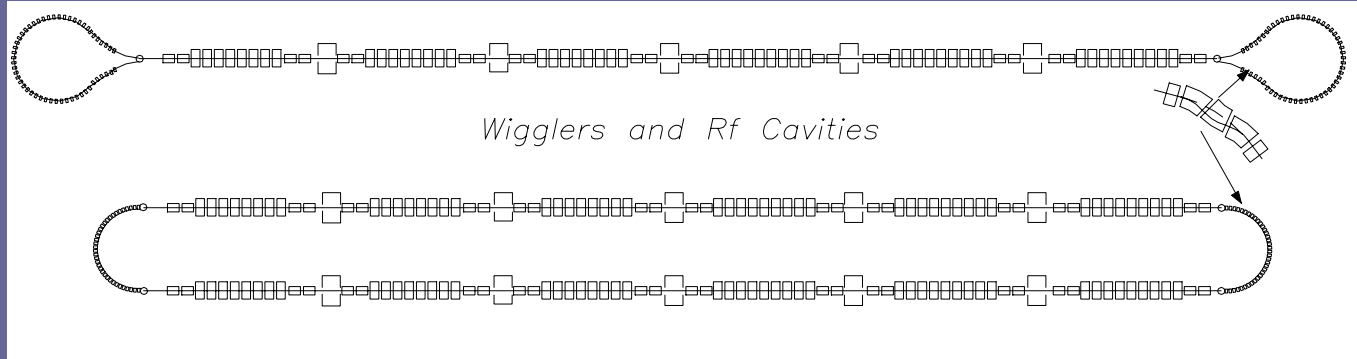


1— is a base. 2—material of the structure is placed on the base. 3—a photoresist is placed at the top. 4—the photoresist is exposed. 5—some of photoresist is removed. 6—material of the structure etched. 7—a new cover of photoresist is placed. 8—extra resist is removed. 9—material of the structure is added. 10—structure etched again.



# INJECTION SOURCE

Fundamental restriction to the minimal emittance  $(\gamma\epsilon_x)(\gamma\epsilon_y)(\gamma\epsilon_s) = (\gamma\epsilon_x)(\gamma\epsilon_y)(\gamma l_b (\Delta p / p_0)) \geq \frac{1}{2} (2\pi\tilde{\lambda}_C)^3 N$



For wiggler dominated cooler equilibrium emittance  $(\gamma\epsilon_x) \cong \frac{1}{2} \cdot \tilde{\lambda}_C \bar{\beta}_x (1 + K_x^2 / 2) \gamma / \rho_x \cong \frac{1}{2} \cdot \tilde{\lambda}_C \bar{\beta}_x (1 + K_x^2 / 2) K_x / \tilde{\lambda}$

Cooling time  $\tau_{cool} \cong (3/2) \cdot (\tilde{\lambda}^2 / r_0 c K^2 \gamma) \sim 8.6 \text{ ms}$ .

$$(\gamma\epsilon_y) \cong \frac{1}{2} \cdot \tilde{\lambda}_C \bar{\beta}_y \gamma / \rho_x \cong \frac{1}{2} \cdot \tilde{\lambda}_C \bar{\beta}_y K_x / \tilde{\lambda}$$

$$K = eH_{\perp} \tilde{\lambda} / mc^2$$

## TEMPERATURE

$$\frac{3}{2} N k_B T \cong N \cdot mc^2 \gamma \left[ \frac{\gamma\epsilon_x}{\beta_x} + \frac{\gamma\epsilon_y}{\beta_y} + \gamma \frac{1}{\gamma^2} \left( \frac{4p_{\parallel}}{p_0} \right)^2 \right] \rightarrow N \cdot mc^2 \gamma \left[ \frac{\gamma\epsilon_x}{\beta_x} + \frac{\gamma\epsilon_y}{\beta_y} + \gamma \left( \frac{1}{\gamma^2} - \left\langle \frac{D}{\beta_x} \right\rangle \right) \left( \frac{4p_{\parallel}}{p_0} \right)^2 \right]$$

$$(\gamma\epsilon_y) \cong 9.5 \cdot 10^{-10} \text{ cm} \cdot \text{rad}$$

$$(\gamma\epsilon_x) \cong 2.5 \cdot 10^{-8} \text{ cm} \cdot \text{rad}$$

# BEAM PARAMETERS

If laser flash lasts  $\tau$  sec and carries energy  $Q$  Joules then maximal field  $E_m \cong 2 \sqrt{\frac{Q}{\epsilon_0 c \tau \lambda l_f}}$

$$Q=10^{-4} \text{ J} \quad \tau \cong 0.1 \text{ ns} \quad \lambda \cong 1 \mu\text{m} \quad Q_{RF}=9 \quad E_m \cong 10 \text{ GeV/m}$$

Bunch population  $N \cong \frac{\eta}{2eI(g)} \sqrt{\frac{\epsilon_0 \lambda_{ac}^3 Q}{c \tau l_f}} \cong 3 \cdot 10^5$  For 5% load

Luminosity  $L = \frac{N^2 f H_B}{4\pi \sigma_x \sigma_y}$   $\gamma \epsilon_x \cong 2.5 \cdot 10^{-8} \text{ cm} \cdot \text{rad}$   $\beta_x \approx \beta_y \approx 0.3 \lambda_{ac}$   $f \cong 1 \text{ kHz}$ ,  $H_B=1$   
 $\gamma \epsilon_x \cong 9.5 \cdot 10^{-10} \text{ cm} \cdot \text{rad}$

$$L \approx 1.7 \cdot 10^{35} \text{ cm}^{-2} \text{ s}^{-1}$$

$$Y_0 \equiv 2\hbar\omega_c / 3E = \gamma H / H_c \sim 10^3$$

Critical energy  $\hbar\omega_c \cong mc^2 \gamma / Y_0$

$$H_c = m^2 c^3 / e\hbar \cong 4.4 \cdot 10^{13}$$

Formation length  $l_F \cong \lambda_C \gamma / Y_0^{2/3}$

Aspect ratio at IP  $\sigma_x / \sigma_y \cong 5$

Transverse size of coherence  $\sigma_{\perp}^{coh} \cong \sqrt{\lambda_{cr} l_F \sigma_b} \cong Y_0^{1/6} \lambda_C$   
 $\sim 3\lambda_C \cong 1.15 \cdot 10^{-10} \text{ cm}$

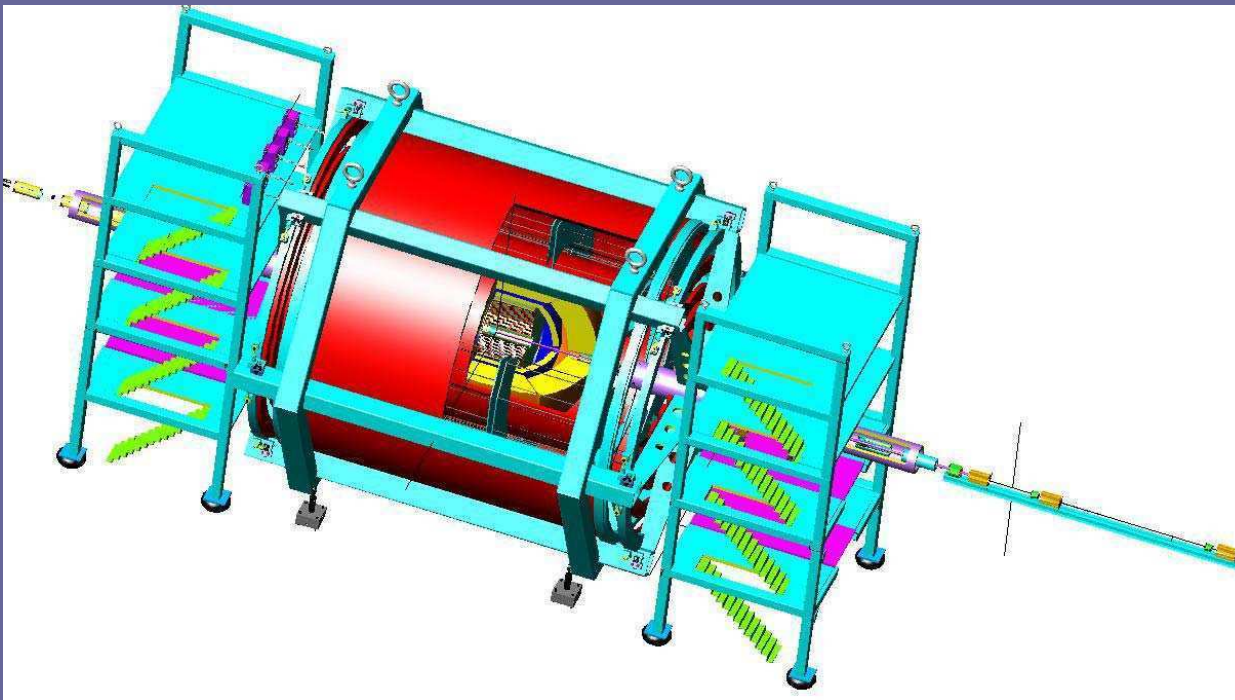
# DETECTOR and IP

There is no magnetic yoke in this detector. Focusing arranged with the help of multiplet of RF quadrupoles on the basis of accelerating structures. The number of RF lenses in multiplet ~200.

RF gradient slowly varies from very strong at closest to IP side to a weak one;  $k \sim 100 \text{ 1/m}^2$

In modular detector the solid angle available for registration is large.

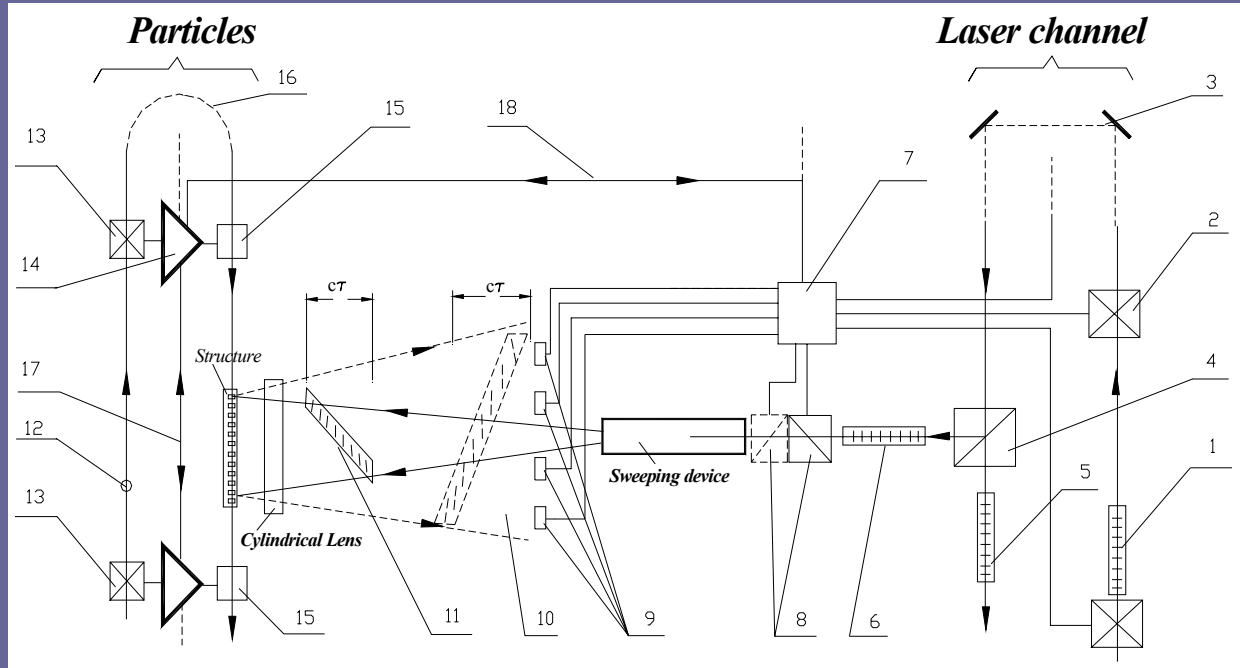
So the lens with 1000 cells reaches the focal distance  $F=20 \text{ cm}$ . Let just remind that these cells will occupy 0.1 cm only.



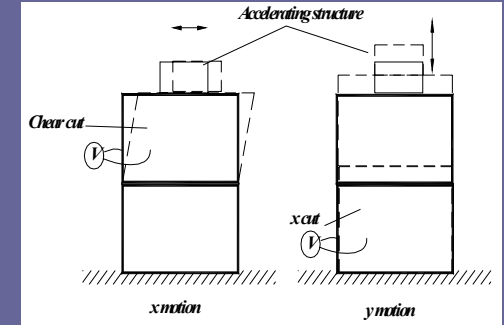
Modular detector

Pixel detectors for  
muon identification

# FEEDBACK AND ALIGNMENT



1—is a driving laser bunch, 2—is transverse position sensor for a laser bunch, 3—is a laser back reflector loop, 4 —is a power splitter, 5—is a driving bunch on the way to next module, 6—is a splitted part of driving laser bunch, 7—is a processor, 8—are the beam deflectors for two transverse directions, 9—is an array of optical sensors, 10—is a reflected laser bunch, 11—is a swepted laser bunch. 12—is an electron/positron bunch on the way to the beginning of accelerator. 13—are the pick up electrodes, 14—is a functional amplifier, 15—is a transverse kickers, 16—is a beam back returning loop, 17,18 —are the lines of the signal processed. Lines across the laser bunch indicate the wavefronts. The back loop 3 located at the beginning of accelerator (acceleration process).



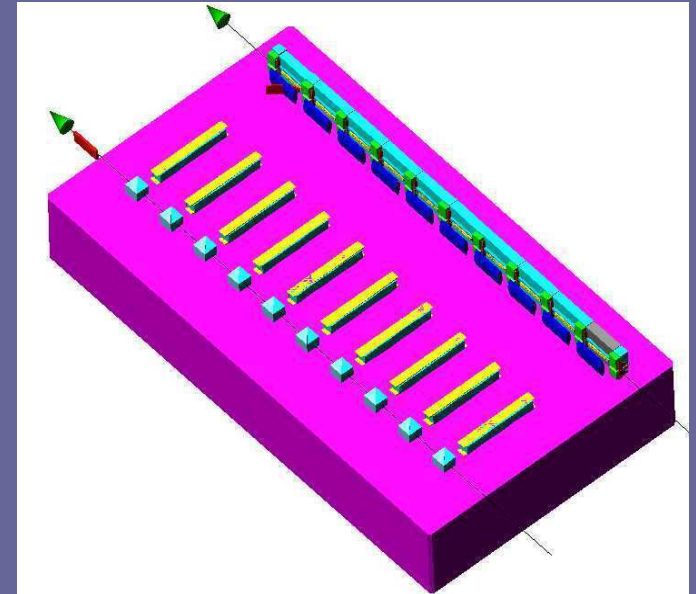
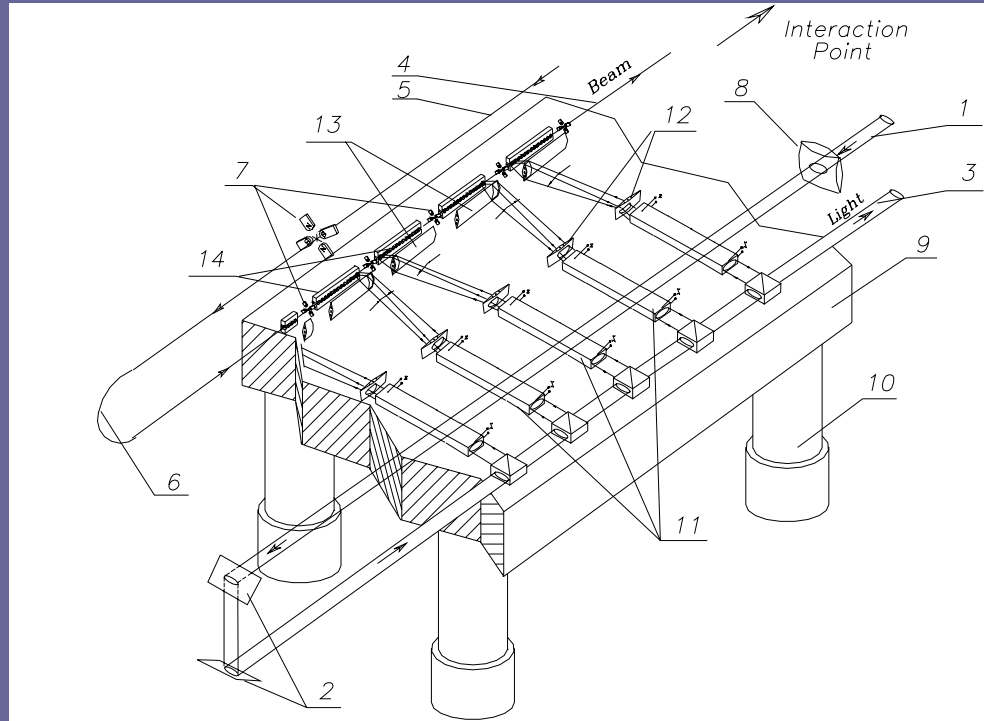
**Movement of structure**

$$(\Delta \mathcal{G})^2 \equiv \left( \frac{\Delta p_{\perp}}{\Delta p_{\parallel}} \right)^2 \ll \frac{\varepsilon}{\beta} \left( \frac{p_{\parallel}}{\Delta p_{\parallel}} \right)^2 = (\Delta \mathcal{G})_{beam}^2 \left( \frac{\gamma}{\Delta \gamma} \right)^2$$

$$\Delta \mathcal{G}_y \cong 2 \cdot 10^{-5}$$

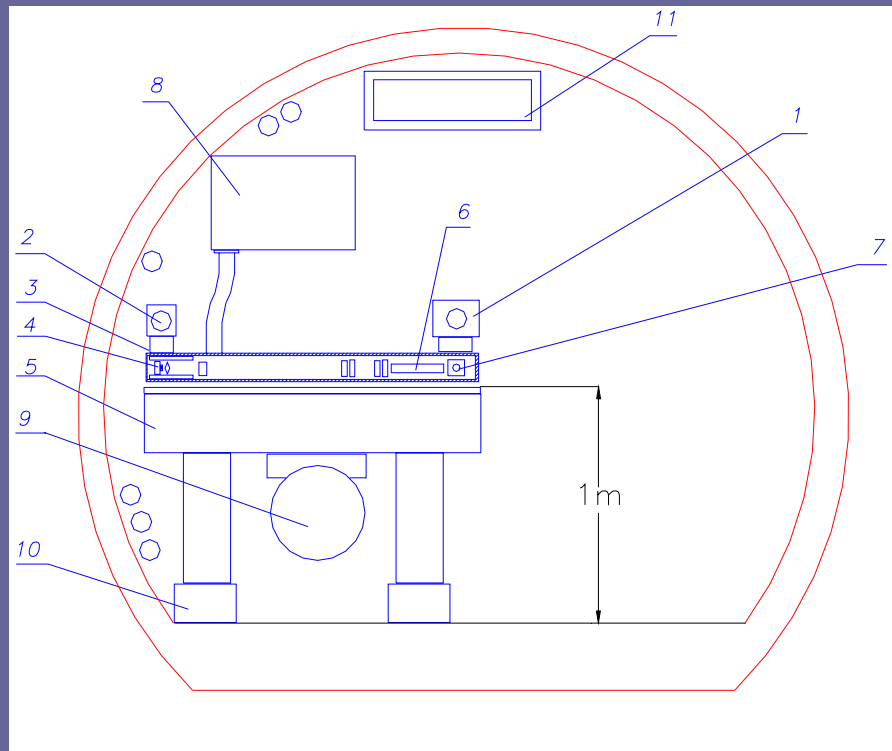
$$\Delta \mathcal{G}_x \cong 7 \cdot 10^{-4}$$

# ACCELERATOR TABLE



Primary laser beam 1 goes to the end of accelerator. Mirrors 2 redirect it back, pos.3, through the sequence of splitters. In the similar way the particle's beam 5, goes through bending system 6 and further through structures to next modules, 4. 7 and 8 –are the focusing elements for the laser and particle's beam respectively. Optical platform 9 is standing on legs 10 with active damping system to minimize vibrations. 13–cylindrical lenses, 14–are the accelerating structures. All elements on the table are located in a vacuumed volume, not shown here.

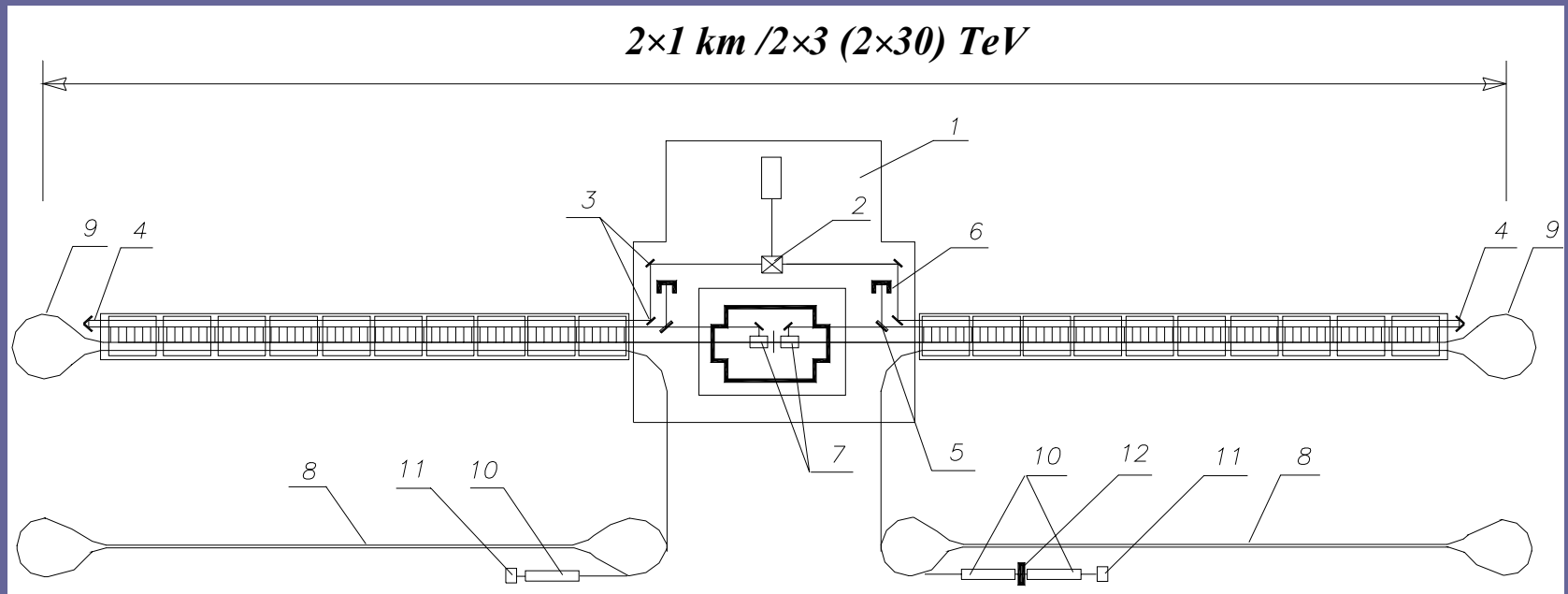
## Cross section of a tunnel with accelerating system for underground location.



Neighboring platforms aligned with help of sensors, installed at the end of each platform. So the sensor installed at one platform touches neighboring one. The sensors are similar to that used in tunneling microscope technique. This system could be made fast enough to exclude influence of ground motion, mostly intensive at lower edge of the spectrum.

1— is a primary optical beam line. 2—is a primary particle's beam line. 3—is a vacuumed container with all equipment. 4—is an accelerating structure with sub systems. 5—is an optical table. 6—is the deflecting device, 7 —is the line for driving optical beam, 8—is a box with equipment for deflecting device and control. 9—is a tube with optical elements for active alignment of all optical tables. 10—is an anti-vibration active system. 11—is a duct for air-conditioning.

# Laser Linear Collider (LLC) complex.



1—is a laser master oscillator platform, 2 —is an optical splitter, 3,4—are the mirrors, 5—is a semi-transparent mirror, 6—is an absorber of laser radiation. 7—are the Final Focus Systems. 8—are the damping systems for preparing particle's beams with small emittances, 9—are the bends for particle's beam. 10—are the accelerating X-band structures, 11—is an electron gun, 12—is a positron converter. The scheme with the damping rings as sources are shown here.

# PARAMETER LIST

|                                               |                                                                 |
|-----------------------------------------------|-----------------------------------------------------------------|
| Wavelength                                    | $\lambda_{ac} \cong 1 \mu m$                                    |
| Energy of $e^+$ beam                          | $2 \times 10 \text{ TeV}$                                       |
| Luminosity                                    | $10^{35} \text{ cm}^{-2} \text{ s}^{-1}$                        |
| Total two-linac length                        | $2 \times 1 \text{ km}$                                         |
| Main linac gradient                           | $10 \text{ GeV/m}$                                              |
| Bunch population                              | $3 \cdot 10^5$                                                  |
| Bunch length                                  | $0.1 \mu m$                                                     |
| No. of bunches/train                          | 30                                                              |
| $\gamma \varepsilon_x / \gamma \varepsilon_y$ | $5 \cdot 10^{-9} / 1 \cdot 10^{-9} \text{ cm} \cdot \text{rad}$ |
| Laser flash energy                            | $2 \times 3 \text{ J}$                                          |
| Laser density                                 | $0.3 \text{ J/cm}^2$                                            |
| Illumination time                             | $0.1 \text{ ps}$                                                |
| Length of section                             | $3 \text{ cm}$                                                  |
| Laser flash energy/section                    | $100 \mu \text{J}$                                              |
| Repetition rate                               | $1 \text{ kHz}$                                                 |
| Laser beam power                              | $2 \times 3 \text{ kW}$                                         |
| Damping ring energy                           | $2 \text{ GeV}$                                                 |
| Damping time                                  | $10 \text{ ms}$                                                 |
| Wall plug power**                             | $2 \times 30 \text{ kW}$                                        |

\*\* Without supplementary electronics.



# CONCLUSIONS

- Nano-technology available creates solid base for accelerator with Travelling Laser Focus.
- Any point on accelerating structure remains illuminated by  $\sim 0.3$  ps only. Laser density  $0.3 \text{ J/cm}^2$
- Lasers for the TLF method need to operate with pulse duration  $\sim 100\text{ps}$ .
- TLF method promises up to  $10 \text{ TeV/km}$  with  $3 \text{ mJ/m}$ . With such high gradients,  $\mu^+\mu^-$ ,  $\pi^+\pi^-$ ,  $\pi p$ ,  $\mu p$  and ion-ion collisions become feasible.
- We conclude that acceleration in a laser-driven linac with TLF method is a present day technology and no physical and technical limitations found on this way.
  - **Testing of this method might be highest priority task for accelerator physics.**

# Particle acceleration by laser

Baifei Shen

Shanghai Institute of Optics and Fine Mechanics, CAS  
ANL

Nov. 28, 2006

# Contents

## 1. Electron acceleration

- Electrons accelerated by laser in vacuum.
- Electrons accelerated by the wake

## 2. Ion acceleration

- Target normal sheath acceleration (TNSA)
- Ion acceleration by light pressure.
- Ion acceleration by a shock

## Electron movement in a planar wave in vacuum

The planar wave is:

$$a(z, t) = a_0 \cos(\omega t - kz)$$
$$a = eA/mc^2$$

For an electron initially rest in front of laser pulse,  
the transversal momentum is :

$$P_{\perp} = \gamma v = a$$

The longitudinal momentum is :

$$p_z = a^2/2$$

The kinetic energy is :

$$K = \gamma - 1 = a^2/2$$

$a=1$  means:

$$I_0 \lambda^2 = 1.37 \times 10^{18} \text{W} \mu\text{m}^2 \text{cm}^{-2}$$

# Electrons accelerated by laser in vacuum

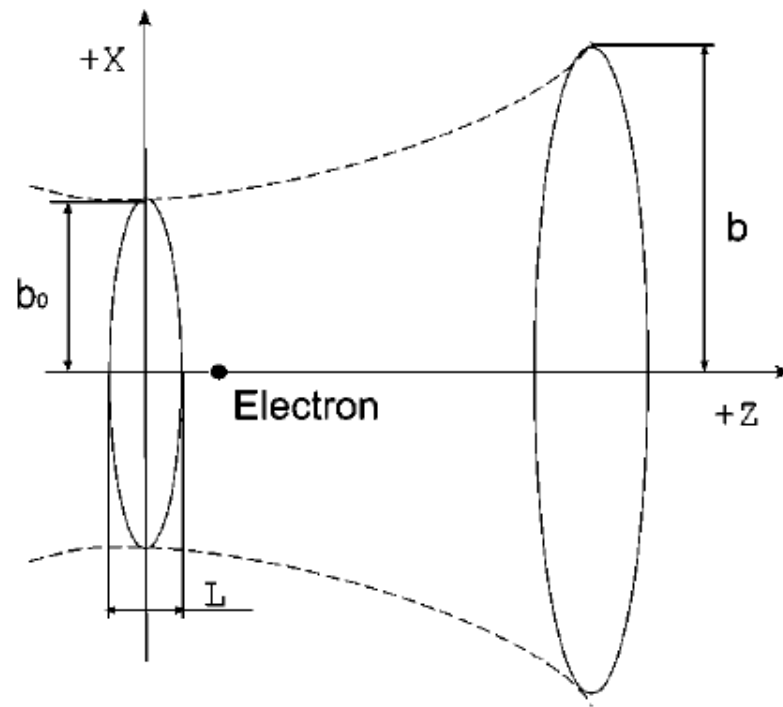


FIG. 1. Schematic geometry of electron acceleration by a circular polarized Gaussian laser beam, we assume that the laser pulse propagates along  $+z$  axis.

$$\mathbf{a} = a_0 \exp(-\eta^2/L^2 - \rho^2/b^2)(b_0/b)\hat{\mathbf{a}},$$

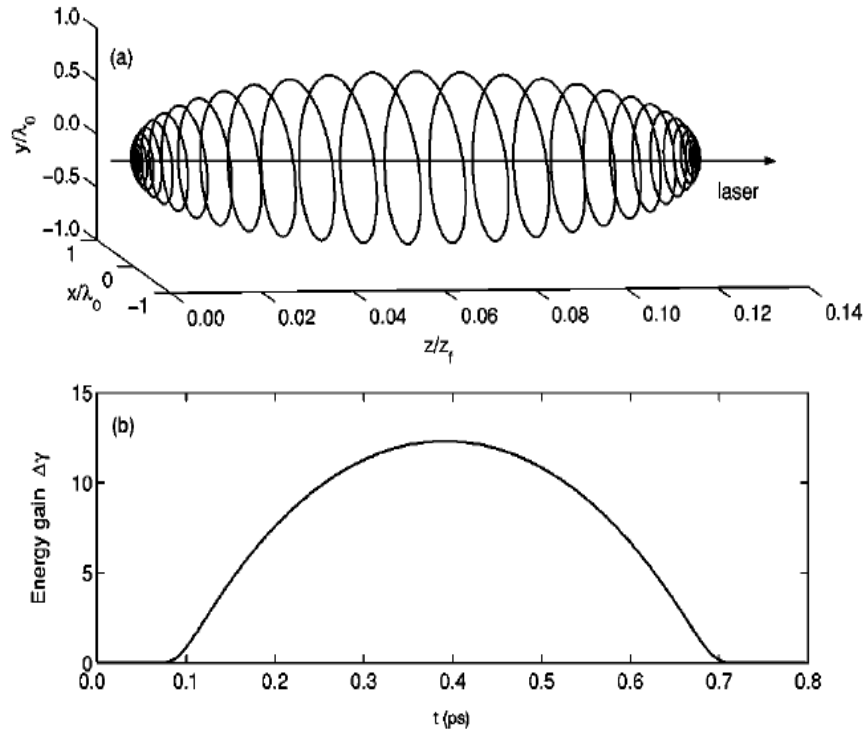


FIG. 2. Electron trajectory in a circular polarized Gaussian pulse electromagnetic wave (a) and electron's energy during the interaction (b) for  $a_0=5$ ,  $L=10\lambda_0$ , and  $b_0=20\lambda_0$ .

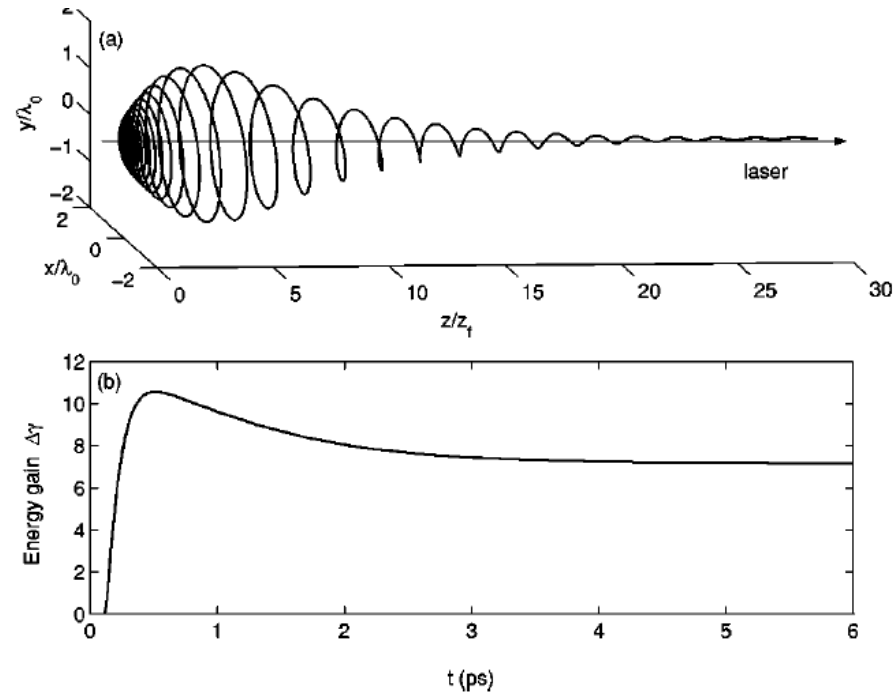


FIG. 3. Electron trajectory in a circular polarized Gaussian pulse electromagnetic wave (a) and electron's energy during the interaction (b) for  $a_0=5$ ,  $L=10\lambda_0$ , and  $b_0=5\lambda_0$ .

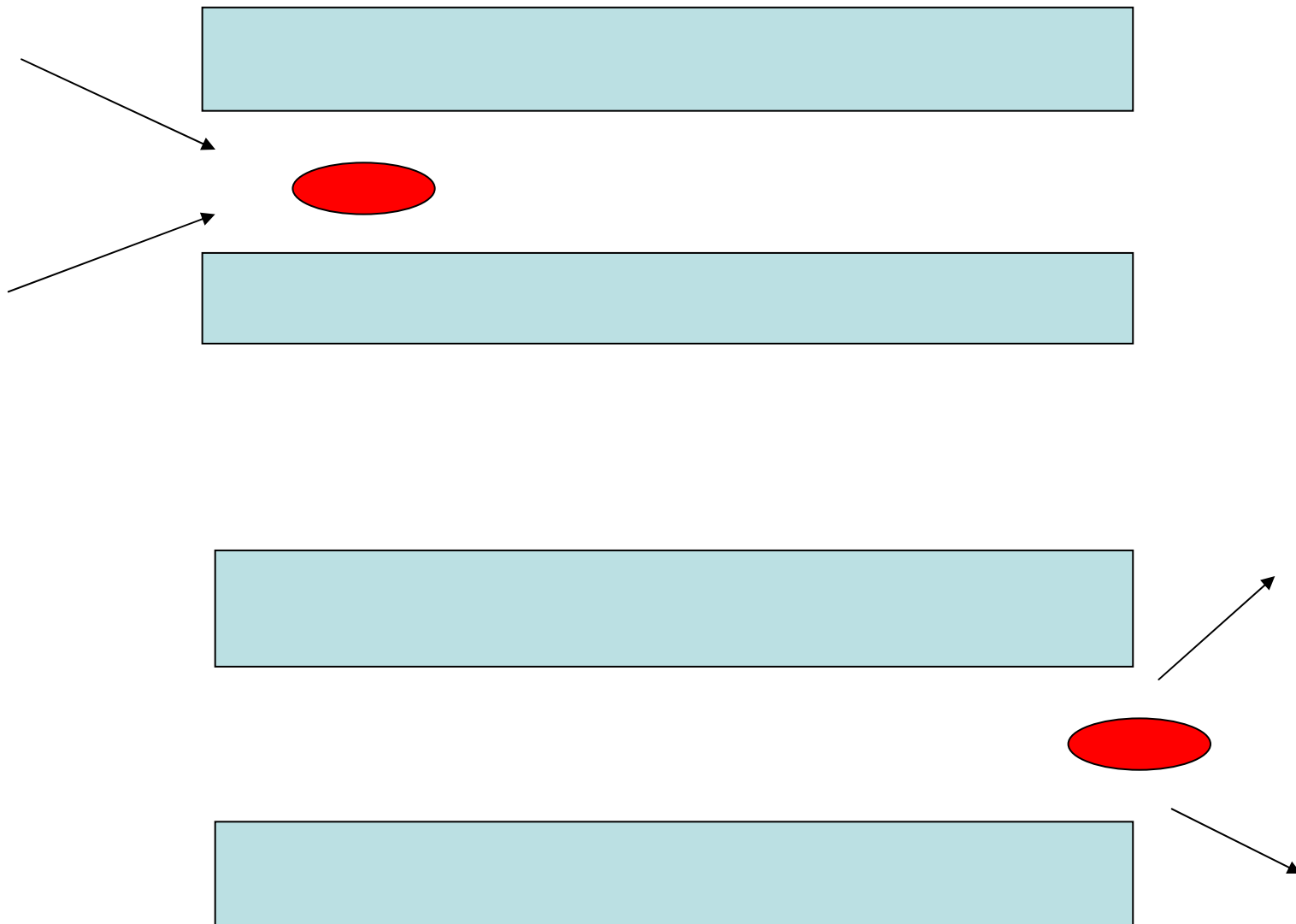
While a planar laser pulse can not accelerate an electron in vacuum, a Gaussian pulse does.

If an electron has an initial velocity, the electron may be accelerated to very high energy.

$$\beta = \frac{\beta_1 + \beta_2}{1 + \beta_1 \beta_2}$$

$$\text{If } \gamma_1, \gamma_2 \gg 1, \quad \gamma = 2\gamma_1\gamma_2$$

The problem is the acceleration is much larger than the Rayleigh length. In order that a laser pulse can propagate longer than Rayleigh length, a preformed plasma channel may be used.

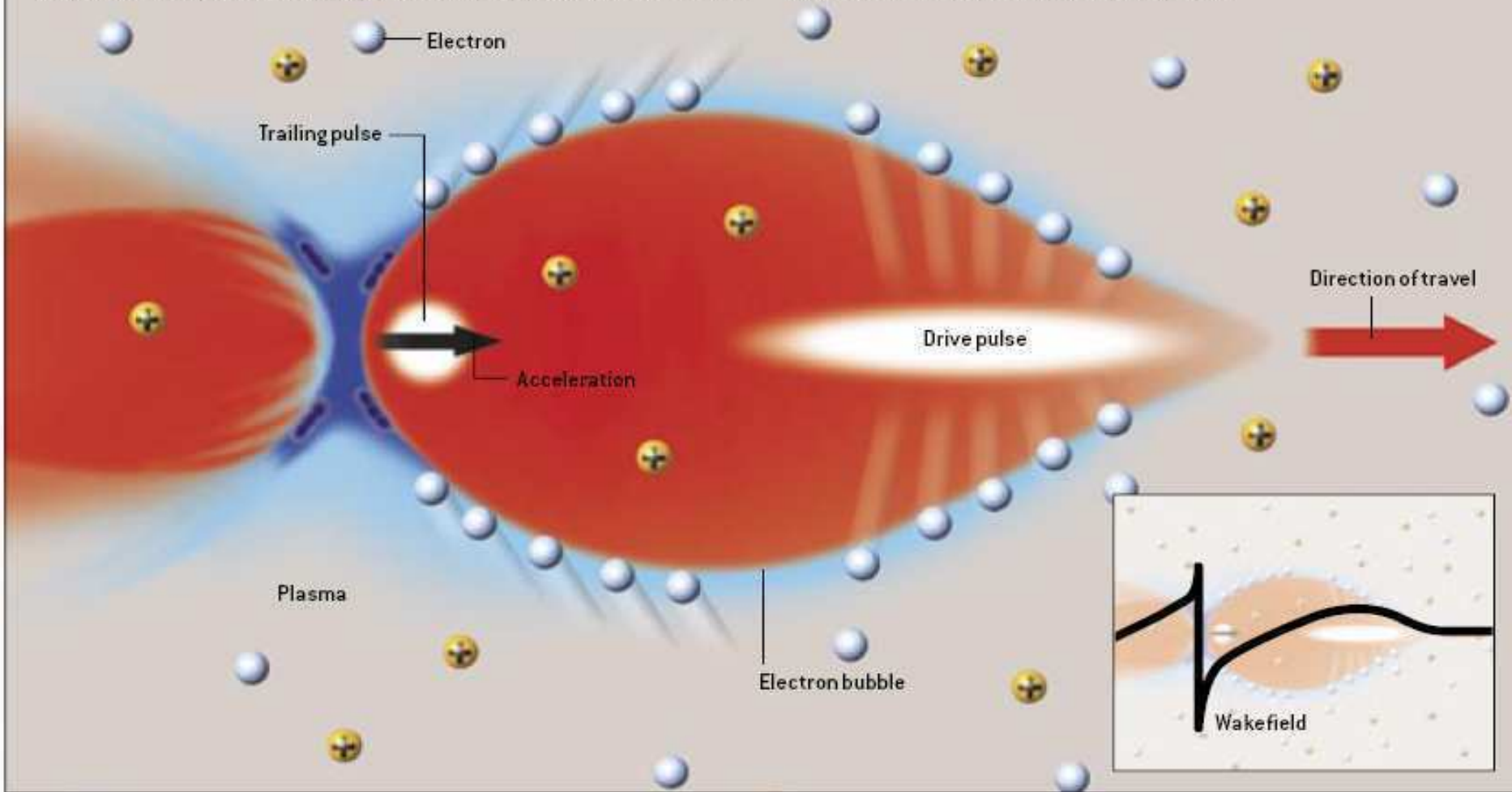




# THE BUBBLE REGIME

Wakefield accelerator relies on a charge disturbance known as a wakefield to provide the driving force. The drive pulse, which can be a short pulse of either a laser or an electron beam, blows the electrons (*blue*) in an ionized gas, or plasma, outward—leaving behind a region of positive charge (*red*). The positive charge pulls the negatively charged electrons back in

behind the drive pulse, forming an electron bubble around the positive region. Along the axis that the beam propagates, the electric field (*plotted below*) resembles a very steep ocean wave about to break. This field—the wakefield—causes a trailing pulse of electrons caught near the rear of the bubble to feel a very strong forward acceleration.

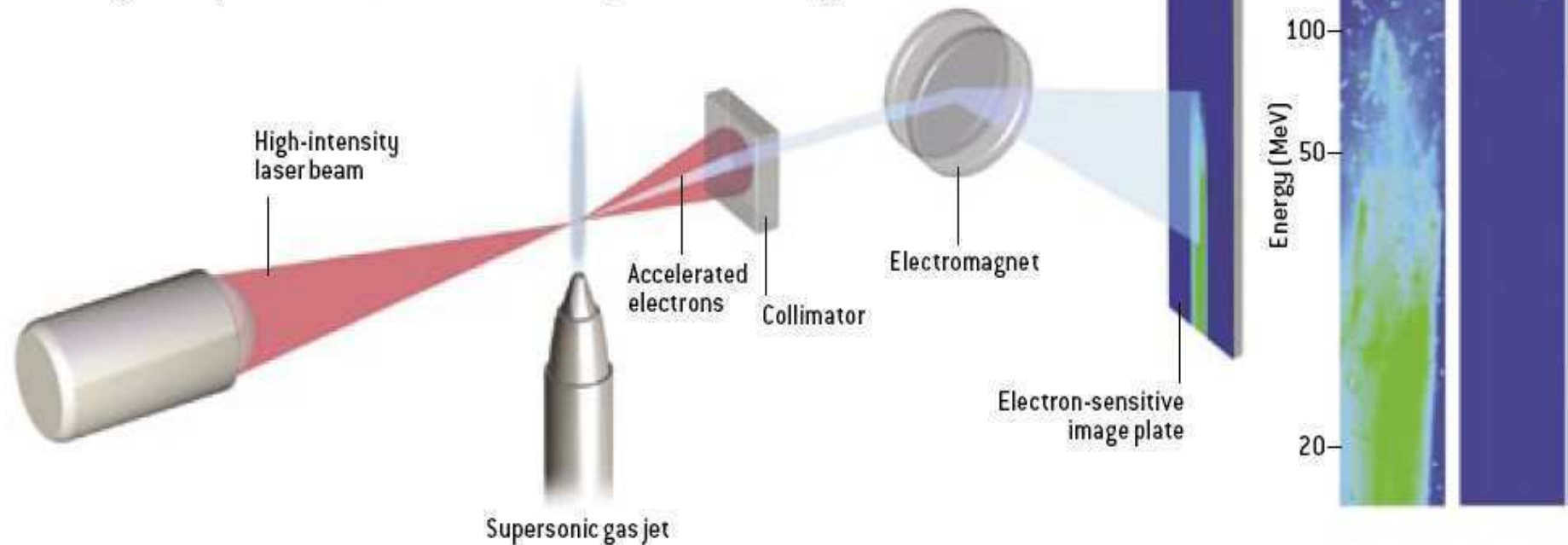


# LASER WAKEFIELD ACCELERATOR

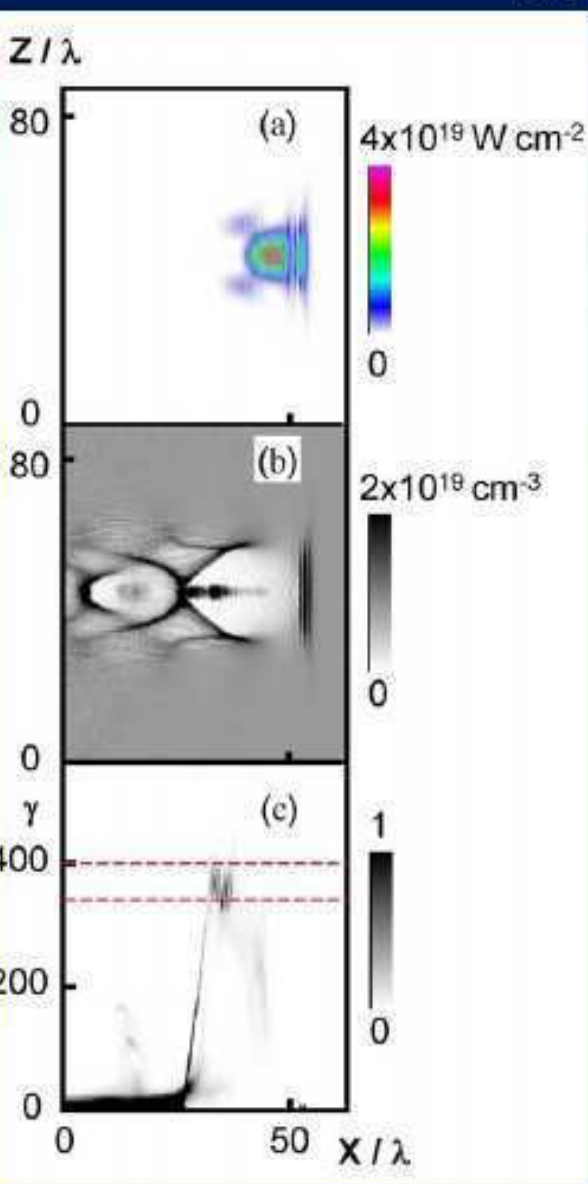
A tabletop plasma accelerator consists of a high-intensity laser beam focused on a supersonic jet of helium gas (*left*). A pulse of the beam produces a plasma in the gas jet, and the wakefield accelerates some of the dislodged electrons. The resulting electron pulse is collimated and passed through a magnetic field, which deflects the electrons by different amounts according to their energy. The whole accelerator can fit on a four-foot-by-six-foot optical table.

Electron beams (*panels at right*) produced by the first tabletop accelerator, at the Laboratory of Applied Optics at the Ecole Polytechnique in France, illustrate how a major obstacle

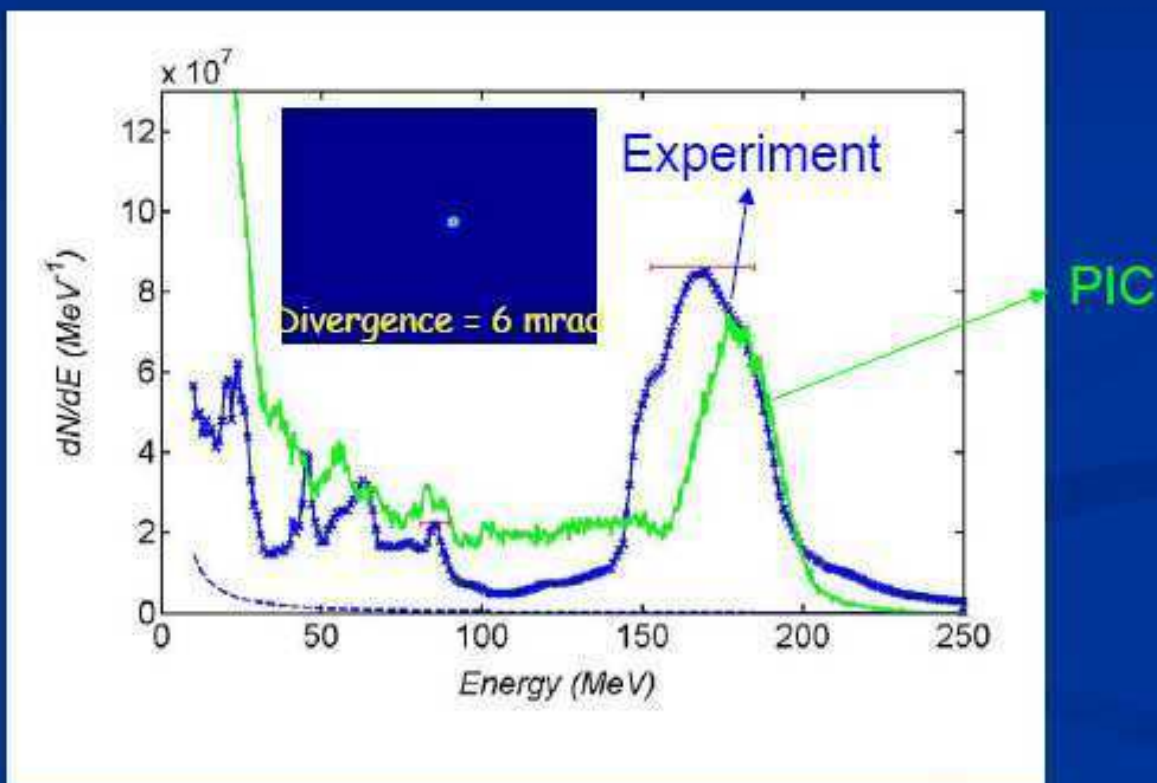
was overcome. Although some electrons were accelerated to 100 MeV, the electron energies ranged all the way down to 0 MeV (*a*). Also, the beam diverged by about a full degree. In contrast, the results from the recently discovered “bubble” regime showed a monoenergetic beam of about 180 MeV with a much narrower angular spread (*b*). Such a beam is of greater use for applications.



# Energy distribution improvements: The Bubble regime



Charge in the peak : 200-300 pC



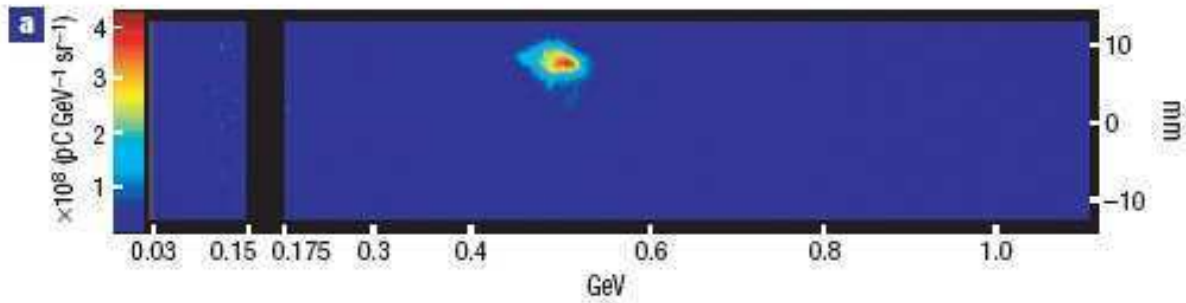
A+ LOA  
J. Faure et al. Nature (2004)



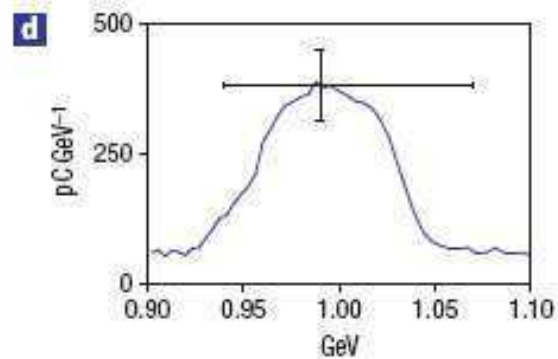
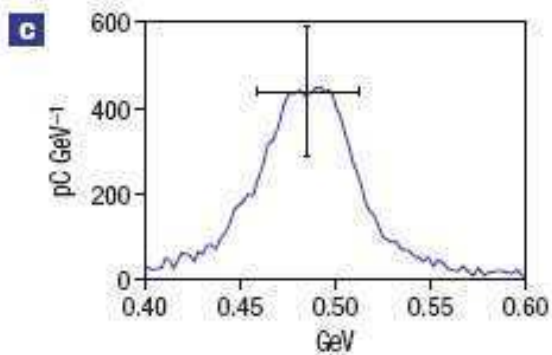
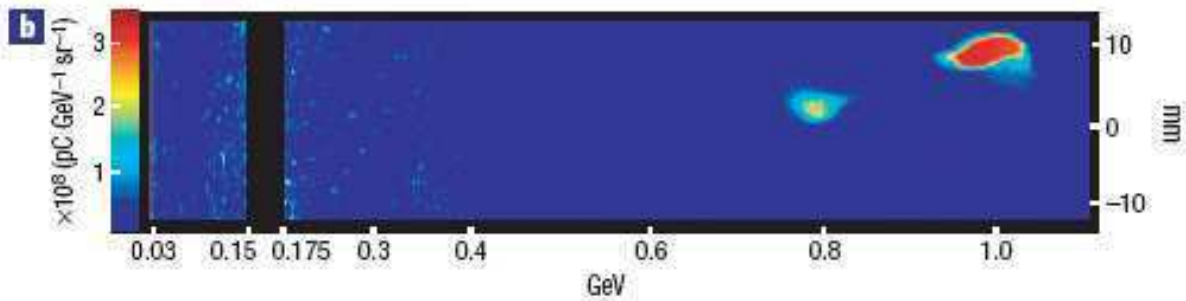
# Quasi-monoenergetic beams reported in the literature

| Name    | Article       | Lab      | Energy<br>[MeV] | dE/E<br>[%] | Charge<br>[pC] | Ne<br>[ $\times 10^{18}/\text{cm}^3$ ] | Intensity<br>[ $\times 10^8 \text{ W}/\text{cm}^2$ ] | $\tau_L/T_p$ | Remark    |
|---------|---------------|----------|-----------------|-------------|----------------|----------------------------------------|------------------------------------------------------|--------------|-----------|
| Mangles | Nature (2004) | RAL      | 73              | 6           | 22             | 20                                     | 2,5                                                  | 1,6          | Channel   |
| Geddes  | Nature (2004) | L'OASIS  | 86              | 2           | 320            | 19                                     | 11                                                   | 2,2          |           |
| Faure   | Nature (2004) | LOA      | 170             | 25          | 500            | 6                                      | 3                                                    | 0,7          |           |
| Hidding | PRL (2006)    | JETI     | 47              | 9           | 0,32           | 40                                     | 50                                                   | 4,6          | Preplasma |
| Hsieh   | PRL (2006)    | IAMS     | 55              |             | 336            | 40                                     |                                                      | 2,6          |           |
| Hosokai | PRE (2006)    | U. Tokyo | 11,5            | 10          | 10             | 80                                     | 22                                                   | 3,0          |           |
| Miura   | APL (2005)    | AIST     | 7               | 20          | 432E-6         | 130                                    | 5                                                    | 5,1          |           |
| Hafz    | PRE (2006)    | KERI     | 4,3             | 93          | 200            | 28                                     | 1                                                    | 33,4         |           |
| Mori    | ArXiv (2006)  | JAERI    | 20              | 24          | 0,8            | 50                                     | 0,9                                                  | 4,5          |           |
| Mangles | PRL (2006)    | Lund LC  | 150             | 20          |                | 20                                     | 5                                                    | 1,4          |           |

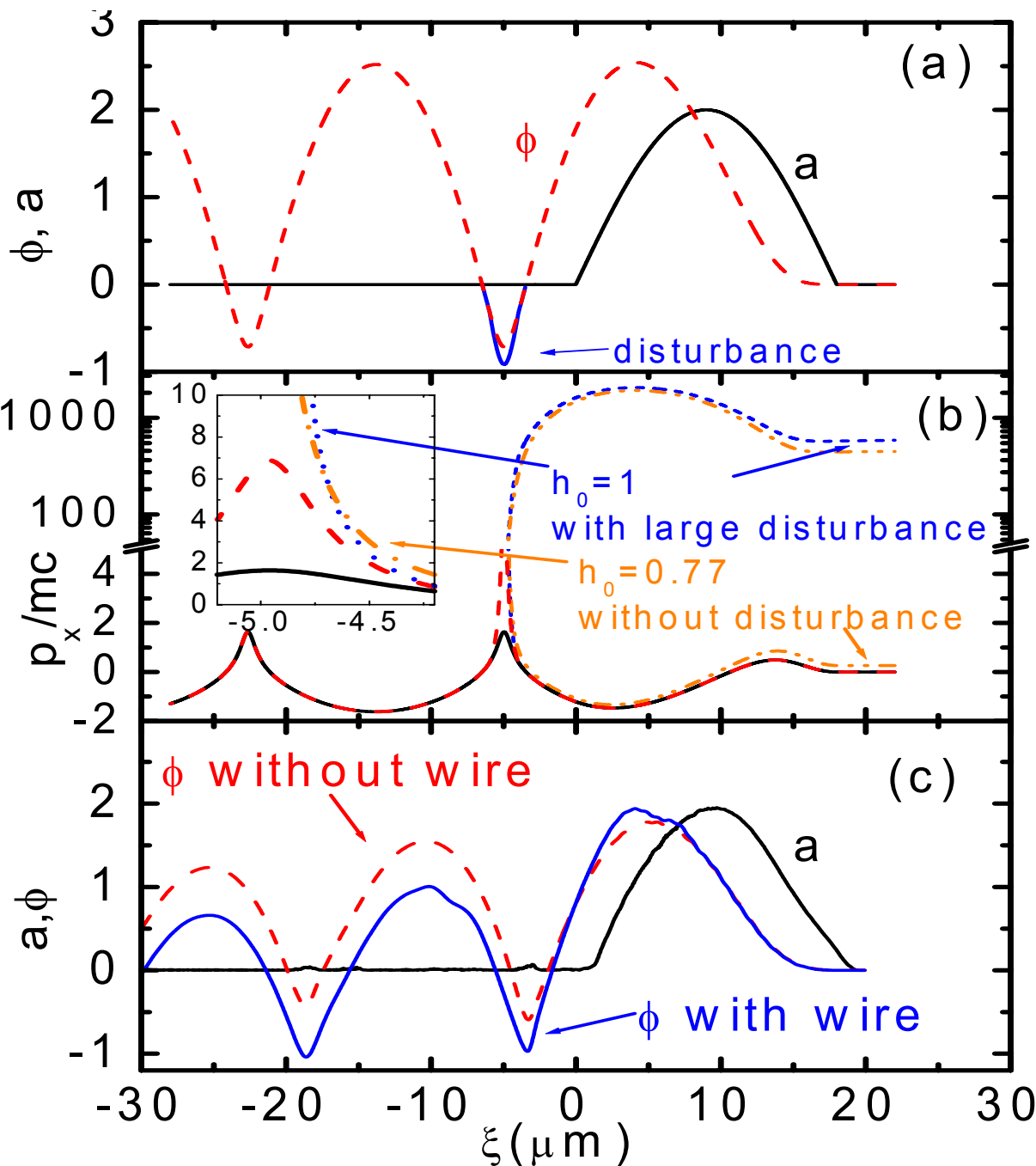
Several groups have obtained quasi monoenergetic e beam but at higher density ( $\tau_L > \tau_p$ )



Plasma length:  
3 cm



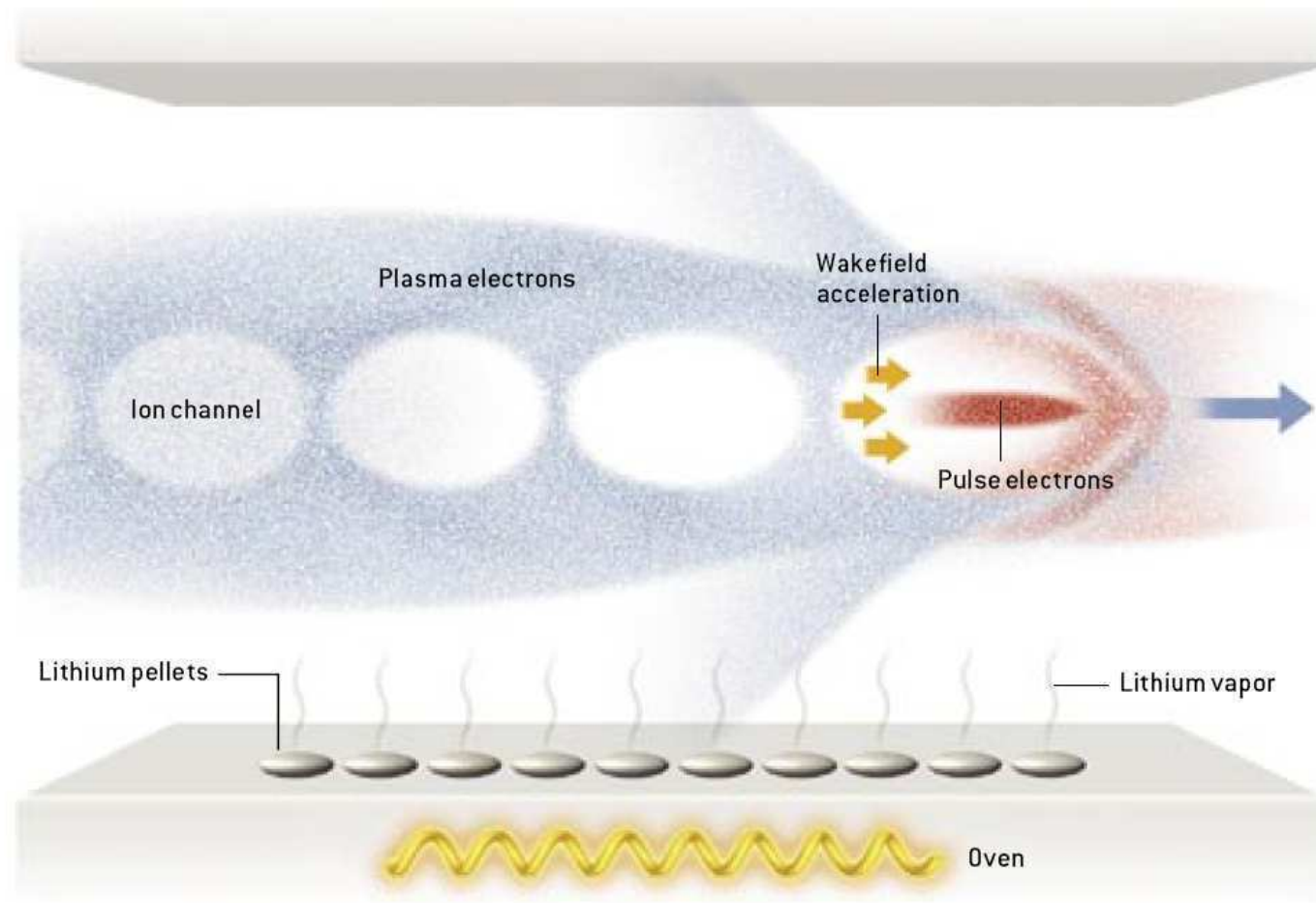
**W. P. LEEMANS, Nature Phys. 2, 296(2006)**



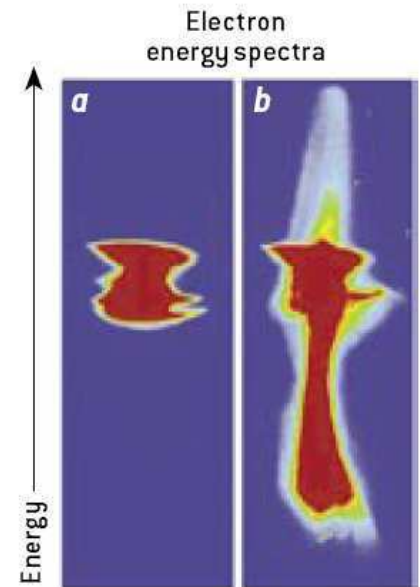
(a) Analytical calculation for the vector potential of the laser pulse and scalar potential for the one-dimensional wake in a plasma of density  $6 \times 10^{18} \text{ cm}^{-3}$  driven by a circularly polarized laser pulse of peak amplitude  $a=2$  and duration 30 fs; (b) Trajectory of electrons under different conditions in the field in (a); (c) Three dimensional particle in cell simulation for the same plasma conditions. The circularly polarized laser pulse is of peak amplitude  $a=1.414$ , duration 30 fs, and a transverse FWHM of  $12 \mu\text{m}$ . The dashed (solid) line shows the vector potential of the wake before (right after) the bubble base hit the wire.

Plasma wakefield acceleration was recently demonstrated in an experiment using a beam of the Stanford Linear Collider (SLC). The accelerator added 4 GeV of energy to an electron beam in just 10 centimeters—an energy gain that would require a 200-meter section of a conventional microwave accelerator.

In the experiment, an oven vaporized lithium pellets. An intense electron pulse (*red*) ionized the vapor to produce a plasma. The pulse blew out the plasma electrons (*blue*), which then set up a wakefield, or a charge disturbance, behind the pulse. Electrons located in that wakefield experienced powerful acceleration (*orange arrows*).



In the absence of the lithium (*a*), SLC's 30-GeV beam was quite mono-energetic (energy is plotted vertically). After passing through 10 centimeters of lithium plasma (*b*), most of the beam particles lost energy in generating the plasma wakefield (*red tail*). The wakefield accelerated a small number of electrons that happened to be at the back of the pulse to higher energy (*blue region at top*).

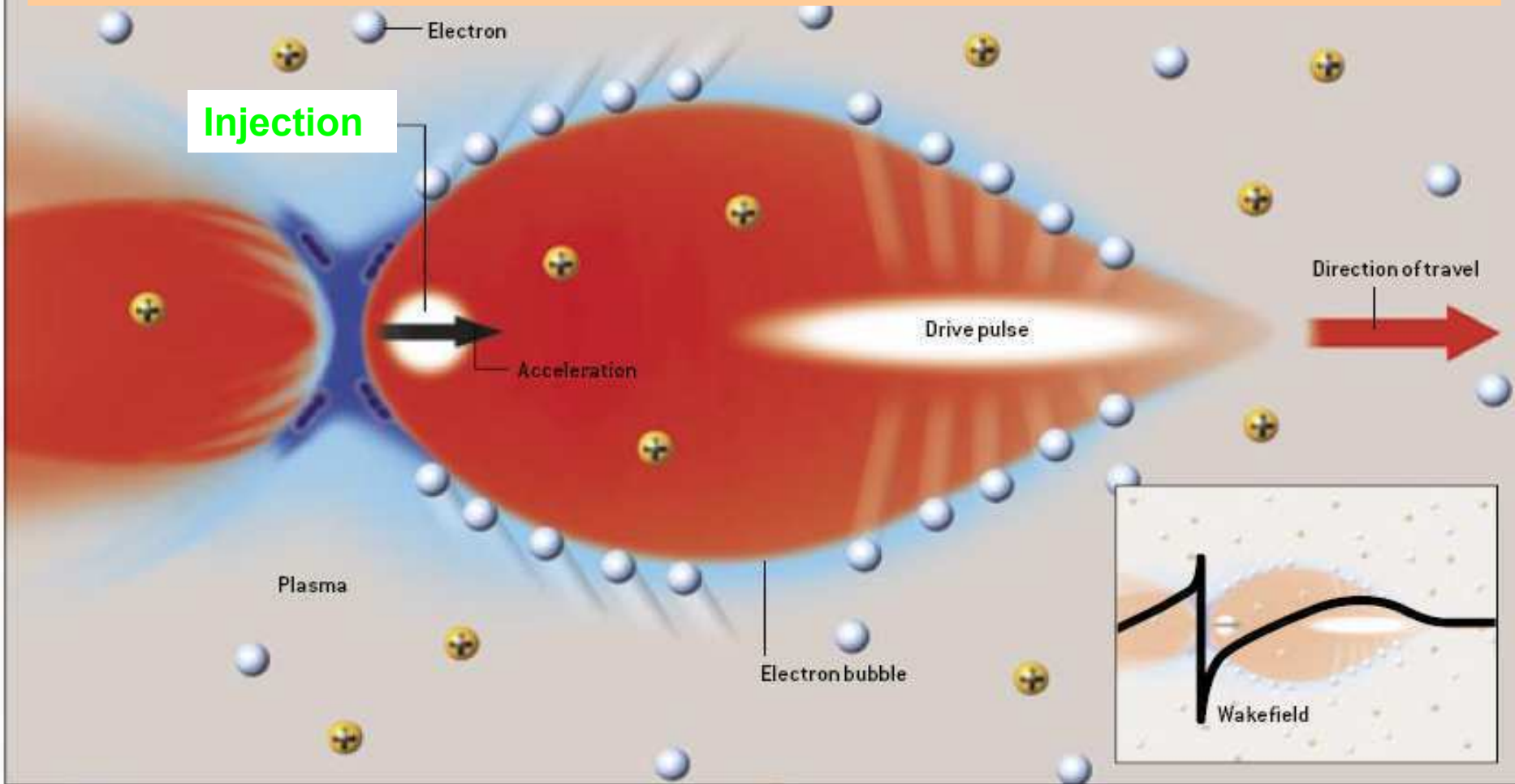


C. Joshi, Scientific America, 41(2006);

M. J. Hogan et al., Phys. Rev. Lett. 95, 054802 (2005).

## THE BUBBLE REGIME

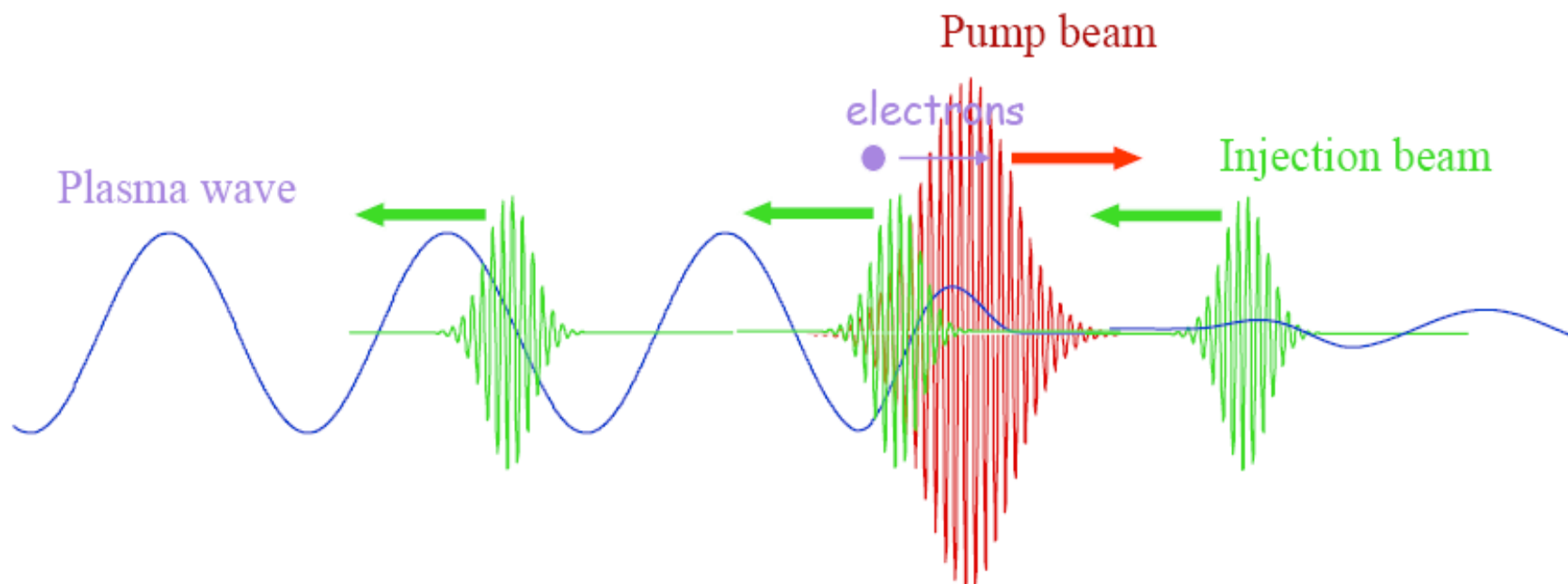
An electron bunch can be injected into a bubble driven by a laser pulse or an electron beam.





# Controlling the injection

Counter-propagating geometry:

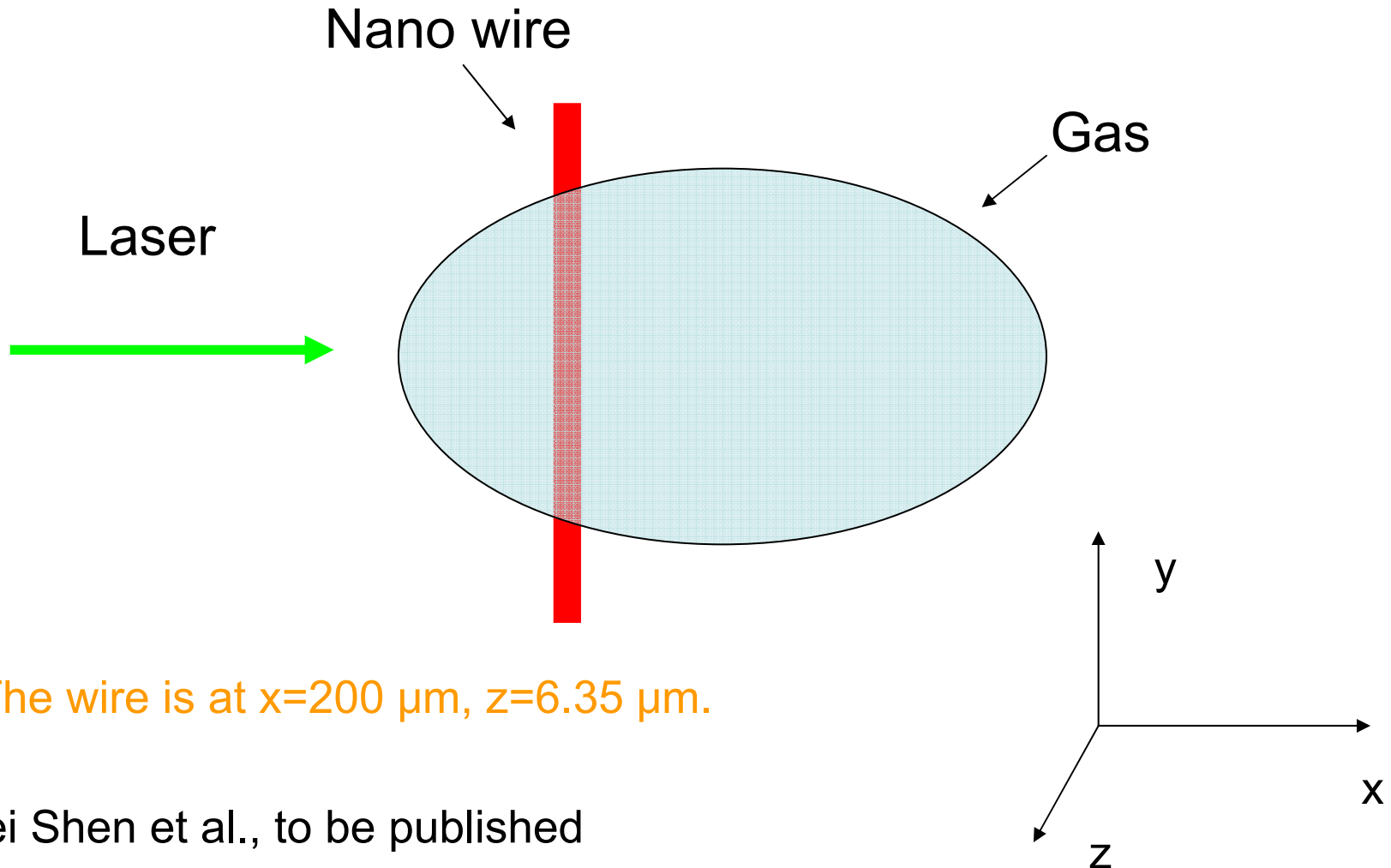


Ponderomotive force of beatwave:  $F_p \sim 2a_0a_1/\lambda_0$  ( $a_0$  et  $a_1$  can be "weak")

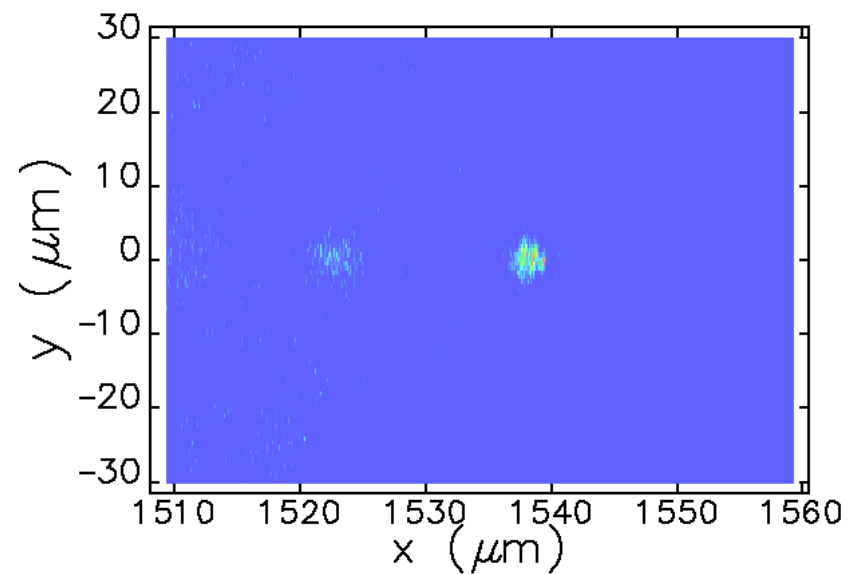
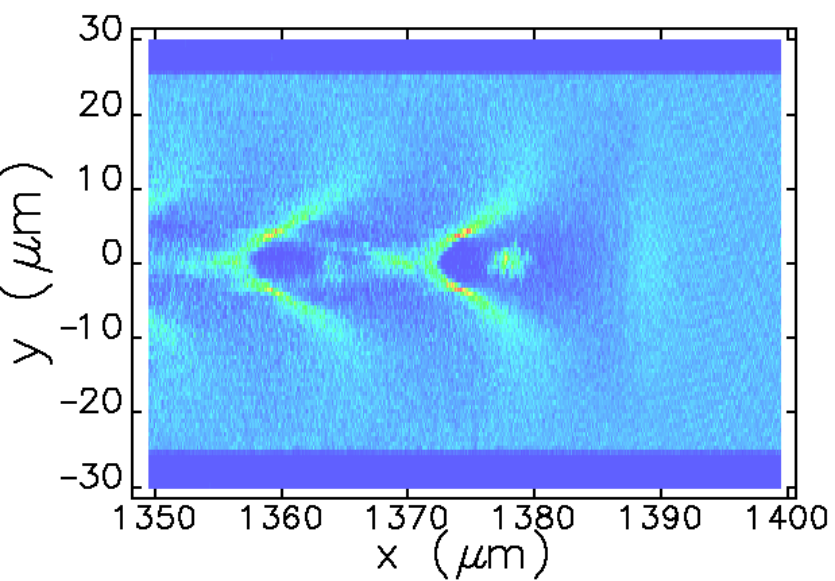
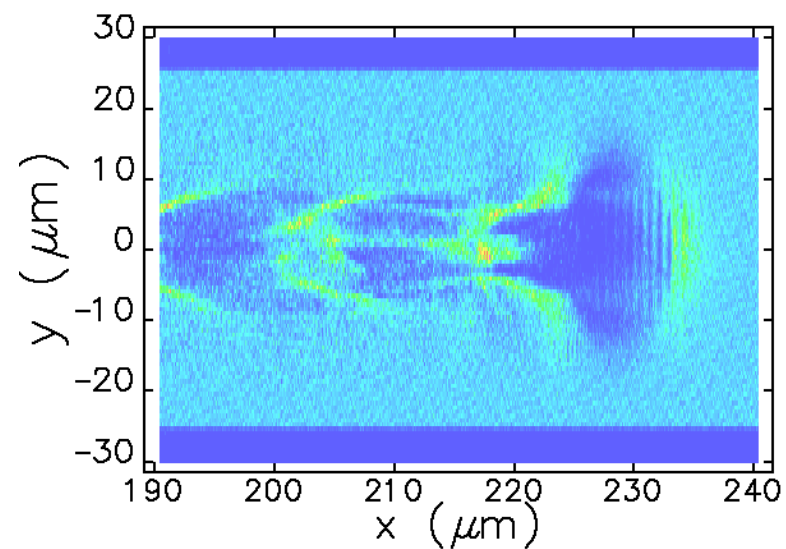
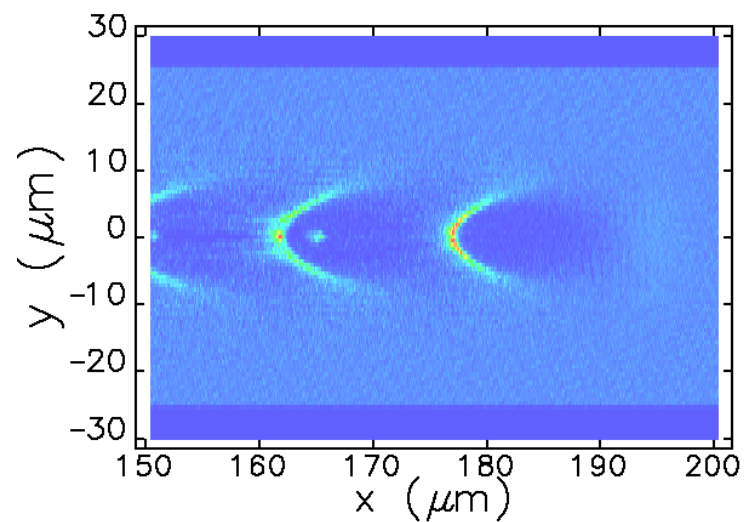
Boost electrons locally and injects them:

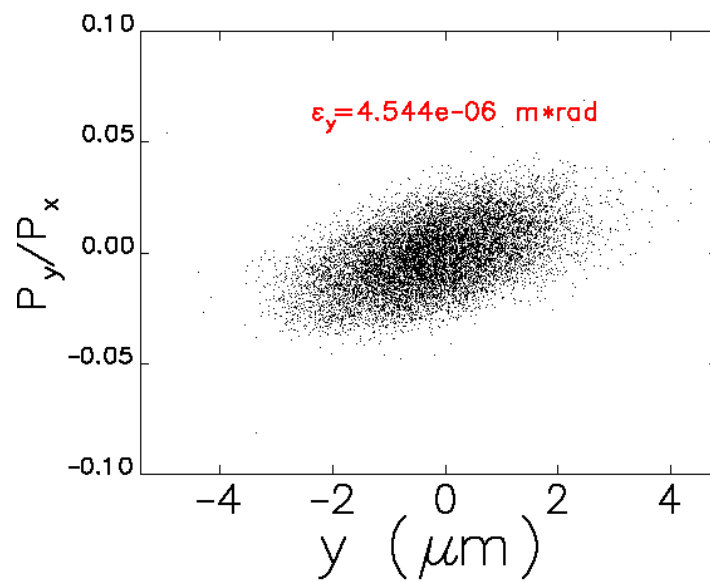
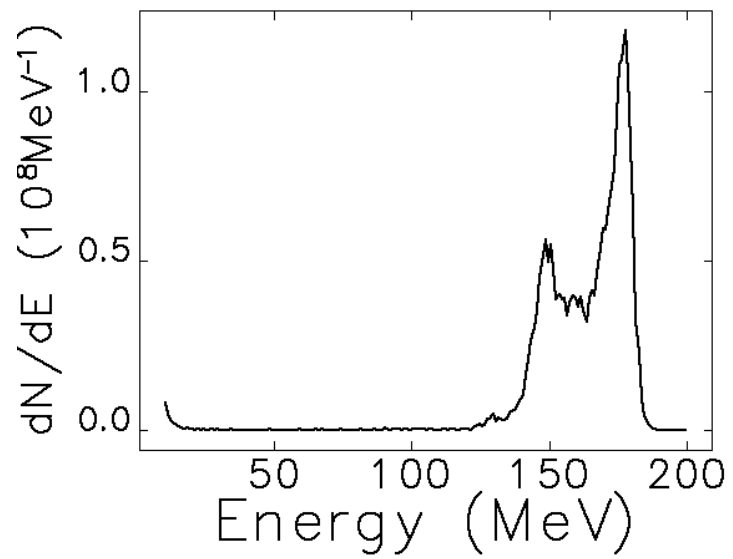
INJECTION IS LOCAL IN FIRST BUCKET

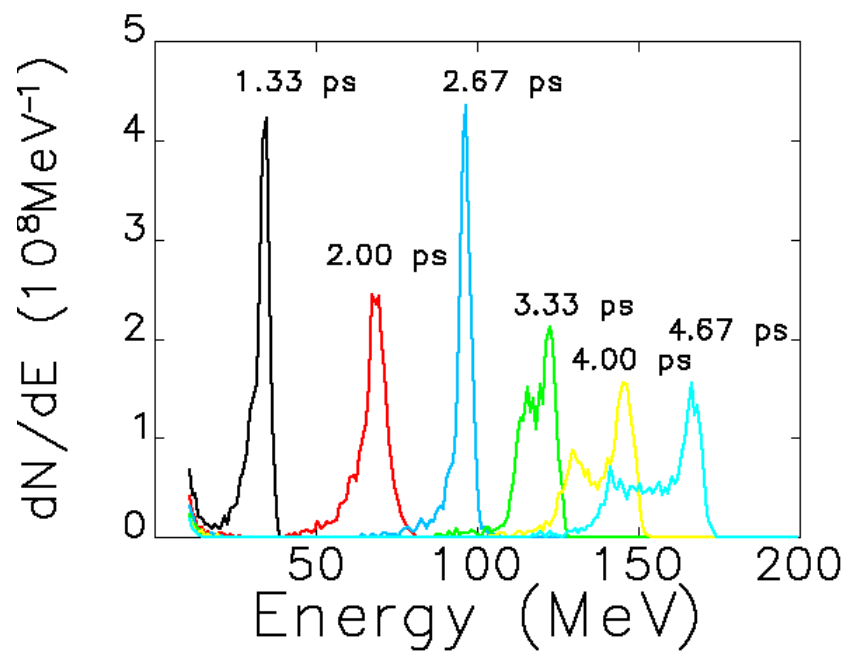
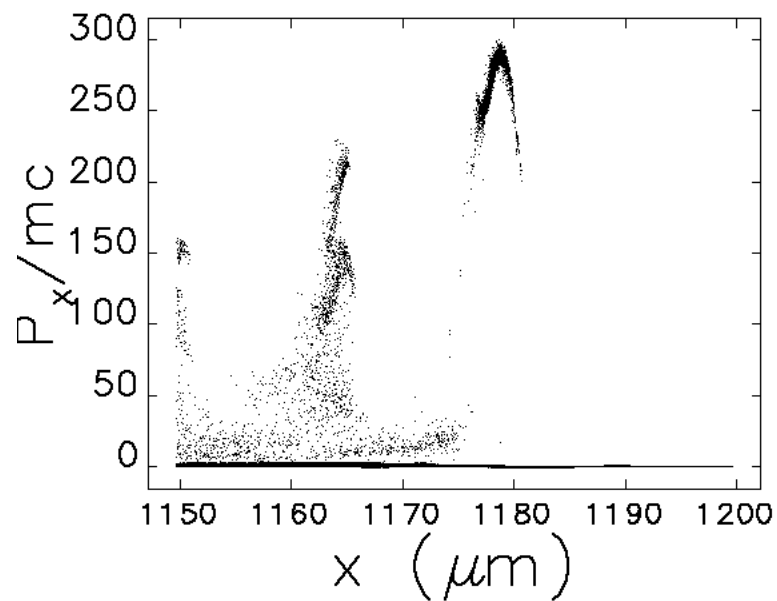
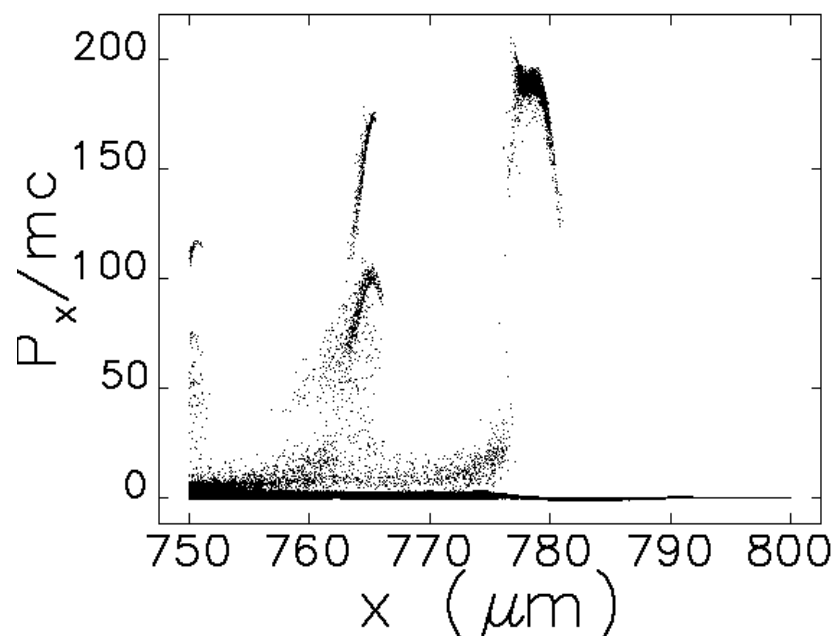
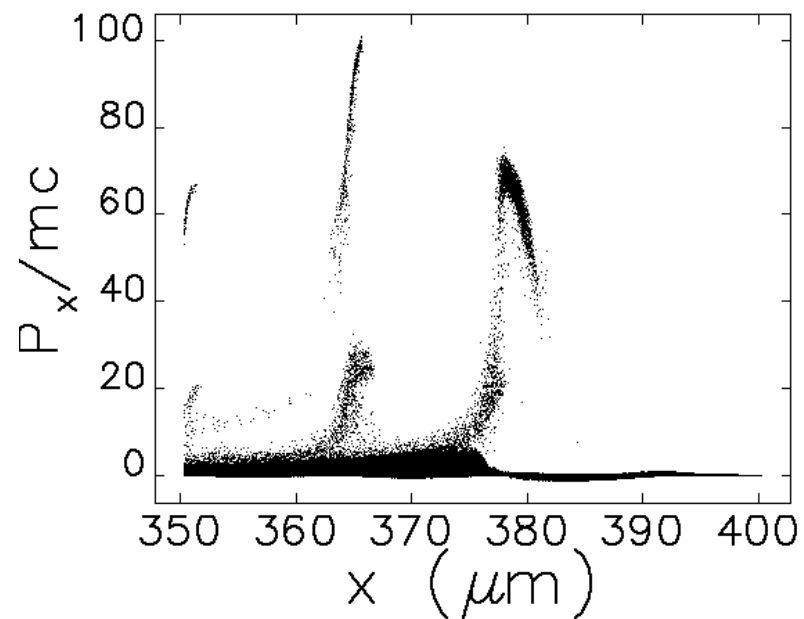
# Wave breaking triggered by a nano wire



**Position  $z = 6.35\ \mu\text{m}$  Charge 370 pC**







# Ion acceleration by laser

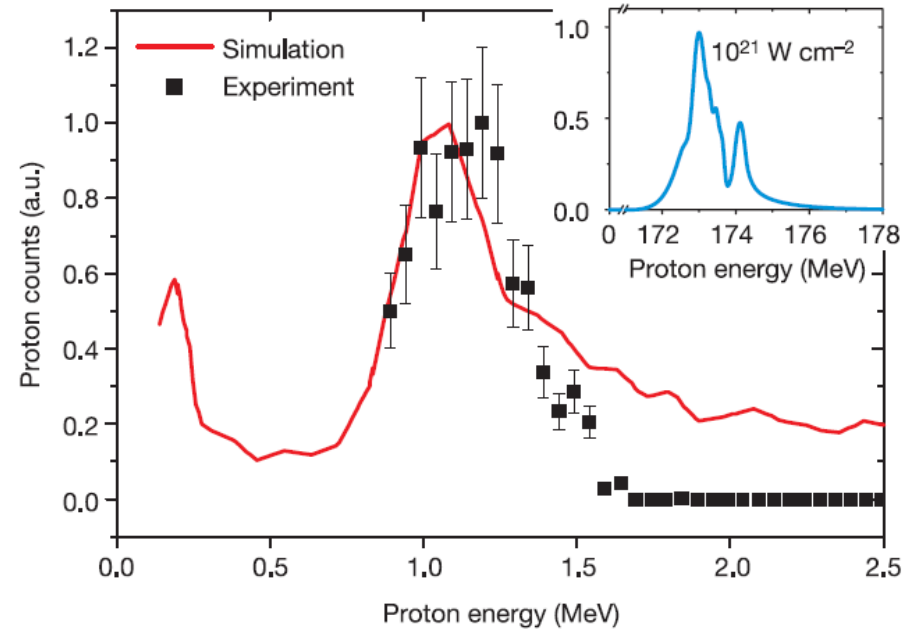
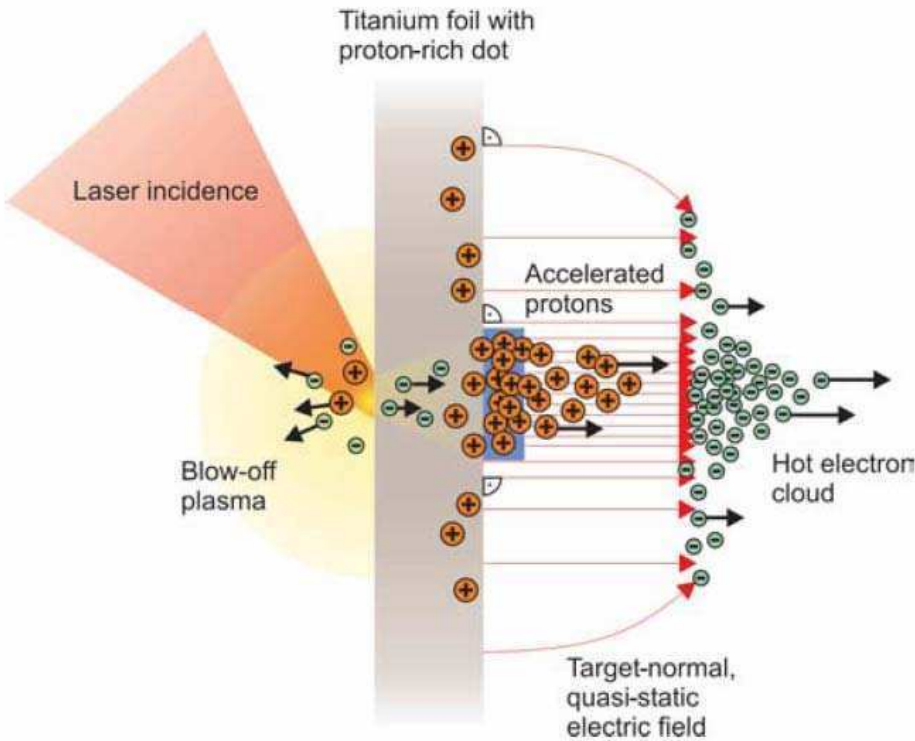


**Figure 4 | Results from simulations and scalability of the technique.**

Comparison of experimental data (black squares) to the proton spectrum obtained from two-dimensional-PIC simulation (red line) for following conditions: laser intensity  $I_L = 3 \times 10^{19} \text{ W cm}^{-2}$ , and target dimensions  $5 \mu\text{m Ti foil} + 0.5 \mu\text{m PMMA dot } (20 \times 20) \mu\text{m}^2$ . Experimental data points comprise the observable energy range on the MCP detector. The statistical uncertainty for the measured data has a value of 20% s.d. as shown by the error bars. In the inset a simulation for a petawatt-laser system demonstrating the scalability of proton acceleration from microstructured targets is shown. The parameters for the simulation are  $I_L = 1.2 \times 10^{21} \text{ W cm}^{-2}$ ,  $5 \mu\text{m Ti foil} + 0.1 \mu\text{m PMMA dot } (2.5 \mu\text{m diameter})$ . The proton spectrum exhibits a narrow peak with relative energy width of  $\Delta E/E \approx 1\%$  at a peak energy of 173 MeV.

H. Schworer, Nature 439,  
445(2006)

# Ion acceleration by laser

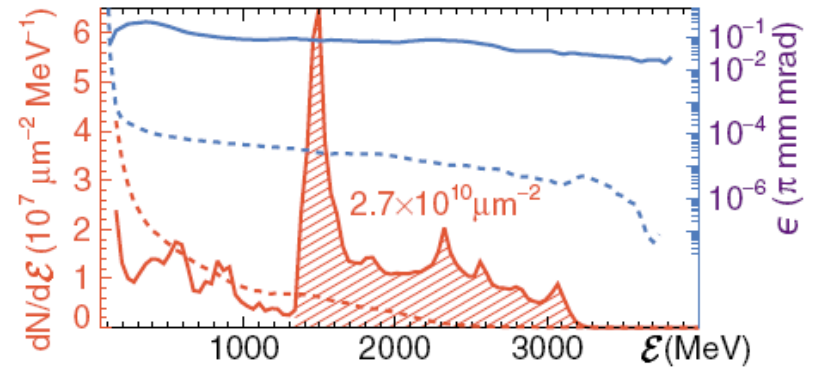
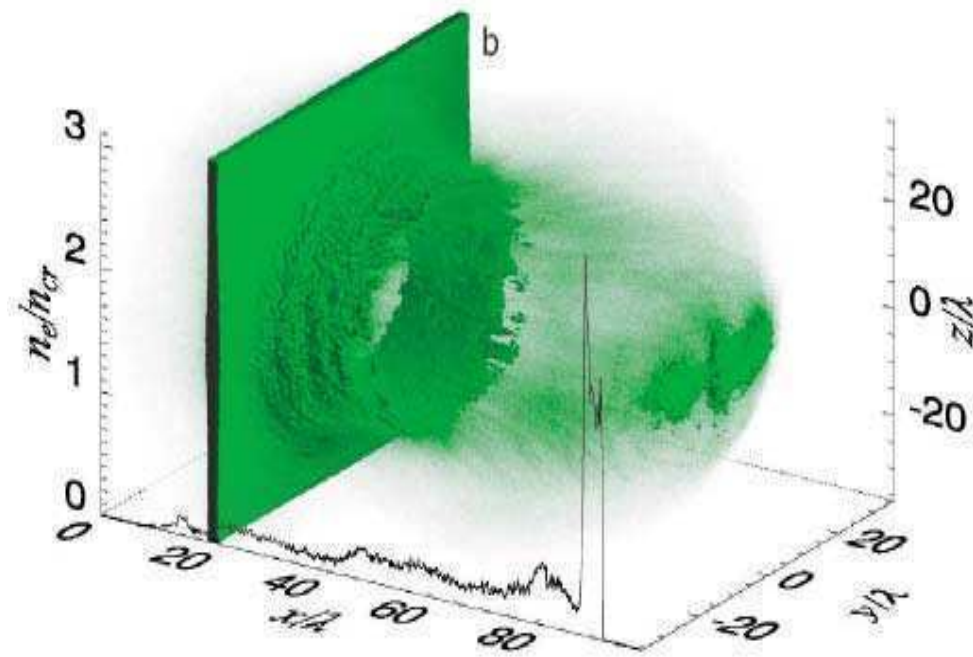
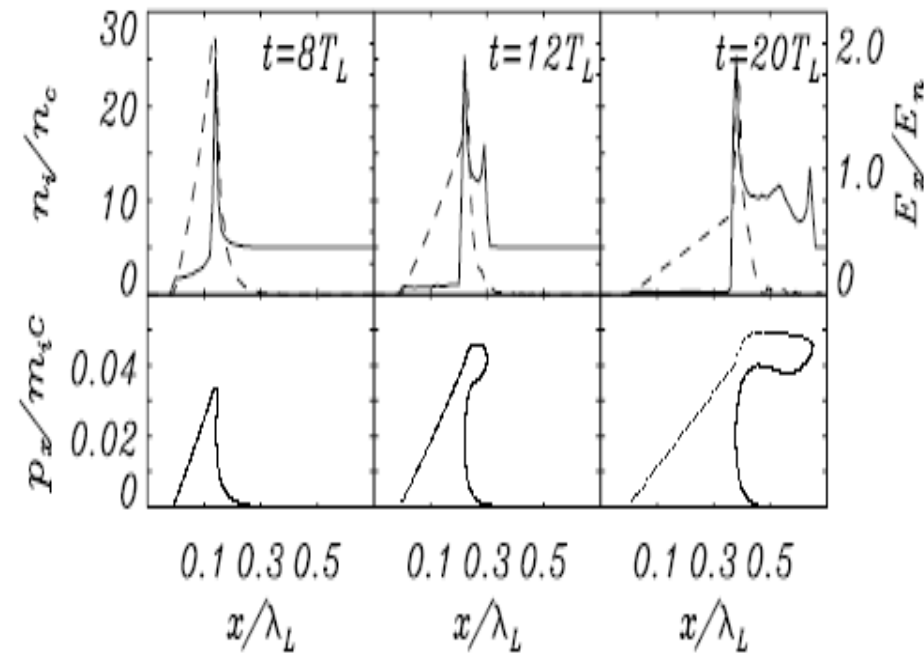
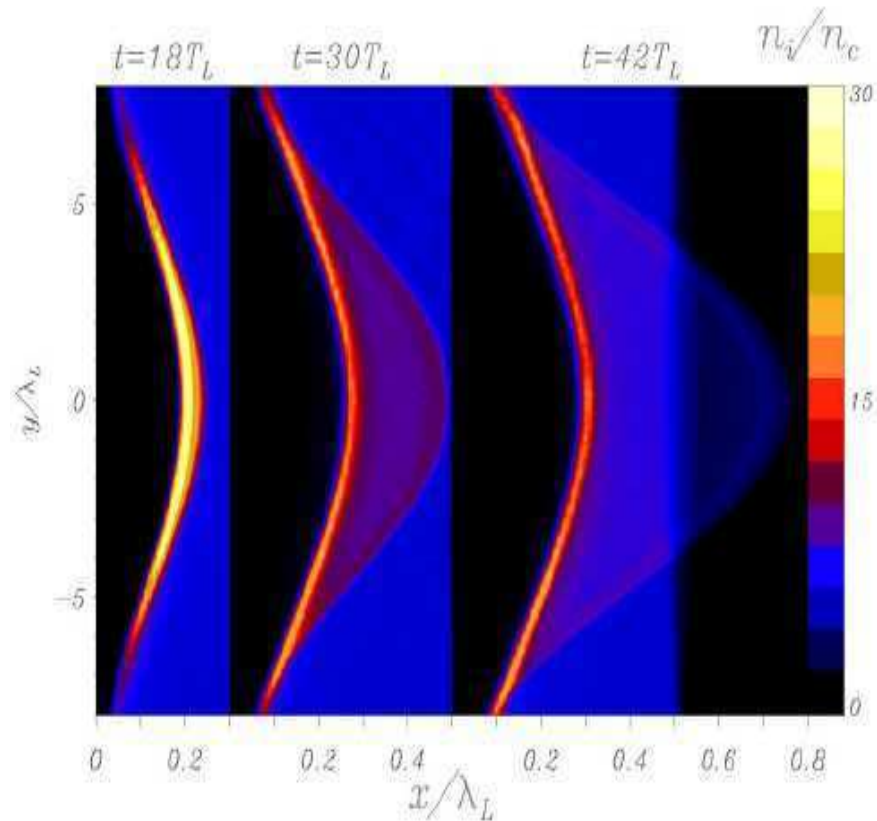


FIG. 3 (color). The energy spectrum (red) and transverse emittance (blue) of ions (solid) and electrons (dashed) located in the box  $50\lambda < x < 80\lambda$ ,  $-\lambda < y$ ,  $z < \lambda$  at  $t = 80 \times 2\pi/\omega$ . The hatched region contains  $2.7 \times 10^{10} \mu\text{m}^{-2}$  particles per cross section. Values correspond to  $\lambda = 1 \mu\text{m}$ .

$$I = 1.37 \times 10^{23} \text{ W/cm}^2$$

T. Esirkepov et al., PRL 92, 175003(2004)

# Ion acceleration by laser



Andrea Macchi, PRL 94, 165003(2005)

$$\frac{v_a}{c} = \sqrt{\frac{Z}{A} \frac{m_e}{m_p} \frac{n_c}{n_e} a_L}$$



# *High Gradient Dielectric Wakefield Structures*

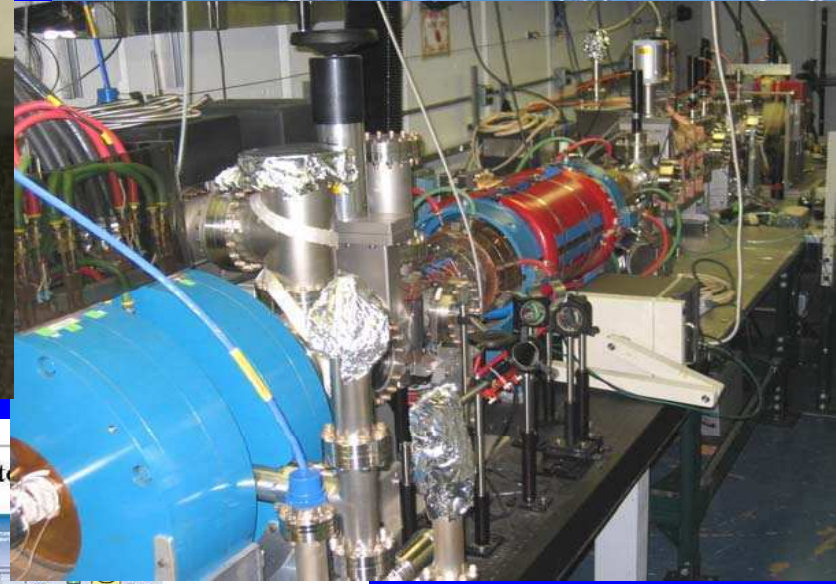
*John G. Power*

*For the Advanced Accelerator R&D Group  
HEP Division  
Argonne National Laboratory*

*Nov 28<sup>th</sup>, 2006*

*Advanced Accelerator R&D at the ILCTA, Fermilab*





# Research Focus

## 1. Advanced Accelerating Structures

### 1. **Dielectric Loaded Accelerating (DLA) Structures**

- *Beam-Driven DLA Structures*
  - **Using the Argonne Wakefield Accelerator Facility**
- *RF-Driven DLA Structures*
  - Collaboration between Argonne, NRL, & SLAC

### 2. **Novel structure investigation** → photonic band gap, left-handed meta-materials.

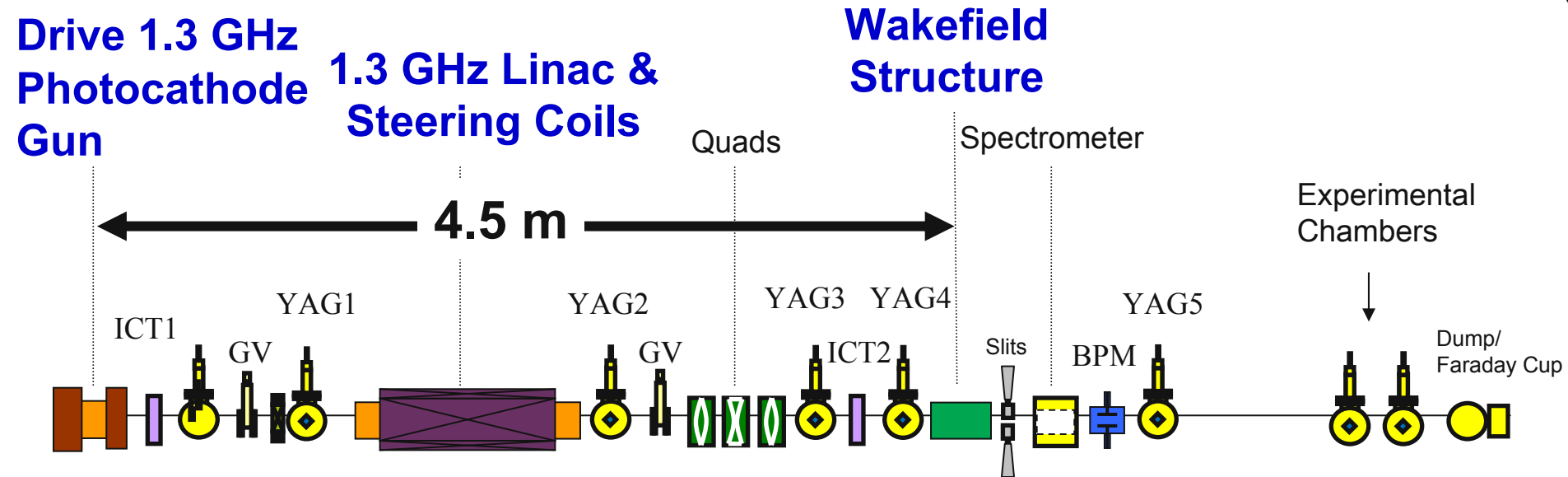
## 2. High-Power/High-Brightness Electron Beams

1. **Fundamental Beam Physics** → beam generation, propagation, & characterization.
2. **High-current beam production** → for beam-driven wakefield acceleration & RF generation schemes.
3. **Beam dynamics in wakefield structures** → BBU control

## 3. Support of existing HEP programs

1. **Positron source for ILC**
2. **Lab Astrophysics**
3. **Providing facilities for external user's research program.**

# AWA Drive Beamline

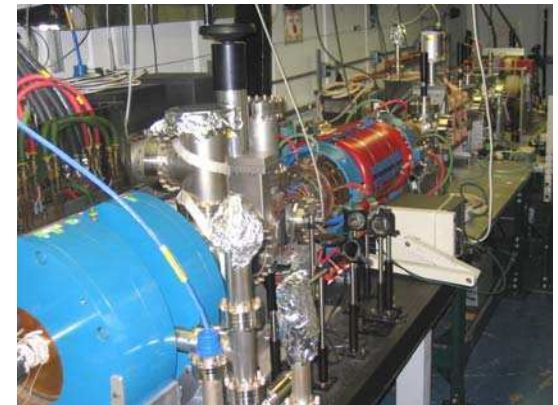


## Single bunch operation

- $Q = 1-100 \text{ nC}$
- Energy = 14 MeV
- High Current = 10 kAmp

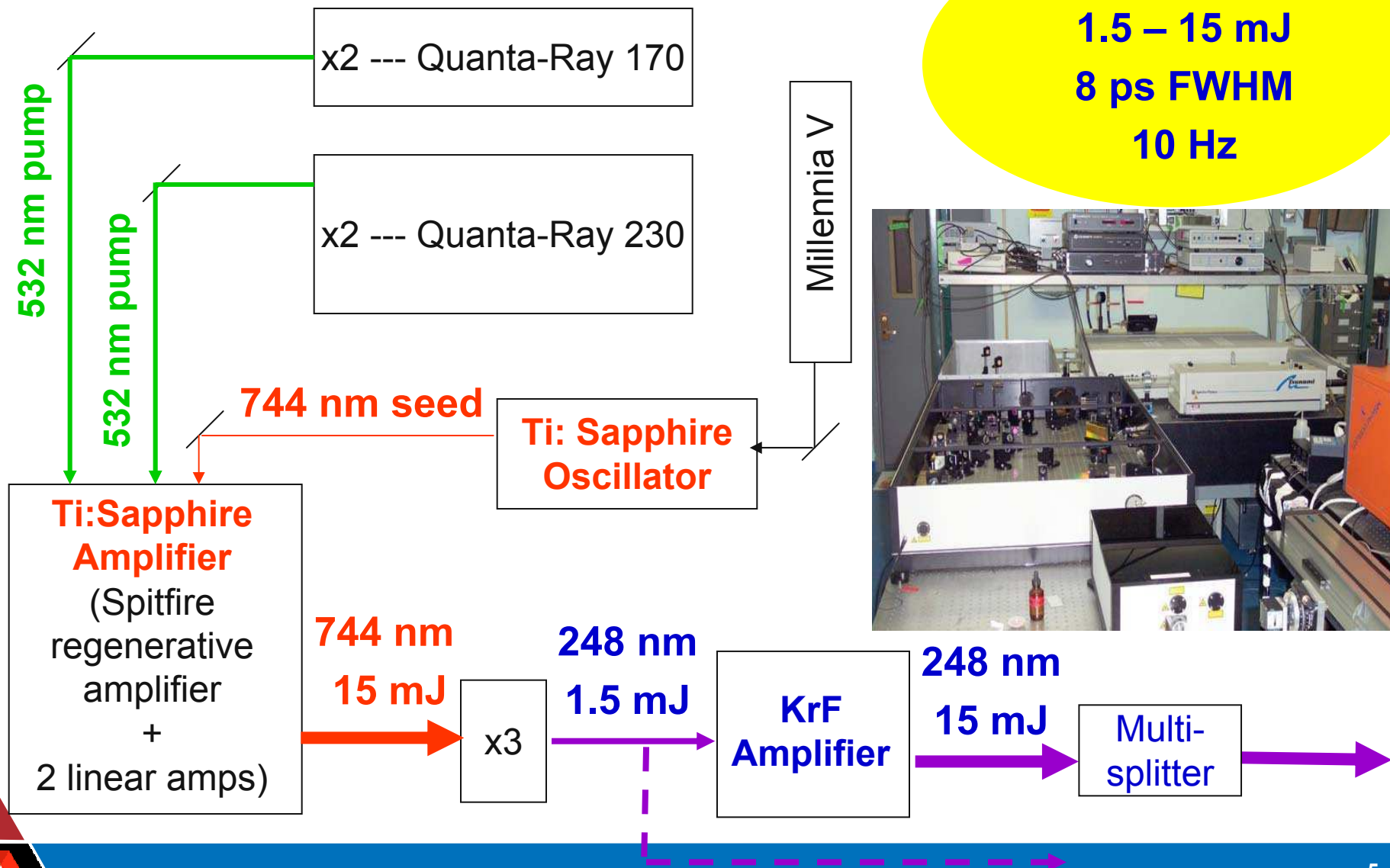
## Bunch train operation

- 4 bunches  $\times 10 \text{ nC}$
- 64 bunches  $\times 50 \text{ nC} \rightarrow 50 \text{ ns}$  long (future)





# AWA Photocathode Laser System



# *Beam-Driven DLA Structures at the Argonne Wakefield Accelerator (AWA) Facility*



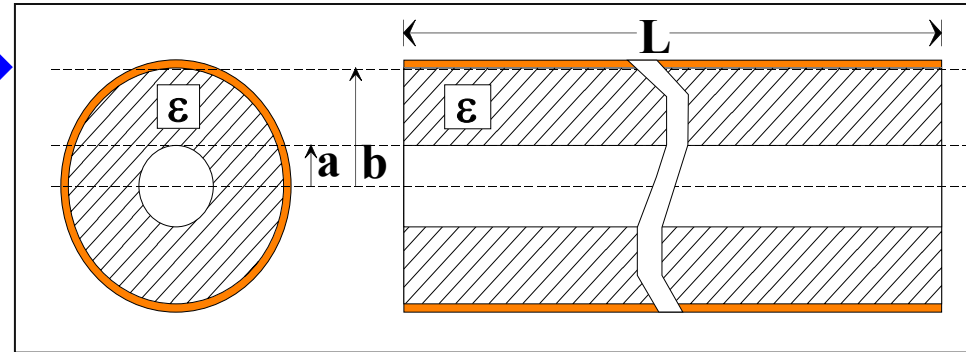
# Dielectric-Loaded Accelerator (DLA) Structures

## (1) Why use dielectrics??

### Slow wave accelerator →

- Dielectric (instead of irises) is used to reduce  $v_{ph}$  to  $c$ .

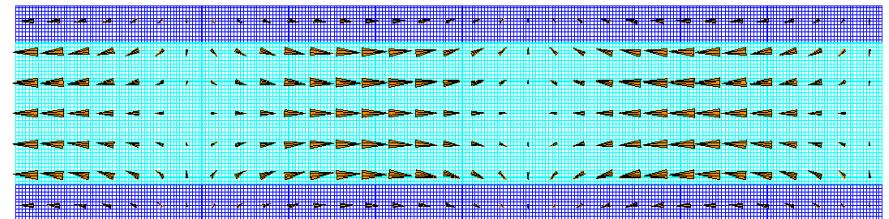
Geometry



### Advantages of DLA →

- Simple geometry
- No field enhancements on irises
- High gradient potential
- Comparable shunt impedance
- Easy to damp HOM

Electric Field Vectors



### Open Questions →

- Breakdown?
- Joule Heating?
- Multipactor?

# Beam-Driven DLA Structures (aka Wakefield Acceleration)

## (2) Why e-Beam Driven?

- GW's of Power transferred by the electron beam.
- Short pulse operation can increase the breakdown threshold.
- More material options:
  - Low and high Q structures produce the same wakefield.

### ➤ Applications

- *Collinear wakefield acceleration schemes*

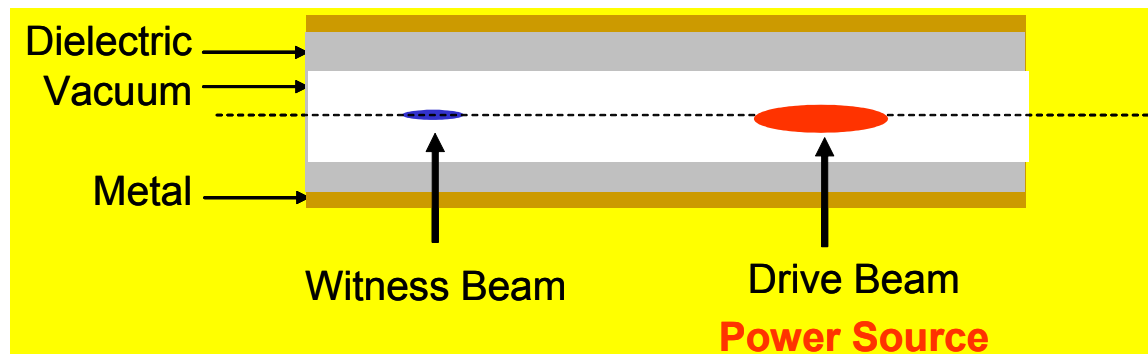
*1. Single Mode*

*2. Multimode*

*3. Enhanced Transformer Ratio*

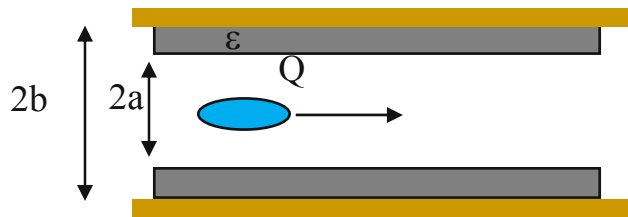
- *Two-beam acceleration*

*1. Dielectric TBA*





# Wakefield Scaling in DLA Structures (a short Gaussian beam)



High Charge  
(photocathode)

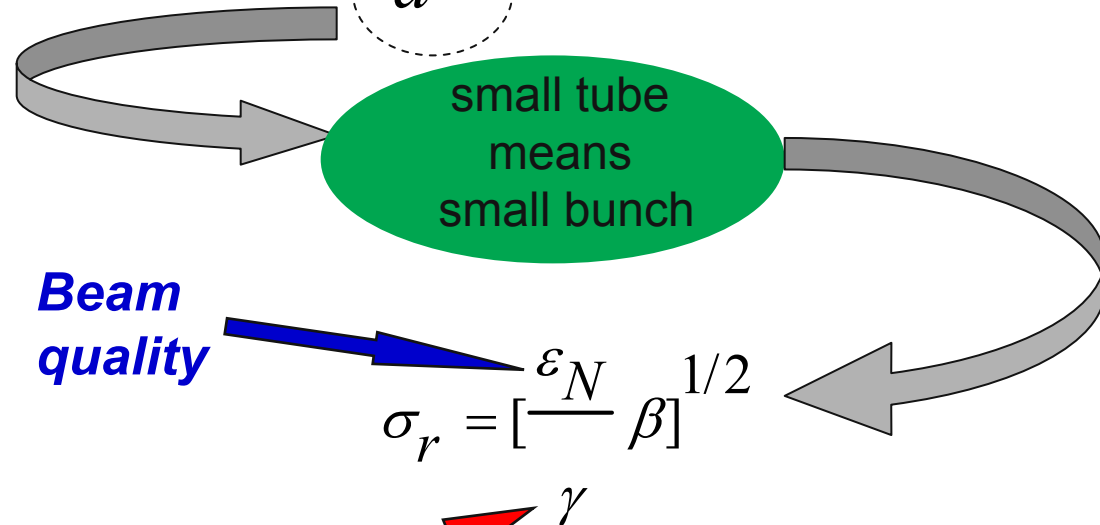
Short Bunch  
(killer!)

Key to Large  $W_z$

DRIVE BEAM

- Charge  $\uparrow$
- Bunch length  $\downarrow$
- Emittance  $\downarrow$
- Energy  $\uparrow$

$$W_z \approx \frac{Q}{a^2} \cos(k_n z) e^{-2 \left( \frac{\pi \sigma_z}{\lambda_n} \right)^2}$$



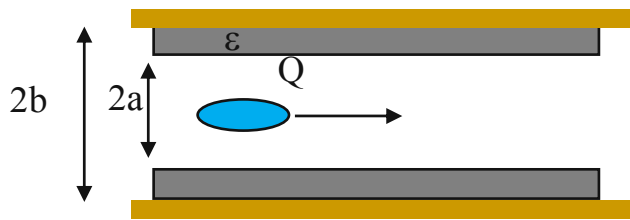
Beam  
quality

$$\sigma_r = \left[ \frac{\epsilon_N}{\beta} \right]^{1/2}$$

Beam energy (= \$\$)

$\gamma$

# Wakefield Scaling in DLA Structures (a short Gaussian beam)



$$W_z \approx \frac{Q}{a^2} \cos(k_n z) e^{-2 \left( \frac{\pi \sigma_z}{\lambda_n} \right)^2}$$

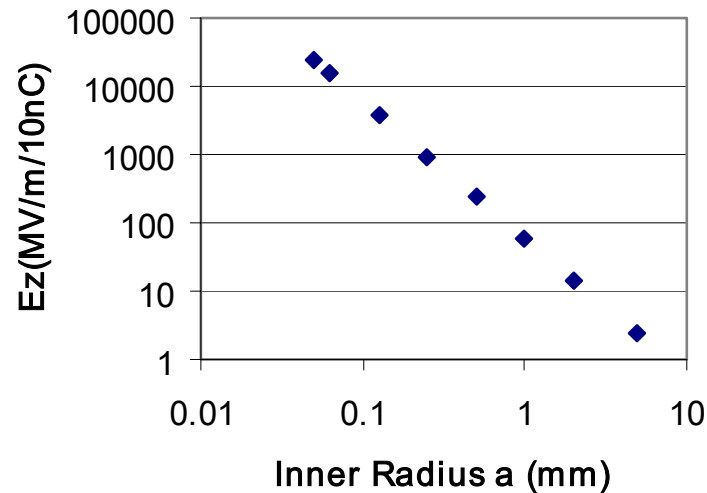
**Key to Large  $W_z$**



**DRIVE BEAM**

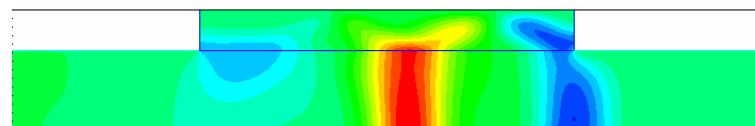
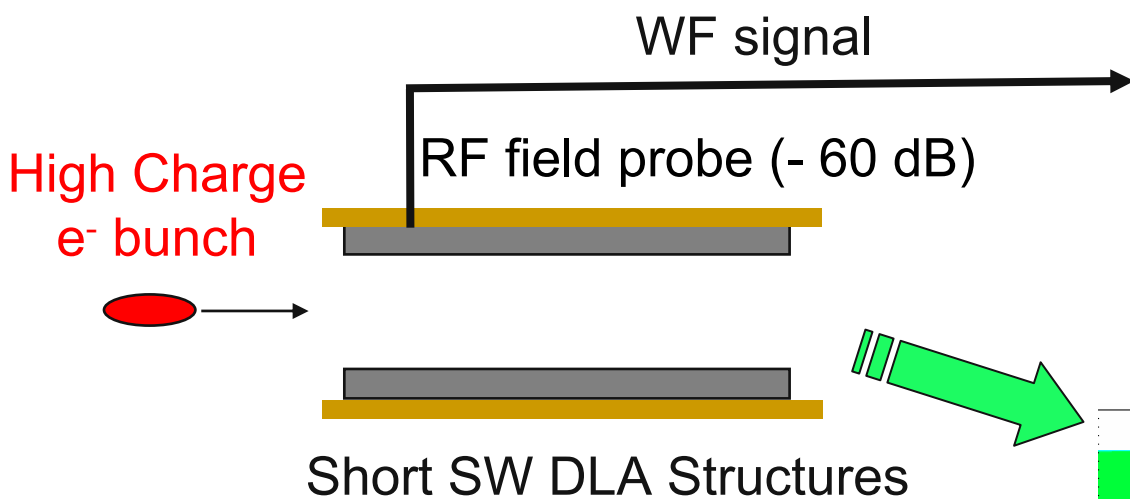
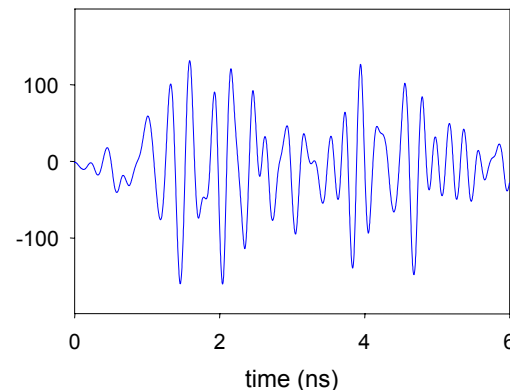
- Charge  $\uparrow$
- Bunch length  $\downarrow$
- Emittance  $\downarrow$
- Energy  $\uparrow$

Wakefield Amplitude Dependence on Inner Radius



# Beam-Driven DLA Structures Tests

Monitor for breakdown



Infer Gradients from MAFIA

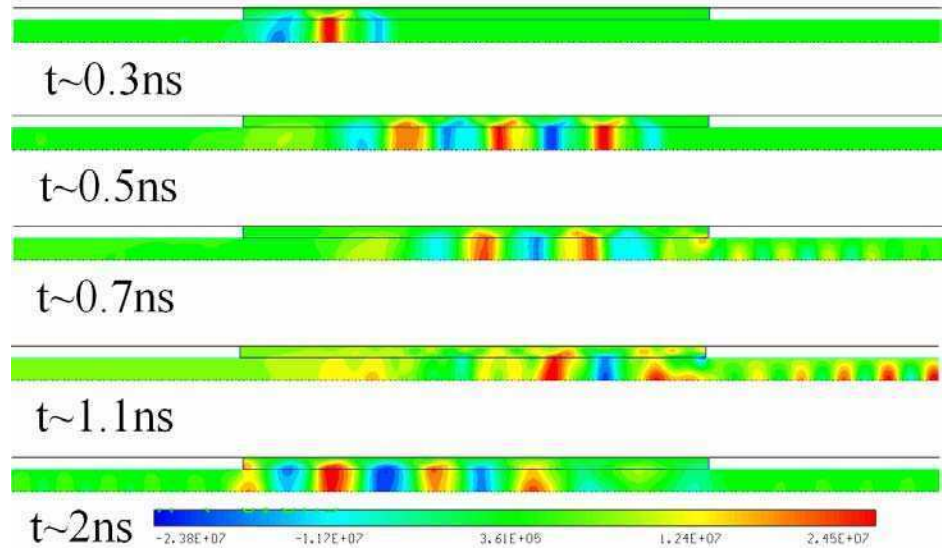
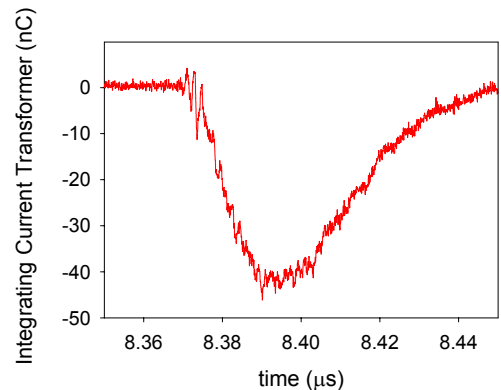
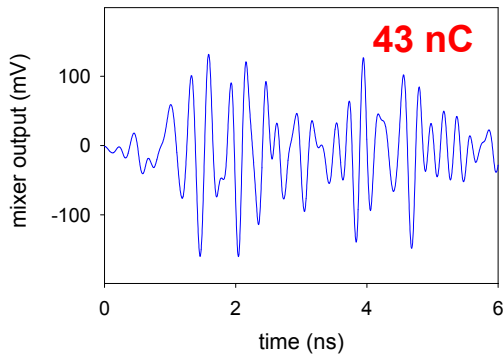
| Structure Parameters             | <i>Structure 1</i> | <i>Structure 2</i> | <i>Structure 3</i> |
|----------------------------------|--------------------|--------------------|--------------------|
| Material                         | Cordierite         | Cordierite         | Cordierite         |
| Dielectric constant              | 4.76               | 4.76               | 4.76               |
| Freq. of TM <sub>01n</sub> modes | ~14 GHz            | ~14 GHz            | ~10 GHz            |
| Inner radius                     | 5 mm               | 5 mm               | 2.75 mm            |
| Outer radius                     | 7.5 mm             | 7.5 mm             | 7.5 mm             |
| Length                           | 102 mm             | 23 mm              | 28 mm              |
| Wakefield Gradient               | 0.5 MV/m/nC        | 0.5 MV/m/nC        | 1 MV/m/nC          |

# Structure 1 (Summer 2005)

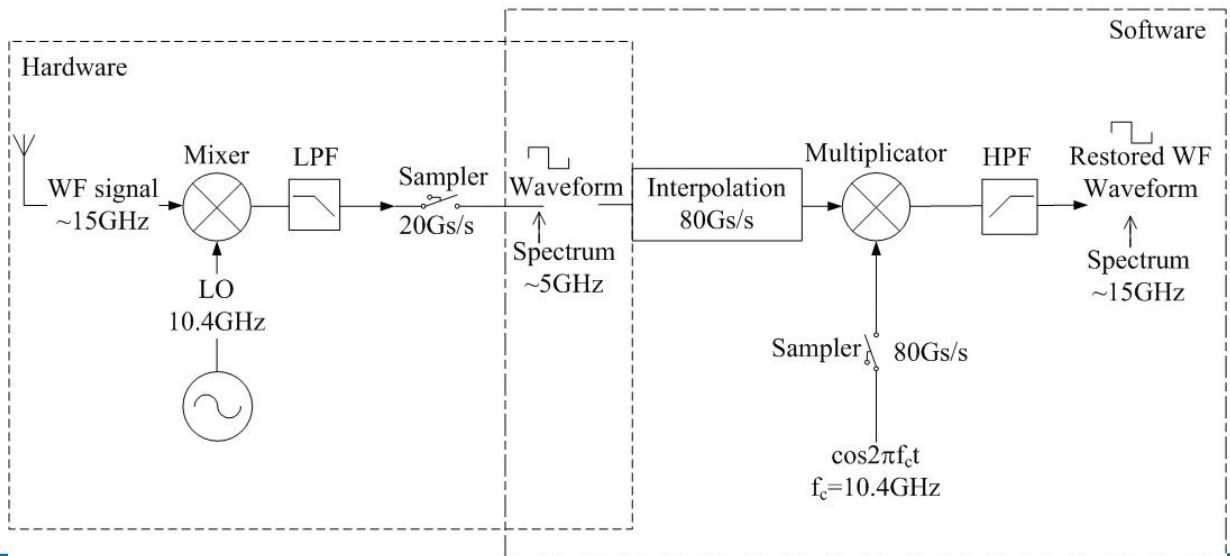
→ long 14GHz structure

23 MV/m gradient.

No signs of breakdown. 😊



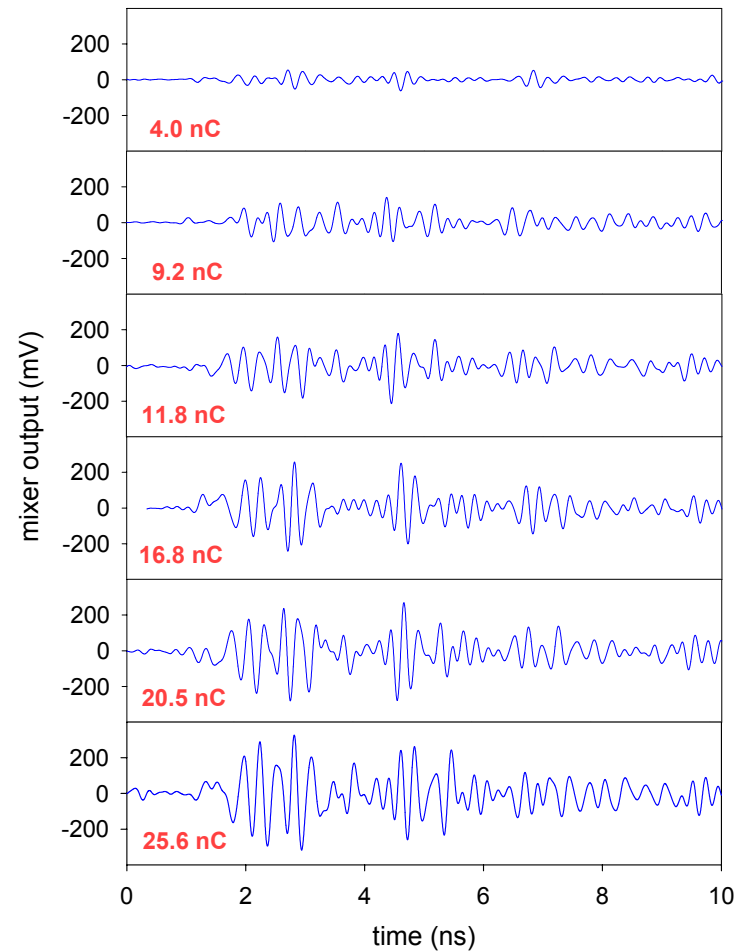
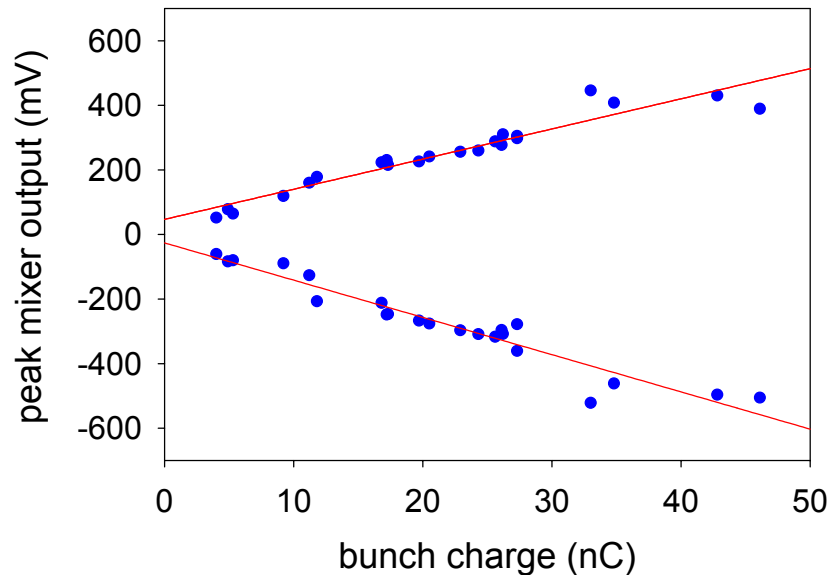
Direct Wakefield Measurement



# Structure 1 (Summer 2005)

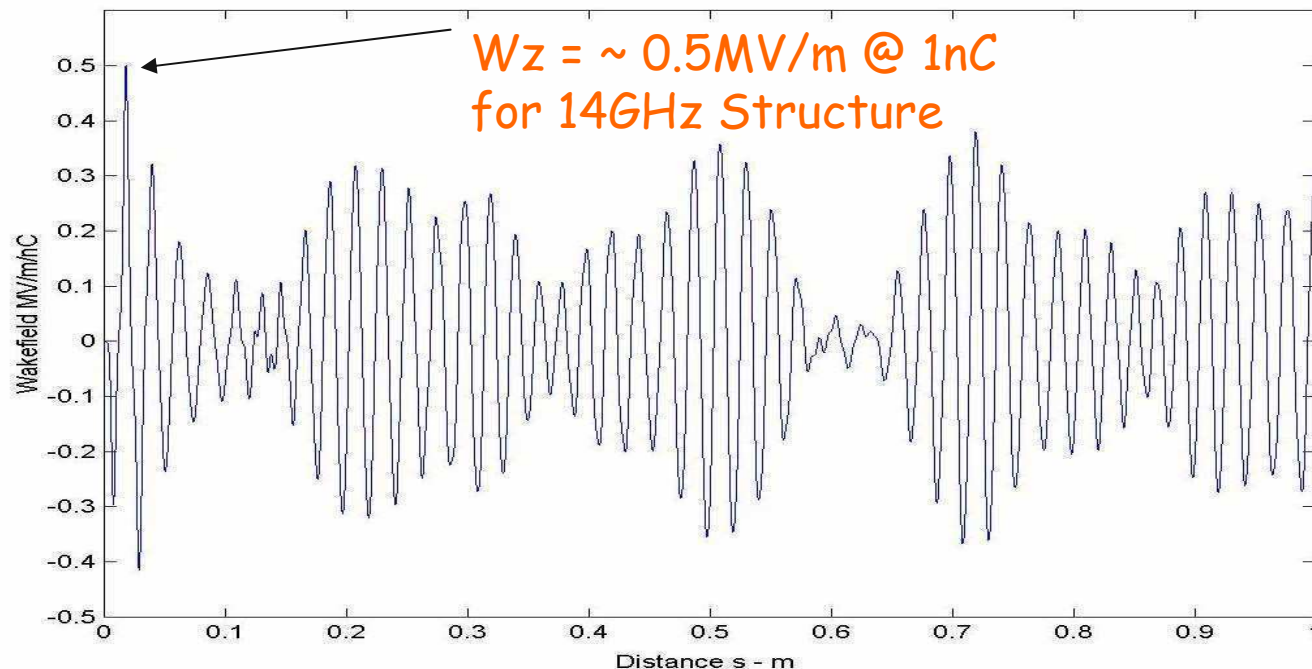
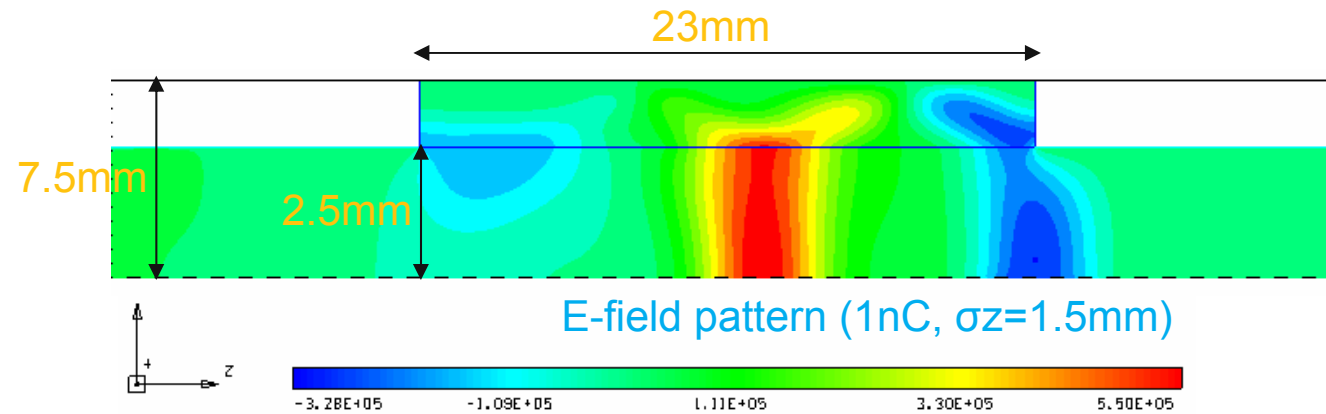
→ long 14GHz structure

## Wakefield Amplitude Charge Scaling



## Structure 2 (Winter 2005-06)

→ MAFIA simulation of wakefield of the short 14GHz structure

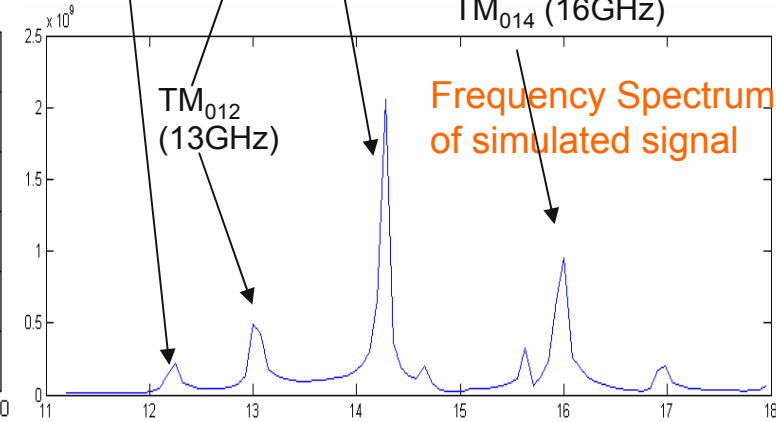
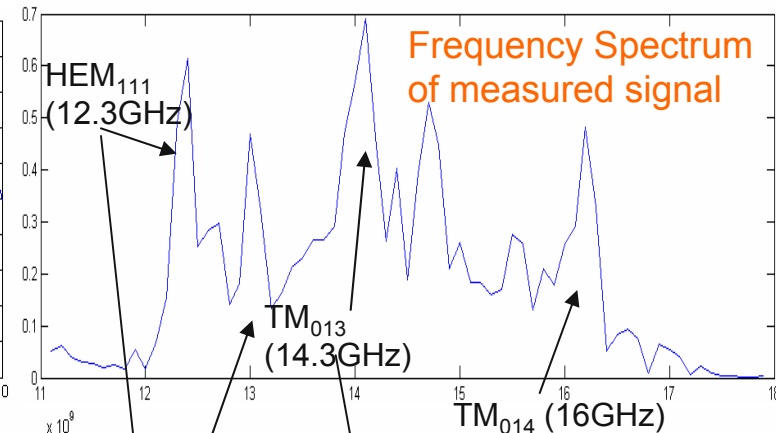
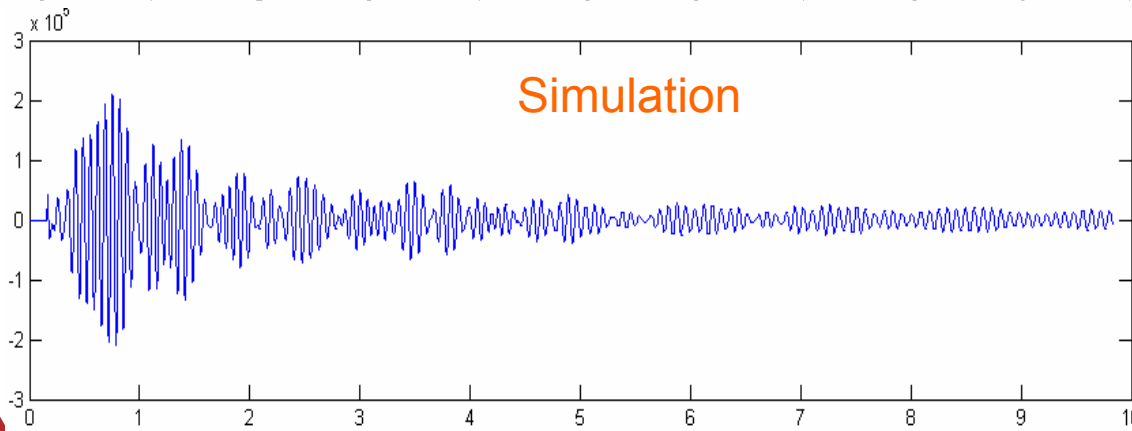
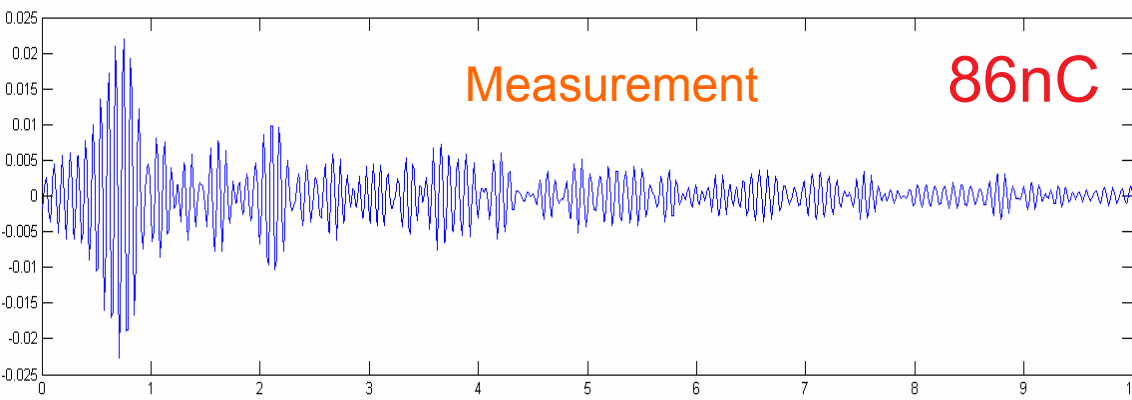


## Structure 2 (Winter 2005-06)

→ Measured and simulated Er probe signals

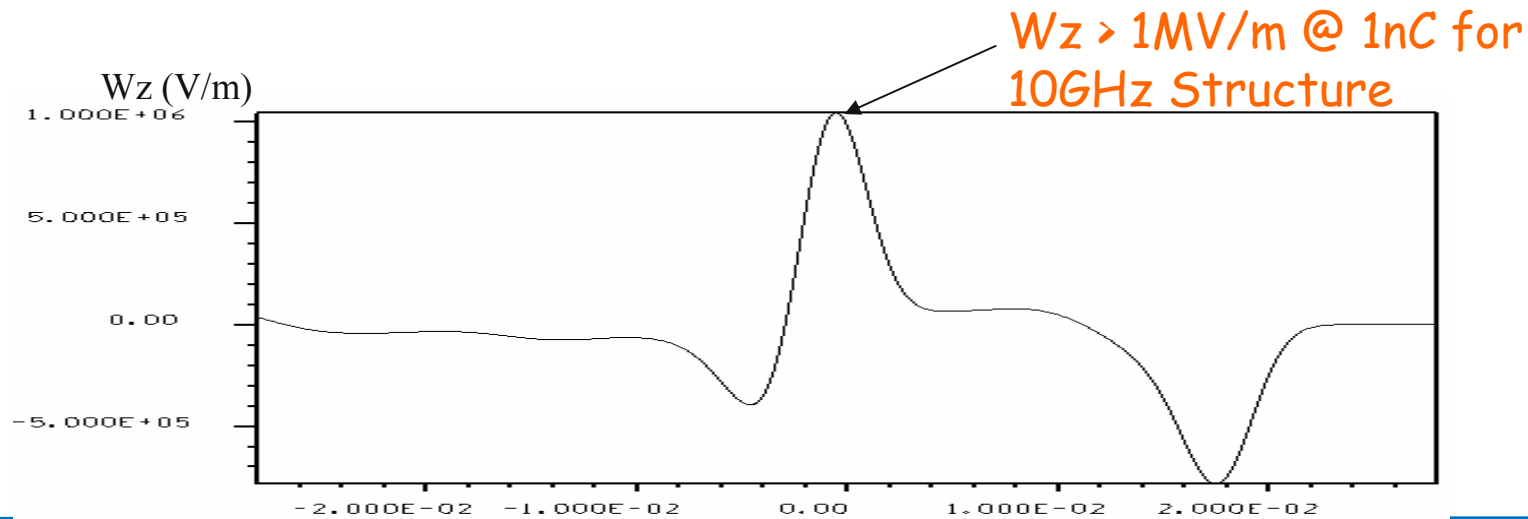
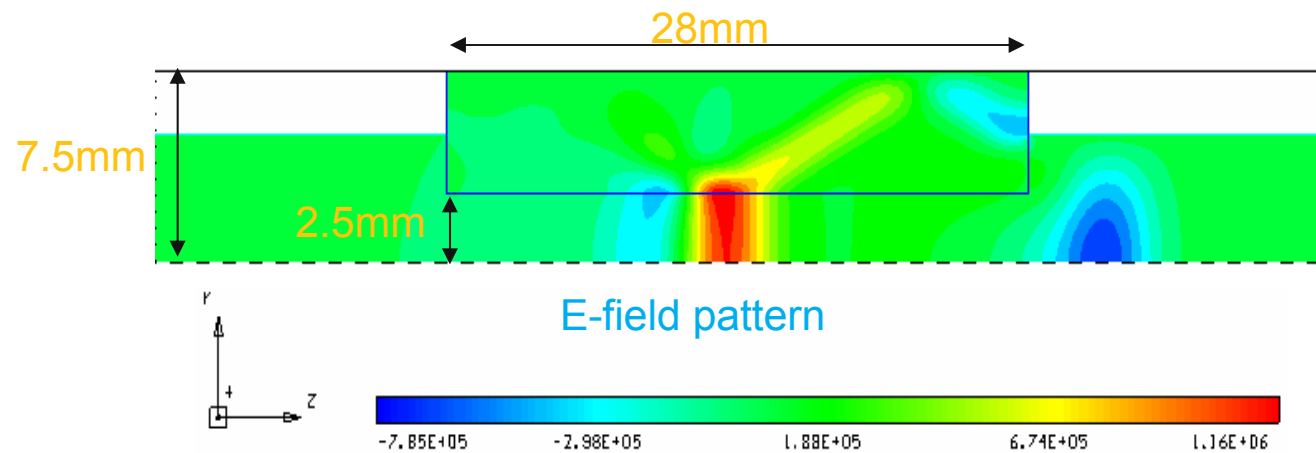
43 MV/m gradient.

No signs of breakdown. 😊



# Structure 3 (Summer 2006)

→ MAFIA simulation of wakefield of the short 10GHz structure

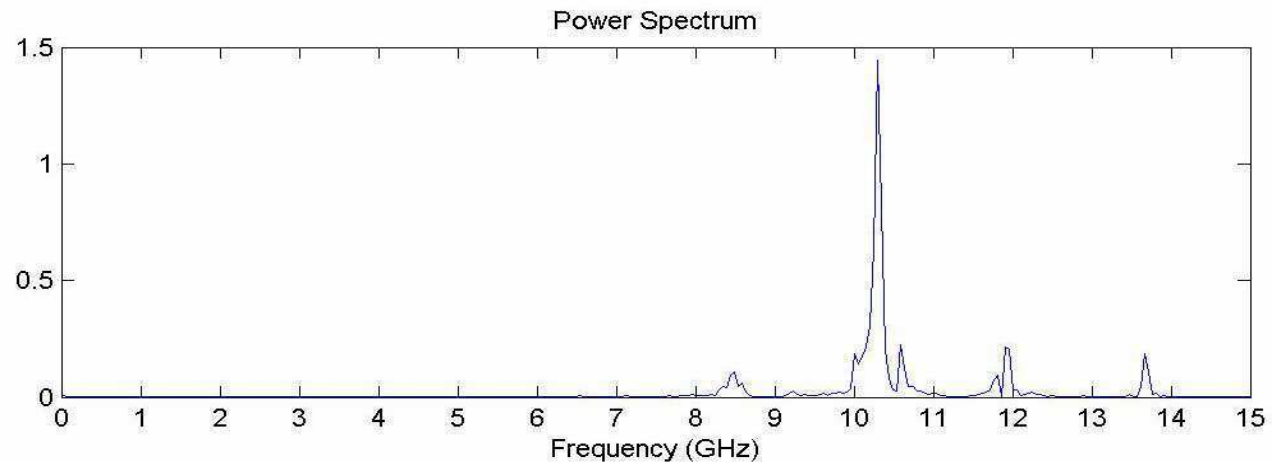
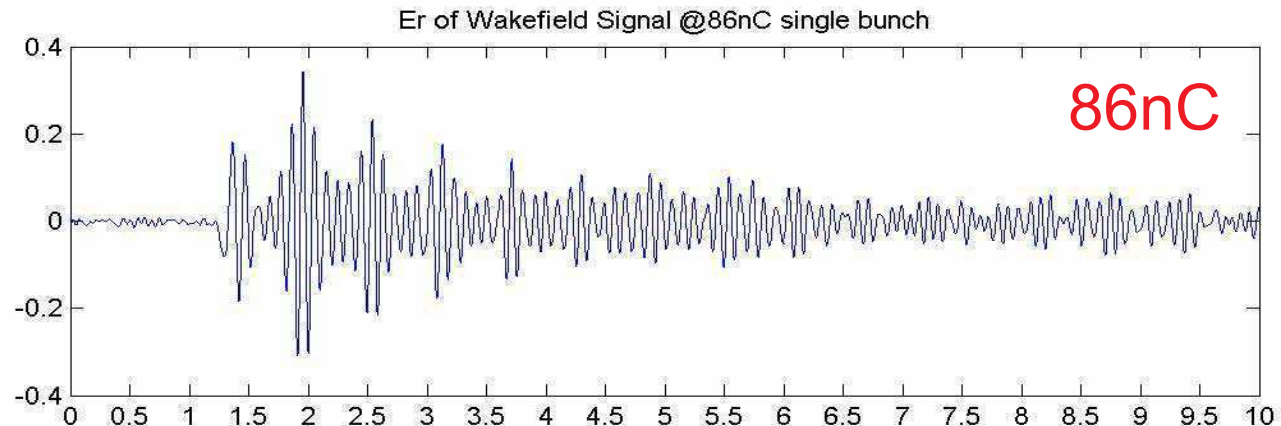




## Structure 3 (Summer 2006)

→ Measured wakefield signal ( $E_r$ ) of the 10GHz short structure  
86 MV/m gradient.

No signs of breakdown. 😊

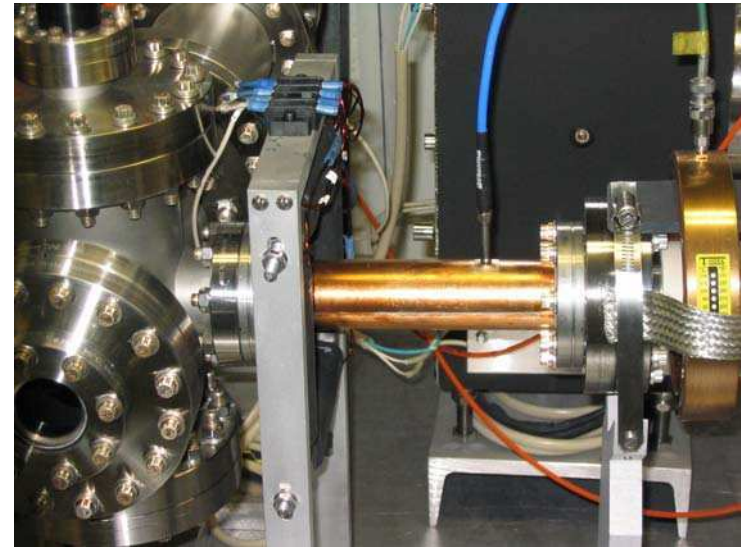


## Short SW DLA Test Summary

- Structure 1 (Summer 2005) 23 MV/m
- Structure 2 (Winter 05/06): 43 MV/m
- Structure 3 (Summer 2006) 86 MV/m

### Next Structure (Near Term Future)

| Structure Parameters             | <i>Structure 4</i> |
|----------------------------------|--------------------|
| Material                         | Cordierite/Quartz  |
| Dielectric constant              | 4.76               |
| Freq. of TM <sub>01n</sub> modes | ~10 GHz            |
| Inner radius                     | 1.9 mm             |
| Outer radius                     | 7.5 mm             |
| Length                           | 102 mm             |
| Wakefield Gradient               | 1.5 MV/m/nC        |



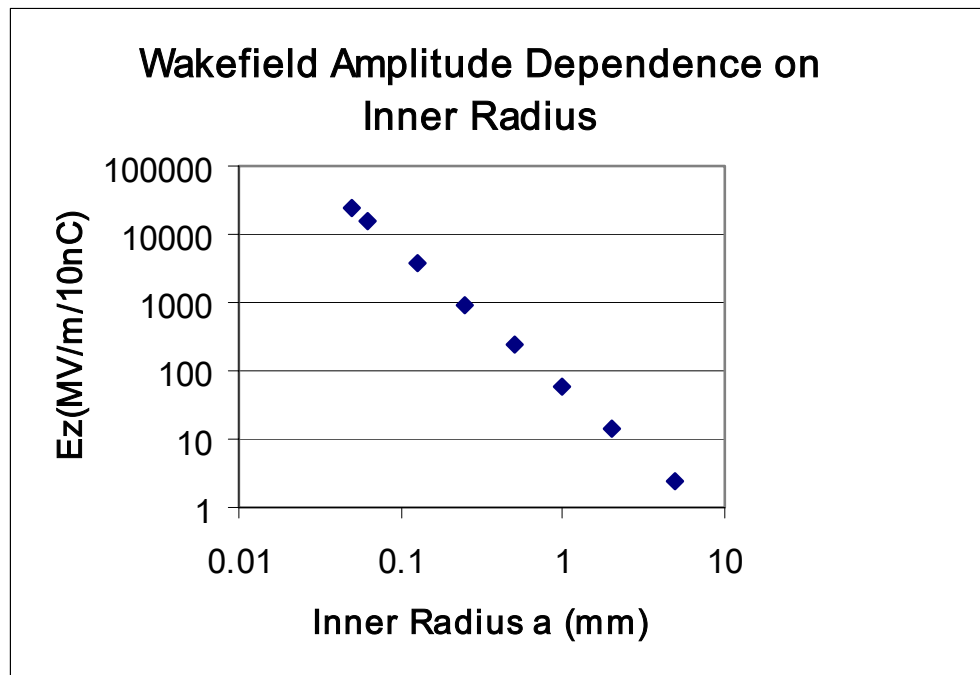
Final assembly in beamline

# *ILCTA dielectric wakefield applications*

## ■ Motivation

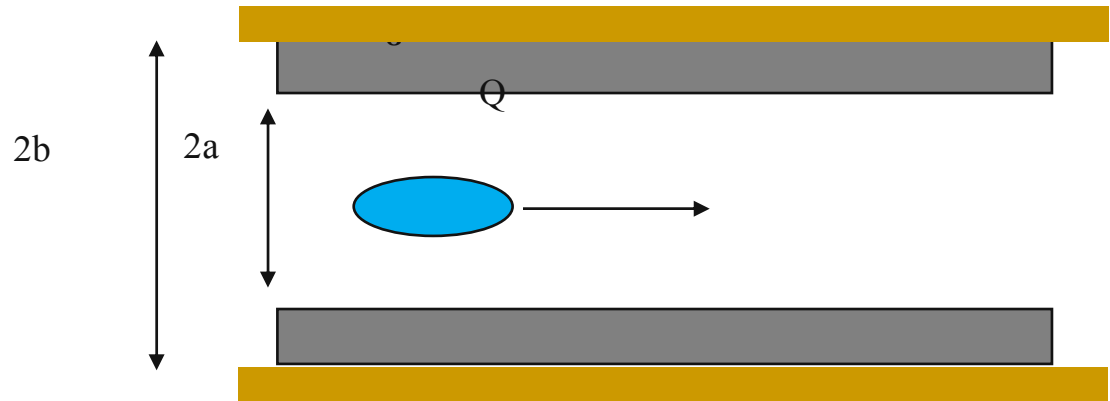
## ■ ILCTA beam parameters → High Gradient

$$W_z \approx \frac{Q}{a^2} \cos(k_n z) e^{-2 \left( \frac{\pi \sigma_z}{\lambda_n} \right)^2}$$



# *ILCTA dielectric wakefield applications*

## ■ Cylindrical dielectric structure



## ■ ILCTA round beam (3.2 nC) parameters

$\sigma_x = 30 \text{ } \mu\text{m}$ ;  
 $\sigma_y = 30 \text{ } \mu\text{m}$ ;  
 $\sigma_z = 400 \text{ } \mu\text{m}$

## Dielectric Structure

$\text{MgTiO}_3$  ;  $\epsilon = 16$

$a = 100 \text{ } \mu\text{m}$ ;  $b = 430 \text{ } \mu\text{m}$ ;

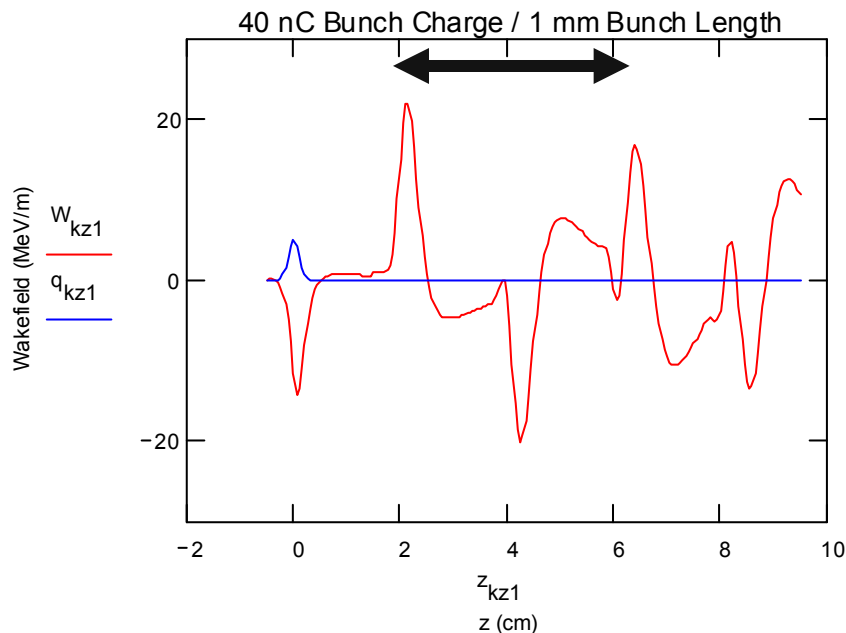
$f = 75 \text{ GHz}$

**Wakefield  $\rightarrow 150 \text{ MV/m}$**

# *ILCTA dielectric wakefield applications*

- Numerical Example
- Use laser beam techniques to generate a closely spaced **witness beam**

75 GHz  $\rightarrow$  13 psec



Measured Energy Change

$L=10$  cm  $\rightarrow$  15 MeV

**$L=1$  m  $\rightarrow$  150 MeV**

However

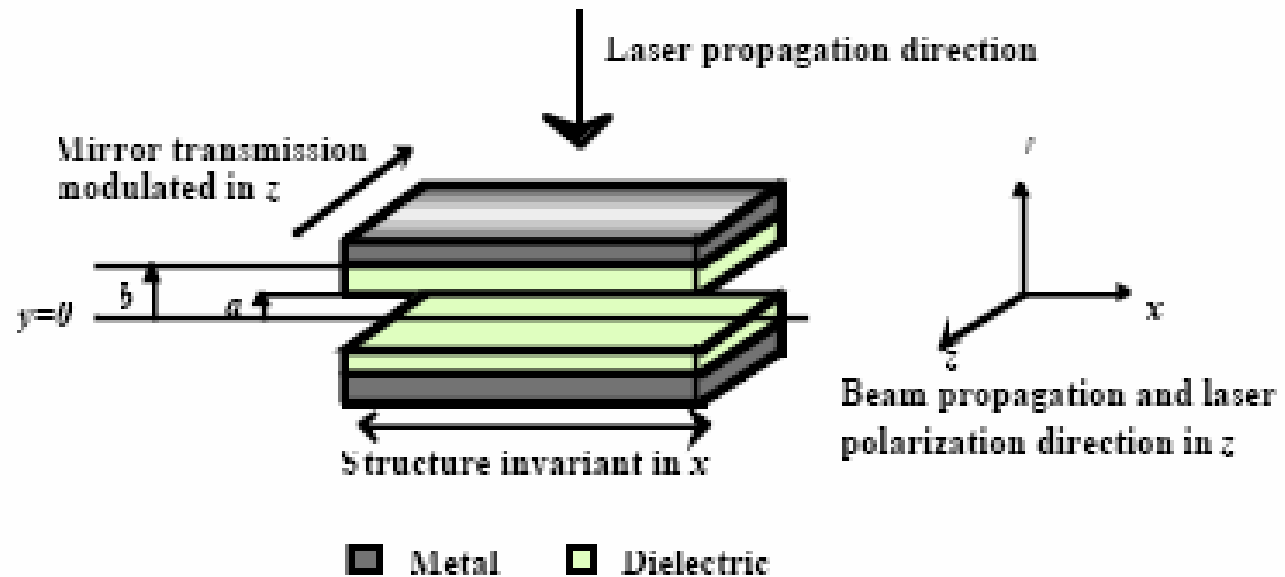
$\rightarrow Wz \sim Q/\sigma Z^2$

Using 72 fsec

$\rightarrow Wz \rightarrow$  GeV/m

# *ILCTA dielectric wakefield applications*

## ■ Planar dielectric structure

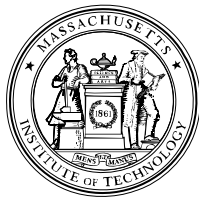


## ■ ILCTA flat beam (3.2 nC) parameters

$\sigma_x = 10 \text{ } \mu\text{m}$ ;  
 $\sigma_y = 100 \text{ } \mu\text{m}$ ;  
 $\sigma_z = 400 \text{ } \mu\text{m}$

**Transverse Wakes →**  
**→ vanish/diminish**  
**→ less BBU**

**High Gradient →  $a = 30 \text{ } \mu\text{m}$**

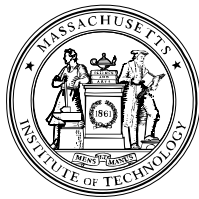


# **Photonic Band Gap Higher Order Mode Coupler for ILC\***

**Jing Zhou**

**Presented at Fermilab  
Nov. 28, 2006**

**\*Supported by DOE Grant No. DE-FG02-95-ER40919**



# Outline



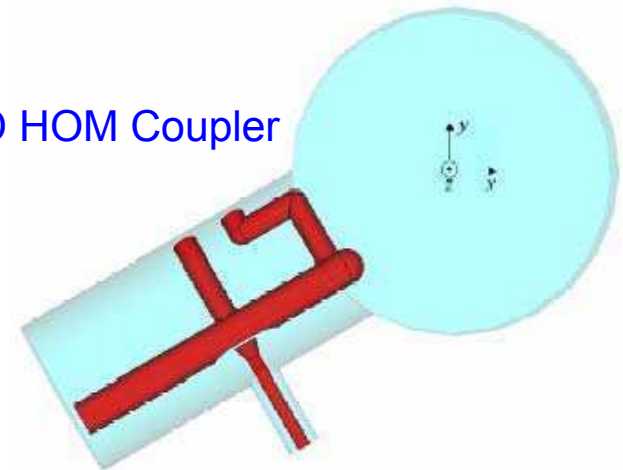
- **Why PBG HOM Coupler**
- **Results of Feasibility Studies**
  - Effects on Operating Mode
  - Effectiveness of PBG HOM Damping
- **Summary and Plans**



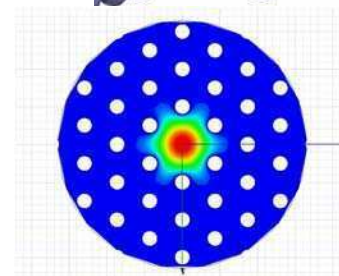
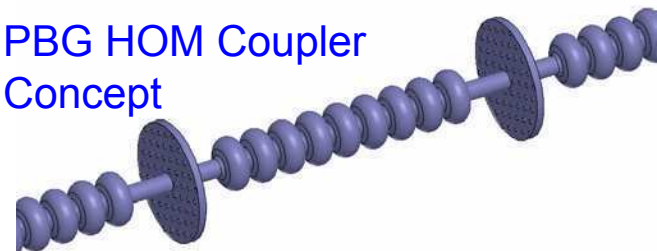
# Motivation

- **Problems with BCD HOM coupler (ILC Report 7-13-06)**
  - Mode asymmetry
  - Insufficient dipole damping
  - Limited knowledge about non-dipole HOM damping
  - High cost
- **PBG HOM coupler solutions**
  - High degree of azimuthal symmetry
  - Allow all unwanted modes to leak out of the structure
  - Potentially much simpler to build, and could reduce costs

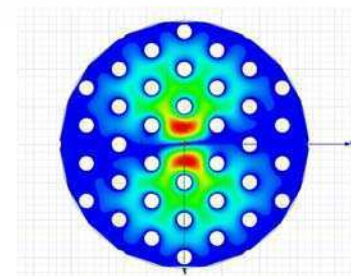
BCD HOM Coupler



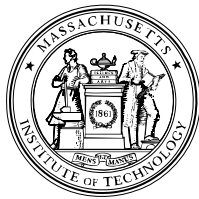
PBG HOM Coupler Concept



(operating)



(BBU)

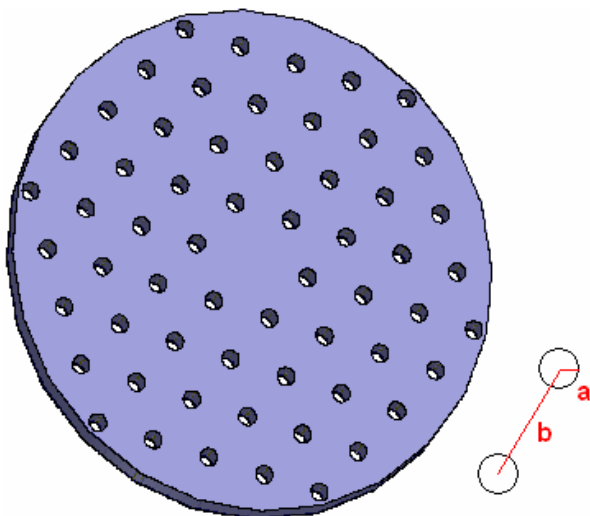


# Goals

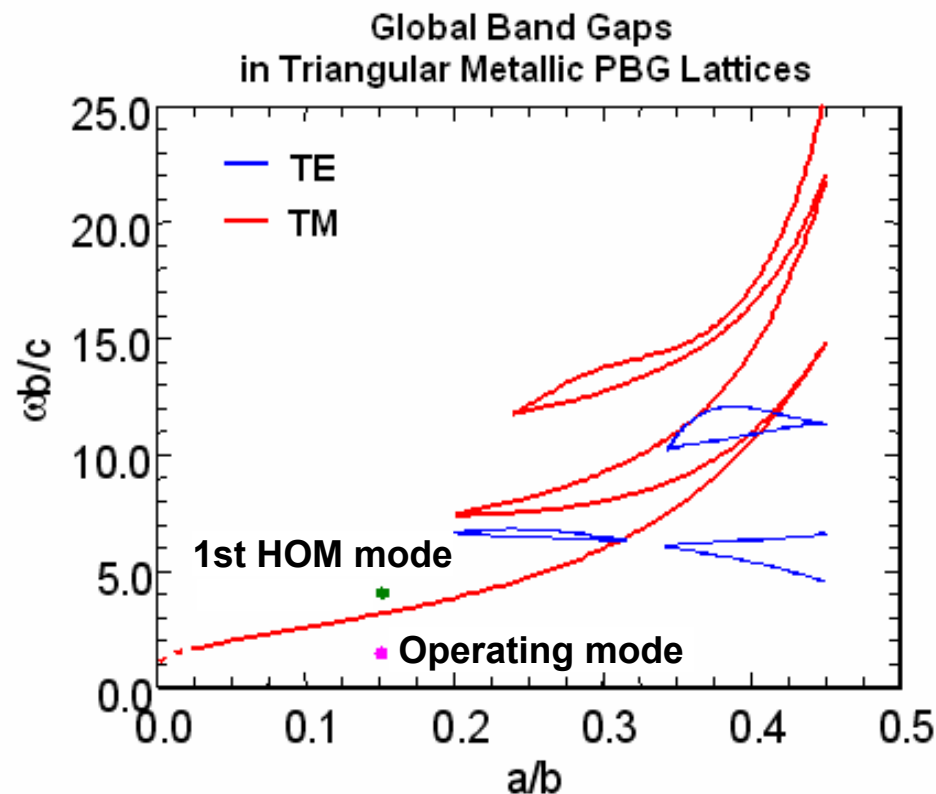


- **Demonstrate that PBG HOM coupler is feasible.**
  - Must preserve operating  $TM_{01}$ -like  $\pi$ -mode to  $Q \geq 10^{10}$ .
  - Must damp HOM wakefields with  $Q \sim 10^5$ .
- **Develop collaborative research on the experimental demonstration.**
- **Build and test PBG HOM coupler.**

- PBG structure designed to trap only TM modes below ~2 GHz.
- Triangular superconducting lattice design
- Propagating modes are damped by outer wall.



$$a = 8.25\text{mm}, b = 55\text{ mm}$$

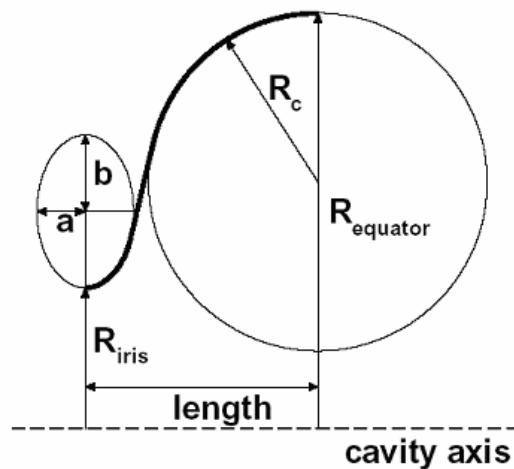


# HFSS Model of TESLA Cavity

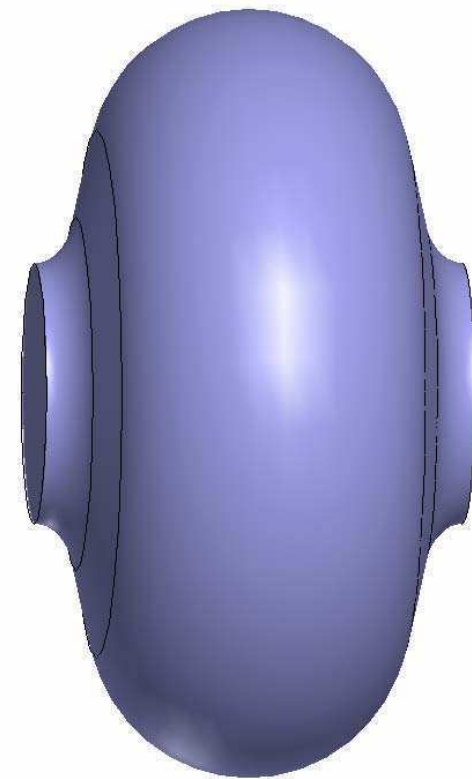
- Created HFSS model of ILC BCD SC cavity, which is the TESLA design.
- Surface conductivity of  $7.2 \times 10^{18}$  S/m
- Simulated TESLA cell supports the  $TM_{01}$ -like mode at 1.299 GHz (1.3 GHz is the intended operating frequency), and  $Q = 1 \times 10^{10}$ .



TESLA RF Unit



TESLA specifications

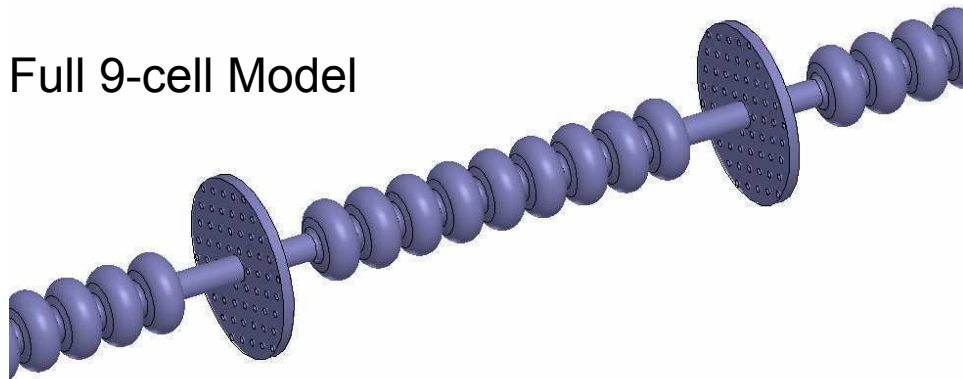


HFSS model of  
TESLA cavity

# HFSS Coupler Models

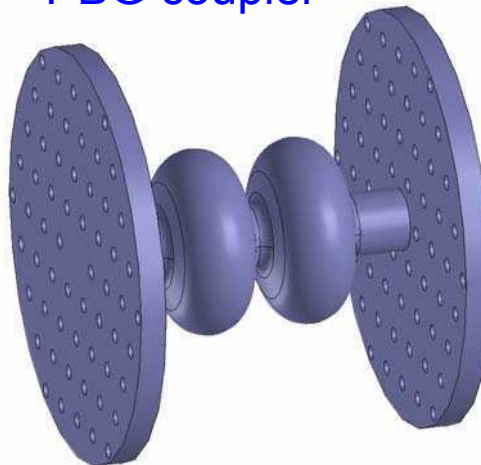
- **Challenging to simulate full 9-cell model**
  - Longitudinal overmoding
  - Computationally intensive
- **Reduced 2-cell model proves to be effective**
  - Two TESLA cells with PBG couplers
  - Two TESLA cells with pillbox couplers

Full 9-cell Model

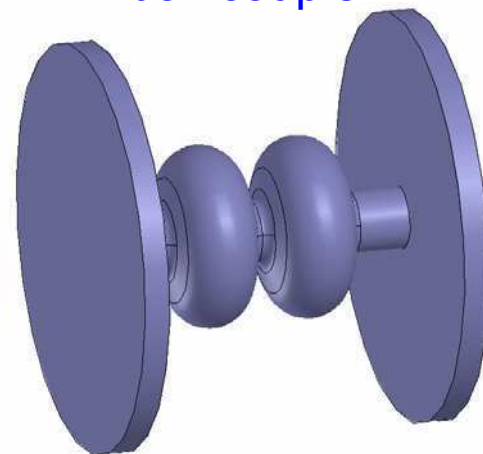


Reduced 2-cell Models

PBG coupler

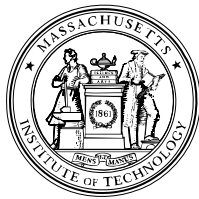


Pillbox coupler





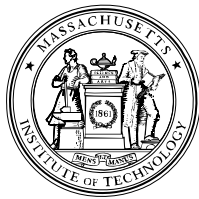




# Results

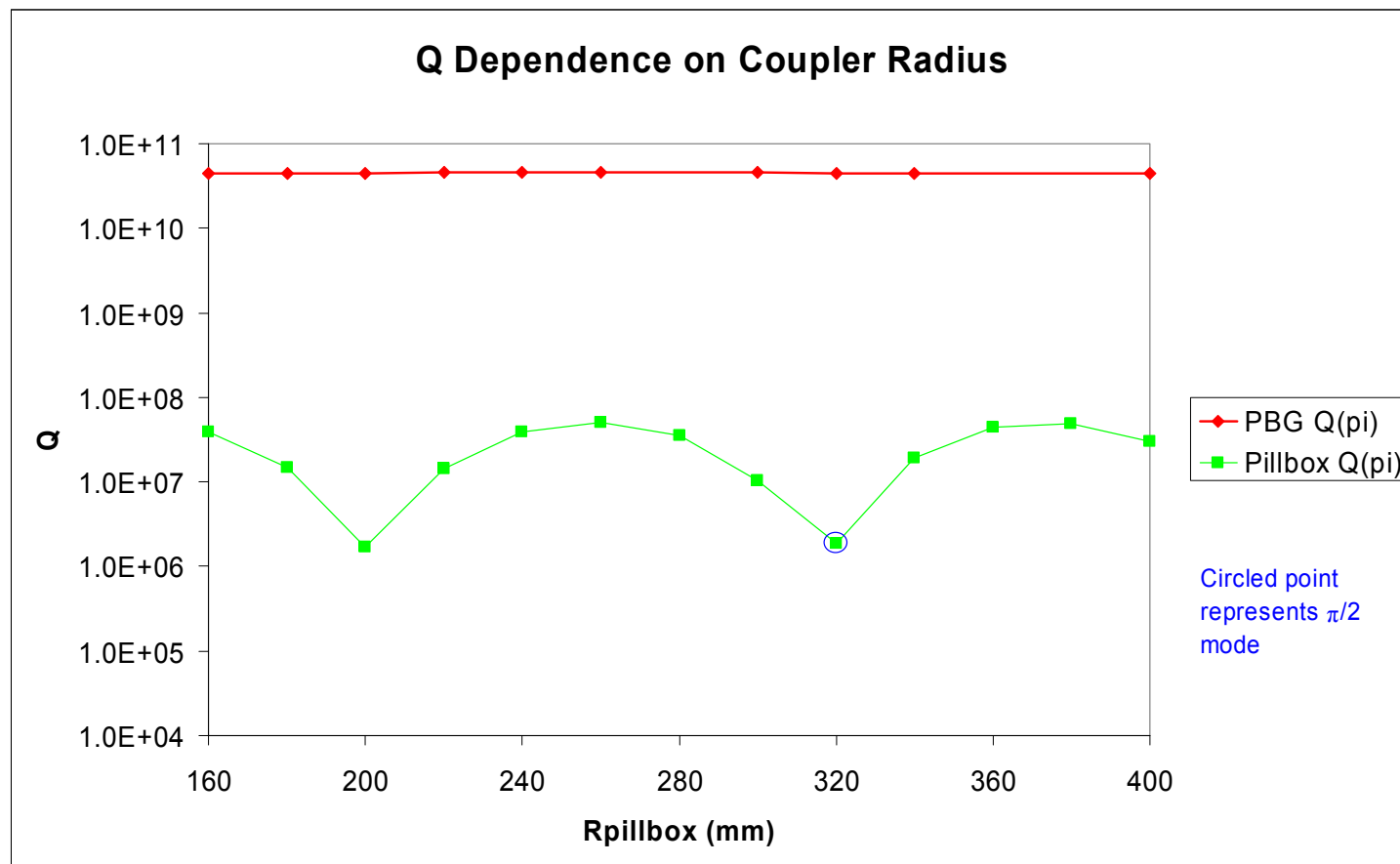
- **PBG HOM coupler meets the goal of maintaining the operating mode.**
- **The simulation model only includes two TESLA cavities, so we expect the Q of the 9-cell setup to be approximately 4.5 times as large, since  $Q_{\text{resonator}} = \omega U/P$ .**

| Coupler type                        | Operating Eigenmode Frequency (GHz) | Q (2-cell system)                     | Estimated Q (9-cell system)                   |
|-------------------------------------|-------------------------------------|---------------------------------------|-----------------------------------------------|
| Pillbox<br>@ Coupler Radius = 35 cm | 1.292                               | $8.562 \times 10^6$                   | $\sim 3.853 \times 10^7$                      |
| <b>PBG</b>                          | <b>1.293</b>                        | <b><math>8.528 \times 10^9</math></b> | <b><math>\sim 3.838 \times 10^{10}</math></b> |

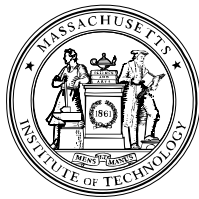


# Dependence on Coupler Radius

- Conducted a test of the relationship between coupler radius and Q-value to ensure the model was robust and realistic.
- PBG coupler Q was insignificantly affected by coupler radius.







# Summary and Plans

- **Developed models and methods for simulating TESLA cavities and PBG HOM couplers.**
- **Verified via HFSS that PBG coupler can sufficiently maintain the TESLA cavity operating mode.**
- **Plans**
  - **Use HFSS models to ascertain whether the PBG coupler can provide the necessary HOM damping.**
  - **Seek collaborative research on the experimental demonstration.**
  - **Build and test PBG HOM coupler at ILCTA.**